ANALYTICAL SOLUTION FOR LOW-THRUST MINIMUM TIME CONTROL OF A SATELLITE FORMATION

DISSERTATION

John Sang-Pil Seo
Major, USAF

AFIT/DS/ENY/04-04

DEPARTMENT OF THE AIR FORCE
AIR UNIVERSITY

AIR FORCE INSTITUTE OF TECHNOLOGY

Wright-Patterson Air Force Base, Ohio

The views expressed in this dissertation are those of the author and do not reflect the official policy or position of the United States Air Force, Department of Defense, or the United States Government.

AFIT/DS/ENY/04-04

ANALYTICAL SOLUTION FOR LOW-THRUST MINIMUM TIME CONTROL OF A SATELLITE FORMATION

DISSERTATION

Presented to the Faculty

Graduate School of Engineering and Management

Air Force Institute of Technology

Air University

Air Education and Training Command

in Partial Fulfillment of the Requirements for the

Degree of Doctor of Philosophy

John Sang-Pil Seo, B.S.E., M.S.E.

Major, USAF

September, 2004

AFIT/DS/ENY/04-04

ANALYTICAL SOLUTION FOR LOW-THRUST MINIMUM TIME CONTROL OF A SATELLITE FORMATION

John Sang-Pil Seo, B.S.E., M.S.E.

Major, USAF

Approved:

/signed/	27 Sep 04
Dr. William E. Wiesel Commitee Chairman	Date
/signed/	27 Sep 04
Dr. Steven G. Tragesser Committee Member	Date
/signed/	27 Sep 04
Maj Richard G. Cobb Committee Member	Date
/signed/	27 Sep 04
Dr. Meir N. Pachter Committee Member	Date
/signed/	27 Sep 04
Dr. Paul J. Wolf Deans Reader	Date

/signed/

Robert A. Calico, Jr
Dean

Dedication

To my Lord and my Savior, Jesus Christ

Acknowledgements

I first thank the almighty and all merciful God for gifting me with all the required talents and furthermore surrounding me with the supportive and loving people to accomplish this task. I pray my efforts have in some way been acceptable to Him.

I thank my research advisor, Dr. William Wiesel, for his teaching, guidance, and assistance, without which I would not be able to complete this arduous work. Next, I would like to thank Dr. Steve Tragesser for his thorough examination of my early research results on the out-of-plane motion as well as securing the sponsorship and the financial support of an outside organization so I could attend and present the preliminary results at a conference in Maui, Hawaii. I also thank my committee members, Maj. Richard Cobb, PhD, and Dr. Meir Pachter for their time in reviewing this manuscript and for their support in this research. I extend my sincere thanks to Dr. Peter Maybeck for serving as my minor advisor and also for providing me with detailed corrections to this dissertation.

I also acknowledge the entire teaching staff of the department of mathematics at AFIT for their availability and sincere wish to help this poor engineering student who would be lost without their insights. I also extend my thanks to numerous other professors, fellow students and professionals at AFIT who have shown compassion and help in this endeavor.

Lastly, but not the least, I sincerely thank my wife and all of my extended family for their constant support and prayers. They do not know the extent to which their support has meant to me. They allowed me to stay focused and at times provided a welcome relief.

John Sang-Pil Seo

Table of Contents

List of Figures

List of Tables

List of Symbols

Symbol		Page
J_2	Earth oblateness perturbation	1-4
e	Eccentricity	1-4
ΔV	Delta-V; Fuel Usage	1-7
R_o	Semi-major axis, or Radius, of Circular Reference Orbit	2-1
x	Radial Relative Position	2-1
y	In-Track Relative Position	2-1
z	Cross-Track Relative Position	2-1
ω	Mean Motion of the Reference Orbit	2-2
$\mu_\oplus$	Gravitational Constant for Earth	2-2
$\dot{x}$	Radial Relative Velocity	2-3
$\dot{y}$	In-Track Relative Velocity	2-3
$\dot{z}$	Cross-Track Relative Velocity	2-3
p	State dimension	2-3
S_N	Target Set	2-4
$\mathbf{x}$	State Vector	2-4
$\mathbf{\Psi}$	Terminal State Constraint	2-4
r	Dimension of constraint	2-4
J	Performance Functional	2-5
t_f	Final or Terminal Time	2-5
U_{max}	Maximum net relative acceleration	2-5
$\boldsymbol{\nu}$	Constant Lagrange multiplier	2-6
$\boldsymbol{\lambda}(t)$	Costate vector	2-6
$H(\mathbf{x}, \mathbf{u}, \boldsymbol{\lambda})$	Control Hamiltonian/Variational Hamiltonian	2-6
$\mathbf{\Phi}_x$	State Transition or Fundamental Matrix	2-8
$\mathbf{x}_o$	Initial state vector	2-8
$\mathbf{\Phi}_\lambda$	Costate Transition or Fundamental Matrix	2-8
$\mathbf{G}$	Controllability Matrix	2-10
λ_x	Radial-position costate	2-10
λ_y	In-track-position costate	2-10
λ_z	Cross-track-position costate	2-10
$\lambda_{\dot{x}}$	Radial-velocity costate	2-10
$\lambda_{\dot{y}}$	In-track-velocity costate	2-10
$\lambda_{\dot{z}}$	Cross-track-velocity costate	2-10
a	Drifting Relative Orbit Parameter	3-2

Symbol		Page
b	Centering Relative Orbit Parameter	3-2
ρ	Relative Orbit Parameter Size	3-2
m	YZ Relative Orbit Parameter	3-2
n	XZ Relative Orbit Parameter	3-2
θ	Relative Orbit Parameter Phase Angle	3-2
M	Amplitude of sinusoidal function	3-11
$D_{(\cdot)}$	Offsets of sinusoidal functions	3-11
ϕ	Phase shift or phase angle of sinusoidal functions	3-11
u_{xo}	Initial control in the radial direction	3-20
u_{yo}	Initial control in the in-track direction	3-20
N	Number of Control Switching	3-27
$\Delta\tau_i$	Time Intervals	5-7
Δa	Change in drifting parameter	5-7
Δb	Change in centering parameter	5-10
Δu_{ij}	Change in control at switch time j for the i-controller	5-10
$\boldsymbol{\Theta}$	Corner State Constraint	6-1
$\boldsymbol{\mu}$	Constant Lagrange Multiplier for Corner State Constraint	6-1
$\boldsymbol{\Delta T}$	Time Interval Vector	E-8

List of Abbreviations

AFIT/DS/ENY/04-04

Abstract

Satellite formations or distributed satellite systems provide advantages not feasible with single satellites. Efficient operation of this platform requires the use of optimal control of the entire satellite formation. While the optimal control theory is well established, only a very simple dynamical system affords an analytical solution. Any practical optimal control problem solve the resulting two-point boundary value (TPBV) problem numerically. In this research, the optimization of satellite formation control is solved analytically. The relative satellite dynamics using Hill's coordinate system and approximations made by Clohessy and Wiltshire, combined with body-fixed thruster control, result in a linearized dynamic system. The minimum use of fuel is important for the longevity of the system; however, understanding the minimum time problem is an a priori requirement for solving the minimum-fuel problem with fixed final time. This dissertation provides the analysis for the minimum time satellite formation control by decoupling the in-plane motion from the out-of-plane motion. While the out-of-plane motion is fully analytic, the in-plane motion is only semi-analytic. The TPBV problem is transformed to solving simultaneous nonlinear equations for the critical control switching times, resulting in an open-loop, bang-bang controller.

ANALYTICAL SOLUTION FOR LOW-THRUST MINIMUM TIME CONTROL OF A SATELLITE FORMATION

I. Introduction

1.1 In the beginning ...

Since the age of enlightenment, many advancements have been made in the study of Celestial Mechanics. Brahe, Kepler, Newton, Euler, Lagrange, Legendre, Gauss, and many more have advanced this study. It was Euler and Lagrange who studied the restricted three-body problem and later (c. 1880) Hill who posed the lunar trajectory (restricted three-body problem of Sun-Earth-moon) in the relative rotating coordinate frame. This initial emphasis in the study of the natural satellites of planets and the moons has shifted to the study of man-made artificial satellites. During the height of the Gemini era, Clohessy and Wiltshire [1] formulated the famous relative motion dynamics using the Hill approach. (Hereinafter the dynamic equations credited to Clohessy and Witshire will be referred to as C-W.) This formulation was the basis for rendezvous or proximity operations. Then in the late 1970's Visher [2] first mentioned the use of "satellite cluster", multiple spacecraft in an cooperative effort working as a single system for communications applications.

The advantage of such a use of multiple spacecraft as a single system was summarized in a recent Air Force Institute of Technology (AFIT) research document by Parker. These advantages include

> "the potential of very large synthetic apertures, modular maintainability and upgradability, graceful degradation, and greatly reduced life cycle costs, beginning with reduced launch costs through the use of multiple smaller launch vehicles." [3]

1.2 Previous Accomplishments

There has been much research in the area of satellite formations, sometimes referred to in the literature as Distributed Satellite Systems (DSSs). DSSs differ from satellite constellation (as in the Global Positioning System) in that the relative distance between members of the satellite clusters are close enough to allow linearization of the gravitational acceleration to first order in relative distance. On the other hand, the distances between the satellites in a constellation is comparable to its semi-major axis. To date, only a few satellites have been flown to take full advantage of proximity operations. This is because there are still technical challenges.

Several organizations have moved into satellite formation feasibility and technical demonstration stage. The United States Air Force and NASA had planned to demonstrate technical feasibility through the TechSat 21 program, which would have investigated satellite formation dynamics as well as micro-satellite and micro-propulsion designs. Using TechSat 21 as a technology demonstrator, they also planned to investigate the distributed mission architecture, sparse aperture sensing, collaborative behavior, and micro-nano-technology [4, 5]. See Figure 1.1 below. The program at the moment has been delayed. Other satellite formation systems are seen in the NASA's Mission to Planet Earth and the NASA-JPL's New Millennium EO-1 programs, in which the EO-1 satellite is in trail 60 ± 6 seconds behind Landsat-7 [6, 7]. NASA Goddard Magnetosphereic Multiscale mission [8] plans to fly a tetrahedron satellite formation in a lunar swingby, twice, to change inclination of the formation from equatorial to polar, an expensive maneuver. European Space Agency (ESA) has also flown Laser Interferometer Space Antenna (LISA) [9] as the satellite formation flying demonstrator. These programs have identified the benefits of satellite formation flying as an earth observing platform.

Research efforts have addressed different aspects of the advantages provided by the formation architecture. They attempt to take advantage of the formation satellites for potential uses in communications, radar mapping, astronomy, and moving target identification. However, an application of DSSs for interferometry requires the relative

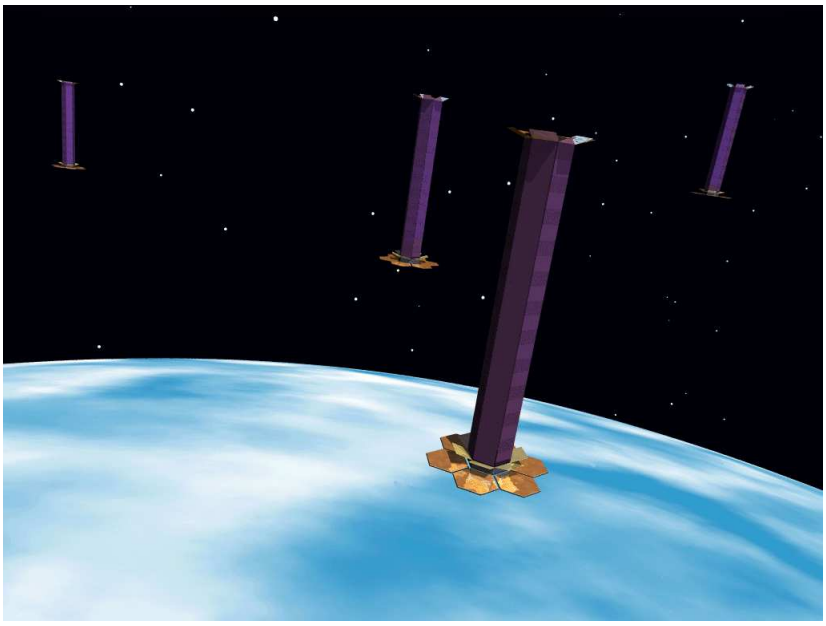

Figure 1.1 US Air Force TechSat 21

navigation knowledge between the satellite members to be on the order of one-tenth of the observing frequency. Therefore, certain operational requirements will dictate the required navigation accuracy of satellite formation. In addition, a high-fidelity model is important for orbit prediction (of control-free formations) as well as long-term control (as in station keeping over a long periods).

Many researchers have initially relied on the relative motion dynamics as posed by Clohessy and Wiltshire. However, the proposed missions for satellite formations require far more precision and for much longer periods than for which C-W equations were initially introduced. The mission duration of DSSs is much longer than the missions for a typical rendezvous, for which the linearized C-W equations were developed. This means minimizing fuel usage to maintain and reconfigure the satellite formation for a long duration is the paramount objective. This leads naturally to the exploitation of "control-free" orbits, sometimes called "Keplerian" or "natural" orbits. These control-free orbits were first based solely on two-body dynamics with circular reference orbit and a perfectly spherical and uniformly dense Earth. The addition of non-spherical earth and

other perturbations introduces secular drift destroying the cluster geometry. However, the perturbations that affect the relative motion are the net difference of perturbations felt by the satellite in the reference orbit and the members of the satellite cluster. This means this effective perturbation on the relative motion is much less than the absolute perturbation felt by the satellites, especially if the satellite cluster consists of identical members as in the Air Force's TechSat 21.

Since then, others have developed variations of C-W equations to include perturbations and allow non-circular reference orbits to generalize relative motion dynamics. Some dynamics models include the dissipative perturbations, such as air drag and solar radiation drag, as well as a non-uniform and non-spherical earth gravity potential.

1.3 Previous Satellite Formation Dynamics Research

Sedwick, Miller and Kong [10] found that the largest error comes from the differential J_2 [1] which introduces secular drift in the relative motion, destroying a stable formation. The next dominant error source is from the non-circular reference orbit. Inalhan et. al [11] showed that even a mildly eccentric reference orbit of e= 0.005, typical of the space shuttle, leads to significant drift in both radial amplitude and in-track direction, which ultimately will destroy the formation geometry if untreated and will require more fuel to null out these neglected effects. Sedwick et. al as well as Wiesel [12] reported that the errors introduced by neglecting the higher order central gravity terms are periodic in nature and should not be counteracted (wasting fuel). The differential drag and differential solar radiation pressure effects decrease with increasing altitude.[10]

Many researchers incorporated J_2 into their model. Schweighart and Sedwick [13] developed a high-fidelity linearized J_2 model. Schaub and Alfriend [14, 15] extended the C-W solution to include first-order oblateness effects using the Delaunay orbital

[1] J_2 is a constant of the second zonal harmonics in describing the earth's gravitational potential using mathematical spherical harmonics.

elements, which the authors noted as being limited because they contain singularities for small values of eccentricity and inclination [16:Chap 2.4.4].

Some researchers incorporated a non-circular reference orbit into their model. Melton [17] expanded the state transition matrix in powers of eccentricity and got errors on the order of 10-20% for reference orbits of small to moderate eccentricity ($0 < e < 0.2$). He used both the cartesian and cylindrical coordinate frame and found the cylindrical coordinate frame to be more accurate as the angular separation between target and chase increased. Kechichian [18] analyzed the relative motion in a general elliptic orbit with respect to a dragging and precessing coordinate frame. Yan, Yang, et. al. [19] developed a model for the lead spacecraft in an elliptical orbit. Yamanaka [20] developed a new state transition matrix for a rendezvous problem with the only assumption being the smallness of the ratio between the relative distance of the satellites and the reference orbit radius. He showed this new state transition matrix reduces to the C-W state transition matrix when $e = 0$. Schaub and Alfriend [21] also developed a dynamics model valid for all eccentricity less than unity. Recently, Ross et. al. [22] employed a purely numerical method through nonlinear programming by posing an optimal control problem to determine zero-fuel orbits that do not assume circular reference orbits.

Hujsak [23] offered a generalization of C-W equation by incorporating both the J_2 and non-zero eccentricity in his debris fragmentation model. In their recent paper by Vaddi and Vadali [24], the authors removed the assumption that went into the development of C-W equations one by one. The results of their corrections (for neglecting J_2 and assuming circular reference orbit) for a duration of 20 orbits showed dramatic improvement in correcting secular drift. Wiesel [25] extended his earlier work in canonical Floquet theory by developing a satellite formation model which incorporates all of the zonal harmonics by linearizing about the periodic relative orbit.

The simplest mathematical description of the relative formation dynamics is the C-W equation. However, it does not incorporate even the J_2 perturbation, it lacks sufficient fidelity for long-term control law synthesis. The higher order effects not modelled by

the C-W solution incite unacceptably high control usage and reduce satellite life spans to impractical durations. In addition, long term drift introduced by the unmodelled perturbations take the system out of the linear region where C-W equation is valid. Although a high-fidelity model is important for relative orbit prediction and long term control, the simpler C-W equation is sufficient if the duration of control is "short" enough to stay within the valid range of the linearization assumptions. In addition, the C-W equation is more mathematically tractable than the higher fidelity models, possibly allowing analytical studies.

1.4 Previous Satellite Formation Control Research

A consensus among researchers in this field is that the fuel usage of a DSSs is one of the most important design parameters. Early works were based on control-free orbits as described in the previous section. However, an operational satellite formation system will require maintenance maneuvers as well as reconfiguration maneuvers. The maintenance maneuvers will be required to zero out any higher order effects not modelled in the orbit prediction algorithm. These effects will build up in time, possibly introducing secular drift. The reconfiguration maneuvers will be required as the operational requirements change, such as change of mission objectives. These maneuvers should be performed with fuel expenditure in mind. Various formulations of the satellite control are possible. The problem may involve a time constraint, or fuel constraint, as well as a power constraint. The time constraint may come to play when the satellite formation must be reconfigured such that the target is in view at a specified time. For any meaningful satellite formation mission, fuel plan dictates the overall mission duration. A satellite system may constrain the power used by the low thrust electric propulsion system. In some instances we may be constrained by more than one constraint at a time. However, the optimal time problem is the basis of all other optimal control problems. For example, an optimal fuel problem must be specified with fixed final time that is greater than or equal to the time optimal solution, otherwise no solution will exist.

Using the logic that the mission duration is governed by when the satellites start to run out of fuel (since the clusters degrade gracefully), it is best to have each member of the satellite formation use fuel at the same rate. Coverstone-Carrol and Prussing [26] have used cooperative control techniques in whch each member (for a rendezvous scenario) is actively controlled to minimize the formation's total fuel expenditure. They found that, as the time allotted for rendezvous is increased, the fuel usage was diminished and, as the power to mass ratio decreased, the optimal control approached that of active/passive rendezvous.

Impulsive control of the satellite clusters have been studied by many in the past. Optimal control of satellite formation using high thrust (impulsive thrust) has been studied by Wiesel [27] using the modal states as well as by Schaub and Alfriend [21] using orbit element feedback. Carter [28] presents a four-impulse optimal rendezvous problem. Ulybyshev [29] develops a linear quadratic controller for long-term formation flying that lead to impulsive burns. This controller counteracts even the periodic disturbances that were not modelled in his "plant" model. The control usage for impulsive controls was optimal (smaller total ΔV) compared to the cases involving continuous control (linear or non-linear). However, impulsive thrusters tend to have low I_{sp}. They consume more fuel mass than the small, higher I_{sp} electric propulsion systems. The loss of ΔV can be partially recovered by employing lighter electric propulsion system.

Satellite formation control using low thrust (or bounded thrust) has been studied extensively by Kechichian in his long series of papers and journal articles. [30, 31, 32, 33, 34, 35] He used non-singular equinoctial orbit elements with dynamics models of varying fidelity to obtain optimal control strategies. DeCou [36] transformed the C-W equations to a U-V plane which is perpendicular to a particular source for interferometry application. Guelman and Aleshin [37] as well as Carter [38] present minimum energy rendezvous with bounded thrust. Guelman and Aleshin further constrained the problem by fixing the terminal-approach direction. Kapila, Yan et al. [39] developed a pulse-based, periodic gain, linear control based on the C-W equation with guaranteed stability.

Using their general elliptical leader model, Yan, Yang et. al [19]presented an output feedback controller. Vadali, Schaub, and Alfriend, [40] presented an orbit maintenance controller using power-limited, electric propulsion. In all of these studies, the control was accomplished by vectored-thrust and the thrust direction was optimized numerically. The cited works assume also that the thrust enters the system non-linearly or the performance functional (cost) is quadratic in control as in the minimum energy problem. Once again we claim that vector thrusting requires three-axis stabilized attitude control and is more expensive than body-fixed thrusters.

The thesis by Irvin [41] investigated minimum fuel reconfiguring techniques using the C-W solution and a variety of feedback design techniques (linear, LQR, SDRE, sliding mode). He found that formation reconfiguration could be accomplished for minimal fuel usage using the simplest of linear techniques. The non-linear controllers such as sliding mode [42], Lyapunov-based [19], adaptive [43, 19], etc. all resulted in higher than acceptable fuel usage for a nominal mission duration of several years. One conclusion that could be drawn from Irvin's study is that, for the short duration of the active control, use of simpler linear C-W equations is valid.

1.5 Current Dissertation Research

The fuel concern for long term formation is crucial for the mission. Thus, the minimum fuel solution could be argued to be more important than the minimum time solution; however, the minimum fuel solution requires first the understanding of the minimum time solution. Therefore, this research has examined the optimization problem, specifically the minimum time control of a satellite member of a formation equipped with low-thrust body-fixed thrusters for a reconfiguration maneuver where only the influence of gravity is considered. Reconfiguration of a satellite formation is required for initial relative orbit insertion as well as for changing the relative orbit formation shape or size. While the full reconfiguration must also address the relative spacing (or phasing) of each satellite, this research only concentrated on achieving the desired final satellite

formation. The issue of spacing each members within a formation must require minimum fuel solution, which this research did not examine, where the specifying of the times naturally addresses the relative phasing.

The linearized C-W model is chosen to derive the minimum time controller because this model is amenable to an analytical solution, while for a short duration of active control, the accuracy is not sacrificed. Other neglected perturbations, such as air drag and solar radiation drag, only introduce small differential perturbations in the relative dynamics, especially if the members of the satellite formation are similar, as in the TechSat 21 system. In this formulation, the Hamiltonian is linear in control due to body-fixed thrusters, but bounded by maximum net relative acceleration. Therefore, the optimal theory provides the minimum time control to be the well-known bang-bang controller that is governed by a switching function, as long as the system is normal.[44]

Since the advancement of the computing and the numerical optimal theory, only the very simple problems are examined analytically. Previous research in this optimal control of satellite formation area has always relied upon numerical solutions. The main focus of this research is to develop an analytical solution to this low-thrust minimum-time control of a satellite in a formation. The algorithm resulting from this research effort can be applied to each members of the formation for the reconfiguration of the entire satellite formation. This analytical study provides insight as well as alternative methods of determining the time optimal control for a satellite formation.

Figure 1.2 illustrates one possible satellite member of a DSS equipped with a body-fixed thrusters, attitude control thrusters and horizon sensors. The geometry and the mass distribution of the satellite will allow the gravitational gradient attitude stabilization; $I_z > I_x \approx I_y$ as was assumed by Milam, Petit and Murray [45]. These subsystems would cost less than a gimballed/vectored thrusters and full three dimensional attitude sensors.

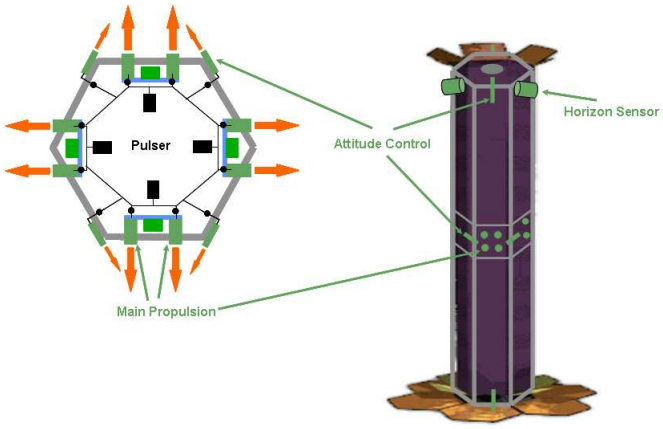

Figure 1.2 Body-fixed thrusters of one DSS satellite

1.6 Research Contributions

Although optimal control theory is mature and many have used it to solve minimum time problems, none have performed a fully analytical study with the satellite formation dynamics. Most relied on numerical solutions using the satisfaction of the Hamiltonian condition as their validation method. This research has performed an analytical study of this problem. The specific contributions stemming from this research include:

i. A costate analysis that was not seen in the literature providing insight to possible optimal control sequences.

ii. Use of time-varying relative orbit parameters for critical time calculations for the in-plane motion.

iii. A fully analytical solution for the out-of-plane motion, which is a general harmonic motion having wide applicability.

These contributions provide an alternative methods to determine the minimum time control of a satellite formation as well as an independent means to verify the optimality of the numerical solutions. For the in-plane problem, the TPBV problem requiring a search in eight-dimensional space was reduced to solving for a root of a single nonlinear equation where the valid range of solution is limited to small subset of the positive real

line. This reduction provides a means for possible real-time (and possibly automated) application of minimum time control of satellites in a formation.

1.7 Dissertation Outline

This dissertation contains 7 chapters, including this introduction which contained much of the literature review. Chapter II presents the elements of the optimal control theory, specifically the minimum-time problem and the necessary and sufficient optimal conditions. Chapter III presents dynamic solutions both for control-free and controlled C-W dynamic system. The importance of costate dynamics, upon which the optimal bang-bang control derives the switching function, is also presented. Chapter IV presents the analytical solution for the out-of-plane motion. Chapter V presents the semi-analytical solution for the in-plane motion. Chapter VI presents the semi-analytical solution for the in-plane motion with initial control-free drift. Chapter VII contains the concluding remarks as well as recommendations for future research.

II. Optimal Time Control of a Satellite Formation

This chapter sets up the optimal time (or minimum time) problem for satellite formation control. Any control problem requires a clear statement of a mathematical model to be controlled (dynamic equations), a desired output of the system (target set), and a set of admissible inputs or controls. An optimal control problem further requires a performance or cost functional which measures the effectiveness of a given control action. [44] These four elements will now be presented for the optimal time control of satellite formation studied in this dissertation.

2.1 Mathematical Model

The fidelity of the dynamics of the satellite formation will dictate the effectiveness of the control problem. Therefore it is important to establish a "good" working dynamics model, where the fidelity and complexity of the models is an important tradeoff. Chapter I discussed many developments of dynamic models of the satellite formation with varying degrees of fidelity.

A high fidelity model would include zonal, tesseral, sectoral harmonics up to certain order, air drag, solar-radiation, and third-body perturbations. The model in the DSST orbit propagator used by many in the literature as the truth model contains many perturbations and the highly non-linear terms. The fully non-linear form is obtained by differencing highly accurate orbital dynamics of each satellite members, but is not conducive to developing an analytical solution.

At the opposite end of the spectrum, the C-W Model is the least accurate, but offers the most mathematically tractable set of equations. The fidelity of this model is a function of the formation separation as well as the duration of the active control for which this model is used. The accuracy of a tighter/smaller formation is better than for a larger formation due to the linearization assumptions of small $\frac{x}{R_o}$, $\frac{y}{R_o}$, and $\frac{z}{R_o}$, where R_o is the circular reference orbit radius, and x, y, and z are the relative positions of the satellite

member with respect to the origin of the reference orbit. Therefore, this approximation becomes inaccurate as time passes and the conditions move away from the valid linear region due to secular drift introduced by neglecting the J_2 effect. This means that C-W equations are not well suited for orbit prediction (or propagation) lasting long durations. However, a low-fidelity model such as the C-W equations will be sufficient for deriving a controller when the duration of control is short enough to stay within the linearization assumptions.

As discussed in Chapter I, the first work in proximity operations was credited to W. H. Clohessy and R. S. Wiltshire back in 1960 at the height of Gemini program, as they sought a solution for rendezvous. Clohessy and Wiltshire applied Hill's approach [1] and similarly simplified the motion by linearizing it about a circular reference orbit. This circular orbit provided the origin[1] for the familiar local coordinate system, with in-plane axes directed along the radial ($\hat{e}_x$) and velocity ($\hat{e}_y$) direction, and the out-of-plane axis ($\hat{e}_z$) direction which is normal to the in-plane. The detail of this first order linearization in this reference frame is in Appendix A. The resulting linearized, constant-coefficient equation[2] as seen in Equation (A.12) is:

$$\begin{aligned} \ddot{x}(t) &= 3\omega^2 x(t) + 2\omega\dot{y}(t) + \tfrac{T_x(t)}{m} \\ \ddot{y}(t) &= -2\omega\dot{x}(t) + \tfrac{T_y(t)}{m} \\ \ddot{z}(t) &= -\omega^2 z(t) + \tfrac{T_z(t)}{m} \end{aligned} \tag{2.1}$$

where ω is the constant mean motion of the circular reference orbit[3]. T_x, T_y, and T_z are the cartesian components of the thrust along the body-axes. It is possible to set up a

[1] This origin is sometimes referred to as the "chief" satellite while the other satellites in the formation are referred as the "slave" or just "member" satellite.

[2] The original paper by Clohessy and Wiltshire notes that H. S. Siefert published the same equations earlier in summer 1959.

[3] $\omega^2 = \mu_\oplus / R_o^3$, where $\mu_\oplus$ is the Earth's gravitational constant

linear system using the state-space form:

$$\begin{bmatrix} \dot{x}(t) \\ \dot{y}(t) \\ \dot{z}(t) \\ \ddot{x}(t) \\ \ddot{y}(t) \\ \ddot{z}(t) \end{bmatrix} = \begin{bmatrix} 0 & 0 & 0 & 1 & 0 & 0 \\ 0 & 0 & 0 & 0 & 1 & 0 \\ 0 & 0 & 0 & 0 & 0 & 1 \\ 3\omega^2 & 0 & 0 & 0 & 2\omega & 0 \\ 0 & 0 & 0 & -2\omega & 0 & 0 \\ 0 & 0 & -\omega^2 & 0 & 0 & 0 \end{bmatrix} \begin{bmatrix} x(t) \\ y(t) \\ z(t) \\ \dot{x}(t) \\ \dot{y}(t) \\ \dot{z}(t) \end{bmatrix} + \begin{bmatrix} 0 & 0 & 0 \\ 0 & 0 & 0 \\ 0 & 0 & 0 \\ 1 & 0 & 0 \\ 0 & 1 & 0 \\ 0 & 0 & 1 \end{bmatrix} \begin{bmatrix} u_x(t) \\ u_y(t) \\ u_z(t) \end{bmatrix} \tag{2.2}$$

where $\dot{x}$, $\dot{y}$, and $\dot{z}$ are the relative velocity components, and

$$\begin{bmatrix} u_x(t) \\ u_y(t) \\ u_z(t) \end{bmatrix} = \begin{bmatrix} \frac{T_x(t)}{m} \\ \frac{T_y(t)}{m} \\ \frac{T_z(t)}{m} \end{bmatrix} \tag{2.3}$$

and $\mathbf{u}^T = [u_x, u_y, u_z]$ is the net/effective acceleration between the member satellite and the reference orbit. Equation (2.2) has the familiar form of a linear, constant-coefficient dynamic system[46].

$$\dot{\mathbf{x}}(t) = \mathbf{A}\mathbf{x}(t) + \mathbf{B}\mathbf{u}(t) \tag{2.4}$$

where the dimension of the state vector, $\mathbf{x}$, is p= 6.

2.2 Desired Output/Target Set

In addition to a mathematical model of the "plant", the optimal control problem needs a target. The target set is important because it determines the size of the solution space. When a single point in $\mathbb{R}^6$ is targeted, the probability of existence of a solution is extremely low. On the other hand, when there is no specific target set[4], it is called free terminal state problem and the probability of the existence of a solution is guaranteed; for the minimum time problem, the solution is the trivial $t_f = 0$. This research has

[4]Mathematically, it is the entire $\mathbb{R}^6$ space.

concentrated on the practical application of satellite control, which requires the satellite to reach a stable relative orbit formation for which the solution space is sufficiently large for existence of solution.

The target set, S_N, is then defined as $S_N = \{\mathbf{x} : \mathbf{x} \in \text{“}Natural\ Orbit\text{”}\}$, where $\mathbf{x}$ is the cartesian relative state vector. By using only the final desired state, $\mathbf{x}_f$, the terminal state constraint can be put in the form

$$\mathbf{\Psi}(\mathbf{x}(t_f), t_f) = \mathbf{0} \tag{2.5}$$

$\mathbf{\Psi}$ is an r-dimensional terminal state constraint vector. A stable relative orbit formation can be described with $r < p$. If $p = r$, as stated earlier, the target set contains a single point in $\mathbb{R}^p$ and the solution space will be very limited. As $p - r$ increases (or, as r decreases), the solution space gets larger.

2.3 Admissible Control

Any physical propulsion system has bounds, whether it is the magnitude of the total thrust available or the maximum vectoring direction. The use of body-fixed thrusting allows the satellite to be equipped with less expensive attitude sensor/controller compared to a vectored thrusting. The loss of ΔV can be shown to be a factor of approximately $(\sqrt{3} - 1)$ when compared to the vectored thrust case. However, it is quite possible that the cost savings in requiring the less expensive components will more than make up the difference. The admissible control for the body-fixed thrusters are then subjected to

$$|u_j(t)| \leq c_j \qquad j = 1, 2, 3 \tag{2.6}$$

where u_j is a component of the control vector and c_j is the maximum allowable thrust in the j^{th} direction. This constraint on the control limits the admissible control to a convex hyper-cube in $\mathbb{R}^3$.

2.4 Performance Functional

The optimal solution depends on the performance functional, J, as well the terminal cost (if any) and whether the terminal time, t_f, is fixed or free. The focus of this research has been on the minimum time (time-optimal) solution. For minimum time control problem [44: Chap. 7], the measure of performance used is

$$J[\mathbf{u}(t)] = t_f - t_o = \int_{t_o}^{t_f} d\tau \tag{2.7}$$

where the control vector $\mathbf{u}$ is not explicitly present in J and the final time, t_f, is not fixed. This dissertation also presents a partial solution for the minimum fuel control problem [44: Chap. 8], for which the measure of performance used is

$$J[\mathbf{u}(t)] = \int_{t_o}^{t_f} \left(\sum_{i=1}^{3} |u_i(t)| \right) d\tau \tag{2.8}$$

where t_f is a fixed value and u_i is the i-th component of the control vector. The result is contained in Appendix H.

In summary, then, this dissertation presents the analysis for minimum time problem defined by the following four elements:

1. The performance functional is, as seen in (2.7), $J[\mathbf{u}(t)] = t_f = \int_0^{t_f} d\tau$, where $t_o = 0$ is fixed and t_f is free.
2. The system equation given in Equation (2.2) is $\dot{\mathbf{x}}(t) = \mathbf{A}\mathbf{x}(t) + \mathbf{B}\mathbf{u}(t)$, a constant coefficient linear system with respect to both the state and the control.
3. The admissible controls for the body-fixed thrusters are bounded as in Equation (2.6), more specifically, $|u_x(t)| \leq U_{max}$, $|u_y(t)| \leq U_{max}$, and $|u_z(t)| \leq U_{max}$, where u_x, u_y, and u_z are the cartesian components of $\mathbf{u}$ and U_{max} is the maximum net relative acceleration available along each coordinate direction.

4. Finally, the target set is the "Natural" orbit (which is now redesignated as the terminal state constraint) expressed in Equation (2.5), $\boldsymbol{\Psi}(\mathbf{x}(t_f), t_f) = \mathbf{0}$. The specific form of this terminal constraint vector will be presented later after the discussion of parameterization.

2.5 Necessary and Sufficient Condition for Optimality

In this section the necessary and sufficient conditions for an optimal solution to the specific problem posed in the previous section are presented. These conditions come from the well established optimal theory summarized by Athans and Falb. For a constant-coefficient, time-invariant system, the necessary and sufficient conditions for optimality can be found in Reference [44].

The performance functional is augmented with both the constant and dynamic Lagrange multipliers ($\boldsymbol{\nu}$ and $\boldsymbol{\lambda}(t)$, respectively) to incorporate the terminal state constraint as well as the dynamic constraints. The modified performance functional becomes:

$$\widetilde{J}[\mathbf{u}(t)] = \boldsymbol{\nu}^T \boldsymbol{\Psi}(\mathbf{x}(t_f), t_f) + \int_0^{t_f} \left(1 + \boldsymbol{\lambda}^T(t) \left[\mathbf{A}\mathbf{x}(t) + \mathbf{B}\mathbf{u}(t) - \dot{\mathbf{x}}(t)\right]\right) dt \tag{2.9}$$

Next, the Hamiltonian, also known as control Hamiltonian or variational Hamiltonian, $H(\mathbf{x}, \mathbf{u}, \boldsymbol{\lambda})$, is defined:

$$H(\mathbf{x}(t), \mathbf{u}(t), \boldsymbol{\lambda}(t)) = 1 + \boldsymbol{\lambda}^T(t) \left[\mathbf{A}\mathbf{x}(t) + \mathbf{B}\mathbf{u}(t)\right] \tag{2.10}$$

where $\boldsymbol{\lambda}(t)$ is the dynamic lagrange multiplier (also known as costate, or adjoint), but referred hereinafter as the costate vector. The Hamiltonian plays an important role in defining the necessary and sufficient conditions in optimal control theory. Incorporating the Hamiltonian into the modified performance functional,

$$\widetilde{J}[\mathbf{u}(t)] = \boldsymbol{\nu}^T \boldsymbol{\Psi}(\mathbf{x}(t_f), t_f) + \int_0^{t_f} \left[H(\mathbf{x}(t), \mathbf{u}(t), \boldsymbol{\lambda}(t)) - \boldsymbol{\lambda}^T(t)\dot{\mathbf{x}}(t)\right] dt \tag{2.11}$$

Calculus of variations is then used to take the first variation of this augmented functional with respect to the state, control, final time, and the terminal state. For an extremum, this first order variation must vanish at the optimal solution. The necessary conditions are derived from forcing this variation to zero, and the details are contained in Appendix C.

Any control from within the hypercube described in Section 2.3 that satisfies all the necessary conditions are only candidates for the optimal controller. The sufficient conditions such as the Legendre, Weirstrauss, Hamilton-Jacobi, etc. are more difficult to evaluate for most problems [44], including the problem under study. However for a linear system posed as a convex problem, the extremum controllers found are guaranteed to be the minimum, if it exists. In fact, the optimal controller relies on Pontryagin's use of Weistrauss condition because the expression for an optimal control does not fall out of the necessary condition. Furthermore, in a conference paper by Chang [47], the necessary condition for the Pontryagin's Minimum Principle[5] is shown to also be the sufficient condition for global optimality. The required condition is that the state not be constrained during the maneuver and that either the end point be fixed or be bounded within a convex set. Our minimum time problem satisfies these conditions and hence the resulting minimum time solution based on Pontryagin's Minimum Principle is globally optimal (i.e. the global minimum).

The necessary and sufficient conditions are:

1. Euler-Lagrange Equations

   Euler-Lagrange equations (sometimes referred to as the canonical equations) provide time-derivatives of the states, $\mathbf{x}$, and costates, $\boldsymbol{\lambda}$:

$$\begin{aligned} \dot{\mathbf{x}}(t) &= \frac{\partial H(t)}{\partial \boldsymbol{\lambda}(t)} = \mathbf{A}\mathbf{x}(t) + \mathbf{B}\mathbf{u}(t) \\ \dot{\boldsymbol{\lambda}}^T(t) &= -\frac{\partial H(t)}{\partial \mathbf{x}(t)} = -\boldsymbol{\lambda}^T(t)\mathbf{A} \end{aligned} \tag{2.12}$$

[5] Originally known as the Pontryagin's Maximum Principle.

The analytical solution to these equations for continuous time is

$$\begin{aligned} \mathbf{x}(t) &= \mathbf{\Phi}_x(t,0)\mathbf{x}(0) + \int_0^t \mathbf{\Phi}_x(t,\tau)\mathbf{B}\mathbf{u}(\tau)d\tau \\ \boldsymbol{\lambda}(t) &= \mathbf{\Phi}_\lambda(t,0)\boldsymbol{\lambda}(0) \end{aligned} \tag{2.13}$$

where $\mathbf{\Phi}_x(t,0) = e^{\mathbf{A}t}$ is the state transition operator and the initial state vector, $\mathbf{x}(0) = \mathbf{x}_o$, is specified.[6] Similarly, the costate transition operator is $\mathbf{\Phi}_\lambda(t,0) = e^{-\mathbf{A}^T t}$ and the boundary condition for the costate is provided by the next necessary condition.[7]

2. Terminal Costate Boundary Condition

   This condition exists because a target set is specified as described earlier in Section 2.2. The necessary condition for the costate at the terminal time is given by

$$\boldsymbol{\lambda}^T(t_f) = \boldsymbol{\nu}^T \frac{\partial \mathbf{\Psi}\left(\mathbf{x}(t_f), t_f\right)}{\partial \mathbf{x}(t_f)} \tag{2.14}$$

   where $\boldsymbol{\nu}$ is constant vector of dimension r. Therefore, the Calculus of Variation has reduced the problem to a Two Point Boundary Value (TPBV) problem. The state equation has the initial condition and the costate has the terminal condition. Numerical solutions of optimal problem uses either a direct method, such as the shooting methods, or an indirect methods, which makes use of gradient information. The optimality validation is provided by the next necessary condition.

3. Transversality Condition and the Hamiltonian

   The Transversality condition shows up when the integration limit of the performance functional is not fixed. This is the case for the minimum time problem in which t_f in Equation (2.7) is free. The transversality condition is a scalar equation

[6] The detailed solution for the state is provided in Appendix A.

[7] In general, if the states are stable forward in time, the costate will be unstable forward in time.

of the form

$$1 + \boldsymbol{\nu}^T \frac{\partial \boldsymbol{\Psi}\left(\mathbf{x}(t_f), t_f\right)}{\partial t_f} + \boldsymbol{\lambda}^T(t_f)\left[\mathbf{A}\mathbf{x}(t_f) + \mathbf{B}\mathbf{u}(t_f)\right] = 0 \tag{2.15}$$

If, however, the terminal state constraint vector ($\boldsymbol{\Psi}$) is not an explicit function of the final time, then this Jacobian is zero.

$$\boldsymbol{\nu}^T \frac{\partial \boldsymbol{\Psi}\left(\mathbf{x}(t_f), t_f\right)}{\partial t_f} = 0 \tag{2.16}$$

The transversality condition can then be considered to be:

$$1 + \boldsymbol{\lambda}^T(t_f)\left[\mathbf{A}\mathbf{x}(t_f) + \mathbf{B}\mathbf{u}(t_f)\right] = 0 \tag{2.17}$$

Furthermore, optimal theory also states that an optimal time controller will result in a constant Hamiltonian that is zero for all $t \in [0, t_f]$. This is why researchers who rely on numerical solutions typically provide a time history of the Hamiltonian. Numerical examples presented in this dissertation will also present this time history.

4. Optimal Control

Typically, one of the necessary conditions, also known as the optimality conditions, provides the means for directly solving for the optimal control. However, when the control enters the Hamiltonian linearly as in Equation (2.10), the optimality condition is

$$H_u(t) = \frac{\partial H(\mathbf{x}, \mathbf{u}, \boldsymbol{\lambda})}{\partial \mathbf{u}(t)} = \boldsymbol{\lambda}^T(t)\mathbf{B} = \mathbf{0}^T \tag{2.18}$$

This does not mean that for an extremum $\boldsymbol{\lambda}(t) = \mathbf{0}\ \forall\ t$ because, if it did, the Hamiltonian will not be zero, violating a necessary condition. It does mean that the $\boldsymbol{\lambda}(t)$ is in the null space generated by $\mathbf{B}$. Notice that the control $\mathbf{u}$ is not present; i.e., the above optimality condition does not provide the minimum time control equation. However, by having the controls bounded as in Equation (2.6), Pontryagin's Mini-

mum Principle [44] provides the stronger sufficient condition. Namely, an optimal control will minimize the Hamiltonian, $H(\mathbf{x}, \mathbf{u}, \boldsymbol{\lambda}(t))$, for all time:

$$\begin{aligned} H(\mathbf{x}^*(t), \mathbf{u}^*(t), \boldsymbol{\lambda}^*(t)) &\leq H(\mathbf{x}(t), \mathbf{u}(t), \boldsymbol{\lambda}(t)) \\ 1 + \boldsymbol{\lambda}^{T*}(t)\left[\mathbf{A}\mathbf{x}^*(t) + \mathbf{B}\mathbf{u}^*(t)\right] &\leq 1 + \boldsymbol{\lambda}^T(t)\left[\mathbf{A}\mathbf{x}(t) + \mathbf{B}\mathbf{u}(t)\right] \\ \boldsymbol{\lambda}^{T*}(t)\left[\mathbf{A}\mathbf{x}^*(t) + \mathbf{B}\mathbf{u}^*(t)\right] &\leq \boldsymbol{\lambda}^T(t)\left[\mathbf{A}\mathbf{x}(t) + \mathbf{B}\mathbf{u}(t)\right] \end{aligned} \tag{2.19}$$

where the asterisk, $()^*$, represents the optimal values. The resulting optimal control is Hamiltonian-minimizing and is the familiar bang-bang controller of the form:

$$u_i^*(t) = \begin{cases} +U_{max} & : \quad \boldsymbol{\lambda}^T(t)\mathbf{b}_i < 0 \\ -U_{max} & : \quad \boldsymbol{\lambda}^T(t)\mathbf{b}_i > 0 \end{cases} \tag{2.20}$$

where $\mathbf{b}_i$ is the i^{th} column of constant matrix $\mathbf{B}$. Reference [44] further states, this form of the solution is only valid for a 'normal' system.[8] That is, the system must be fully controllable and $\boldsymbol{\lambda}^T(t)\mathbf{b}_i$ not be zero for any open interval of time. The controllability matrix, $\mathbf{G}$, for any linear time invariant system provides the necessary condition for controllability. Provided that (for this 6-state problem)

$$\mathbf{G} = \left[\mathbf{B}|\mathbf{A}\mathbf{B}|\mathbf{A}^2\mathbf{B}|\mathbf{A}^3\mathbf{B}|\mathbf{A}^4\mathbf{B}|\mathbf{A}^5\mathbf{B}\right] \tag{2.21}$$

has full rank, i.e. rank of $\mathbf{G} = n = 6$, the system is completely controllable. Furthermore, as will be presented in Chapter III the $\boldsymbol{\lambda}^T(t)\mathbf{b}_i$ is zero only on a set made of isolated times called the control switching times (or critical times). Therefore, the system under study provided in Equation (2.12) is 'normal', hence Equations (2.22), (2.23), and (2.24) are the global minimum solutions. For $\boldsymbol{\lambda}^T = [\lambda_x \ \lambda_y \ \lambda_z \ \lambda_{\dot{x}} \ \lambda_{\dot{y}} \ \lambda_{\dot{z}}]$, where λ_x, λ_y, and λ_z are the position costates and $\lambda_{\dot{x}}$, $\lambda_{\dot{y}}$, and $\lambda_{\dot{z}}$ are the velocity costates, Equation (2.20) can be expressed more compactly

[8] For an 'abnormal' or 'singular' system, the optimal control is more difficult to obtain.

using the signum function[9]:

$$u_x^*(t) = -sgn\{\lambda_{\dot{x}}(t)\}U_{max} \tag{2.22}$$

$$u_y^*(t) = -sgn\{\lambda_{\dot{y}}(t)\}U_{max} \tag{2.23}$$

$$u_z^*(t) = -sgn\{\lambda_{\dot{z}}(t)\}U_{max} \tag{2.24}$$

2.6 Summary

In this chapter, the elements of an optimal control problem, specifically, for the minimum time problem were presented. They include the performance functional, mathematical model, the admissible control, and the target set. Because the optimal theory is well established, the form of the optimal solution is known to be a bang-bang controller. The remainder of the this dissertation will rely on these necessary and sufficient conditions to develop an analytical solution for minimum time control of satellite formation.

[9] $sgn\{x\} = \begin{cases} +1 & : \quad x > 0 \\ 0 & : \quad x = 0 \\ -1 & : \quad x < 0 \end{cases}$

III. Satellite Formation Dynamics

In Chapter II, the four elements of the minimum time control problem addressed in this dissertation, as well as the necessary and sufficient conditions, were discussed. This chapter provides in greater detail the specific solution of the Euler-Lagrange equations, Equation (2.12), given in Section 2.5. First, the well known control-free dynamics is examined. Next, the controlled dynamics is examined along with the vital costate dynamics.

3.1 Control-Free State Dynamics

The control-free state dynamics are discussed in many Astrodynamics texts.[48, 16] They are presented here to set up the discussion of parameterization and for completeness. The control-free ($u_x = u_y = u_z = 0$) state solution to Equation (2.2) for the positions only[1] are

$$\begin{aligned} x(t) &= (4 - 3\cos(\omega t))\, x_o + \tfrac{\dot{x}_o}{\omega}\sin(\omega t) + \tfrac{2\dot{y}_o}{\omega}(1 - \cos(\omega t)) \\ y(t) &= 6\,(\sin(\omega t) - \omega t)\, x_o + y_o + \tfrac{2\dot{x}_o}{\omega}(\cos(\omega t) - 1) \\ &\quad + \tfrac{\dot{y}_o}{\omega}(-3\omega t + 4\sin(\omega t)) \\ z(t) &= \tfrac{\dot{z}_o}{\omega}\sin(\omega t) + z_o\cos(\omega t) \end{aligned} \tag{3.1}$$

Yeh and Sparks [49] re-parameterized this solution in terms of six relative orbit parameters: a, b, ρ, m, n, and θ_o.[2] These parameters replace the six constants of motion;

[1] The state solution for the relative velocity is simply the time derivative of Equation (3.1) and is also presented in AppendixA.

[2] Appendix B.2 presents the detailed description of the parameterization.

namely, the initial state conditions: x_o, y_o, z_o, $\dot{x}_o$, $\dot{y}_o$, and $\dot{z}_o$.

$$a = \frac{2\dot{y}_o + 4\omega x_o}{\omega} \tag{3.2a}$$

$$b = \frac{\omega y_o - 2\dot{x}_o}{\omega} \tag{3.2b}$$

$$\rho^2 = (x_o - a)^2 + \left(\frac{\dot{x}_o}{\omega}\right)^2 \tag{3.2c}$$

$$m = \frac{\dot{z}_o\dot{x}_o - z_o\omega^2(a - x_o)}{\dot{x}_o^2 + \omega^2(a - x_o)^2} \tag{3.2d}$$

$$n = \frac{z_o\dot{x}_o\omega + \dot{z}_o\omega(a - x_o)}{2\left[\dot{x}_o^2 + \omega^2(a - x_o)^2\right]} \tag{3.2e}$$

$$\tan\theta_o = \frac{\omega(x_o - a)}{\dot{x}_o} \tag{3.2f}$$

The drift parameter, a, is the offset of the relative satellite formation in the $\hat{e}_x$ direction. This parameter must be zero for each satellite in the DSS to prevent in-track secular drift. The centering parameter, b, is the offset of the entire relative formation in the $\hat{e}_y$ direction. This parameter is chosen to be zero for an even distribution about the origin of the reference frame. For stable and centered formations, this reduces the degree of freedom to the remaining four, per satellite: the size of the formation (ρ), the slope of the formation projected in the x-z plane (m), the slope of the formation projected in the y-z plane (n), and the initial phase angle (θ_o). This transformation to relative orbit parameters will also allow easy specification of natural orbits.

Equation (3.1) along with the time derivatives can now be expressed using these relative orbit parameters:

$$\begin{aligned}
x(t) &= \rho \sin(\omega t + \theta_o) + a \\
y(t) &= 2\rho \cos(\omega t + \theta_o) - \tfrac{3\omega}{2} a t + b \\
z(t) &= m\rho \sin(\omega t + \theta_o) + n2\rho \cos(\omega t + \theta_o) \\
&= m\left[x(t) - a\right] + n\left[y(t) + \tfrac{3\omega}{2} a t - b\right] \\
\dot{x}(t) &= \omega\rho \cos(\omega t + \theta_o) \\
\dot{y}(t) &= -2\omega\rho \sin(\omega t + \theta_o) - \tfrac{3\omega}{2} a \\
\dot{z}(t) &= m\omega\rho \cos(\omega t + \theta_o) - 2n\omega\rho \sin(\omega t + \theta_o)
\end{aligned} \tag{3.3}$$

The constraints found by Schaub and Alfriend [14] in reducing the degrees of freedom for control-free formations to four are now easily seen using these relative orbit parameters, where a and b are required to be zero. Yeh and Sparks [49] presented special cases of satellite formations using these relative orbit parameters. By choosing $n = 0$ and $m = \pm\sqrt{3}$, the formation will be circular in full three-dimensional space. By choosing $m = 0$ and $n = \pm 0.5$, the formation has a circular projection as seen from the ground directly below the origin; i.e. radial projection. For a non-dispersing formation centered on the reference orbit ($a = 0 = b$), the initial relative positions and velocities are:

$$x_o = \rho \sin\theta_o \tag{3.4a}$$

$$y_o = 2\rho \cos\theta_o \tag{3.4b}$$

$$z_o = m\rho \sin\theta_o + 2n\rho \cos\theta_o \tag{3.4c}$$

$$\dot{x}_o = \rho\omega \cos\theta_o \tag{3.4d}$$

$$\dot{y}_o = -2\rho\omega \sin\theta_o \tag{3.4e}$$

$$\dot{z}_o = m\rho\omega \cos\theta_o - 2n\rho\omega \sin\theta_o \tag{3.4f}$$

To simplify the analysis, for the remainder of this dissertation, canonical units are used. The reference orbit radius, R_o, is normalized to unity as well as the earth gravity

constant, $\mu_\oplus$, reducing the mean motion to unity; $\omega = 1$. This means that all relative distances are normalized by R_o and the times are also normalized by the orbital period of the reference orbit.[3] The relative velocities are normalized by the uniform speed of the reference circular orbit ($\sqrt{\mu_\oplus/R_o}$) and the accelerations are normalized by $\mu_\oplus/R_o^2$.

The control-free dynamics of the C-W Equation, provided in (2.2), decouples to out-of-pane (z-motion) and in-plane motions (xy-motion). It is instructive to examine these two control-free dynamics separately.

3.1.1 Control-Free Out-of-Plane State Dynamics. The differential equation for the out-of-plane motion becomes, $\ddot{z}(t) = -z(t)$. In state space form,

$$\begin{bmatrix} \dot{z}(t) \\ \ddot{z}(t) \end{bmatrix} = \begin{bmatrix} 0 & 1 \\ -1 & 0 \end{bmatrix} \begin{bmatrix} z(t) \\ \dot{z}(t) \end{bmatrix}$$
$$\dot{\mathbf{x}}_z(t) = \mathbf{A}_z \mathbf{x}_z(t) \tag{3.5}$$

The state is now $\mathbf{x}_z = [z \ \dot{z}]^T$. This homogeneous system has a unique property; namely that $\mathbf{A}_z$is skew-symmetric ($\mathbf{A}_z^T = -\mathbf{A}_z$). The homogeneous solution is $\mathbf{x}_z(t) = e^{\mathbf{A}_z t}\mathbf{x}_z(0)$, where

$$e^{\mathbf{A}_z t} = \begin{bmatrix} \cos(t) & \sin(t) \\ -\sin(t) & \cos(t) \end{bmatrix} \tag{3.6}$$

and the initial state vector, $\mathbf{x}_z(0) = [z_o \ \dot{z}_o]^T$.[4] As predicted by the mathematical theory for the self-adjoint system, the Euclidean norm of the homogeneous solution is a constant.[44]

$$\begin{aligned} < \mathbf{x}_z(t), \mathbf{x}_z(t) > &= < e^{\mathbf{A}_z t}\mathbf{x}_z(0), e^{\mathbf{A}_z t}\mathbf{x}_z(0) > \\ &= < \mathbf{x}_z(0), e^{\mathbf{A}_z^T t} e^{\mathbf{A}_z t}\mathbf{x}_z(0) > \\ &= < \mathbf{x}_z(0), e^{(\mathbf{A}_z^T + \mathbf{A}_z)t}\mathbf{x}_z(0) > \\ ||\mathbf{x}_z(t)||^2 &= < \mathbf{x}_z(0), \mathbf{x}_z(0) > = \ ||\mathbf{x}_z(0)||^2 = R_{zo}^2 \end{aligned} \tag{3.7}$$

[3] $t = 2\pi$ is equivalent to one period of the reference orbit.

[4] The initial out-of-plane state is given in terms of the relative orbit parameters in Equation (3.4).

This is easily seen by parameterizing the state solution with the trajectory radius and phase angle:

$$\begin{aligned} z(t) &= R_{zo}\sin(t+\phi_o) \\ \dot{z}(t) &= R_{zo}\cos(t+\phi_o) \\ R_{zo} &= \sqrt{z_o^2+\dot{z}_o^2} \\ \phi_o &= \tan\left(\tfrac{z_o}{\dot{z}_o}\right) \end{aligned} \tag{3.8}$$

where the phase angle is measured clockwise from the positive $\dot{z}$-axis. The trajectory of the control-free out-of-plane motion can be visualized easily in the state-phase space. The homogeneous state trajectories form circles centered about the origin, as it is for a perfect harmonic motion. See Figure 3.1 below.

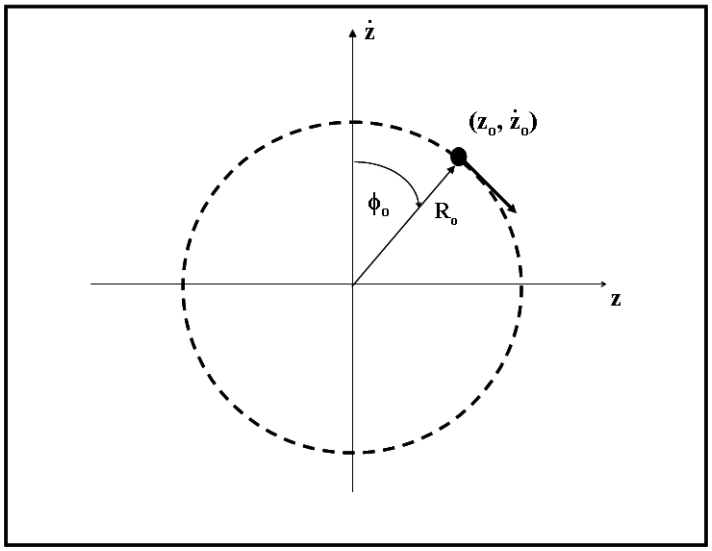

Figure 3.1 Control-free out-of-plane trajectory in state-phase space

3.1.2 Control-Free In-Plane State Dynamics. The in-plane motion is not so easily visualized because it is four-dimensional. The homogeneous dynamic equation in

state-space is

$$\begin{bmatrix} \dot{x}(t) \\ \dot{y}(t) \\ \ddot{x}(t) \\ \ddot{y}(t) \end{bmatrix} = \begin{bmatrix} 0 & 0 & 1 & 0 \\ 0 & 0 & 0 & 1 \\ 3 & 0 & 0 & 2 \\ 0 & 0 & -2 & 0 \end{bmatrix} \begin{bmatrix} x(t) \\ y(t) \\ \dot{x}(t) \\ \dot{y}(t) \end{bmatrix} \tag{3.9}$$

$$\dot{\mathbf{x}}_{xy}(t) = \mathbf{A}_{xy}\mathbf{x}_{xy}(t) \tag{3.10}$$

The state is now $\mathbf{x}_{xy} = [x\ y\ \dot{x}\ \dot{y}]^T$. This homogeneous linear differential equation has an analytical solution.

$$\mathbf{x}_{xy}(t) = \mathbf{\Phi}_x(t,0)\mathbf{x}_{xy}(0) \tag{3.11}$$

where the state transition matrix $\mathbf{\Phi}_x(t,0) = e^{\mathbf{A}_{xy}t}$. The explicit solution was presented in Equation (3.3) using the relative orbit parameters.

While it is difficult to visualize the trajectory in four dimensions, it is helpful to plot the trajectory in multiple 2-D plots. In Figure 3.2 below, two stable control-free trajectories are plotted with labels $u = \dot{x}$ and $v = \dot{y}$. The dashed trajectory is generated with $\rho = 1$ and the solid trajectory is generated with $\rho = 2$. The "Position Plane" shows the typical 2-to-1 ratio ellipse for stable (non-drifting) orbits. Notice that the "Velocity Plane" depicts the trajectory in the familiar 2-to-1 ratio ellipse. Also, notice that both trajectories are stable, centered orbits and how this translates into a line on the "Drifting Plane" and "Centering Plane" with slopes of -0.5 and +0.5, respectively. Also note that when $a = b = 0$, the "Radial Plane" and "In-Track Plane" motions are pure harmonics.

3.2 Costate Dynamics

The control-free state dynamics were presented in detail in the previous two sections and before examining the controlled state dynamics, the costate dynamics must be examined first. This is because the costate determines the switching function for the optimal bang-bang controller presented in Equations (2.22), (2.23), and (2.24). The costate

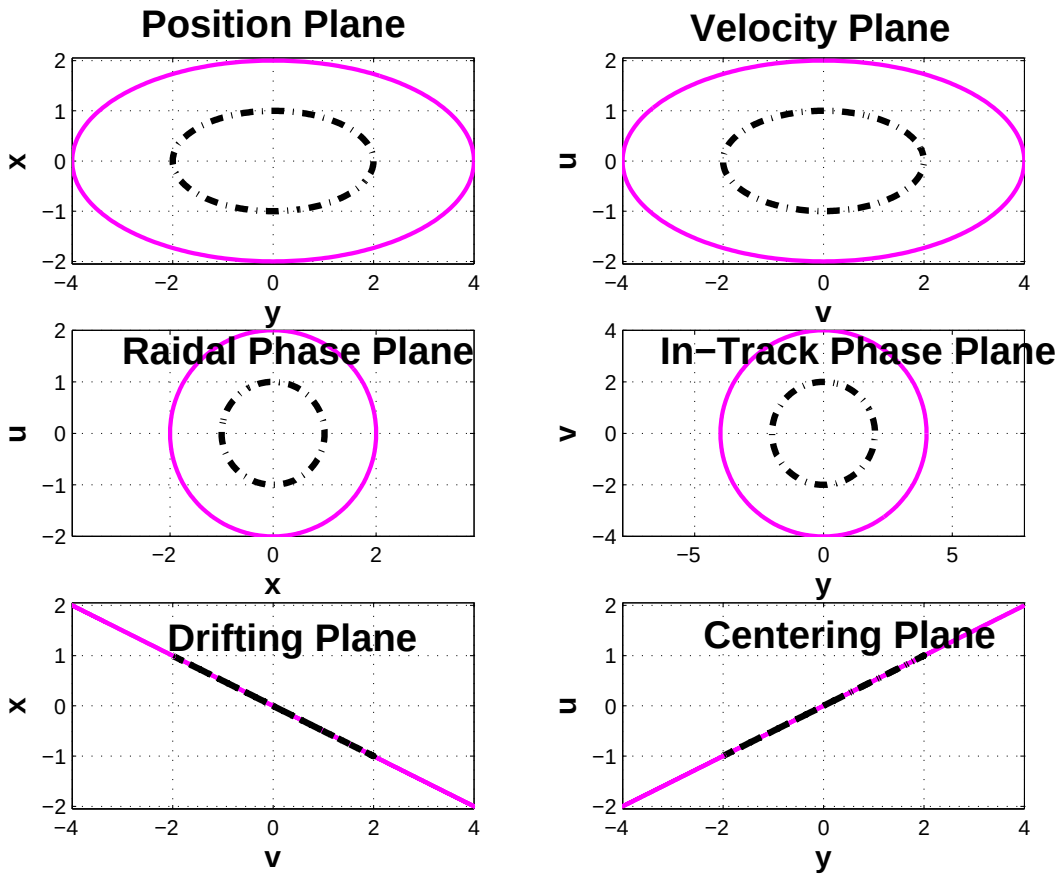

Figure 3.2 The in-plane motion trajectory in six 2-D plots

dynamic equation provided in Equation (2.12) in state-space form, $\dot{\boldsymbol{\lambda}}(t) = -\mathbf{A}^T\boldsymbol{\lambda}(t)$, has analytical solution $\boldsymbol{\lambda}(t) = \boldsymbol{\Phi}_\lambda(t,0)\boldsymbol{\lambda}(0)$. More explicitly, $\boldsymbol{\Phi}_\lambda(t,0) = e^{-\mathbf{A}^T t}$ is

$$e^{-\mathbf{A}^T t} = \begin{bmatrix} 4-3\cos t & -6\sin t+6t & 0 & -3\sin t & 6\cos t-6 & 0 \\ 0 & 1 & 0 & 0 & 0 & 0 \\ 0 & 0 & \cos t & 0 & 0 & \sin t \\ -\sin t & 2\cos t-2 & 0 & \cos t & 2\sin t & 0 \\ -2\cos t+2 & 3t-4\sin t & 0 & -2\sin t & -3+4\cos t & 0 \\ 0 & 0 & -\sin t & 0 & 0 & \cos t \end{bmatrix} \tag{3.12}$$

Knowing the costate vector at any one time provides the costate vector at any other time, past and future, through this costate transition (or fundamental) matrix. Hence,

the optimal control can be determined from a costate vector of any time. Notice that the costate solution also decouples the out-of-plane costate motion from the in-plane costate motion. As was done in the previous section, the two decoupled costate motions are examined next separately.

3.2.1 Out-of-Plane Costate Dynamics. The out-of-plane costate motion is also a simple harmonic because the out-of-plane system is self-adjoint:[5]

$$e^{-\mathbf{A}_z^T t} = \begin{bmatrix} \cos t & \sin t \\ -\sin t & \cos t \end{bmatrix} = e^{\mathbf{A}_z t} \tag{3.13}$$

The trajectory in costate-phase space also forms a simple circle centered about the origin. This can be seen by writing out the solutions more explicitly,

$$\begin{aligned} \lambda_z(t) &= \lambda_{zo}\cos t + \lambda_{\dot{z}o}\sin t \\ \lambda_{\dot{z}}(t) &= -\lambda_{zo}\sin t + \lambda_{\dot{z}o}\cos t \end{aligned} \tag{3.14}$$

Now,

$$\lambda_z^2(t) + \lambda_{\dot{z}}^2(t) = \lambda_{zo}^2 + \lambda_{\dot{z}o}^2 = R_{z\lambda}^2 \tag{3.15}$$

describes the (constant) radius of the circular trajectory in the costate-phase space. So, the trajectories of both the state (homogeneous; i.e. uncontrolled) and costate are circles in their own respective phase spaces. See Figure 3.3 below. Of the two costates for the out-of-plane motion, it is the velocity costate that governs the optimal control. As was presented in the Hamilton-minimizing controller in Equation (2.24), $u_z^*(t) = -sgn\{\lambda_{\dot{z}}(t)\}U_{max}$. Therefore, the optimal control will be $+U_{max}$ when $\lambda_{\dot{z}}(t) < 0$ and $-U_{max}$ when $\lambda_{\dot{z}}(t) > 0$ with the switching occurring at $\lambda_{\dot{z}}(t) = 0$. In terms of the "trajectory" in the costate phase space, whenever the costate pair is in the upper half plane, the control is negative and vice versa. Notice that the times between switchings

[5]For the out-of-plane motion, $d(\lambda_z(t))/dt = \lambda_{\dot{z}}(t)$.

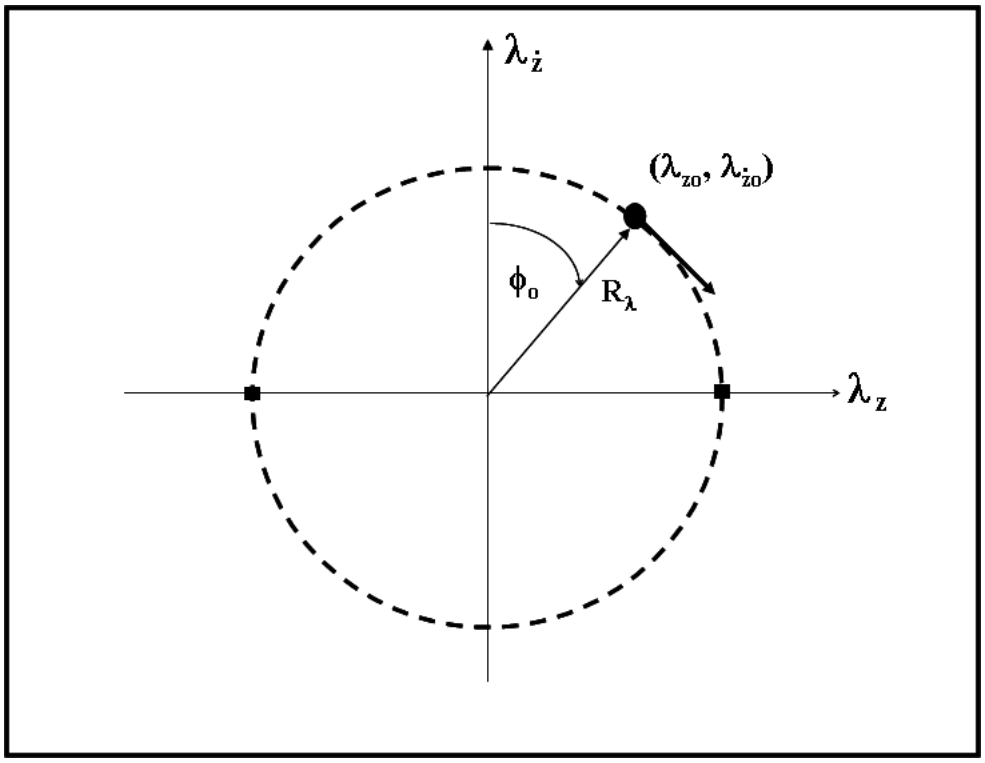

Figure 3.3 Out-of-plane costate trajectory

is a fixed π (canonical) units of time[6]. Since the canonical units are used in this study, the angles in the phase space are equal to the time; physical time is equal to $\omega t = \phi$, where ϕ is the angle in the phase space. In addition, as the name bang-bang controller suggests, the optimal control sequence is either

$$u_z^* = \{+U_{max}, -U_{max}, +U_{max}, -U_{max}, ...\} \tag{3.16}$$

or

$$u_z^* = \{-U_{max}, +U_{max}, -U_{max}, +U_{max}, ...\} \tag{3.17}$$

where the only difference is in the sign of the initial control.

[6]This is true except for the first and the last switches, which may be less than π canonical units of time each.

For a general N number of control switches, the control switching times and the optimal control can be expressed as

$$t_{k+1} = t_k + \pi \qquad k \in \{1, 2, ..., N-1\} \tag{3.18}$$

$$u_{zk} = (-1)^k u_{zo} \qquad k \in \{1, 2, ..., N\} \tag{3.19}$$

where u_{zo} is either $+U_{max}$ or $-U_{max}$. Thus, the out-of-plane problem is considered to have a single subcase (of alternating switching) with two options for initial control.

3.2.2 In-Plane Costate Dynamics. The in-plane costate motion is also difficult to visualize. However, closer examination of the in-plane costate solution provides insight to the possible optimal control sequences and critical control switch times. The fundamental matrix for the in-plane costate dynamics is

$$e^{-\mathbf{A}_{xy}^T t} = \begin{bmatrix} 4 - 3\cos t & -6\sin t + 6t & -3\sin t & 6\cos t - 6 \\ 0 & 1 & 0 & 0 \\ -\sin t & 2\cos t - 2 & \cos t & 2\sin t \\ -2\cos t + 2 & 3t - 4\sin t & -2\sin t & -3 + 4\cos t \end{bmatrix} \tag{3.20}$$

Note that the solution for the costate corresponding to the in-track position $\lambda_y(t) = \lambda_{yo}$ is a constant.[7] Since the optimal control is based on the two velocity costates, the behavior for the in-plane motion is examined in more detail:

$$\lambda_{\dot{x}}(t) = (-\lambda_{xo} + 2\lambda_{\dot{y}o})\sin t + (2\lambda_{yo} + \lambda_{\dot{x}o})\cos t - 2\lambda_{yo} \tag{3.21}$$

$$\lambda_{\dot{y}}(t) = -2(2\lambda_{yo} + \lambda_{\dot{x}o})\sin t + 2(-\lambda_{xo} + 2\lambda_{\dot{y}o})\cos t + (2\lambda_{xo} - 3\lambda_{\dot{y}o}) + 3\lambda_{yo}t \tag{3.22}$$

Earlier, it was noted that $\lambda_y(t) = \lambda_{yo}$, which means that $\lambda_{\dot{x}}$ is sinusoidal with a constant offset of $-2\lambda_{yo}$. This also means that $\lambda_{\dot{y}}$ is not only sinusoidal with an offset of $2\lambda_{xo} - 3\lambda_{\dot{y}o}$, but it also changes linearly in time with a slope of $3\lambda_{yo}$. Rewriting these two velocity

[7] For the in-plane motion, $d(\lambda_x(t))/dt \neq \lambda_{\dot{x}}(t)$ and $d(\lambda_y(t))/dt \neq \lambda_{\dot{y}}(t)$. Note that $\frac{d\lambda_x(t)}{dt} = -3\lambda_{\dot{x}}(t)$.

costate equations using amplitude, M, offsets, $D_{(\cdot)}$, and phase angles, ϕ,

$$\lambda_{\dot{x}}(t) = M \sin\left(t - \phi + \frac{\pi}{2}\right) + D_{\dot{x}} \tag{3.23a}$$

$$\lambda_{\dot{y}}(t) = -2M \sin(t - \phi) + D_{\dot{y}} + 3\lambda_{yo} t \tag{3.23b}$$

$$M = \sqrt{\left(-\lambda_{xo} + 2\lambda_{\dot{y}o}\right)^2 + \left(2\lambda_{yo} + \lambda_{\dot{x}o}\right)^2} \tag{3.23c}$$

$$\tan\phi = \frac{-\lambda_{xo} + 2\lambda_{\dot{y}o}}{2\lambda_{yo} + \lambda_{\dot{x}o}} \tag{3.23d}$$

$$D_{\dot{x}} = -2\lambda_{yo} \tag{3.23e}$$

$$D_{\dot{y}} = (2\lambda_{xo} - 3\lambda_{\dot{y}o}) \tag{3.23f}$$

Note that both $\lambda_{\dot{x}}(t)$ and $\lambda_{\dot{y}}(t)$ have the same period of 2π. The two velocity costates are out of phase with each other by $\pi/2$ as well as having different offsets. These cannot be set arbitrarily since they are coupled through the four constants of costate motion. These two velocity costate equations is important since the minimum time optimal bang-bang controller is a function of these two costates, as was presented in Equations (2.22) and (2.23): $u_x^*(t) = -sgn\{\lambda_{\dot{x}}(t)\}U_{max}$ and $u_y^*(t) = -sgn\{\lambda_{\dot{y}}(t)\}U_{max}$.

As was presented in the out-of-plane costate discussion, it is essential to know what control sequences are possible and what relations exist for the critical control switching times. Without knowing the costate dynamics, all combination and permutations of the x-control and y-control switchings as well as simultaneous switchings may be expected to be possible. However, the two velocity costates are coupled through the four initial costate values, limiting the possible control sequences.

As stated earlier, $\lambda_{\dot{x}}(t)$ is a pure sinusoid with an offset, $D_{\dot{x}} = -2\lambda_{yo}$. See Equation (3.23). This means that the roots (x-crossings) of this equation are given at regular intervals, provided that the offset is smaller than the amplitude. The first two zero-

crossings (t_{x1} and t_{x2}) of $\lambda_{\dot{x}}(t)$ are written in terms of the principle solution to $\cos^{-1}(\cdot)$,

$$\begin{aligned} t_{x1} &= \cos^{-1}\left(-\frac{D_{\dot{x}}}{M}\right) + \phi \\ t_{x2} &= 2\pi - \cos^{-1}\left(-\frac{D_{\dot{x}}}{M}\right) + \phi \\ t_{x3} &= t_{x1} + 2\pi \\ t_{x4} &= t_{x2} + 2\pi \end{aligned} \tag{3.24}$$

and so on. These times partly form the in-plane critical control switching times.

It was also noted earlier, that $\lambda_{\dot{y}}(t)$ is sinusoid with a ramp, $3\lambda_{yo}t$, and an offset, $D_{\dot{y}} = 2\lambda_{xo} - 3\lambda_{\dot{y}o}$ in the $\lambda_{\dot{y}}$-equation. $\lambda_{\dot{y}}(t)$, in general, cannot be solved for roots (y-crossings), as it was done for the x-crossings, unless the ramp term is zero. Notice that λ_{yo} controls both the offset for $\lambda_{\dot{x}}(t)$ as well as the ramp in $\lambda_{\dot{y}}(t)$. This says that, for $\lambda_{yo} \neq 0$, unlike $\lambda_{\dot{x}}(t)$, only a finite number of roots exist. If $\lambda_{yo} = 0$, $\lambda_{\dot{y}}(t)$ exhibits the same behavior as $\lambda_{\dot{x}}(t)$ and the y-crossings can be analytically found. Now, if $|\lambda_{yo}|$ is small, there will be many roots and conversely, as $|\lambda_{yo}|$ increases, there will be fewer and fewer roots. The y-crossing times, in addition to the x-crossings, will completely determine the in-plane critical control switching times.

It is important to find out whether the x-controls and y-controls switch simultaneously ad-infinitum. Since $\lambda_{\dot{y}}(t)$ has a ramp, in order for these two functions (of time) to have the same roots (recall they have the same frequency), this ramp term must vanish: i.e., $\lambda_{yo} = 0$. This means that for $\lambda_{\dot{x}}(t)$, the offset is now zero; $D_{\dot{x}} = 0$. Furthermore, the roots for $\lambda_{\dot{x}}(t)$ will now be at regular intervals of π canonical units of time; $t_{x(i+1)} = t_{x(i)} + \pi$. This means that the $\lambda_{\dot{y}}(t)$ must also have zero offset, $D_{\dot{y}} = 0$, requiring $2\lambda_{xo} = 3\lambda_{\dot{y}o}$. The two velocity costates now reduce to:

$$\begin{aligned} \lambda_{\dot{x}}(t) &= \lambda_{\dot{x}o}\cos t + \frac{1}{2}\lambda_{\dot{y}o}\sin t \\ \lambda_{\dot{y}}(t) &= \lambda_{\dot{y}o}\cos t - 2\lambda_{\dot{x}o}\sin t = 2\frac{d}{dt}\left[\lambda_{\dot{x}}(t)\right] \end{aligned} \tag{3.25}$$

Since the optimal control is a function of the signs of the velocity costates and not the magnitudes, only the phases must be equal. In other words, for the two equations to have the same roots, the two velocity costates must be scale multiples of each other: i.e., $\lambda_{\dot{x}}(t) = \alpha\lambda_{\dot{y}}(t)$ for $\alpha \in \mathbb{R}^1$:

$$\lambda_{\dot{x}}(t) - \alpha\lambda_{\dot{y}}(t) = (\lambda_{\dot{x}o} - \alpha\lambda_{\dot{y}o})\cos t + \left(\frac{1}{2}\lambda_{\dot{y}o} + 2\alpha\lambda_{\dot{x}o}\right)\sin t = 0 \tag{3.26}$$

Now, since $\{\cos(t),\ \sin(t)\}$ form an independent set (or orthogonal pair), the coefficients are set to zero. Writing them in a matrix form,

$$\begin{bmatrix} 1 & -\alpha \\ 2\alpha & \frac{1}{2} \end{bmatrix} \begin{bmatrix} \lambda_{\dot{x}o} \\ \lambda_{\dot{y}o} \end{bmatrix} = \begin{bmatrix} 0 \\ 0 \end{bmatrix} \tag{3.27}$$

A non-trivial solution can exist only if the two equations are linearly dependent or if the left matrix is singular. The determinant of the left matrix is $2\alpha^2 + \frac{1}{2} = 0$. The only roots to this quadratic are $\alpha = \pm\frac{1}{2}i$, complex numbers. This contradicts the assumption that $\alpha \in \mathbb{R}^1$. Hence x- and y-controls cannot switch simultaneously ad infinitum.

An alternative proof with the same assumptions of $D_{\dot{x}} = 0 = D_{\dot{y}}$ is provided. Equations (3.23a) and (3.23b) are now

$$\begin{aligned} \lambda_{\dot{x}}(t) &= M\cos(t-\phi) \\ \lambda_{\dot{y}}(t) &= -2M\sin(t-\phi) = 2M\cos\left(t + \frac{\pi}{2} - \phi\right) \end{aligned} \tag{3.28}$$

The only way for these two equations to have the same zeros is for the phasing to be equal (or be off by $2n\pi$).

$$-\phi = \frac{\pi}{2} - \phi + 2n\pi \tag{3.29}$$

However, this equation cannot be satisfied by any ϕ. So, the same conclusion is drawn: that simultaneous control switching is not possible ad infinitum.

Although multiple simultaneous control switching is not possible, a single simultaneous control switching is possible. This is because of the ramp term in the $\lambda_{\dot{y}}(t)$ equation. Without loss of generality, a simultaneous crossing can occur at either the first x-crossing or the second x-crossing. Begin by re-examining Equations (3.23a) and (3.23b). For convenience, $\phi = 0$ is chosen, which means $\lambda_{xo} = 2\lambda_{\dot{y}o}$ is required. Choosing to work with the first x-crossing,

$$\lambda_{\dot{x}}(t_{x1}) = M\cos(t_{x1}) - 2\lambda_{yo} = 0 \tag{3.30}$$

$$\lambda_{\dot{y}}(t_{x1}) = 2M\cos\left(t_{x1} + \frac{\pi}{2}\right) + \lambda_{\dot{y}o} + 3\lambda_{yo}t_1 = 0 \tag{3.31}$$

$$M = |2\lambda_{yo} + \lambda_{\dot{x}o}| \tag{3.32}$$

Before continuing, $\lambda_{\dot{x}}(t)$ must be guaranteed to have a zero-crossing, i.e. that the offset, $|D_{\dot{x}}|$, is not larger than the amplitude, M. See Figures 3.4(a) below where the offset is larger than the amplitude.

$$\frac{|D_{\dot{x}}|}{M} = \frac{|2\lambda_{yo}|}{|2\lambda_{yo} + \lambda_{\dot{x}o}|} \leq 1 \tag{3.33a}$$

$$4\lambda_{yo}^2 \leq (2\lambda_{yo} + \lambda_{\dot{x}o})^2 \tag{3.33b}$$

$$0 \leq \lambda_{\dot{x}o}(4\lambda_{yo} + \lambda_{\dot{x}o}) \tag{3.33c}$$

This says that for $\lambda_{yo} = k\lambda_{\dot{x}o}$, where $k \geq \frac{1}{4}$, x-crossings are guaranteed. Substituting this into the above equations and solving for t_1 and M, they become functions of k.

$$t_{x1} = cos^{-1}\left(\frac{2k}{2k+1}\right) \tag{3.34a}$$

$$M = (2k+1)\lambda_{\dot{x}o} \tag{3.34b}$$

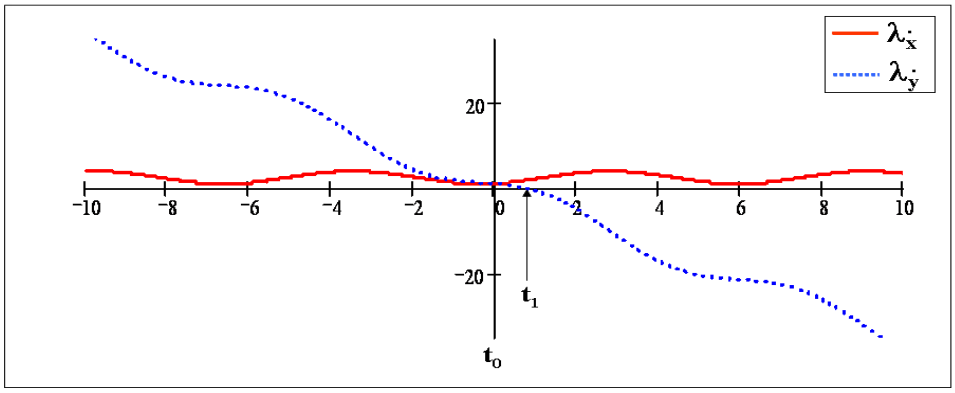

(a) **No X-Control Switching, Single Y-control Switch**

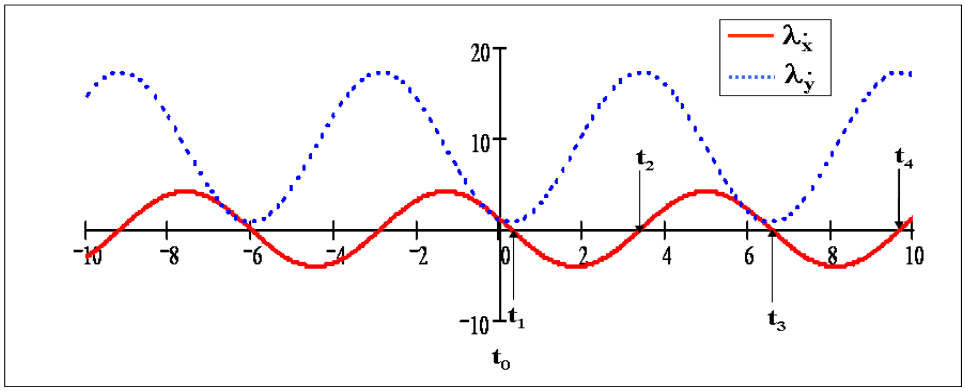

(b) **No Y-Control Switching, Regular X-Control Switch**

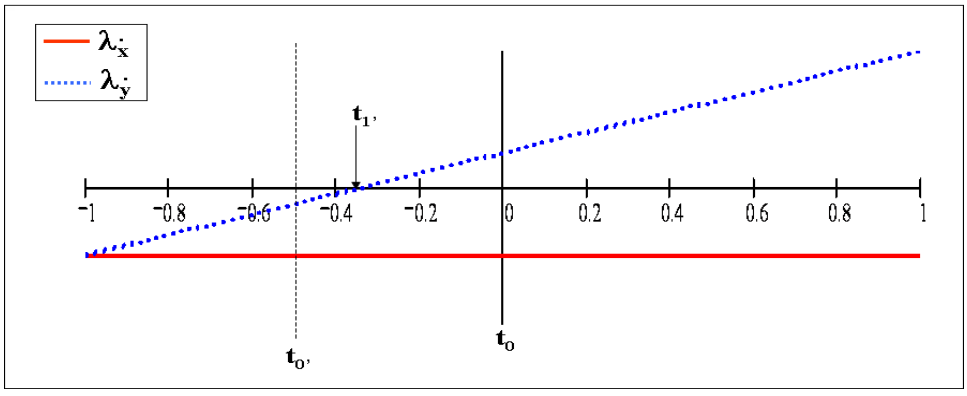

(c) **No Control Switching.**

Figure 3.4 Velocity costate for subcases with single control switching.

When these are substituted back into $\lambda_{\dot{y}}(t_{x1}) = 0$,

$$\lambda_{\dot{y}o} = [2(2k+1)\sin(t_{x1}) - 3kt_{x1}]\,\lambda_{\dot{x}o} = f(k)\lambda_{\dot{x}o} \tag{3.35}$$

Then for an initial costate of

$$\boldsymbol{\lambda}_o = \begin{bmatrix} 2f(k) \\ k \\ 1 \\ f(k) \end{bmatrix} \lambda_{\dot{x}o} \tag{3.36}$$

both the x-control and the y-control are guaranteed to cross at the first x-crossing. For this feasibility analysis, $k = 1$ is chosen, to ensure that $\lambda_{\dot{x}}(t)$ has zeros, and for convenience, $\lambda_{\dot{x}o}$ is set to 1. This results in first two non-negative x-crossing times for $\lambda_{\dot{x}}$ to be $t_{x1} = \cos^{-1}(2/3)$ and $t_{x2} = 2\pi - \cos^{-1}(2/3)$. Using the results of this example, the two plots in Figure 3.5 are generated. Notice that, using the solution from t_{x1}, the simultaneous crosses occur at the first non-negative crossing overall (labelled "t_1" in Figure 3.5(a)), but using the solution from t_{x2}, the simultaneous crosses occur at the third non-negative zero crossing overall (labelled "t_3" in Figure 3.5(b)), which is still the second $\lambda_{\dot{x}}(t)$ crossing. This is because both $\lambda_{\dot{x}}(t)$ and $\lambda_{\dot{y}}(t)$ have the same frequency but out-of-phase by $\pi/2$. Notice that in this example the time interval between the y-crossings is short in comparison to the x-crossings. An analytical expression of this second y-crossing is not available, but it is bounded above by the next x-crossing. A single simultaneous crossing was demonstrated as being possible, however, this case is too specific to be used for determining a general optimal control sequence.

The most general case is the single control switch, alternating between the x- and y-controls. Alternating control switching is possible when only the ramp term in $\lambda_{\dot{y}}(t)$ is eliminated. See the plot in Figure 3.6(a), where λ_{yo} is set to 0 to remove the ramp. In addition, the y-offset is removed in the plot by setting $2\lambda_{xo} = 3\lambda_{\dot{y}o}$. Both functions are now pure sinusoids where $\lambda_{\dot{y}}(t)$ has double the amplitude and the phase is off by $\pi/2$.

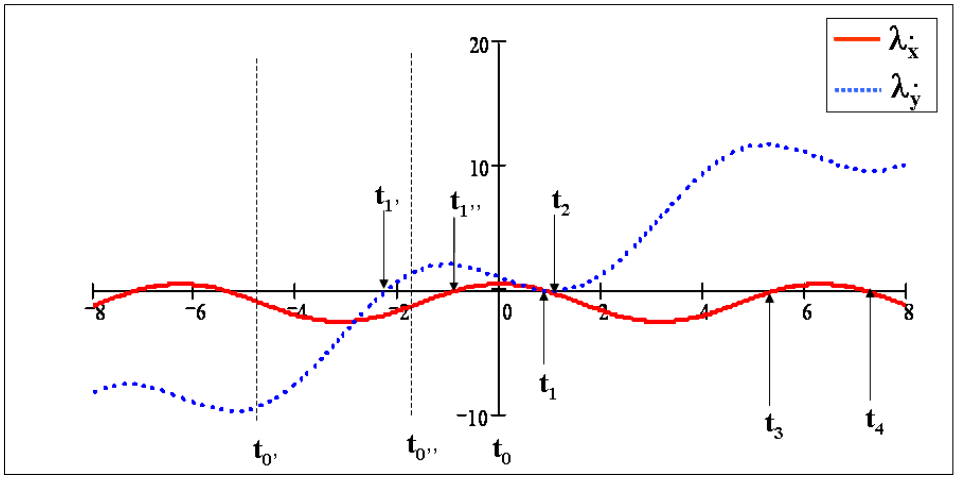

(a) Single simultaneous switch at t_{x1}

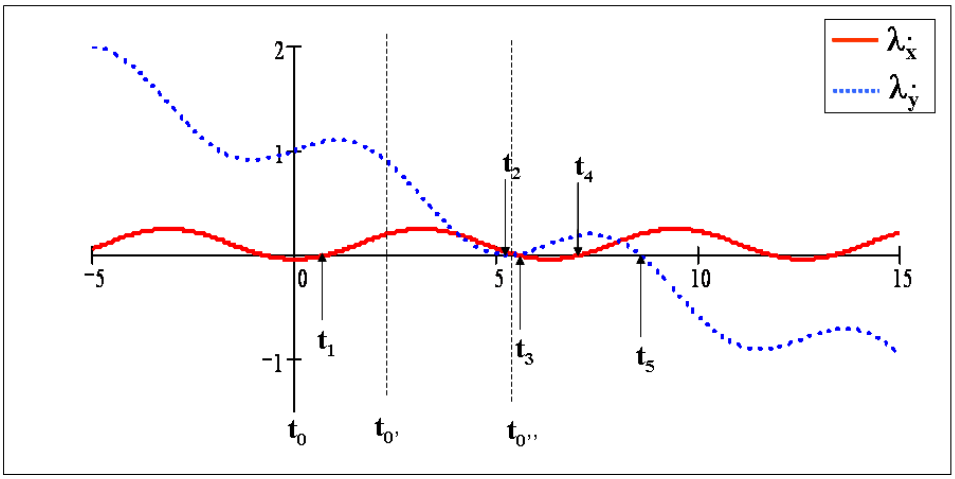

(b) Single simultaneous switch at t_{x2}

Figure 3.5 Velocity costate for subcases with single simultaneous control switching.

The time intervals between the alternating zero-crossings must be less than or equal to the half-period of these two sinusoidal functions, namely π.

In the plot in Figure 3.6(b), another relationship between $\lambda_{\dot{x}}(t)$ and $\lambda_{\dot{y}}(t)$ is illustrated. Here, the ramp exists ($\lambda_{yo} \neq 0$), but it is small enough that $\lambda_{\dot{x}}(t)$ has roots ($|D_{\dot{x}}/M| \leq 1$). Then there is a finite number of y-control switching, but infinite number (but at regular interval) of x-control switchings.

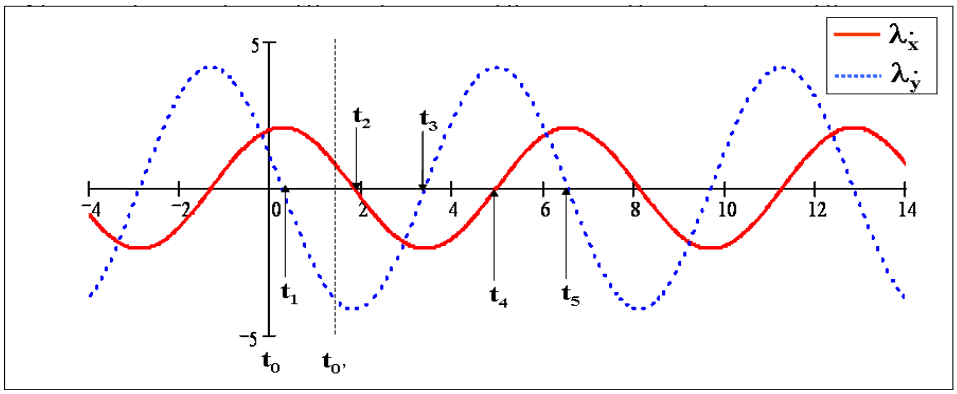

(a) **Alternating control switching (Y-X-Y-X-...)**

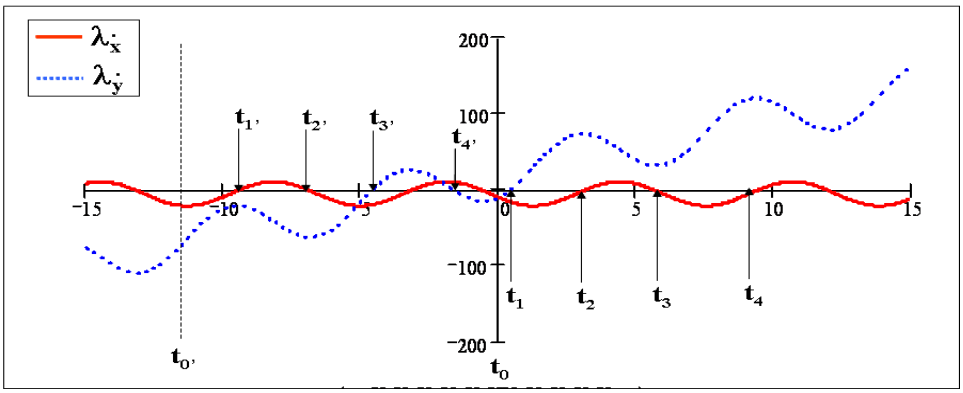

(b) **Repeating x-control switching (X-X-X-...)**

Figure 3.6 Velocity costate for subcases with single control switching.

It is also possible to have the x-offset in $\lambda_{\dot{x}}(t)$ be larger than the amplitude. See Figure 3.4(a). However, because the offset in $\lambda_{\dot{x}}(t)$ is proportional to the ramp in $\lambda_{\dot{y}}(t)$, when λ_{yo} is large, only a single y-crossing is possible. In these type of scenarios, the x-control is held constant until the final time while the y-control switches once at $t = t_{y1} \in [0, t_f]$. Conversely, the ramp can be zeroed out and the offset in $\lambda_{\dot{y}}(t)$ can be greater than its magnitude. See Figure 3.4(b). This time the y-control does not change during the maneuver. Since the x-control now has no offset, it switches regularly at every half-period of the reference orbit.

It is also possible that the sinusoidal portions of $\lambda_{\dot{x}}(t)$ and $\lambda_{\dot{y}}(t)$ vanish. In other words, the amplitude, M, is zero. Then, the $\lambda_{\dot{x}}(t)$ stays constant while $\lambda_{\dot{y}}(t)$ changes linearly in time. See Figure 3.4(c). Finally, there are two degenerate cases: 1) $\lambda_{\dot{x}}(t) = 0 \; \forall \; t$ and $\lambda_{\dot{y}}(t) = \lambda_{\dot{y}o}$, a constant, and 2) $\lambda_{\dot{x}}(t) = \lambda_{\dot{y}}(t) = 0 \; \forall \; t$.

Up to this point, it was shown that simultaneous control switching can happen at most once. However, this is a very special case since it necessarily limits the number of y-control switch with the two of those times being very close to each other. See Figure 3.5. For the general problem of minimum time maneuvering of a satellite formation, many control switches are needed to achieve our final desired relative orbit. However, in the in-plane motion, the number of critical control switching times required must be equivalent to r, the number of terminal state constraint. Since the in-plane natural orbit can be described using three relative orbit parameters (a_f, b_f, and ρ_f at the final time), a minimum of two control switches are needed to satisfy them. The three critical times corresponding to the two control switches are t_1, t_2, and t_f. If however, all four parameters are specified (now including θ_f), the target set contains a single point in $\mathbb{R}^4$ and four critical times (corresponding to three control switches) is required; t_1, t_2, t_3 and t_f. This costate analysis revealed that, in general, the control switch will be either the x-control or the y-control at each control switch time, but not both.

Next, the possible optimal control sequences for the case of three control switches are presented for completeness. Note that the possible optimal control sequences for the case requiring two control switches will be contained within this larger set.

Subcase I. (Y-X-Y)

In the plot of Figure 3.6(a), the velocity costates are plotted with the initial control, $\mathbf{u}_o = [-U_{max} \; -U_{max}]^T$. The first control switch is in the y-control at t_1, followed by the x-control switch at t_2, and the final control switch at t_3 is again the y-control.

Then, the sequence of control is

$$\begin{bmatrix} -U_{max} \\ -U_{max} \end{bmatrix}_{\mathbf{u}_o} \rightarrow \begin{bmatrix} -U_{max} \\ +U_{max} \end{bmatrix}_{\mathbf{u}_1} \rightarrow \begin{bmatrix} +U_{max} \\ +U_{max} \end{bmatrix}_{\mathbf{u}_2} \rightarrow \begin{bmatrix} +U_{max} \\ -U_{max} \end{bmatrix}_{\mathbf{u}_3} \tag{3.37}$$

and obviously, multiplying the entire sequences by -1,

$$\begin{bmatrix} +U_{max} \\ +U_{max} \end{bmatrix}_{\mathbf{u}_o} \rightarrow \begin{bmatrix} +U_{max} \\ -U_{max} \end{bmatrix}_{\mathbf{u}_1} \rightarrow \begin{bmatrix} -U_{max} \\ -U_{max} \end{bmatrix}_{\mathbf{u}_2} \rightarrow \begin{bmatrix} -U_{max} \\ +U_{max} \end{bmatrix}_{\mathbf{u}_3} \tag{3.38}$$

Notice that all four initial conditions for this subcase are not possible. It is not possible get $\mathbf{u}_o = \pm[+U_{max} \ -U_{max}]^T$ because the phasing in $\lambda_{\dot{x}}(t)$ and $\lambda_{\dot{y}}(t)$ is not arbitrary. This means that $u_{xo}/u_{yo} = +1$ for this type of subcase, where u_{xo} is the initial control in the x-direction and u_{yo} is the initial control in the y-direction. For this subcase, we also know that t_f must occur prior to the next x-control switch. However, the time interval between two consecutive x-control switch is known be 2π. So, the time interval, $t_f - t_2$, must be less than 2π.

Subcase II. (X-Y-X)

In the plot of Figure 3.6(a), imagine the plot shifted in time so that $t_{o'}$ is the zero time. Then, the x-control switches at $t_{1'}$ (t_2 on the plot), y-control switches at $t_{2'}$ (t_3 on the plot), and x-control switches at $t_{3'}$ (t_4 on the plot). Then the sequence of control is

$$\begin{bmatrix} -U_{max} \\ +U_{max} \end{bmatrix}_{\mathbf{u}_o} \rightarrow \begin{bmatrix} +U_{max} \\ +U_{max} \end{bmatrix}_{\mathbf{u}_1} \rightarrow \begin{bmatrix} +U_{max} \\ -U_{max} \end{bmatrix}_{\mathbf{u}_2} \rightarrow \begin{bmatrix} -U_{max} \\ -U_{max} \end{bmatrix}_{\mathbf{u}_3} \tag{3.39}$$

multiplying the entire set of results by -1,

$$\begin{bmatrix} +U_{max} \\ -U_{max} \end{bmatrix}_{\mathbf{u}_o} \rightarrow \begin{bmatrix} -U_{max} \\ -U_{max} \end{bmatrix}_{\mathbf{u}_1} \rightarrow \begin{bmatrix} -U_{max} \\ +U_{max} \end{bmatrix}_{\mathbf{u}_2} \rightarrow \begin{bmatrix} +U_{max} \\ +U_{max} \end{bmatrix}_{\mathbf{u}_3} \tag{3.40}$$

Notice again, that not all four initial conditions are possible for this subcase. The initial control $\mathbf{u}_o = \pm[+U_{max} \ +U_{max}]^T$ is not possible because the phasing in $\lambda_{\dot{x}}(t)$ and $\lambda_{\dot{y}}(t)$ is not arbitrary. This means that $u_{xo}/u_{yo} = -1$ for this type of subcase. For this subcase, t_f must occur prior to the next y-control switch. However, the time interval between two consecutive y-control switch must be 2π when $\lambda_{\dot{y}}(t)$ is a pure sinusoid. So, $t_f - t_2 < 2\pi$. In addition, $t_3 - t_1 = 2\pi$ because that is the time interval between two consecutive x-control switches.

Subcase III. (Y-X-X)

In the plot of Figure 3.6(b), the velocity costates are plotted with the initial control, $\mathbf{u}_o = [+U_{max} \ +U_{max}]^T$. The y-control switches at t_1, followed by the x-control switching at t_2 and at t_3. Then the sequence of control is

$$\begin{bmatrix} +U_{max} \\ +U_{max} \end{bmatrix}_{\mathbf{u}_o} \rightarrow \begin{bmatrix} +U_{max} \\ -U_{max} \end{bmatrix}_{\mathbf{u}_1} \rightarrow \begin{bmatrix} -U_{max} \\ -U_{max} \end{bmatrix}_{\mathbf{u}_2} \rightarrow \begin{bmatrix} +U_{max} \\ -U_{max} \end{bmatrix}_{\mathbf{u}_3} \tag{3.41}$$

and obviously, multiplying the entire sequences by -1,

$$\begin{bmatrix} -U_{max} \\ -U_{max} \end{bmatrix}_{\mathbf{u}_o} \rightarrow \begin{bmatrix} -U_{max} \\ +U_{max} \end{bmatrix}_{\mathbf{u}_1} \rightarrow \begin{bmatrix} +U_{max} \\ +U_{max} \end{bmatrix}_{\mathbf{u}_2} \rightarrow \begin{bmatrix} -U_{max} \\ +U_{max} \end{bmatrix}_{\mathbf{u}_3} \tag{3.42}$$

Notice again that not all four initial conditions are possible for this subcases. The initial controls of $\mathbf{u}_o = \pm[+U_{max} \ -U_{max}]^T$ is not possible because the phasing in $\lambda_{\dot{x}}(t)$ and $\lambda_{\dot{y}}(t)$ is not arbitrary. This means that $u_{xo}/u_{yo} = +1$ for this type of subcase.

Subcase IV. (X-X-Y)

In the plot of Figure 3.6(b), imagine the plot shifted in time so that $t_{o'}$ is the zero time. Then, the x-control switches at $t_{1'}$ and $t_{2'}$. The y-control switches at $t_{3'}$.

Then the sequence of control is

$$\begin{bmatrix} +U_{max} \\ +U_{max} \end{bmatrix}_{\mathbf{u}_o} \rightarrow \begin{bmatrix} -U_{max} \\ +U_{max} \end{bmatrix}_{\mathbf{u}_1} \rightarrow \begin{bmatrix} +U_{max} \\ +U_{max} \end{bmatrix}_{\mathbf{u}_2} \rightarrow \begin{bmatrix} +U_{max} \\ -U_{max} \end{bmatrix}_{\mathbf{u}_3} \tag{3.43}$$

and obviously, multiplying the entire sequences by -1,

$$\begin{bmatrix} -U_{max} \\ -U_{max} \end{bmatrix}_{\mathbf{u}_o} \rightarrow \begin{bmatrix} +U_{max} \\ -U_{max} \end{bmatrix}_{\mathbf{u}_1} \rightarrow \begin{bmatrix} -U_{max} \\ -U_{max} \end{bmatrix}_{\mathbf{u}_2} \rightarrow \begin{bmatrix} -U_{max} \\ +U_{max} \end{bmatrix}_{\mathbf{u}_3} \tag{3.44}$$

Notice that not all four initial conditions are possible for this subcases. Initial controls of $\mathbf{u}_o = \pm[+U_{max} \ -U_{max}]^T$ is not possible. This means that $u_{xo}/u_{yo} = +1$ for this type of subcase.

Subcase V. (X-X-X)

In the plot of Figure 3.4(b), the x-control switches at t_2, t_3, and t_4 while the y-control stays constant. Then the sequence of control is

$$\begin{bmatrix} -U_{max} \\ -U_{max} \end{bmatrix}_{\mathbf{u}_o} \rightarrow \begin{bmatrix} +U_{max} \\ -U_{max} \end{bmatrix}_{\mathbf{u}_1} \rightarrow \begin{bmatrix} -U_{max} \\ -U_{max} \end{bmatrix}_{\mathbf{u}_2} \rightarrow \begin{bmatrix} +U_{max} \\ -U_{max} \end{bmatrix}_{\mathbf{u}_3} \tag{3.45}$$

and obviously, multiplying the both sequences by -1,

$$\begin{bmatrix} +U_{max} \\ +U_{max} \end{bmatrix}_{\mathbf{u}_o} \rightarrow \begin{bmatrix} -U_{max} \\ +U_{max} \end{bmatrix}_{\mathbf{u}_1} \rightarrow \begin{bmatrix} +U_{max} \\ +U_{max} \end{bmatrix}_{\mathbf{u}_2} \rightarrow \begin{bmatrix} -U_{max} \\ +U_{max} \end{bmatrix}_{\mathbf{u}_3} \tag{3.46}$$

For this subcase only, all four initial control pairs are possible. By shifting in time such that $\lambda_{\dot{x}}(t) < 0$, the initial controls can have opposite signs. This means that $u_{xo}/u_{yo} = \pm 1$ for this type of subcase.

In each of these subcases, the ratio of initial control pair is either $u_{xo}/u_{yo} = +1$ or $u_{xo}/u_{yo} = -1$, but not both (except for subcase V). Whereas in the out-of-plane analysis

in Section 3.2.1, there was one subcase and two initial control options, now there are five subcases and two initial control vector options for $N = 3$. In other words, of the four possible choices for the initial control:

$$\mathbf{u}_o = \begin{bmatrix} u_{xo} \\ u_{yo} \end{bmatrix} \in \left\{ \begin{bmatrix} U_{max} \\ U_{max} \end{bmatrix}, \begin{bmatrix} U_{max} \\ -U_{max} \end{bmatrix}, \begin{bmatrix} -U_{max} \\ U_{max} \end{bmatrix}, \begin{bmatrix} -U_{max} \\ -U_{max} \end{bmatrix} \right\} \tag{3.47}$$

only two are viable for each of the subcases (except for subcase V). This is because $\lambda_{\dot{y}}(t)$ is always $\pi/2$ ahead in phase of $\lambda_{\dot{x}}(t)$, independent of the ϕ. As seen earlier, by writing the velocity costate Equations (3.21) as

$$\begin{aligned} \lambda_{\dot{x}}(t) &= M\cos(t-\phi) - 2\lambda_{yo} \\ \lambda_{\dot{y}}(t) &= 2M\cos\left(t + \frac{\pi}{2} - \phi\right) + 3\lambda_{yo}t + (2\lambda_{xo} - 3\lambda_{\dot{y}o}) \end{aligned}$$

it is clear that the phasing difference is exactly $\pi/2$. The number of y-controls is sensitive to the y-position costate, λ_y, which is a constant. It introduces the offset in the $\lambda_{\dot{x}}(t)$ as well as the ramp term in the $\lambda_{\dot{y}}(t)$, which are the switching functions of the x- and y-controllers, respectively. A non-zero λ_{yo} means the number of y-control switchings is limited to some finite number. If both offsets are zero[8], then the y-control can switch periodically without limit. Similarly, in general, the x-controls can switch without limit as long as the magnitude of the x-offset is less than the amplitude, $|D_{\dot{x}}| < M$.

In Figure 3.7 below, a "stable" costate trajectory is presented where the labels correspond to $x = \lambda_x(t)$, $y - \lambda_y(t)$, $u = \lambda_{\dot{x}}(t)$, and $v = \lambda_{\dot{y}}(t)$. As was seen in the state dynamics where $a = 0 = b$ resulted in non-drifting stable relative orbit, a "stable" costate orbit is generated similarly when $\lambda_{yo} = 0$ and $2\lambda_{xo} = 3\lambda_{\dot{y}o}$. In the state phase space, focus is on the y-x position-plane where the stable relative orbit forms a 2-to-1 elliptical path about the reference orbit. However, for the costate, the $\lambda_{\dot{y}}$-$\lambda_{\dot{x}}$ velocity-plane is more

[8] $D_{\dot{x}} = 0 \rightarrow \lambda_y = 0$ and $D_{\dot{y}} = 0 \rightarrow 2\lambda_{xo} = 3\lambda_{\dot{y}o}$.

important because the switching function for the time-optimal bang-bang controller are functions of the velocity costates.

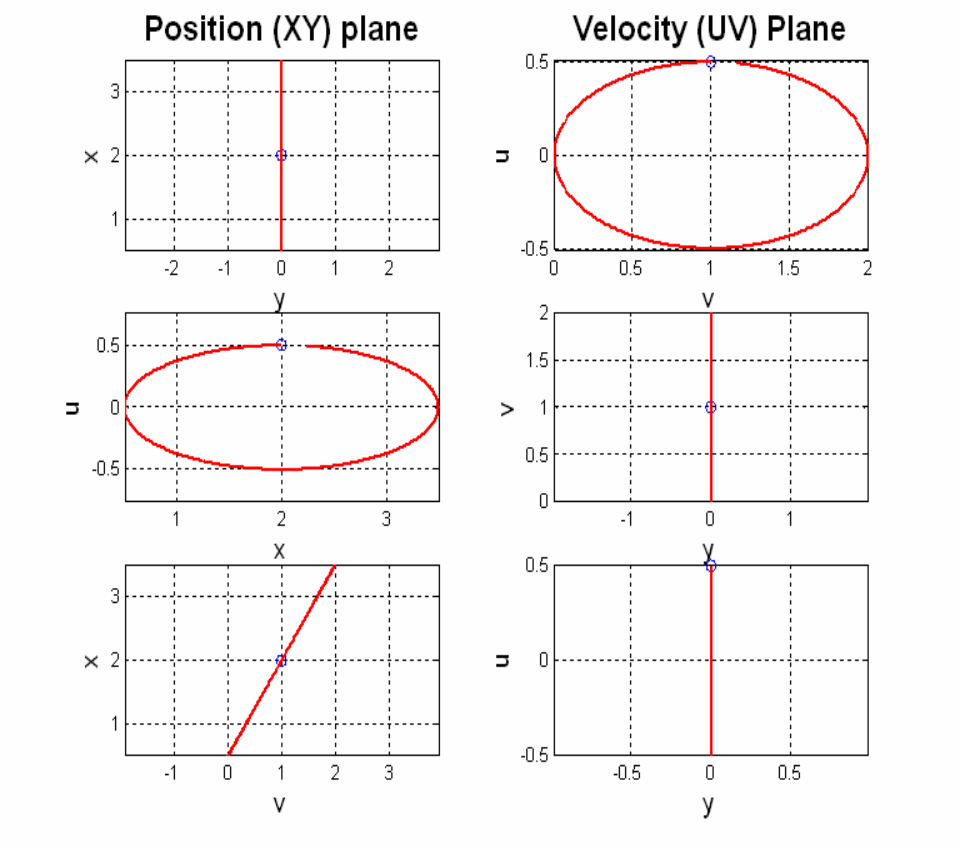

Figure 3.7 In-plane costate trajectory in costate-phase space

Prior to this analysis, all permutations and combinations of control switching, including multiple simultaneous control switches seemed possible. This costate analysis reduces the number of combinations from 27×4 to just 5×2 for the case of three control switches. See Table 3.1 below. For the case of two control switches, $N = 2$, there are three subcases with two initial control vector options.

3.3 Controlled State Dynamics

Having learned the behavior of the costate dynamics, the switching functions for the optimal bang-bang controller, the controlled state dynamics is now examined. The

Table 3.1 Table of possible control sequences with various initial controls for $N = 3$.

Control Sequence	$\mathbf{u}_o^I = \begin{bmatrix} +U_{max} \\ +U_{max} \end{bmatrix}$	$\mathbf{u}_o^{II} = \begin{bmatrix} +U_{max} \\ -U_{max} \end{bmatrix}$	$\mathbf{u}_o^{III} = \begin{bmatrix} -U_{max} \\ +U_{max} \end{bmatrix}$	$\mathbf{u}_o^{IV} = \begin{bmatrix} -U_{max} \\ -U_{max} \end{bmatrix}$
Y-X-Y	Yes	–	–	Yes
X-Y-X	–	Yes	Yes	–
Y-Y-X	–	–	–	–
X-X-Y	Yes	–	–	Yes
Y-Y-Y	–	–	–	–
X-X-X	Yes	–	–	Yes
Y-X-X	Yes	–	–	Yes
X-Y-Y	–	–	–	–
XY-X-Y	Yes*	–	–	Yes*
XY-Y-X	Yes*	–	–	Yes*
XY-Y-Y	–	–	–	–
XY-X-X	–	–	–	–
X-XY-Y	Yes*	–	–	Yes*
Y-XY-X	Yes*	–	–	Yes*
Y-XY-Y	–	–	–	–
X-XY-X	–	–	–	–
X-Y-XY	Yes*	–	–	Yes*
Y-X-XY	Yes*	–	–	Yes*
Y-Y-XY	–	–	–	–
X-X-XY	–	–	–	–
XY-XY-X	–	–	–	–
XY-XY-Y	–	–	–	–
XY-X-XY	–	–	–	–
XY-Y-XY	–	–	–	–
X-XY-XY	–	–	–	–
Y-XY-XY	–	–	–	–
XY-XY-XY	–	–	–	–

* These are plausible, but too specific to include as the general subcases.

insight gained in the previous section was that the optimal controls will be piece-wise constant functions of time changing their signs when the corresponding velocity costate changes sign (crosses zero). In addition, it was determined that only certain control

sequences are considered to be possibly optimal. As before, the two decoupled motions are now examined separately.

3.3.1 Controlled Out-of-Plane Dynamics. The control-free state dynamics case was already examined in Section 3.1.1. Now the controlled out-of-plane motion is examined. The dynamic equation, $\ddot{z}(t) = -z(t) + u_z(t)$ can be written in state-space form as:

$$\begin{aligned} \begin{bmatrix} \dot{z}(t) \\ \ddot{z}(t) \end{bmatrix} &= \begin{bmatrix} 0 & 1 \\ -1 & 0 \end{bmatrix} \begin{bmatrix} z(t) \\ \dot{z}(t) \end{bmatrix} + \begin{bmatrix} 0 \\ 1 \end{bmatrix} u_z(t) \\ \dot{\mathbf{x}}_z(t) &= \mathbf{A}_z \mathbf{x}_z(t) + \mathbf{B}_z u_z(t) \end{aligned} \tag{3.48}$$

where the single control in the z-direction is u_z where $|u_z(t)| \leq U_{max}$. The above linear differential equation has solution of the form,

$$\mathbf{x}(t) = e^{\mathbf{A}_z t}\mathbf{x}_z(0) + \int_0^t e^{\mathbf{A}_z(t-\tau)}\mathbf{B}_z u_z(\tau) d\tau \tag{3.49}$$

For a constant control $u_z(t) = u_{zo}\ \forall t \in [0, t]$, the explicit solution is

$$\begin{bmatrix} z(t) \\ \dot{z}(t) \end{bmatrix} = \begin{bmatrix} \cos(t) & \sin(t) \\ -\sin(t) & \cos(t) \end{bmatrix} \begin{bmatrix} z_o \\ \dot{z}_o \end{bmatrix} + \begin{bmatrix} 1 - \cos(t) \\ \sin(t) \end{bmatrix} u_{zo} \tag{3.50}$$

With no controls (homogeneous solution), the state dynamics were shown in Section 3.1.1 to be a perfect harmonic motion where trajectories formed circles centered about the origin. When a constant $\pm U_{max}$ is applied, the trajectory continues to be a circle, but now centered about $(\pm U_{max}, 0)$. See Figure 3.8 where R_{z-} and R_{z+} represent the radius of the circular trajectories generated by using $-U_{max}$ and $+U_{max}$ controls, respectively. Therefore, the reachable state from any given initial state is a function of both the initial state and the magnitude of U_{max}.

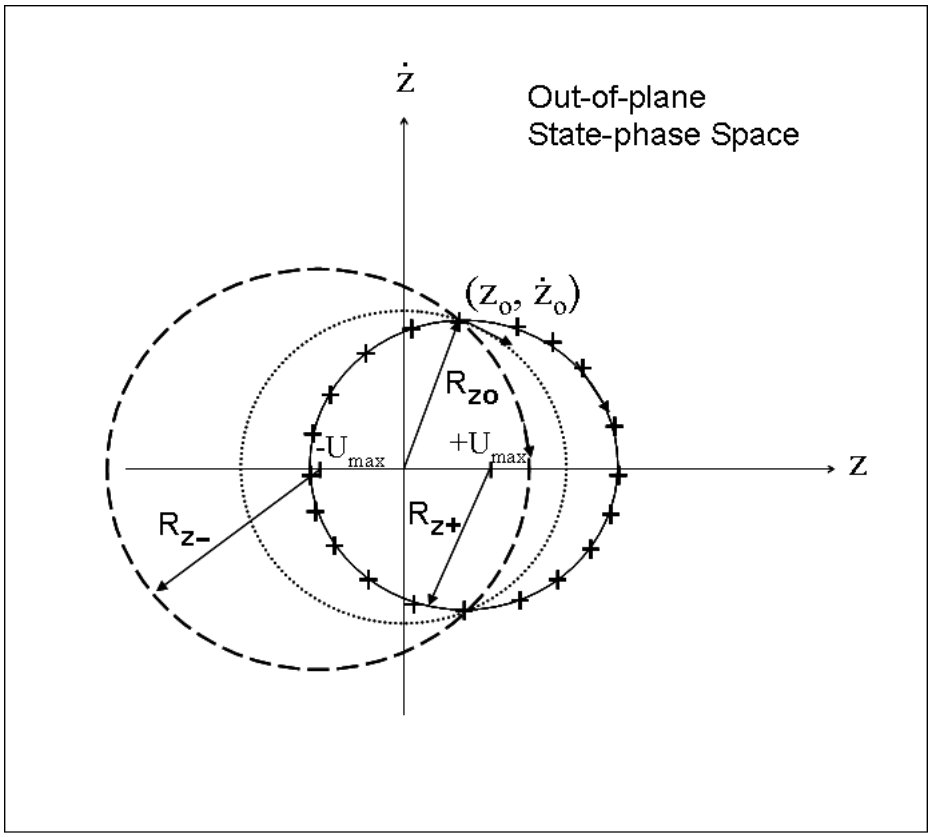

Figure 3.8 Out-of-plane state-phase space diagram .

For a general solution with N number of control switches, the control switching times of $t_{k+1} = t_k + \pi$ and the optimal control of $u_{zk} = (-1)^k u_{zo}$ were presented in Equations (3.18) and (3.19). Then, for $t_N < t < t_f$, the general out-of-plane state solution is

$$\mathbf{x}_z(t) = e^{\mathbf{A}_z t}\mathbf{x}_z(0) + \int_0^{t_1} e^{\mathbf{A}_z(t-\tau)}\mathbf{B}_z u_{zo} d\tau + \sum_{k=1}^{N-1}\left(\int_{t_k}^{t_{k+1}} e^{\mathbf{A}_z(t-\tau)}\mathbf{B}_z u_{zk} d\tau\right) + \int_{t_N}^{t} e^{\mathbf{A}_z(t-\tau)}\mathbf{B}_z u_{zN} d\tau \quad (3.51)$$

As will be presented later in Chapter IV, this equation plays an important role in the analytical solution for the out-of-plane problem.

3.3.2 Controlled In-Plane Dynamics. The control-free state dynamics were already examined in Section 3.1.2. Now the controlled in-plane motion is examined.

$$\begin{bmatrix} \dot{x}(t) \\ \dot{y}(t) \\ \ddot{x}(t) \\ \ddot{y}(t) \end{bmatrix} = \begin{bmatrix} 0 & 0 & 1 & 0 \\ 0 & 0 & 0 & 1 \\ 3 & 0 & 0 & 2 \\ 0 & 0 & -2 & 0 \end{bmatrix} \begin{bmatrix} x(t) \\ y(t) \\ \dot{x}(t) \\ \dot{y}(t) \end{bmatrix} + \begin{bmatrix} 0 & 0 \\ 0 & 0 \\ 1 & 0 \\ 0 & 1 \end{bmatrix} \begin{bmatrix} u_x(t) \\ u_y(t) \end{bmatrix} \tag{3.52}$$

$$\dot{\mathbf{x}}_{xy}(t) = \mathbf{A}_{xy}\mathbf{x}_{xy}(t) + \mathbf{B}_{xy}\mathbf{u}_{xy}(t) \tag{3.53}$$

For a constant control of $\mathbf{u}_{xyo} = \begin{bmatrix} u_{xo} & u_{yo} \end{bmatrix}^T$, the explicit in-plane state solution is

$$\mathbf{x}_{xy}(t) = \mathbf{\Phi}_x(t,0)\mathbf{x}_{xy}(0) + \left[\int_0^t \mathbf{\Phi}_x(t,\tau)\mathbf{B}_{xy}d\tau\right]\mathbf{u}_{xyo}$$

$$\begin{bmatrix} x(t) \\ y(t) \\ \dot{x}(t) \\ \dot{y}(t) \end{bmatrix} = \begin{bmatrix} \rho_o \sin(t+\theta_o) + a_o \\ 2\rho_o \cos(t+\theta_o) - \frac{3}{2}a_o t + b_o \\ \rho_o \cos(t+\theta_o) \\ -2\rho_o \sin(t+\theta_o) - \frac{3}{2}a_o \end{bmatrix} + \begin{bmatrix} 1-\cos t & 2t - 2\sin t \\ -2t + 2\sin t & -\frac{3}{2}t^2 + 4 - 4\cos t \\ \sin t & 2 - 2\cos t \\ -2 + 2\cos t & -3t + 4\sin t \end{bmatrix} \begin{bmatrix} u_{xo} \\ u_{yo} \end{bmatrix} \tag{3.54}$$

where the homogeneous part was written using the in-plane relative orbit parameters. Then, for a general N control switches, the in-plane state solution for $t_N < t < t_f$,

$$\mathbf{x}_{xy}(t) = \begin{bmatrix} \rho_o \sin(t+\theta_o) + a_o \\ 2\rho_o \cos(t+\theta_o) - \frac{3}{2}a_o t + b_o \\ \rho_o \cos(t+\theta_o) \\ -2\rho_o \sin(t+\theta_o) - \frac{3}{2}a_o \end{bmatrix} + \left[\int_0^{t_1} \mathbf{\Phi}_x(t,\tau)\mathbf{B}_{xy} d\tau\right] \mathbf{u}_{xyo} + \sum_{k=1}^{N-1} \left[\int_{t_k}^{t_{k+1}} \mathbf{\Phi}_x(t,\tau)\mathbf{B}_{xy} d\tau\right] \mathbf{u}_{xyk} + \left[\int_{t_N}^{t} \mathbf{\Phi}_x(t,\tau)\mathbf{B}_{xy} d\tau\right] \mathbf{u}_{xyN} \quad (3.55)$$

As will be presented later in Chapter V, this equation plays an important role in the analytical solution of the critical control switching times.

3.4 Summary

In this chapter, first the control-free solutions for the state dynamic equation were presented, where the out-of-plane and in-plane motions decoupled. Therefore, these two motions were discussed separately. The relative orbit parameters were also presented in this chapter, along with state-phase space diagrams allowing visualization of state trajectories. Next, the costate dynamics were discussed, which was necessary for presenting the controlled state solutions. With the knowledge of state and costate dynamics as well as the form of the optimal control law, the full optimal control problem is now ready to be solved. The following two chapters present the analytical solutions for the out-of-plane motion and the in-plane motion in this order, respectively.

IV. Minimum Time Control for Out-of-plane Motion

Quickly reviewing pertinent information from the previous chapters, the costate trajectory for the out-of-plane motion was found to be identical to the state trajectory, due to the out-of-plane system being self-adjoint. The out-of-plane costate phase space trajectory analysis provided the insight that the time interval between two control switches must be π canonical units of time. The optimal control was shown to be dependent on the velocity costate, which determines the switching functions. Furthermore, this velocity costate is a function of the initial costate vector. Therefore, if the initial costate vector can be calculated, the full solution for the optimal control is achieved. So, the objective of this chapter is to calculate this initial costate vector analytically, for a given initial and final state[1] and a fixed U_{max}.

The approach is to examine some simple cases to gain insight into this problem. The problem for no control switching case ($N = 0$)[2] is solved first; i.e., the initial control is held constant from $t = 0$ to $t = t_f$. Then the case of a single control switch ($N = 1$) is examined next, which is then followed by the case with two control switches ($N = 2$). This process is continued until the general solution is obtained.

4.1 Single Controlled Arc (No Switching: $N = 0$)

In this case, there is only one controlled arc with no control switch. The duration of active control for the $N = 0$ case must necessarily be less than π (canonical) units of time. Otherwise, the costate trajectory, which as half-period of π, will cross from lower half to upper half plane (or vice versa) and our bang-bang controller must switch controls.

[1]The initial state is considered specified, $\mathbf{x}_z(0) = [z_o \ \dot{z}_o]^T = \mathbf{x}_{zo}$. The desired final state is also specified, $\mathbf{x}_{zf} = [z_f \ \dot{z}_f]^T$ and is considered a constant vector.

[2]For N control switches, there are $N + 1$ controlled arcs.

Before proceeding, the target set must first be specified; i.e., the specific terminal constraint vector, $\mathbf{\Psi}$, must be addressed. $\mathbf{\Psi}$ determines the existence of a solution. The terminal state constraint $\mathbf{\Psi}_z(\mathbf{x}_z(t_f), t_f)$ for the out-of-plane problem can be expressed in terms of the desired final states, $(z_f, \dot{z}_f)$.

$$\mathbf{\Psi}_z(\mathbf{x}_z(t_f), t_f) = \mathbf{x}_z(t_f) - \mathbf{x}_{zf} = \begin{bmatrix} z(t_f) - z_f \\ \dot{z}(t_f) - \dot{z}_f \end{bmatrix} = \mathbf{0} \tag{4.1}$$

Notice that the constraints do not contain t_f explicitly; i.e., $\mathbf{\Psi}(\mathbf{x}_z(t_f), t_f) = \mathbf{\Psi}(\mathbf{x}_z(t_f))$. This eliminates the second term in Equation (2.15), leaving only the Hamiltonian as the transversality condition. Notice also that the number of constraints equals the number of states, $r_z = p_z = 2$, and the target set is a single point. Then, for the minimum-time maneuver to reach this point, the final state is assumed to lie along the controlled circular trajectory in the state phase space and within a π arc of the initial state. This is illustrated in Figure 4.1, where the solid dark circle is the initial orbit trajectory. The controlled trajectories marked by the '+' and '−' symbols forms the reachable set when the target set is a single point. The solution will exist only if the $\mathbf{x}_{zf}$ lie on either of these controlled trajectories. The solution space is very limited.

Instead, if only the final radius[3] is targeted, the terminal state constraint could be put in the form

$$\mathbf{\Psi}_z(\mathbf{x}_z(t_f)) = \mathbf{x}_z^T(t_f)\mathbf{x}_z(t_f) - \mathbf{x}_{zf}^T\mathbf{x}_{zf} = 0 \tag{4.2}$$

Notice this form also is not explicit in t_f. In this case, the reachable set is larger. In Figure 4.1, this larger reachable set is shown as the shaded ring around the origin. The inner radius is the closest approach to the origin and the outer radius is the farthest departure from the origin.

Then, for this analysis, Equation (4.2) is referenced as $\mathbf{\Psi}_z^I$ and Equation (4.1) is referenced as $\mathbf{\Psi}_z^{II}$, where the superscript denotes the number of final states being targeted.

[3] $R_z(t_f) = \sqrt{< \mathbf{x}_z(t_f), \mathbf{x}_z(t_f) >}$

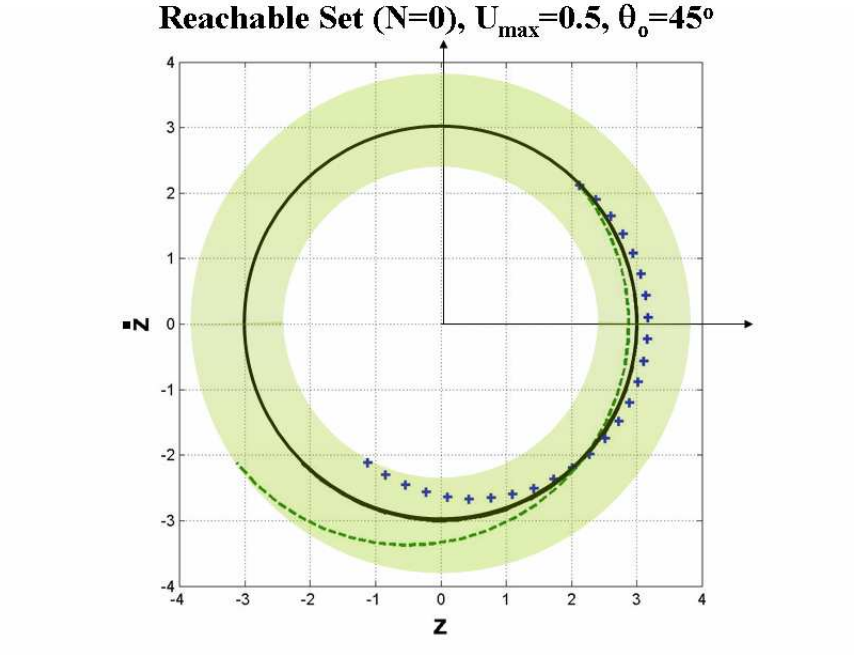

Figure 4.1 Reachable Region for (N=0).
The solid dark circle is the initial orbit trajectory for which the initial state vector, $\mathbf{x}_{zo}$ is located in the first quadrant. The controlled trajectories marked by the '+' and '−' symbols forms the reachable set when the target set is the desired final state, $\mathbf{x}_{zf}$. The shaded region is the reachable set when only the final radius is targeted.

The reachable set is also a function of the initial state, specifically, the initial phase angle, θ_o. In Figure 4.2, the reachable set is plotted for four different the $\mathbf{x}_{zo}$; one plot for each quadrant. The full range can be visualized by plotting the reachable range as a function of initial phase angle. In Figure 4.3, the reachable range in terms of the radius of the desired orbit is plotted for full range of θ_o for the case of $U_{max} = 0.5$ and $R_{zo} = 1.5$. Notice that the maximum range is located at θ_o of $\pi/2$ and $3\pi/2$. Also note that there are gaps in the region $R_{zo} \pm 2U_{max}$ where some of the states cannot be reached, even when only the final radius is targeted. The gaps can be filled only when the satellite is permitted to coast prior to initiating active control. The importance of a target set is very clear. It has direct affect on the reachable state and the existence of solution.

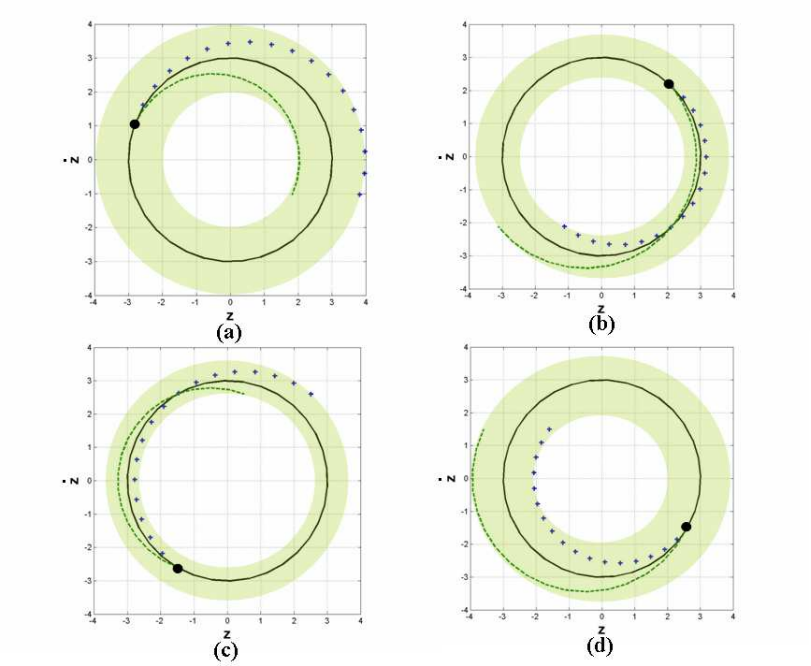

Figure 4.2 Reachable Region for (N=0).

Figure 4.2(a)-(d) illustrate the reachable set is a function of the initial state, specifically, θ_o. The initial state is represented by the dark circles.

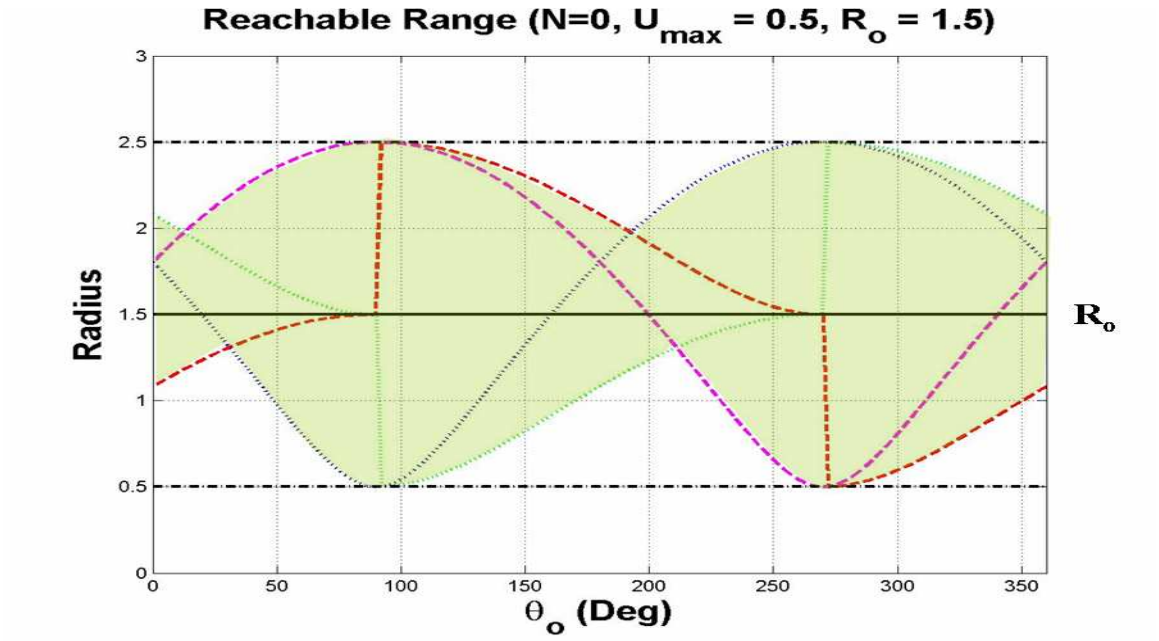

Figure 4.3 Reachable Range for (N=0).

Final Time Calculation

Three equations are needed for the three unknowns: t_f and the two initial costate vector pair. First the final time can be calculated by explicitly writing out the state solution at $t = t_f$. Since the optimal controller is constant, $\mathbf{B}_z u_z(\tau) = \mathbf{B}_z u_{zo}$ may be moved outside the integral in Equation (3.49), and the resulting solution was presented in Equation (3.50). Now, rearranging the solution at $t = t_f$, it becomes:

$$\begin{bmatrix} z_f - u_{zo} \\ \dot{z}_f \end{bmatrix} = \begin{bmatrix} z_o - u_{zo} & \dot{z}_o \\ \dot{z}_o & -(z_o - u_{zo}) \end{bmatrix} \begin{bmatrix} \cos(t_f) \\ \sin(t_f) \end{bmatrix} \tag{4.3}$$

However, the final time depends on which terminal state constraint is used. When using $\mathbf{\Psi}_z^I$, only the final trajectory (a new circle in the state phase space) is targeted (the specified final phase angle is not targeted):

$$\begin{aligned} R_{zf}^2 &= R_z(t_f)^2 = z^2(t_f) + \dot{z}^2(t_f) \\ R_{zf}^2 &= \left[(z_o - u_{zo})\cos(t_f) + \dot{z}_o \sin(t_f) + u_{zo}\right]^2 \\ &\quad + \left[(u_{zo} - z_o)\sin(t_f) + \dot{z}_o \cos(t_f)\right]^2 \\ R_{zf}^2 - R_{zo}^2 &+ 2u_{zo}(z_o - u_{zo}) = 2u_o(z_o - u_o)\cos(t_f) + 2\dot{z}_o u_{zo}\sin(t_f) \\ \frac{R_{zf}^2 - R_{zo}^2}{2u_{zo}(z_o - u_{zo})} &+ 1 = \cos(t_f) + \frac{\dot{z}_o}{(z_o - u_{zo})}\sin(t_f) \end{aligned} \tag{4.4}$$

By defining some intermediate constants, $c_1 = (R_{zf}^2 - R_{zo}^2)/(2u_{zo}(z_o - u_{zo})) + 1$ and $c_2 = \dot{z}_o/(z_o - u_{zo})$,

$$c_1 - \cos(t_f) = c_2 \sin(t_f) = \pm c_2 \sqrt{1 - \cos^2(t_f)} \tag{4.5}$$

This equation is quadratic in $\cos(t_f)$ and has an analytical solution of

$$\cos(t_f) = \frac{c_1 \pm c_2\sqrt{1 + c_2^2 - c_1^2}}{1 + c_2^2} \tag{4.6}$$

where the sign is chosen such that t_f is less than π. For a physically meaningful solution, the discriminant must be greater than zero for non-complex $\cos(t_f)$. After manipulating the discriminant, the inequality constraint that must be satisfied is

$$\left(R_{zf}^2 - z_o^2\right) - \frac{z_o}{u_{zo}}\left(R_{zf}^2 - R_{zo}^2\right) - \frac{\left(R_{zf}^2 - R_{zo}^2\right)^2}{4U_{max}^2} \geq 0 \tag{4.7}$$

Since a priori knowledge is not known for u_{zo}, Equation (4.6) must be solved twice, once for $u_{zo} = +U_{max}$ and once for $u_{zo} = -U_{max}$. The resulting final times may be labelled as t_f^+ and t_f^-, respectively, and the minimum time would be the smaller of the two; $t_f = min(t_f^+,\ t_f^-)$ which satisfies the state equation. This only gets the state on the same size orbit. To reach the desired point, the satellite coasts until the desired final phase is reached.

Another way to reach the desired point requires the terminal state constraint be in the form of Equation (4.1). Then to calculate the final time, Cramer's Rule is applied to directly to Equation (4.3) to obtain the expression for $\cos(t_f)$[4,5]:

$$\cos(t_f) = \frac{\dot{z}_o\dot{z}_f + (z_o - u_o)(z_f - u_o)}{(z_o - u_o)^2 + \dot{z}_o^2} \tag{4.8}$$

This must also be solved twice, once for $u_{zo} = +U_{max}$ and once for $u_{zo} = -U_{max}$. In this case, a solution may not exist because the target set is a single point in $\mathbb{R}^2$.

Final Velocity Costate and Hamiltonian

With one of three unknowns (final time) determined, two more equations are need to determine the initial costate vector. For the $N = 0$ case of no control switching, if $t_f = \pi$, the costate trajectory must lie entirely in the upper (or lower) half plane, and $\lambda_{\dot{z}o} = \lambda_{\dot{z}}(t_f) = 0$. Furthermore, the initial costate vector is unique. However, if $t_f < \pi$,

[4]The principle range of $\cos^{-1}(\cdot)$ is 0 to π, which has the proper range for $N = 0$ case where $t_f \leq \pi$.

[5]The other solution is $\sin(t_f) = \frac{\dot{z}_o(z_f - u_o) - \dot{z}_f(z_o - u_o)}{(z_o - u_o)^2 + \dot{z}_o^2}$. These equations can also be derived purely from geometry.

the resulting initial costate vector is not unique because there are an infinite number of arcs having arc length equal equal $t_f < \pi$ that are entirely in the upper half (or in the lower half plane). However, a unique solution is possible in part by forcing $\lambda_{\dot{z}}(t_f)$ to be zero; i.e., treating t_f as a control switching time. One of the two required equations is derived from the velocity costate Equation (3.14) at the final time:

$$\lambda_{\dot{z}}(t_f) = -\sin(t_f)\lambda_{zo} + \cos(t_f)\lambda_{\dot{z}o} = 0 \tag{4.9}$$

which is linear in the initial costate vector and will provide means to calculate the initial costate vector algebraically.

The final equation is now derived. As mentioned Section 2.5, optimal theory says that the Hamiltonian stays constant. Without much difficulty, this can be shown to be true[6]:

$$\begin{aligned}
H(t_f) &= 0 \\
1 &+ \boldsymbol{\lambda}^T(t_f)\left[\mathbf{A}\mathbf{x}(t_f) + \mathbf{B}\mathbf{u}(t_f)\right] = 0 \\
1 &+ \boldsymbol{\lambda}_o^T e^{-\mathbf{A}t_f}\mathbf{A}\left[e^{\mathbf{A}t_f}\mathbf{x}_o + \int_0^{t_f} e^{\mathbf{A}(t_f-\tau)}d\tau\mathbf{B}\mathbf{u}_o\right] + \boldsymbol{\lambda}_o^T e^{-\mathbf{A}t_f}\mathbf{B}\mathbf{u}_o = 0 \\
1 &+ \boldsymbol{\lambda}_o^T\mathbf{A}\mathbf{x}_o + \boldsymbol{\lambda}_o^T e^{-\mathbf{A}t_f}\mathbf{A}\int_0^{t_f} e^{\mathbf{A}(t_f-\tau)}d\tau\mathbf{B}\mathbf{u}_o + \boldsymbol{\lambda}_o^T e^{-\mathbf{A}t_f}\mathbf{B}\mathbf{u}_o = 0 \\
1 &+ \boldsymbol{\lambda}_o^T\mathbf{A}\mathbf{x}_o + \boldsymbol{\lambda}_o^T\mathbf{A}\int_0^{t_f} e^{-\mathbf{A}\tau}d\tau\mathbf{B}\mathbf{u}_o + \boldsymbol{\lambda}_o^T e^{-\mathbf{A}t_f}\mathbf{B}\mathbf{u}_o = 0 \\
1 &+ \boldsymbol{\lambda}_o^T\mathbf{A}\mathbf{x}_o + \boldsymbol{\lambda}_o^T\left[\mathbf{I} - e^{-\mathbf{A}t_f}\right]\mathbf{B}\mathbf{u}_o + \boldsymbol{\lambda}_o^T e^{-\mathbf{A}t_f}\mathbf{B}\mathbf{u}_o = 0 \\
1 &+ \boldsymbol{\lambda}_o^T\left[\mathbf{A}\mathbf{x}_o + \mathbf{B}\mathbf{u}_o\right] = 0
\end{aligned} \tag{4.10}$$

[6]This derivation is valid for both the out-of-plane system as well as the in-plane system. Hence the subscripts are omitted.

In addition, the product of $\mathbf{A}$ and $e^{-\mathbf{A}t}$ commute and was used in the derivation.[7] Writing this more explicitly, the third and final required equation is obtained:

$$\dot{z}_o\lambda_{zo} - (z_o - u_{zo})\lambda_{\dot{z}o} = -1 \tag{4.11}$$

Initial Costate Vector

Now, Equations (4.9) and (4.11) can be put in a 2x2 matrix form because both equations are linear the initial costate vector,

$$\begin{bmatrix} -\sin(t_f) & \cos(t_f) \\ \dot{z}_o & -(z_o - u_{zo}) \end{bmatrix} \begin{bmatrix} \lambda_{zo} \\ \lambda_{\dot{z}o} \end{bmatrix} = \begin{bmatrix} 0 \\ -1 \end{bmatrix} \tag{4.12}$$

The initial costate vector is

$$\lambda_{zo} = \begin{bmatrix} \lambda_{zo} \\ \lambda_{\dot{z}o} \end{bmatrix} = \begin{bmatrix} -\sin(t_f) & \cos(t_f) \\ \dot{z}_o & -(z_o - u_{zo}) \end{bmatrix}^{-1} \begin{bmatrix} 0 \\ -1 \end{bmatrix} \tag{4.13}$$

When the final time solution from either Equation (4.8) or (4.6) is substituted in, the initial costate vector become a non-linear function of the initial, final state, and U_{max}. For example, using Equation (4.8), the initial costate vector is

$$\lambda_{zo} = -\frac{\dot{z}_o\dot{z}_f + (z_o - u_{zo})(z_f - u_{zo})}{\dot{z}_f[(z_o - u_{zo})^2 + \dot{z}_o^2]} \tag{4.14}$$

$$\lambda_{\dot{z}o} = \frac{\dot{z}_f(z_o - u_{zo}) - \dot{z}_o(z_f - u_{zo})}{\dot{z}_f[(z_o - u_{zo})^2 + \dot{z}_o^2]} \tag{4.15}$$

Phasing with Single Arc

[7] This commutability is clear when the product is written out in the infinite series.

A very special phasing maneuver will also require a single arc.[8] The target trajectory is the same as the initial trajectory (R_{zf}=R_{zo}), but ahead or behind the original state. This phasing can only happen if the initial state (Point A in Figure 4.4) is in the first or the third quadrant; i.e., $z_o\dot{z}_o > 0$. Then the final state, which can be reached with

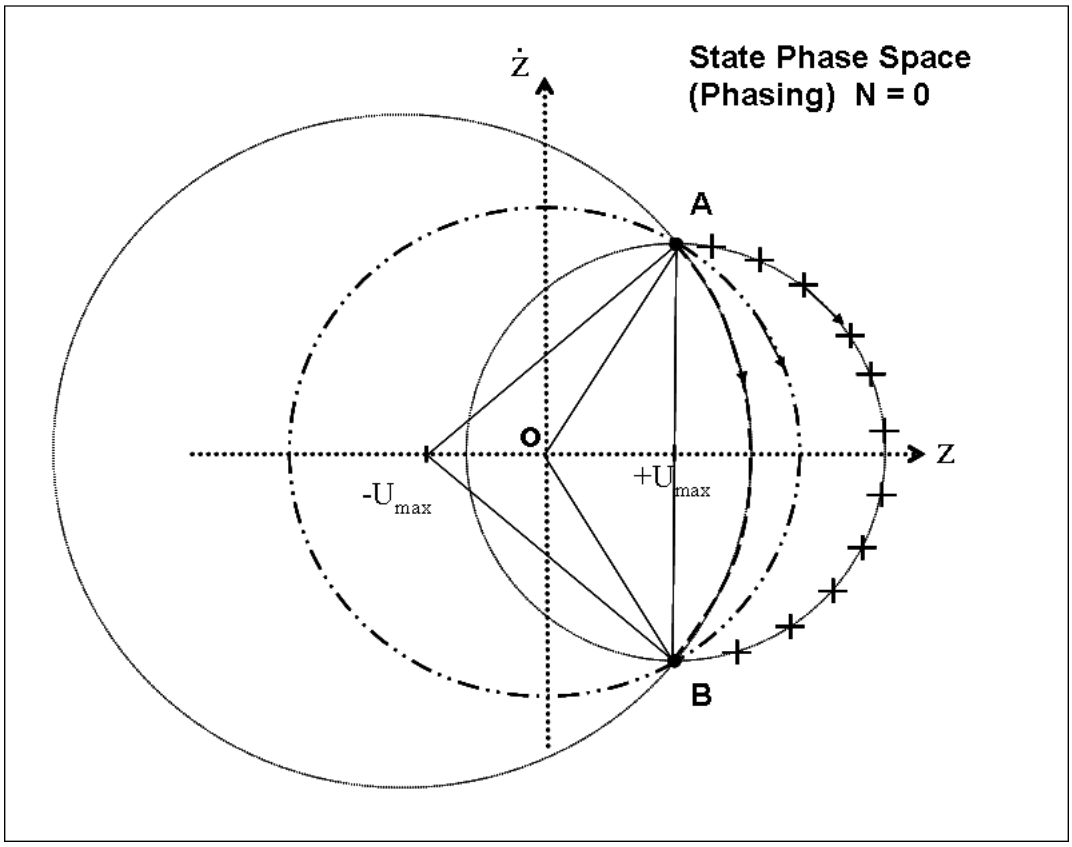

Figure 4.4 Phasing with single arc.

a single arc, is symmetric with respect to the z-axis, Point B in Figure 4.4:

$$\begin{aligned} z_f &= z_o \\ \dot{z}_f &= -\dot{z}_o \end{aligned} \tag{4.16}$$

[8]Less restrictive phasing is presented in Section 4.2 with $N = 1$.

Then it takes the original state on the initial orbit

$$t^o = \tan^{-1}\left(\frac{2z_o\dot{z}_o}{z_o^2+\dot{z}_o^2}\right) \tag{4.17}$$

amount of time (uncontrolled) to reach Point B; equivalent to the angle subtended by A-o-B. It takes

$$t^{\pm} = \tan^{-1}\left(\frac{2\dot{z}_o(z_o-u^{\pm})}{(z_o-u^{\pm})^2-\dot{z}_o^2}\right) \tag{4.18}$$

on the two controlled arcs, subtended angles A-$+U_{max}$-B and A-$-U_{max}$-B, respectively.[9] The amount of phasing that can be achieved with a single arc is

$$\begin{aligned}\Delta\phi^+ &= t^o - t^+ \\ \Delta\phi^- &= t^o - t^-\end{aligned} \tag{4.19}$$

In Figure (4.4) above, $t^- < t^o < t^+ = \pi$.

4.2 Two Arcs (One Switch: $N = 1$)

In this case, there are two controlled arcs with one control switch. For $N = 1$, the control switches once at $t = t_1$ with the control changing to $u_{z1} = -u_{zo}$, which means $\lambda_{\dot{z}}(t_1) = 0$. This situation can arise in three ways. The first way is when the target is the desired final state and R_{zf} is within R_{zo} $+2U_{max}$. The second way is when only the the final orbit radius is targeted and R_{zf} is outside R_{zo} $+2U_{max}$ but within R_{zo} $+4U_{max}$. The final way is when phasing is desired: R_{zf}=R_{zo}. In Figure 4.5, the reachable range is displayed as was done done earlier in Figure 4.3 for the $N = 0$ case. The darker shaded region is exactly the same as in Figure 4.3, and the lighter shaded region (in addition to the dark shaded region) is the reachable set for $N = 1$ when the target is the final orbit radius only. Notice how the lower bound is reflected by the $R_z = 0$. The origin can only

[9]The superscript $\pm$ corresponds to $+U_{max}$ or $-U_{max}$.

be reached at specific and isolated initial phases. Again, the gaps of unreachable states can be removed if initial coasting is permitted.

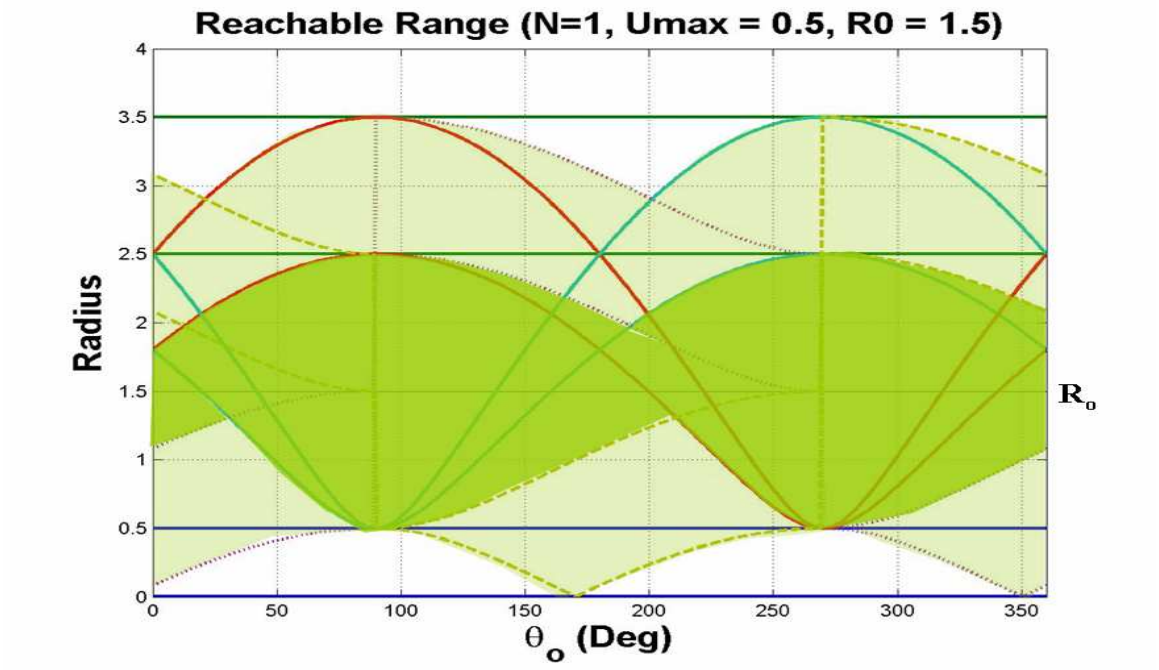

Figure 4.5 Reachable Range for (N=1).

Final Time Calculation

For $N = 1$, the final time calculation requires more steps due to the addition of t_1; the number of unknowns is now one more than for the $N = 0$ case. Instead of solving for t_f directly, t_f is broken into two parts corresponding to two controlled arcs: t_1 and $(t_f - t_1)$. The final time, t_f^*[10] is just the sum of t_1 and $(t_f - t_1)$, where each time interval is less than π:

$$t_f^* = t_1 + (t_f - t_1) \tag{4.20}$$

[10]The asterisk now represents the optimal (minimum-time) quantities.

First, the controlled state solution is written at $t = t_1$, the first control switch time:

$$\begin{bmatrix} z_1 - u_{zo} \\ \dot{z}_1 \end{bmatrix} = \begin{bmatrix} z_o - u_{zo} & \dot{z}_o \\ \dot{z}_o & -(z_o - u_{zo}) \end{bmatrix} \begin{bmatrix} \cos(t_1) \\ \sin(t_1) \end{bmatrix} \tag{4.21}$$

where the state at t_1 is not yet known. Applying the linear algebra as before, an expression for t_1 is obtained:

$$\sin(t_1) = \frac{\dot{z}_o(z_1 - u_{zo}) - \dot{z}_1(z_o - u_{zo})}{(z_o - u_{zo})^2 + \dot{z}_o^2} \tag{4.22}$$

$$\cos(t_1) = \frac{\dot{z}_o\dot{z}_1 + (z_o - u_{zo})(z_1 - u_{zo})}{(z_o - u_{zo})^2 + \dot{z}_o^2} \tag{4.23}$$

The cosine equation is used to calculate t_1 because the principle range of arc-cosine properly generates $t_1 \leq \pi$. Next, the final state, $\mathbf{x}_{zf}$, is related to the state at t_1, $\mathbf{x}_{z1}$, by

$$\begin{bmatrix} z_f - u_{z1} \\ \dot{z}_f \end{bmatrix} = \begin{bmatrix} z_1 - u_{z1} & \dot{z}_1 \\ \dot{z}_1 & -(z_1 - u_{z1}) \end{bmatrix} \begin{bmatrix} \cos(t_f - t_1) \\ \sin(t_f - t_1) \end{bmatrix} \tag{4.24}$$

and the resulting solution for $(t_f - t_1) \leq \pi$ is determined using the cosine equation:

$$\cos(t_f - t_1) = \frac{\dot{z}_1\dot{z}_f + (z_1 - u_{z1})(z_f - u_{z1})}{\dot{z}_f^2 + (z_f - u_{z1})^2} \tag{4.25}$$

By substituting $u_{z1} = -u_{zo}$,

$$\cos(t_f - t_1) = \frac{\dot{z}_1\dot{z}_f + (z_1 + u_{zo})(z_f + u_{zo})}{\dot{z}_f^2 + (z_f + u_{zo})^2} \tag{4.26}$$

becomes a function of $\mathbf{x}_{zo}$, $\mathbf{x}_{z1}$, $\mathbf{x}_{zf}$, and u_{zo}.

To solve for the state at t_1, $\mathbf{x}_{z1}$, the two controlled arcs are visualized in the state-phase space. $\mathbf{x}_{z1}$ is the intersection of these two controlled circular arcs. One is centered about u_{zo} starting at $\mathbf{x}_{zo}$, and the second centered about u_{z1}, terminating at $\mathbf{x}_{zf}$. In Figure 4.6 below, a numerical example is presented in which $\mathbf{x}_{zo}$ is in the first quadrant

and $\mathbf{x}_{zf}$ is in the third quadrant with $t_1 = 110^o$ and $(t_f - t_1) = 150^o$. To calculate $\mathbf{x}_{z1}$,

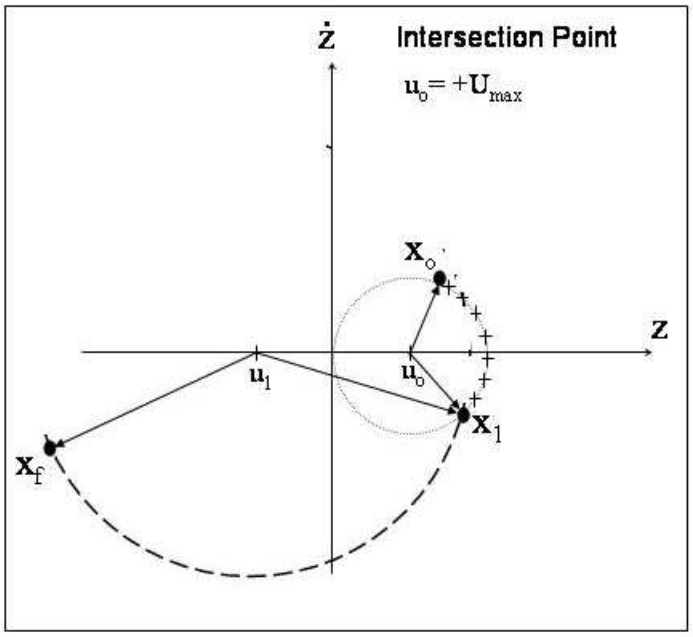

Figure 4.6 State trajectory for $N = 1$.

two expressions for the radius of the first arc (with the center at u_{zo}) expressed using both $\mathbf{x}_{z1}$ and $\mathbf{x}_{zo}$ are equated.

$$(z_1 - u_{zo})^2 + \dot{z}_1^2 = (z_o - u_{zo})^2 + \dot{z}_o^2 \tag{4.27}$$

Next, two expressions for the radius of the second arc (with the center at u_{z1}), expressed using both $\mathbf{x}_{z1}$ and $\mathbf{x}_{zf}$, are also equated.

$$(z_1 - u_{z1})^2 + \dot{z}_1^2 = (z_f - u_{z1})^2 + \dot{z}_f^2 \tag{4.28}$$

Performing some algebraic reduction and solving for z_1 and $\dot{z}_1$,

$$\begin{aligned} z_1 &= \frac{R_f^2 - R_o^2}{4u_{zo}} + \frac{z_o + z_f}{2} && (4.29) \\ \dot{z}_1^2 &= (z_o - u_{zo})^2 + \dot{z}_o^2 - (z_1 - u_{zo})^2 \\ &= (z_f + u_{zo})^2 + \dot{z}_f^2 - (z_1 + u_{zo})^2 && (4.30) \end{aligned}$$

where the correct sign on $\dot{z}_1$ is determined by the initial state since the trajectory can only travel in one direction: clockwise and with $t_1 < \pi$; a quadrant check is required. Now Equations (4.23) and (4.20) are no longer dependent on $\mathbf{x}_{z1}$. They are strictly functions of $\mathbf{x}_{zo}$, $\mathbf{x}_{zf}$, and u_{zo}.

For the case of targeting anywhere on the final orbit (R_{zf}=R_{zo}), the minimum-time solution is achieved by switching when $\dot{z}(t_1) = 0$. Maximum change in radius occurs when the velocity is zero; i.e., $dR_z(t)/dt = 0$. When $\dot{z}_o < 0$, application of positive control increases the radius at the maximum rate and the reverse is also true. So, $u_{zo} = sign\{\dot{z}_o\}U_{max}$. This means the state at t_1 is:

$$\begin{aligned} z_1 &= sign\{\dot{z}_o\}\left[\sqrt{(z_o - u_{zo})^2 + \dot{z}_o^2} + U_{max}\right] && (4.31) \\ \dot{z}_1 &= 0 && (4.32) \end{aligned}$$

for which t_1 can be easily derived using the state solution:

$$\begin{bmatrix} z_1 - u_{zo} \\ 0 \end{bmatrix} = \begin{bmatrix} z_o - u_{zo} & \dot{z}_o \\ \dot{z}_o & -(z_o - u_{zo}) \end{bmatrix} \begin{bmatrix} \cos(t_1) \\ \sin(t_1) \end{bmatrix} \quad (4.33)$$

can be solved for $\cos(t_1)$ using Cramer's rule,

$$\cos(t_1) = \frac{(z_o - u_{zo})(z_1 - u_{zo})}{\dot{z}_o^2 + (z_o - u_{zo})^2} \quad (4.34)$$

Next, another intersection point needs to be calculated. One arc is centered about u_{z1} starting at $\mathbf{x}_{z1}$ and the second arc is centered about the origin (due to coasting)

terminating at the desired final state. Using the same approach of equating radii:

$$\begin{aligned}(z_1 - u_{z1})^2 + \dot{z}_1^2 &= (z_2 - u_{z1})^2 + \dot{z}_2^2 \\ z_2^2 + \dot{z}_2^2 &= z_f^2 + \dot{z}_f^2 = R_{zf}^2 \end{aligned} \tag{4.35}$$

Performing some algebraic reduction and solving for z_2 and $\dot{z}_2$,

$$z_2 = \frac{R_{z1}^2 - R_{zf}^2}{2u_{zo}} + z_1 \tag{4.36}$$

$$\dot{z}_2^2 = R_{zf}^2 - z_2^2 \tag{4.37}$$

Then, the state at t_2, $\mathbf{x}_{z2}$, is used to determine $(t_2 - t_1)$ as was done in Equation (4.26) for $(t_f - t_1)$.

$$\cos(t_2 - t_1) = \frac{\dot{z}_1\dot{z}_2 + (z_1 + u_{zo})(z_2 + u_{zo})}{\dot{z}_2^2 + (z_2 + u_{zo})^2} \tag{4.38}$$

Finally, $(t_f - t_2)$ is the amount of coasting (uncontrolled arc) time to achieve the desired final state:

$$\cos(t_f - t_2) = \frac{z_2 z_f + \dot{z}_2\dot{z}_f}{z_2^2 + \dot{z}_2^2} \tag{4.39}$$

The total final time for the case of targeting the final orbit with terminal cruise is then the sum of two controlled arcs and one uncontrolled arc.

$$t_f^* = t_1 + (t_2 - t_1) + (t_f - t_2) \tag{4.40}$$

Costate at $t = t_1$ and Hamiltonian

The velocity costate Equation (3.14) at the $t = t_1$ is used to obtain one of two equations required to solve for the initial costate vector:

$$\lambda_{\dot{z}}(t_1) = -\sin(t_1)\lambda_{zo} + \cos(t_1)\lambda_{\dot{z}o} = 0 \tag{4.41}$$

The Hamiltonian condition is used again for the final required equation. The details are longer than the $N = 0$ case, but still straightforward:

$$1 + \boldsymbol{\lambda}_o^T \left[\mathbf{A}_z \mathbf{x}_{zo} + \mathbf{B}_z \mathbf{u}_o - 2e^{-\mathbf{A}_z t_1} \mathbf{B}_z u_{zo} \right] = 0 \tag{4.42}$$

where the last term can be simplified with the knowledge of $\lambda_{\dot{z}}(t_1) = 0$:

$$\begin{aligned} -2\boldsymbol{\lambda}_o^T e^{-\mathbf{A}_z t_1} \mathbf{B}_z u_{zo} &= -2 \left[e^{-\mathbf{A}_z^T t_1} \boldsymbol{\lambda}_o \right]^T \mathbf{B}_z u_{zo} \\ &= -2 \left[\boldsymbol{\lambda}^T(t_1) \mathbf{B}_z \right] u_{zo} \\ &= -2\lambda_{\dot{z}}(t_1) u_{zo} = -2 \cdot 0 \cdot u_{zo} = 0 \end{aligned} \tag{4.43}$$

Therefore, the Hamiltonian condition is identical to Equation (4.11).

Initial Costate Vector

Now, Equations (4.41) and (4.11) can be put into a 2x2 matrix form because both equations are linear with respect to the initial costate vector:

$$\begin{bmatrix} -\sin(t_1) & \cos(t_1) \\ \dot{z}_o & -(z_o - u_{zo}) \end{bmatrix} \begin{bmatrix} \lambda_{zo} \\ \lambda_{\dot{z}o} \end{bmatrix} = \begin{bmatrix} 0 \\ -1 \end{bmatrix} \tag{4.44}$$

The initial costate vector is

$$\boldsymbol{\lambda}_o = \begin{bmatrix} \lambda_{zo} \\ \lambda_{\dot{z}o} \end{bmatrix} = \begin{bmatrix} -\sin(t_1) & \cos(t_1) \\ \dot{z}_o & -(z_o - u_{zo}) \end{bmatrix}^{-1} \begin{bmatrix} 0 \\ -1 \end{bmatrix} \tag{4.45}$$

which has the same form as the solution for $N = 0$ case. See Equation (4.13).

Phasing with Two Controlled Arcs

When the phasing provided by Equation (4.19) using a single arc is insufficient, two arcs may be used to obtain a different amount of phasing. In this scenario, the terminal

state is not symmetric as it was for the $N = 0$ phasing. In Figure 4.7 below, a phasing maneuver with two arcs is presented in the state-phase space in which the initial state is at $\mathbf{x}_{zo} = (1, 1)$ (Point 'A') and the final state at $\mathbf{x}_{zf} = (-\sqrt{2}, 0)$ (Point1'C') is on the same orbit. First, the controlled satellite moves from Point 'A' ($\phi = 45^o$) to Point 'B', along an arc centered about Point 'm', using $u_{zo} = -U_{max} = -0.5$ for 114.34^o. Then, the control switches to $u_{z1} = +0.5$ bringing the satellite along an arc centered about Point 'p' to Point 'C' ($\phi = 270^o$), for a duration of 68.32^o. During the total maneuvering time of 182.66^o, the original satellite would have moved to Point 'D' ($\phi = 227.66^o$ on the original orbit. The resulting total phasing ($\Delta\phi = 42.34^o$) is the angle subtended by D-O-C.[11]

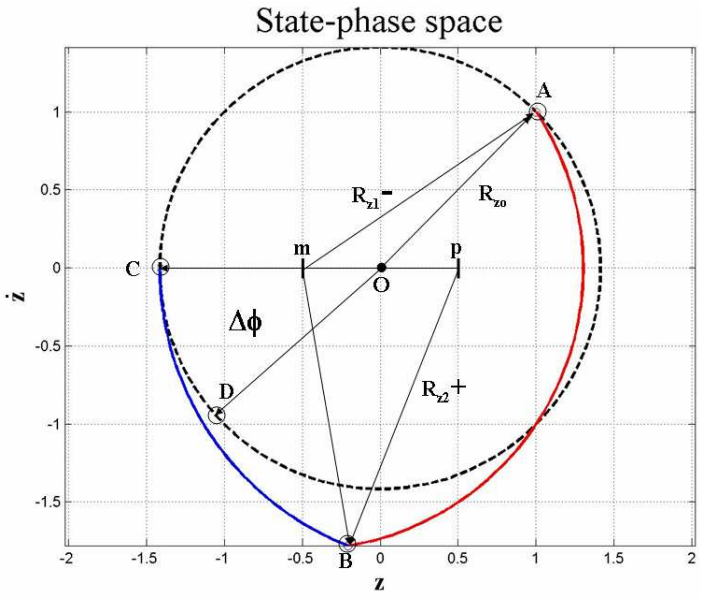

Figure 4.7 Out-of-plane phasing maneuver with two arcs ($N = 1$).

4.3 Three Arcs (Two Switches: $N = 2$)

This situation can arise in two ways. The first way is when the target is the desired final state and R_{zf} is within $R_{zo} + 4U_{max}$. The second way is when only the the final

[11] Recall, angles are equivalent to canonical time. All ϕ's are with respect to Point 'O' on the original orbit.

orbit radius is targeted and R_{zf} is outside R_{zo} $+4U_{max}$ but within R_{zo} $+6U_{max}$.[12] For $N = 2$, the control switches twice. The first control switch is at $t = t_1$ with the control changing to $u_{z1} = -u_{zo}$, which means $\lambda_{\dot{z}}(t_1) = 0$. The second control switch occurs at $t = t_2$ with the control changing to $u_{z2} = -u_{z1} = u_{zo}$, which means $\lambda_{\dot{z}}(t_2) = 0$. With the addition of t_2, the number of unknowns is now one more than for the $N = 1$ case.

The second controlled arc from t_1 to t_2 must necessarily last for π (canonical) units of time.[13] This means that the state at t_2, $\mathbf{x}_{z2}$, can be easily related to the state at t_1, $\mathbf{x}_{z1}$, by the appropriate use of Equation (3.50) with $t = t_2 - t_1 = \pi$:

$$\begin{bmatrix} z(t_2) \\ \dot{z}(t_2) \end{bmatrix} = \begin{bmatrix} -1 & 0 \\ 0 & -1 \end{bmatrix} \begin{bmatrix} z_1 \\ \dot{z}_1 \end{bmatrix} + \begin{bmatrix} 2 \\ 0 \end{bmatrix} u_{z1} = \begin{bmatrix} z_2 \\ \dot{z}_2 \end{bmatrix} \tag{4.46}$$

and using $u_{z1} = -u_{zo}$,

$$\mathbf{x}_{z2} = \begin{bmatrix} z_2 \\ \dot{z}_2 \end{bmatrix} = \begin{bmatrix} -z_1 - 2u_{zo} \\ -\dot{z}_1 \end{bmatrix} \tag{4.47}$$

Equation (4.21) is still valid and results in the same solution for the first control switch time, t_1, as in Equation (4.23). This time, the final state is a function of the state at $t_2 = t_1 + \pi$,

$$\begin{bmatrix} z_f - u_{z2} \\ \dot{z}_f \end{bmatrix} = \begin{bmatrix} z_2 - u_{z2} & \dot{z}_2 \\ \dot{z}_2 & -(z_2 - u_{z2}) \end{bmatrix} \begin{bmatrix} \cos(t_f - t_2) \\ \sin(t_f - t_2) \end{bmatrix} \tag{4.48}$$

From Equation (4.47), $z_2 - u_{z2} = -(z_1 + 3u_{zo})$ and $\dot{z}_2 = -\dot{z}_1$ using $u_{z2} = u_{zo}$. Substituting these into the above equation yields:

$$\begin{bmatrix} z_f - u_{zo} \\ \dot{z}_f \end{bmatrix} = \begin{bmatrix} -(z_1 + 3u_{zo}) & -\dot{z}_1 \\ -\dot{z}_1 & z_1 + 3u_{zo} \end{bmatrix} \begin{bmatrix} \cos(t_f - t_2) \\ \sin(t_f - t_2) \end{bmatrix} \tag{4.49}$$

[12] There will be gaps in the reachable region unless initial coasting is permitted.

[13] This is the reason that phasing maneuver (R_{zf}=R_{zo}) is not be optimal (minimum time) with $N > 1$ and is not considered in this or future sections.

Solving for $t_f - t_2$,

$$\cos(t_f - t_2) = \frac{\dot{z}_1 \dot{z}_f + (z_1 + 3u_{zo})(z_f - u_{zo})}{\dot{z}_1^2 + (z_1 + 3u_{zo})^2} \tag{4.50}$$

The final time, t_f is just

$$\begin{aligned} t_f^* &= t_1 + (t_2 - t_1) + (t_f - t_2) \\ &= t_1 + \pi + (t_f - t_2) \end{aligned} \tag{4.51}$$

Again the state at t_1 must be calculated. This time $\mathbf{x}_{z1}$ is determined by looking for two intersections of three controlled arcs where the middle arc is a half-circle centered about u_{z1}. The first and third arcs are centered about u_{zo} as in Figure 4.8 below.

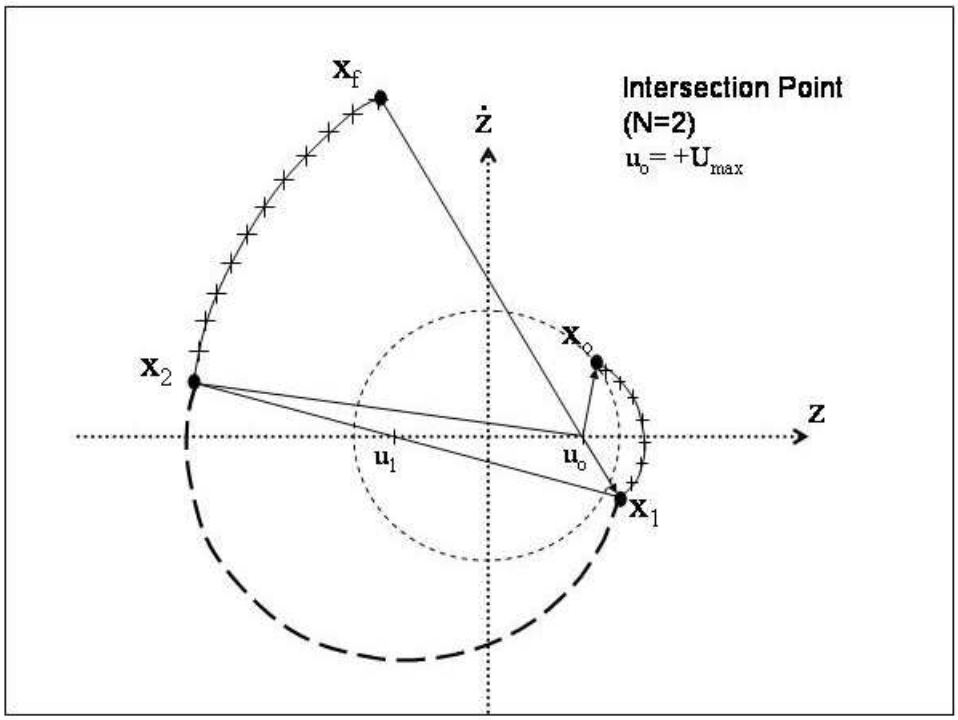

Figure 4.8 State trajectory for $N = 2$.

Equating the expressions for the appropriate radii, these two equations:

$$(z_1 - u_{zo})^2 + \dot{z}_1^2 = (z_o - u_{zo})^2 + \dot{z}_o^2 \tag{4.52}$$

$$(z_2 - u_{z2})^2 + \dot{z}_2^2 = (z_f - u_{z2})^2 + \dot{z}_f^2 \tag{4.53}$$

must be solved for z_1 and $\dot{z}_1$. Substituting the state at t_2 by Equation (4.47) and $u_{z2} = u_{zo}$,

$$(z_1 - u_{zo})^2 + \dot{z}_1^2 = (z_o - u_{zo})^2 + \dot{z}_o^2 \tag{4.54}$$

$$(-z_1 - 3u_{zo})^2 + (-\dot{z}_1)^2 = (z_f - u_{zo})^2 + \dot{z}_f^2 \tag{4.55}$$

The solution to these two equations for z_1 and $\dot{z}_1$ is:

$$z_1 = \frac{R_f^2 - R_o^2}{8u_{zo}} + \frac{z_o - z_f}{4} - u_{zo} \tag{4.56}$$

$$\begin{aligned} \dot{z}_1^2 &= (z_o - u_{zo})^2 + \dot{z}_o^2 - (z_1 - u_{zo})^2 \\ &= (z_f - u_{zo})^2 + \dot{z}_f^2 - (z_1 + 3u_{zo})^2 \end{aligned} \tag{4.57}$$

where the correct sign on $\dot{z}_1$ must again be determined by the initial state since the trajectory can only travel clockwise on the state phase space.

For targeting anywhere on the final orbit, a minimum-time solution requires that the first control switch occur when $\dot{z}(t_1) = 0$, which means π unit of time later $\dot{z}(t_2) = -\dot{z}(t_1) = 0$ and $z(t_2) = -z(t_1) + 2u_{z1}$:

$$z_1 = sign\{\dot{z}_o\}\left[\sqrt{(z_o - u_{zo})^2 + \dot{z}_o^2} + U_{max}\right] \tag{4.58}$$

$$z_2 = -sign\{\dot{z}_o\}\left[\sqrt{(z_o - u_{zo})^2 + \dot{z}_o^2} + U_{max}\right] - 2u_{zo} \tag{4.59}$$

$$\dot{z}_1 = 0 = \dot{z}_2 \tag{4.60}$$

The first switch time, t_1, can again be easily calculated using Equation (4.34). Another intersection point must be calculated to determine the time interval of the last controlled

arc. This time, the intersection is between the last controlled arc and the final orbit. Labelling this intersection point $\mathbf{x}_{z3}$, $(t_3 - t_2)$ can be calculated as was done in Equation (4.38). Then $(t_f - t_3)$ will simply be the coasting time to reach the desired final state, similarly provided in Equation (4.40).

Velocity Costate at t_1 and Hamiltonian

Equation (4.41) is still valid. It is also possible to use the velocity costate equation at t_2,

$$\lambda_{\dot{z}}(t_2) = \lambda_{zo}\sin(t_2) - \lambda_{\dot{z}o}\cos(t_2) = 0 \tag{4.61}$$

The Hamiltonian condition for this $N = 2$ case is

$$\begin{aligned} 1 \;+\; & \boldsymbol{\lambda}_o^T \left[\mathbf{A}_z\mathbf{x}_{zo} + \mathbf{B}_z u_{zo} - 2e^{-\mathbf{A}_z t_1}\mathbf{B}_z u_{zo} + 2e^{-\mathbf{A}_z t_2}\mathbf{B}_z u_{zo}\right] = 0 \\ 1 \;+\; & \boldsymbol{\lambda}_o^T \left[\mathbf{A}_z\mathbf{x}_{zo} + \mathbf{B}_z u_{zo} - 4e^{-\mathbf{A}_z t_1}\mathbf{B}_z u_{zo}\right] = 0 \end{aligned} \tag{4.62}$$

since $t_2 = t_1 + \pi$, $e^{-\mathbf{A}_z t_2} = e^{-\mathbf{A}_z(t_1+\pi)} = e^{-\mathbf{A}_z t_1}e^{-\mathbf{A}_z \pi} = -e^{-\mathbf{A}_z t_1}$. However, as it was in the $N = 1$ case, $\boldsymbol{\lambda}_o^T e^{-\mathbf{A}_z t_1}\mathbf{B}_z = 0$. Thus, the Hamiltonian condition remains the same as in Equation (4.11).

The initial costate vector is also the same when (4.41) is used as Equation (4.45). Or with (4.61), the initial costate vector becomes:

$$\lambda_{zo} = \begin{bmatrix} \lambda_{zo} \\ \lambda_{\dot{z}o} \end{bmatrix} = \begin{bmatrix} -\sin(t_2) & \cos(t_2) \\ \dot{z}_o & -(z_o - u_{zo}) \end{bmatrix}^{-1} \begin{bmatrix} 0 \\ -1 \end{bmatrix} \tag{4.63}$$

which has the same form as the solution for $N = 0$ case. See Equation (4.13).

4.4 General Case (N Switches)

The trend that is generated in the analysis is that N switchings of controls will be required in one of two ways. The first is when the target is the desired final state

and R_{zf} is within $R_{zo} + 2NU_{max}$. The second is when only the the final orbit radius is targeted and R_{zf} is outside $R_{zo} + 2NU_{max}$, but within $R_{zo} + 2(N+1)U_{max}$. There are $N+1$ controlled arcs, where all the arcs, except the first and the last, must necessarily be π arc lengths:

$$\begin{aligned} t_1 &< \pi \\ t_2 - t_1 &= \pi \\ &\cdot \\ &\cdot \\ &\cdot \\ t_N - t_{N-1} &= \pi \\ t_f - t_N &< \pi \end{aligned} \tag{4.64}$$

and the optimal control switches signs back and forth from $+U_{max}$ to $-U_{max}$ and in general for the k^{th} arc, $u_{zk} = (-1)^k u_{zo}$ where u_{zo} is the initial control arc. Therefore, two time intervals are the only unknowns: the first and the last. The first time interval is the first switching time, t_1, and the last time interval is $t_f - t_N$.

Final Time Calculations

In order to calculate the two critical time intervals, the state at t_1 must always be calculated. $\mathbf{x}_{z1}$ is obtained by examining two specific intersections. When the final state is targeted, the first intersection is between the first and second controlled arcs. The second intersection of interest is between the N^{th} arc and the final arc. All the arcs except the first and the last arcs are half-circles centered alternatingly about u_{z1} and u_{zo}. The first and final arcs are centered about u_{zo} and u_{zN}. After equating the two expressions for the radii, the following two equations can be solved for z_1 and $\dot{z}_1$:

$$(z_1 - u_{zo})^2 + \dot{z}_1^2 = (z_o - u_{zo})^2 + \dot{z}_o^2 \tag{4.65a}$$

$$(z_N - u_{zN})^2 + \dot{z}_N^2 = (z_f - u_{zN})^2 + \dot{z}_f^2 \tag{4.65b}$$

where the state at t_N is a function of the state at t_1. For the kth state,

$$\begin{bmatrix} z_k \\ \dot{z}_k \end{bmatrix} = \begin{bmatrix} (-1)^{k-1} z_1 + 2(-1)^{k-1} u_{zo} \\ (-1)^{k-1} \dot{z}_1 \end{bmatrix} \tag{4.66}$$

and for the Nth state,

$$\begin{bmatrix} z_N \\ \dot{z}_N \end{bmatrix} = \begin{bmatrix} (-1)^{N-1} z_1 + 2(-1)^{N-1} (N-1) u_{zo} \\ (-1)^{N-1} \dot{z}_1 \end{bmatrix} \tag{4.67}$$

Now Equations (4.65a) and (4.65b) can be solved for the state at t_1, $\mathbf{x}_{z1}$, the components of which are required values to solve for t_1 in Equation (4.23):

$$z_1 = \frac{R_f^2 - R_o^2}{4N u_{zo}} + \frac{z_o - (-1)^N z_f}{2N} - (N-1) u_{zo} \tag{4.68}$$

$$\begin{aligned} \dot{z}_1^2 &= (z_o - u_{zo})^2 + \dot{z}_o^2 - (z_1 - u_{zo})^2 \\ &= [z_f - (-1)^N u_{zo}]^2 + \dot{z}_f^2 - [z_1 + (2N-1) u_{zo}]^2 \end{aligned} \tag{4.69}$$

where the sign of $\dot{z}_1$ must be tested based on initial state and u_{zo}.

The final time interval is solved using

$$\begin{bmatrix} z_f - u_{zN} \\ \dot{z}_f \end{bmatrix} = \begin{bmatrix} z_N - u_{zN} & \dot{z}_N \\ \dot{z}_N & -(z_N - u_{zN}) \end{bmatrix} \begin{bmatrix} \cos(t_f - t_N) \\ \sin(t_f - t_N) \end{bmatrix} \tag{4.70}$$

with $u_{zN} = (-1)^N u_{zo}$. Solving for $t_f - t_N$ with z_N given by Equation (4.67),

$$\cos(t_f - t_N) = \frac{\dot{z}_1 \dot{z}_f + [z_1 + (2N-1) u_{zo}][z_f - (-1)^N u_{zo}]}{\dot{z}_N^2 + (z_N + u_{zN})^2} \tag{4.71}$$

The final time, t_f^*, is then

$$t_f^* = t_1 + (N-1)\pi + (t_f - t_N) \tag{4.72}$$

For the case of targeting the final radius (R_{zf}=R_{zo}), $\mathbf{x}_{z1}$ and t_1 are provided by Equations (4.31) and (4.34), in which the velocity state at all intermediate switching times is zero. Furthermore, an additional intersection point between the last controlled arc and the final orbit must be determined as was done for $N = 1$. Labelling this intersection point $\mathbf{x}_{zN+1}$, the final controlled time interval $(t_{N+1} - t_N)$ is calculated as was done in Equation (4.38) for $N = 1$ case. Next, the cruising time interval, $(t_f - t_{N+1})$, is calculated as was done in Equation (4.40) for $N = 1$. Finally, the total final time has the same express as in Equation (4.72) with an additional coasting time required to reach the desired final state:

$$t_f^* = t_1 + (N-1)\pi + (t_{N+1} - t_N) + (t_f - t_{N+1}) \tag{4.73}$$

Velocity Costate at t_1 and Hamiltonian

At each control switch time, the velocity costate must be zero; $\lambda_{\dot{z}}(t_k) = 0 \forall\ k \in \{1, 2, ..., N\}$. The Hamiltonian remains constant and zero:

$$\begin{aligned}
1 \quad &+ \quad \boldsymbol{\lambda}_o^T \left[\mathbf{A}_z \mathbf{x}_{zo} + \mathbf{B}_z u_{zo} + 2 \left(\sum_{i=1}^{i=N} (-1)^i e^{-\mathbf{A}_z t_i} \right) \mathbf{B}_z u_{zo} \right] = 0 \\
1 \quad &+ \quad \boldsymbol{\lambda}_o^T \left[\mathbf{A}_z \mathbf{x}_{zo} + \mathbf{B}_z u_{zo} \right] - 2N \boldsymbol{\lambda}_o^T e^{-\mathbf{A}_z t_1} \mathbf{B}_z u_{zo} = 0 \\
1 \quad &+ \quad \boldsymbol{\lambda}_o^T \left[\mathbf{A}_z \mathbf{x}_{zo} + \mathbf{B}_z u_{zo} \right] = 0
\end{aligned} \tag{4.74}$$

since $\boldsymbol{\lambda}_o^T e^{-\mathbf{A}_z t_1} \mathbf{B}_z = 0$. This validates the constancy of the Hamiltonian required in the optimization theory. Using Equation (4.41) and (4.11), the initial costate vector is provided by Equation (4.45) for all $N \geq 1$.

The total fuel usage, in the canonical units[14], is simply[15]

$$\Delta V = t_f^* U_{max} \tag{4.75}$$

since, for a bang-bang controller, the controls are on from $t = 0$ to $t = t_f$.

4.5 General Algorithm

Many equations were presented in this Chapter. The general algorithm for the out-of-plane minimum time control is now summarized. The initial state, final desired state, as well as the maximum allowable acceleration are assumed as given and fixed.

1. Calculate R_{zo} and R_{zf}:

$$R_{zo} = ||\mathbf{x}_{zo}|| = \sqrt{< \mathbf{x}_{zo}^T, \mathbf{x}_{zo} >} \tag{4.76}$$

$$R_{zf} = ||\mathbf{x}_{zf}|| = \sqrt{< \mathbf{x}_{zf}^T, \mathbf{x}_{zf} >} \tag{4.77}$$

   If $R_{zf} = R_{zo}$, then a phasing maneuver is requested. Furthermore, if $\dot{z}_f = -\dot{z}_o$, then $N = 0$, else $N = 1$.

2. For a non-phasing maneuver, determine the optimal starting N for the given initial and final state via

$$N = \left\lfloor \left| \frac{R_{zf} - R_{zo}}{2U_{max}} \right| \right\rfloor \tag{4.78}$$

   where $\lfloor \cdot \rfloor$ is the floor operator which rounds the argument down to the nearest integer. As was presented in Figure 4.5, there is an overlap of reachable range for consecutive numbers of switchings, so, Equation (4.78) only serves as the starting point.

[14] The times are normalized by the orbital period of the reference orbit. The accelerations are normalized by $\sqrt{\frac{\mu_\oplus}{R_o}}$. The velocities are normalized by the uniform speed of the circular reference orbit.

[15] For the case of targeting the final orbit radius only, the coasting time interval is subtracted first before multiplying by U_{max}.

3. Guess the initial control, u_{zo}. If $R_{zf} > R_{zo}$, use

$$u_{zo} = sign\{\dot{z}_o\}U_{max} \tag{4.79}$$

4. Solve for the state at the first control switch (if $N > 0$). $\mathbf{x}_{z1}$ is found by using Equation (4.68). Then use Equation (4.23) to calculate t_1 using both the positive and negative roots of $\dot{z}_1$. Determine the correct t_1 by propagating the initial costate from $t = 0$ to t_1. Only one of the roots will be correct; choose the correct $\dot{z}_1$ and t_1.
5. Determine the final controlled time interval using Equation (4.71). Then determine the total final time by Equation (4.72).
6. Propagate the initial state using the control switching times and the corresponding controls to verify the calculated final state is the desired final state. If the calculated final state does not agree with the desired final state, repeat previous steps with the same N, but opposite u_{zo}.
7. If both $u_{zo} = +U_{max}$ and $u_{zo} = -U_{max}$ lead to no solution when both the R_{zf} and ϕ_f are targeted, repeat previous steps after incrementing N by one, up to maximum of two. If N becomes too large, the initial assumption of short duration may be violated, making the C-W dynamics less accurate.
8. If the solution is not achieved, then require only that R_{zf} be met; i.e., increase the solution space. Repeat previous steps using Equations appropriate for targeting final orbit radius.

4.6 Out-of-Plane Numerical Example

The above analytical results were numerically simulated using MATLAB®. For the simulation, the maximum net relative acceleration was $U_{max} = 0.25$, the initial state was $\mathbf{x}_{zo}= \begin{bmatrix} 1.0 & 1.0 \end{bmatrix}^T$ and the desired final state was chosen arbitrarily to generate a large N; $\mathbf{x}_{zf}= \begin{bmatrix} -3.0 & 3.0 \end{bmatrix}^T$. Following the algorithm above:

Step 1. $R_{zo} = \sqrt{2}$ and $R_{zf} = \sqrt{18}$. The target radius is larger that the initial orbit, thus it is not a phasing maneuver.

Step 2.

$$N = \left\lfloor \frac{|R_{zf} - R_{zo}|}{2U_{max}} \right\rfloor = 5 \tag{4.80}$$

Using $N = 5$ did not produce the proper solution for either initial control. Therefore, N was incremented by one until a solution was found; the optimal N, for this example was 7.

Step 3. $u_{zo} = sign\{\dot{z}_o\}U_{max} = +0.25$ did not produce the correct solution. For $N = 7$ u_{zo} $= -U_{max} = -0.25$.

Step 4. The correct state at the first control switch using $N = 7$ and $u_{zo}= -0.25$ produced $\mathbf{x}_{z1} = \begin{bmatrix} -0.93 & -1.45 \end{bmatrix}^T$ and $t_1 = 2.683$ radians in canonical units of time.

Step 5. The final controlled time interval was $(t_f - t_N) = 1.0793$ radians for $N = 7$ and $u_{zo}= -0.25$.

Step 6. Total final time was $t_f = 22.6122$ radians, which translates to approximately 3.6 times the reference orbital period. This length of time should keep the C-W dynamics within the linearized region.

In Figure 4.9, the state trajectory is plotted where the solid circles are the switching points. Notice how the trajectory spirals outward and how, at each control switch point, the velocities are one of two values, forming two horizontal lines. In Figure 4.10, the costate trajectory is plotted in the costate-phase space. Little information is obtained from this plot. However, the velocity costate is plotted (dashed curve) along with the optimal control (solid curve) in Figure 4.11. The optimality is confirmed by plotting the time history of the Hamiltonian. See Figure 4.12 and note the y-scale; i.e., Hamiltonian remains zero from $t = 0$ to t_f.

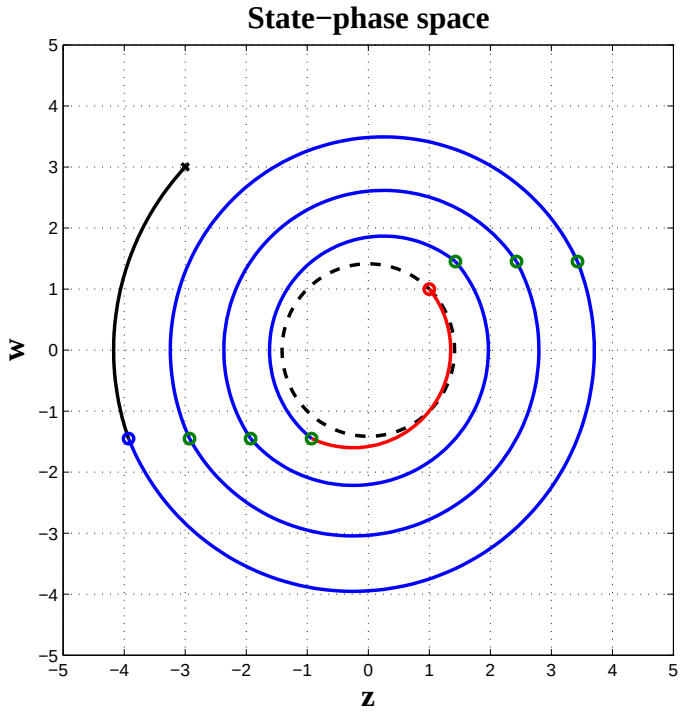

Figure 4.9 State trajectory for out-of-plane numerical example ($N = 7$).

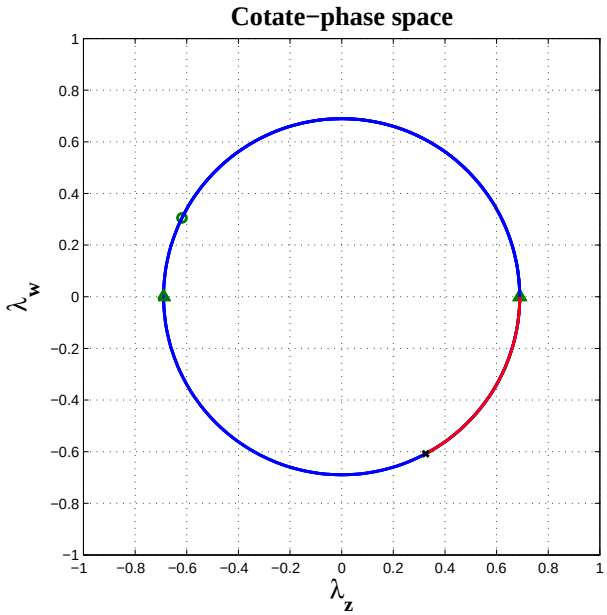

Figure 4.10 Costate trajectory for out-of-plane numerical example ($N = 7$).

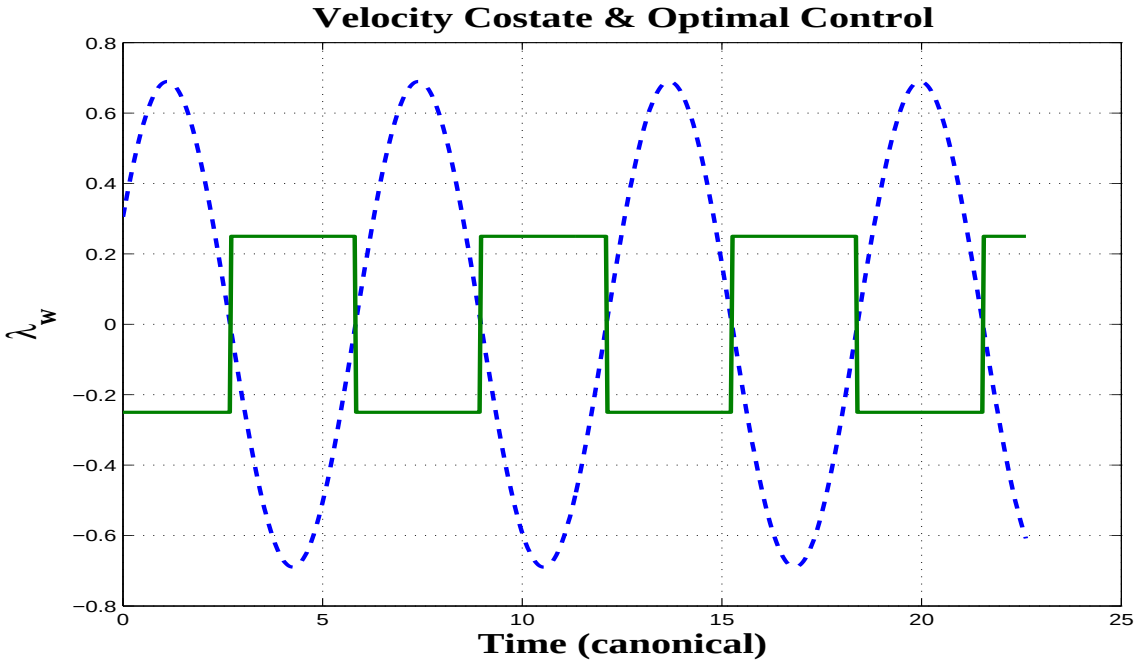

Figure 4.11 Velocity costate and optimal control for out-of-plane numerical example ($N = 7$).

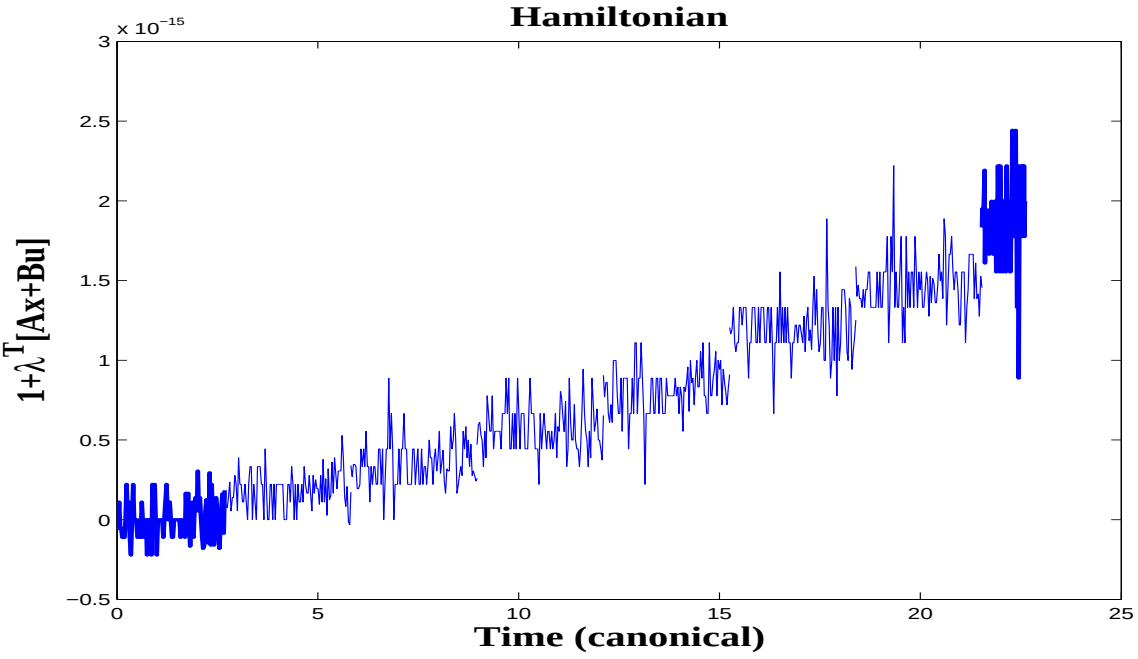

Figure 4.12 Hamiltonian for out-of-plane numerical example ($N = 7$).

4.7 Summary

In this chapter, the analytical solution for the minimum-time solution for the out-of-plane motion was presented. Graphical insight obtained from the state- and costate-phase space provided the necessary information, such as the vital state at the first control switch, $\mathbf{x}_{z1}$, to solve the problem. Phasing can be performed using either one ($N = 0$) or two ($N = 1$) control arcs. This chapter also presented the solution algorithm for two different target sets.[16] The results for the in-plane motion will be similarly presented in the following chapter.

[16]The results of this chapter along with minimum fuel solution were presented in the AIAA/AAS Astrodynamics Specialist Conference held in February 2004 at Maui, Hawaii.[50]

V. Minimum Time Control for In-Plane Motion

In the previous chapter, the analytical minimum time solution for out-of-plane motion problem was presented. The difference between the in-plane and out-of-plane motion is drastic. While the out-of-plane motion was harmonic, the in-plane motion is coupled and difficult to visualize. This chapter develops the analysis of the minimum-time control problem for in-plane motion.

The approach is similar to the out-of-plane analysis in that the case of no control switch is examined first. Then the case of one control switch is considered and so on, up to $N = 3$ switchings case, until generalization is possible. For the in-plane motion, the stable final orbit can be described using three of the four relative orbit parameters, for the case in which the final phase angle is not specified. Specifying the final phase angle will unnecessarily restrict our solution space for practical formation control problems. Thus, two control switches, with three critical times (t_1, t_2, and t_f), are all that are required to satisfy the desired final relative orbit parameters, a_f, b_f, and ρ_f. For practical application, the target set is the natural orbit requiring that $a_f = 0 = b_f$, leaving ρ_f to be specified. Then, by coasting once on the final orbit, the final phase angle will be reached within 2π canonical units of time (or one revolution of the reference orbit later). Therefore, this chapter presents only the $N = 2$ case.[1]

5.1 Review of Pertinent Information for In-plane Motion

First, the established necessary conditions for the minimum time from Chapter II as well the discussions of the in-plane costate dynamics from Chapter III are reexamined. The costate analysis provided the necessary information to eliminate non-optimal control switch sequences as well as reveal the relationship among the control switching times.

[1]The analysis for the $N = 3$ case of meeting all four relative orbit parameters is contained in Appendix E.

For $N = 2$, the controls are piece-wise constants:

$$\mathbf{u}(t) = \begin{cases} \mathbf{u}_o, & 0 \le t < t_1 \\ \mathbf{u}_1, & t_1 \le t < t_2 \\ \mathbf{u}_2, & t_2 \le t \le t_f \end{cases} \tag{5.1}$$

where t_1 and t_2 are control switching times. The four possible choices of initial control were shown in Equation (3.47), of which only two may be applicable for each of the subcases as was discussed in earlier Section 3.2.2. The possible optimal control sequences for the $N = 2$ case were presented as being a subset of the $N = 3$ case. The three subcases are described here briefly. Recall, the optimal control based on the Pontryagin's Minimum Principle (Hamilton-minimizing) was the bang-bang type: $u_x^*(t) = -sgn\{\lambda_{\dot{x}}(t)\}U_{max}$ and $u_y^*(t) = -sgn\{\lambda_{\dot{y}}(t)\}U_{max}$.

Subcase I. X-control Switch Only (X-X)

In this subcase, only the x-control switches at t_1 and at t_2 while the y-control is held constant. The period of the switching functions (velocity costates) is 2π, which means t_f must be less than the next x-crossing. Otherwise, another x-crossing would occur before t_f. For this subcase, the initial control pair is restricted to $u_{xo}/u_{yo} = +1$. Then the only possible sequence of control for this subcase are

$$\begin{bmatrix} -U_{max} \\ -U_{max} \end{bmatrix}_{\mathbf{u}_o} \rightarrow \begin{bmatrix} +U_{max} \\ -U_{max} \end{bmatrix}_{\mathbf{u}_1} \rightarrow \begin{bmatrix} -U_{max} \\ -U_{max} \end{bmatrix}_{\mathbf{u}_2} \tag{5.2}$$

and

$$\begin{bmatrix} +U_{max} \\ +U_{max} \end{bmatrix}_{\mathbf{u}_o} \rightarrow \begin{bmatrix} -U_{max} \\ +U_{max} \end{bmatrix}_{\mathbf{u}_1} \rightarrow \begin{bmatrix} +U_{max} \\ +U_{max} \end{bmatrix}_{\mathbf{u}_2} \tag{5.3}$$

Note that for this subcase, $\mathbf{u}_2 = \mathbf{u}_o$.

Subcase II. (X-Y)

In this subcase, the x-control switches at t_1 followed by a y-control switch at t_2. This

means that t_f is less than the next x-crossing. For this subcase, the initial control pair is restricted to $u_{xo}/u_{yo} = -1$ due to the fixed phasing difference between $\lambda_{\dot{y}}(t)$ and $\lambda_{\dot{x}}(t)$ of $\pi/2$. Then the two possible sequences of controls are

$$\begin{bmatrix} -U_{max} \\ +U_{max} \end{bmatrix}_{\mathbf{u}_o} \rightarrow \begin{bmatrix} +U_{max} \\ +U_{max} \end{bmatrix}_{\mathbf{u}_1} \rightarrow \begin{bmatrix} +U_{max} \\ -U_{max} \end{bmatrix}_{\mathbf{u}_2} \tag{5.4}$$

and

$$\begin{bmatrix} +U_{max} \\ -U_{max} \end{bmatrix}_{\mathbf{u}_o} \rightarrow \begin{bmatrix} -U_{max} \\ -U_{max} \end{bmatrix}_{\mathbf{u}_1} \rightarrow \begin{bmatrix} -U_{max} \\ +U_{max} \end{bmatrix}_{\mathbf{u}_2} \tag{5.5}$$

Note that for this subcase, $\mathbf{u}_2 = -\mathbf{u}_o$.

Subcase III. (Y-X)

In this subcase, the y-control switches at t_1 followed by a x-control switch at t_2. In this subcase, t_f must be less than the next y-crossing. For this subcase, the initial control pair is restricted to $u_{xo}/u_{yo} = +1$. Then the two sequences of controls are

$$\begin{bmatrix} -U_{max} \\ -U_{max} \end{bmatrix}_{\mathbf{u}_o} \rightarrow \begin{bmatrix} -U_{max} \\ +U_{max} \end{bmatrix}_{\mathbf{u}_1} \rightarrow \begin{bmatrix} +U_{max} \\ +U_{max} \end{bmatrix}_{\mathbf{u}_2} \tag{5.6}$$

and

$$\begin{bmatrix} +U_{max} \\ +U_{max} \end{bmatrix}_{\mathbf{u}_o} \rightarrow \begin{bmatrix} +U_{max} \\ -U_{max} \end{bmatrix}_{\mathbf{u}_1} \rightarrow \begin{bmatrix} -U_{max} \\ -U_{max} \end{bmatrix}_{\mathbf{u}_2} \tag{5.7}$$

Note that for this subcase, $\mathbf{u}_2 = -\mathbf{u}_o$.

The solution to the controlled in-plane motion was presented in Equation (3.55) for a general number, N, of control switches. For the remainder of this chapter, the subscript $(\cdot)_{xy}$ denoting the in-plane motion is dropped.[2] The state is $\mathbf{x} = [x\ y\ \dot{x}\ \dot{y}]^T$ and

[2]The variables are still normalized by $R_o = 1 = \mu_\oplus$ and $\omega = 1$.

the analytical solution of the dynamics is

$$\mathbf{x}(t) = \begin{bmatrix} \rho_o \sin(t+\theta_o) + a_o \\ 2\rho_o \cos(t+\theta_o) - \frac{3}{2}a_o t + b_o \\ \rho_o \cos(t+\theta_o) \\ -2\rho_o \sin(t+\theta_o) - \frac{3}{2}a_o \end{bmatrix} + \left[\int_0^{t_1} \mathbf{\Phi}_x(t,\tau)\mathbf{B}d\tau\right]\mathbf{u}_o + \left[\int_{t_1}^{t_2} \mathbf{\Phi}_x(t,\tau)\mathbf{B}d\tau\right]\mathbf{u}_1 + \left[\int_{t_2}^{t} \mathbf{\Phi}_x(t,\tau)\mathbf{B}d\tau\right]\mathbf{u}_2 \quad (5.8)$$

for $t > t_2$. While it is difficult to visualize the trajectory in 4 dimension, it is helpful to plot the trajectory in multiple 2-D plots. In Section 3.1.2, the control-free in-plane motion was shown in Figure 3.2. As soon as the control is applied, the trajectory moves off of the 2-1 ellipse and the stable relative orbit is destroyed. Taking advantage of the parameterization of the control-free motion that was presented in Chapter III, relative orbit parameters for the in-plane motion can be viewed as being instantaneously provided by the same Equation (3.3). Therefore, at any given t,

$$a(t) = 4x(t) + 2\dot{y}(t) \quad (5.9)$$

$$b(t) = y(t) - 2\dot{x}(t) \quad (5.10)$$

$$\rho(t) = [x(t) - a(t)]^2 + \dot{x}(t)^2 \quad (5.11)$$

The initial state, $\mathbf{x}(0) = \mathbf{x}_o$, is considered fixed, and the terminal state constraints can be put into the form:

$$\mathbf{\Psi}(\mathbf{x}(t_f), t_f) = \mathbf{x}(t_f) - \mathbf{x}_f = \mathbf{0} \quad (5.12)$$

Notice that the constraint does not contain t_f explicitly; i.e. $\mathbf{\Psi}(\mathbf{x}(t_f), t_f) = \mathbf{\Psi}[\mathbf{x}(t_f)]$. However, instead of using the states, when the relative formation parameters are applied,

the terminal constraint equations become:

$$\boldsymbol{\Psi}[\mathbf{x}(t_f), t_f] = \begin{bmatrix} a(t_f) - a_f \\ b(t_f) - b_f \\ \rho^2(t_f) - \rho_f^2 \end{bmatrix} = \begin{bmatrix} 4x(t_f) + 2\dot{y}(t_f) - a_f \\ y(t_f) - 2\dot{x}(t_f) - b_f \\ (x(t_f) - a(t_f))^2 + \dot{x}^2(t_f) - \rho_f^2 \end{bmatrix} \tag{5.13}$$

which does not contain t_f explicitly. The form of terminal state constraint is important because it affects both the terminal costate boundary condition and the transversality condition, as well as the existence of solutions. The second form using the relative orbit parameters is more advantageous because the relative orbit parameters are considered constants of the relative motion. Therefore, the second form was used for this research.

The costate terminal condition was given in Equation (2.14). Using the form in Equation (5.13),

$$\frac{\partial \boldsymbol{\Psi}\left(\mathbf{x}(t_f), t_f\right)}{\partial \mathbf{x}(t_f)} = \begin{bmatrix} 4 & 0 & 0 & 2 \\ 0 & 1 & -2 & 0 \\ -3(x(t_f) - a(t_f)) & 0 & 2\dot{x}(t_f) & -4(x(t_f) - a(t_f)) \end{bmatrix} \tag{5.14}$$

where Equations (5.9), (5.10), and (5.11) were used in the intermediate derivations.

As was discussed in Section 2.5, the transversality condition from the optimal theory is reduced to $\boldsymbol{\nu}^T \frac{\partial \boldsymbol{\Psi}\left(\mathbf{x}(t_f), t_f\right)}{\partial t_f} = 0$ because the optimal theory also tells us that the Hamiltonian remains zero for all time, $t \in [0\ t_f]$. Separating these two conditions[3],

$$\boldsymbol{\nu}^T \frac{\partial \boldsymbol{\Psi}\left(\mathbf{x}(t_f), t_f\right)}{\partial t_f} = 0 \tag{5.15}$$

$$H(t) = 1 + \boldsymbol{\lambda}^T(t)\left[\mathbf{A}\mathbf{x}(t) + \mathbf{B}\mathbf{u}(t)\right] = 0 \tag{5.16}$$

With all the necessary conditions in hand, the in-plane motion analysis begins by examining the simpler cases and gradually increased the complexity. The case in which

[3]Notice that $\frac{\partial \boldsymbol{\Psi}(\mathbf{x}(t_f), t_f)}{\partial t_f} = \mathbf{0}$ because the terminal state constraint is not an explicit function of t_f.

no control switch is required ($N = 0$) is examined first; i.e., the initial control is held constant from $t = 0$ to $t = t_f$. Then the $N = 1$ case with a single control switch is examined next and so forth.

The reachable state from any given initial state is a function of both that initial state and the magnitude of U_{max}.[4] For this analysis, the final state $\mathbf{x}_f$ is assumed to be "close" enough to the initial state $\mathbf{x}_o$ to require only two control switches. That is, the final relative orbit can be reached with only two control switches. For $N = 2$, there are seven unknowns: three critical control switch times (t_1, t_2, t_f) and the initial costate vector.

The results for the two control switch case ($N = 2$), specifically, the derivation for the initial costate vector of the minimum-time problem in the XY-plane, will now be presented in the same order as was done for the out-of-plane motion. The critical times are calculated first. Then, the initial costate vector is determined.

5.2 Critical Control Switch Times

The three critical times for $N = 2$ are found using three of the four relative orbit parameters: a, b, and ρ. First examined is the drifting parameter with $a(t)$, followed by the centering parameter, $b(t)$, and finally the relative size parameter, $\rho(t)$.

[4]For a typical stable centered orbit, the initial state is a function of ρ_o and θ_o as defined in Appendix B.2 because $a_o = 0 = b_o$.

As was done in the out-of-plane analysis, these times will be calculated using the dynamic solution. The explicit state solution at time t_f using Equation (5.8) is

$$\mathbf{x}(t_f) = \begin{bmatrix} \rho_o \sin(t_f + \theta_o) + a_o \\ 2\rho_o \cos(t_f + \theta_o) - \frac{3}{2} a_o t_f + b_o \\ \rho_o \cos(t_f + \theta_o) \\ -2\rho_o \sin(t_f + \theta_o) - \frac{3}{2} a_o \end{bmatrix} + \left[\int_0^{t_1} \mathbf{\Phi}_x(t_f, \tau) \mathbf{B} d\tau \right] \begin{bmatrix} u_{xo} \\ u_{yo} \end{bmatrix}$$
$$+ \left[\int_{t_1}^{t_2} \mathbf{\Phi}_x(t_f, \tau) \mathbf{B} d\tau \right] \begin{bmatrix} u_{x1} \\ u_{y1} \end{bmatrix} + \left[\int_{t_2}^{t_f} \mathbf{\Phi}_x(t_f, \tau) \mathbf{B} d\tau \right] \begin{bmatrix} u_{x2} \\ u_{y2} \end{bmatrix} \quad (5.17)$$

Using the analytical results from Equation (5.17) in the equation for drifting parameter, $a(t_f) = 4x(t_f) + 2\dot{y}(t_f)$ reduces to

$$a(t_f) = a_f = a_o + 2u_{yo}\Delta\tau_1 + 2u_{y1}\Delta\tau_2 + 2u_{y2}\Delta\tau_3 \quad (5.18)$$

where , $\Delta\tau_1 = t_1$, $\Delta\tau_2 = t_2 - t_1$, and $\Delta\tau_3 = t_f - t_2$. Also, $t_f = \Delta\tau_1 + \Delta\tau_2 + \Delta\tau_3$. These time intervals ($\Delta\tau_i$) are more useful than the absolute times. Instead of requiring the switching times be in correct order (i.e. $0 \leq t_1 \leq t_2 \leq t_f$), each time interval will now be required to be non-negative. Notice the lack of x-control in this equation. This makes some intuitive sense since the drift is in the y-direction and the controls in this in-track direction will affect the final drifting parameter. Defining $\Delta a = a_o - a_f$ as the change in drifting parameter,

$$\frac{\Delta a}{2u_{yo}} + \Delta\tau_1 + \frac{u_{y1}}{u_{yo}}\Delta\tau_2 + \frac{u_{y2}}{u_{yo}}\Delta\tau_3 = 0 \quad (5.19)$$

Equation (5.19) can be used to reduce the unknowns from three to two; i.e., one of the three time intervals can be expressed in terms of the other two:[5]

$$\Delta\tau_3 = -\frac{1}{\frac{u_{y2}}{u_{yo}}} \left[\frac{\Delta a}{2u_{yo}} + \Delta\tau_1 + \frac{u_{y1}}{u_{yo}}\Delta\tau_2 \right] = -\frac{u_{y2}}{u_{yo}} \left[\frac{\Delta a}{2u_{yo}} + \Delta\tau_1 + \frac{u_{y1}}{u_{yo}}\Delta\tau_2 \right] \quad (5.20)$$

[5] $u_{yo}/u_{y2} = u_{y2}/u_{yo} = \pm 1$ was used in Equation (5.20).

For the three subcases of $N = 2$, this first set of equation is used to examine what constraints are placed on the time intervals and their combinations when they are required to be non-negative. These constraints on the time intervals can be used as a test for existence of solution and are presented here for each subcase.

Subcase I. X-control Switch Only

When only the x-control is switching, $u_{y1} = u_{y2} = u_{yo}$. Equation (5.19) becomes

$$t_f = -\frac{1}{2}\frac{\Delta a}{u_{yo}} \tag{5.21}$$

Requiring the final time to be non-negative, the initial y-control must be

$$u_{yo} = -sgn\{\Delta a\}U_{max} \tag{5.22}$$

This means that the final time is a function of Δa for a fixed U_{max}; $t_f = \Delta\tau_1 + \Delta\tau_2 + \Delta\tau_3 = \frac{1}{2}|\Delta a|/U_{max}$. Then, each of the time intervals is also bounded by

$$0 \leq \{\Delta\tau_1, \Delta\tau_2, \Delta\tau_3\} \leq \frac{1}{2}\frac{|\Delta a|}{U_{max}} \tag{5.23}$$

Notice also that, if the maneuver is from one non-drifting orbit to another, that is $a_o = 0 = a_f$, then $\Delta a = 0$ and $t_f = 0$. This implies that this subcase is not suitable for this type of maneuver. Practical use of formation control is from one stable orbit to another, and in these cases the number of subcases is reduced from three to two.

Subcase II. X-control Switch followed by Y-control Switch

In this subcase, the x-control switches first at t_1 and then the y-control switches at t_2. So, $u_{y1} = u_{yo}$, and $u_{y2} = -u_{y1} = -u_{yo}$. Then, Equation (5.19), after some algebra, can

be used to solve for the final time:

$$t_f = -\frac{1}{2}\frac{\Delta a}{u_{yo}} + 2\Delta\tau_3 \tag{5.24}$$

For positive final time, $\Delta\tau_3 \geq \max\{0, \Delta a/(4u_{yo})\}$. However, when the equation is written as,

$$2\Delta\tau_3 = t_f + \frac{1}{2}\frac{\Delta a}{u_{yo}} \tag{5.25}$$

for positive time interval $\Delta\tau_3$, $t_f \geq \max\{0, -\Delta a/(2u_{yo})\}$. Now, if the y-control is set to

$$u_{yo} = -sgn\{\Delta a\}U_{max} \tag{5.26}$$

the final time must satisfy

$$t_f \geq \frac{1}{2}\frac{|\Delta a|}{U_{max}} \tag{5.27}$$

and $0 < \Delta\tau_3 < t_f$. However, if y-control is set to

$$u_{yo} = +sign\{\Delta a\}U_{max} \tag{5.28}$$

the final time is required to be positive while $t_f > \Delta\tau_3 \geq |\Delta a|/(4U_{max})$.

Subcase III. Y-Control Switch followed by X-control Switch

In this subcase, the y-control switches first at t_1 and then the x-control switches at t_2. So, $u_{y1} = -u_{yo}$, and $u_{y2} = u_{y1} = -u_{yo}$. Then, Equation (5.19), after some algebra, can be used to solve for the final time:

$$t_f = \frac{1}{2}\frac{\Delta a}{u_{yo}} + 2\Delta\tau_1 \tag{5.29}$$

For positive final time, $\Delta\tau_1 \geq \max\{0, -\Delta a/(4u_{yo})\}$. However, when the equation is written as

$$2\Delta\tau_1 = t_f - \frac{1}{2}\frac{\Delta a}{u_{yo}} \tag{5.30}$$

and restraining $\Delta\tau_1 \geq 0$, $t_f \geq \max\{0, \Delta a/(2u_{yo})\}$. Now if the y-control is set to $u_{yo} = +sign\{\Delta a\}U_{max}$, then

$$t_f \geq \frac{1}{2}\frac{|\Delta a|}{U_{max}} \tag{5.31}$$

while $0 < \Delta\tau_1 < t_f$. If $u_{yo} = -sgn\{\Delta a\}U_{max}$, the final time must be non-negative and $t_f > \Delta\tau_1 > |\Delta a|/(4U_{max})$. The constraint on the y-control for this subcase is somewhat opposite of subcases II.

Analysis of the drifting parameter for the three subcases just examined, provides insight to the possible initial y-control as a function of Δa as well as constraints on time intervals and the final time. Next to be examined is the centering parameter with $b(t_f) = b_f$ specified. In a similar method, the solution from Equation (5.17) is used in the equation for centering parameter, $b(t_f) = y(t_f) - 2\dot{x}(t_f)$. The initial reduction is of the form:

$$\begin{aligned} 0 =& \frac{\Delta b}{u_{yo}} - 2\frac{u_{xo}}{u_{yo}}\left(\Delta\tau_1 + \frac{u_{x1}}{u_{xo}}\Delta\tau_2 + \frac{u_{x2}}{u_{xo}}\Delta\tau_3\right) + \frac{3}{2}\frac{a_o}{u_{yo}}t_f \\ &+ \frac{3}{2}\left(\frac{\Delta u_{y1}}{u_{yo}}(t_f - t_1)^2 + \frac{\Delta u_{y2}}{u_{yo}}(t_f - t_2)^2 - t_f^2\right) \end{aligned} \tag{5.32}$$

where $\Delta b = b_o - b_f$ is the change in centering parameter and Δu_{ij} is the change in control at switch time j in the i-controller. Now, substituting in the Equation (5.20), the equation becomes a function of $\Delta\tau_1$ and $\Delta\tau_2$. Then, $\Delta\tau_2$ can be solved in terms of $\Delta\tau_1$ (or, vice versa),

$$\begin{aligned} & \left(\frac{u_{y2}}{u_{yo}} - \frac{u_{y1}}{u_{yo}}\right)\Delta\tau_2^2 \\ + & \left[\frac{u_{xo}}{u_{yo}}\left(\frac{u_{x2}}{u_{xo}}\frac{u_{y1}}{u_{yo}}\frac{u_{y2}}{u_{yo}} - \frac{u_{x1}}{u_{xo}}\right)\frac{4}{3} + \left(\frac{u_{y1}}{u_{yo}}\frac{u_{y2}}{u_{yo}} - 1\right)\frac{a_o}{u_{yo}} + \left(\frac{u_{y1}}{u_{yo}}\frac{u_{y2}}{u_{yo}} - 1\right)2\Delta\tau_1\right]\Delta\tau_2 \\ + & \left(\frac{u_{y2}}{u_{yo}} - 1\right)\Delta\tau_1^2 + \left[\frac{u_{xo}}{u_{yo}}\left(\frac{u_{x2}}{u_{xo}}\frac{u_{y2}}{u_{yo}} - 1\right)\frac{4}{3} + \frac{a_o}{u_{yo}}\left(\frac{u_{y2}}{u_{yo}} - 1\right)\right]\Delta\tau_1 \\ + & \frac{u_{y2}}{u_{yo}}\left(\frac{2}{3}\frac{u_{xo}}{u_{yo}}\frac{u_{x2}}{u_{xo}} + \frac{1}{4}\frac{(a_o + a_f)}{u_{yo}}\right)\frac{\Delta a}{u_{yo}} + \frac{2}{3}\frac{\Delta b}{u_{yo}} = 0 \end{aligned} \tag{5.33}$$

This equation is written as a quadratic function of $\Delta\tau_2$ in terms of $\Delta\tau_1$. Restricting the discriminant of this quadratic function to be non-negative in order to ensure a physically meaningful time interval, additional constraints are obtained for each of the subcases.

Subcase I. X-control Switch Only

For this subcase, the coefficient of the quadratic is zero and $\Delta\tau_2$ can be solved directly in terms of the problem parameters,

$$\Delta\tau_2 = -\frac{3}{32}\frac{u_{xo}}{u_{yo}}\frac{(a_o + a_f)}{u_{yo}}\frac{\Delta a}{u_{yo}} - \frac{1}{4}\left(\frac{u_{xo}}{u_{yo}}\frac{\Delta b}{u_{yo}} + \frac{\Delta a}{u_{yo}}\right) \tag{5.34}$$

From earlier analysis, the initial control of $u_{yo} = -sgn\{\Delta a\}U_{max}$ is required. Now, by restraining $0 \leq \Delta\tau_2 \leq \frac{1}{2}|\Delta a|/U_{max}$ (see discussion above), a new constraint is obtained,

$$\left|\frac{\Delta b}{|\Delta a|} - \frac{3}{8}\frac{(a_o + a_f)}{U_{max}}\right| \leq 1 \tag{5.35}$$

for a non-zero Δa. Notice that not every combination of initial and desired values of a and b will satisfy this inequality and the solution will then not exist. Therefore, in some instances, subcase I will not be a viable control sequence option. If the inequality holds for a given problem, $\Delta\tau_3$ can be solved in terms of $\Delta\tau_1$ by substituting Equation (5.34) into Equation (5.20),

$$\begin{aligned}\Delta\tau_3 &= \frac{1}{2}\frac{|\Delta a|}{U_{max}} - \Delta\tau_1 - \Delta\tau_2 \\ &= \frac{1}{4}\frac{|\Delta a|}{U_{max}} - \Delta\tau_1 + \frac{3}{32}\frac{u_{xo}}{u_{yo}}\frac{(a_o + a_f)}{sign\{\Delta a\}}\frac{|\Delta a|}{U_{max}^2} - \frac{1}{4}\frac{u_{xo}}{u_{yo}}\frac{\Delta b}{sign\{\Delta a\}U_{max}}\end{aligned} \tag{5.36}$$

Subcase II. X-control Switch followed by Y-control Switch

For this subcase, a quadratic equation of $\Delta\tau_2$ in terms of $\Delta\tau_1$ is obtained,

$$\Delta\tau_2^2 + \left(2\Delta\tau_1 + \frac{a_o}{u_{yo}} + \frac{4}{3}\right)\Delta\tau_2 + \left[\Delta\tau_1^2 + \frac{a_o}{u_{yo}}\Delta\tau_1 + \left(\frac{1}{3} + \frac{1}{8}\frac{(a_o + a_f)}{u_{yo}}\right)\frac{\Delta a}{u_{yo}} - \frac{1}{3}\frac{\Delta b}{u_{yo}}\right] = 0 \quad (5.37)$$

where for this subcase only $u_{xo}/u_{yo} = -1$ is allowed. The discriminant of this quadratic equation must be required to be non-negative for non-complex time interval:

$$\frac{4}{3}\Delta\tau_1 + \frac{1}{4}\left(\frac{a_o}{u_{yo}}\right)^2 - \left(\frac{1}{3} + \frac{1}{8}\frac{(a_o + a_f)}{u_{yo}}\right)\frac{\Delta a}{u_{yo}} + \frac{1}{3}\frac{\Delta b}{u_{yo}} + \frac{4}{9} + \frac{2}{3}\frac{a_o}{u_{yo}} > 0 \quad (5.38)$$

which places a constraint on $\Delta\tau_1$.

$$\Delta\tau_2 = -\frac{2}{3} - \frac{1}{2}\frac{a_o}{u_{yo}} - \Delta\tau_1 \pm \sqrt{\frac{4}{3}\Delta\tau_1 + \frac{1}{4}\left(\frac{a_o}{u_{yo}}\right)^2 - \left(\frac{1}{3} + \frac{1}{8}\frac{(a_o + a_f)}{u_{yo}}\right)\frac{\Delta a}{u_{yo}} + \frac{1}{3}\frac{\Delta b}{u_{yo}} + \frac{4}{9} + \frac{2}{3}\frac{a_o}{u_{yo}}} \quad (5.39)$$

where only the positive real roots will be considered. It seems reasonable to take the smallest of the two non-negative real roots, but the non-negative root which leads to minimum t_f will be the answer. For this subcase,

$$\Delta\tau_3 = -\frac{2}{3} - \frac{1}{2}\frac{a_f}{u_{yo}} + \sqrt{\frac{4}{3}\Delta\tau_1 + \frac{1}{4}\left(\frac{a_o}{u_{yo}}\right)^2 - \left(\frac{1}{3} + \frac{1}{8}\frac{(a_o + a_f)}{u_{yo}}\right)\frac{\Delta a}{u_{yo}} + \frac{1}{3}\frac{\Delta b}{u_{yo}} + \frac{4}{9} + \frac{2}{3}\frac{a_o}{u_{yo}}} \quad (5.40)$$

which is now considered as a function of $\Delta\tau_1$ only. Finally,

$$\begin{aligned} t_f &= \Delta\tau_1 + \Delta\tau_2 + \Delta\tau_3 \\ &= -\frac{1}{2}\frac{a_o + a_f}{u_{yo}} - \frac{4}{3} \\ &\quad + 2\sqrt{\frac{4}{3}\Delta\tau_1 + \frac{1}{4}\left(\frac{a_o}{u_{yo}}\right)^2 - \left(\frac{1}{3} + \frac{1}{8}\frac{(a_o + a_f)}{u_{yo}}\right)\frac{\Delta a}{u_{yo}} + \frac{1}{3}\frac{\Delta b}{u_{yo}} + \frac{4}{9} + \frac{2}{3}\frac{a_o}{u_{yo}}} \end{aligned} \quad (5.41)$$

Subcase III. Y-Control Switch followed by X-control Switch

For this subcase, $\Delta\tau_2$ could be solved as a nonlinear function of $\Delta\tau_1$,

$$\Delta\tau_2 = -\frac{u_{xo}}{u_{yo}}\frac{3}{4}\left(\Delta\tau_1 + \frac{a_o}{u_{yo}}\right)\Delta\tau_1 + \frac{1}{4}\left(\frac{\Delta a}{u_{yo}} + \frac{u_{xo}}{u_{yo}}\frac{\Delta b}{u_{yo}}\right) - \frac{3}{32}\frac{u_{xo}}{u_{yo}}\frac{(a_o + a_f)}{u_{yo}}\frac{\Delta a}{u_{yo}} \tag{5.42}$$

Substituting this into Equation 5.20,

$$\begin{aligned}\Delta\tau_3 &= \frac{1}{2}\frac{\Delta a}{u_{yo}} + \Delta\tau_1 - \Delta\tau_2 \\ &= \Delta\tau_1 + \frac{u_{xo}}{u_{yo}}\frac{3}{4}\left(\Delta\tau_1 + \frac{a_o}{u_{yo}}\right)\Delta\tau_1 + \frac{1}{4}\left(\frac{\Delta a}{u_{yo}} - \frac{u_{xo}}{u_{yo}}\frac{\Delta b}{u_{yo}}\right) + \frac{3}{32}\frac{u_{xo}}{u_{yo}}\frac{(a_o + a_f)}{u_{yo}}\frac{\Delta a}{u_{yo}}\end{aligned} \tag{5.43}$$

is now a function of $\Delta\tau_1$ only.

Finally, the relative orbit size parameter is examined with $\rho(t_f) = t_f$. Again, using the solution from Equation (5.17) in the equation for relative formatino size parameter, $\rho^2(t_f) = [x(t_f) - a(t_f)]^2 + \dot{x}^2(t_f)$, a large equation is obtained:

$$
\begin{aligned}
\frac{\rho_f^2-\rho_o^2}{2U_{max}^2} &= 5+\frac{1}{2}\left(\frac{\Delta u_{x1}}{u_{xo}}\right)^2+\frac{1}{2}\left(\frac{\Delta u_{x2}}{u_{xo}}\right)^2+2\left(\frac{\Delta u_{y1}}{u_{yo}}\right)+2\left(\frac{\Delta u_{y2}}{u_{yo}}\right)^2 \\
&-2\frac{\rho_o}{u_{yo}}\cos\theta_o-\frac{u_{xo}}{u_{yo}}\frac{\rho_o}{u_{yo}}\sin\theta_o+\frac{\Delta u_{y1}}{u_{yo}}2\frac{\rho_o}{u_{yo}}\cos(\Delta\tau_1+\theta_o)+\frac{u_{xo}}{u_{yo}}\frac{\Delta u_{x1}}{u_{xo}}\frac{\rho_o}{u_{yo}}\sin(\Delta\tau_1+\theta_o) \\
&-\left(\frac{\Delta u_{x1}}{u_{xo}}+\frac{\Delta u_{y1}}{u_{yo}}4\right)\cos\Delta\tau_1+\frac{u_{xo}}{u_{yo}}\left(\frac{\Delta u_{y1}}{u_{yo}}-\frac{\Delta u_{x1}}{u_{xo}}\right)2\sin\Delta\tau_1 \\
&+\left(\frac{\Delta u_{x1}}{u_{xo}}\frac{\Delta u_{x2}}{u_{xo}}+\frac{\Delta u_{y1}}{u_{yo}}\frac{\Delta u_{y2}}{u_{yo}}4\right)\cos\Delta\tau_2+\frac{u_{xo}}{u_{yo}}\left(\frac{\Delta u_{y1}}{u_{yo}}\frac{\Delta u_{x2}}{u_{xo}}-\frac{\Delta u_{x1}}{u_{xo}}\frac{\Delta u_{y2}}{u_{yo}}\right)2\sin\Delta\tau_2 \\
&+\left(\frac{u_{x2}}{u_{xo}}\frac{\Delta u_{x2}}{u_{xo}}+\frac{u_{y2}}{u_{yo}}\frac{\Delta u_{y2}}{u_{yo}}4\right)\cos\Delta\tau_3+\frac{u_{xo}}{u_{yo}}\left(\frac{u_{x2}}{u_{xo}}\frac{\Delta u_{y2}}{u_{yo}}-\frac{u_{y2}}{u_{yo}}\frac{\Delta u_{x2}}{u_{xo}}\right)2\sin\Delta\tau_3 \\
&-\left(\frac{\Delta u_{x2}}{u_{xo}}+\frac{\Delta u_{y2}}{u_{yo}}4\right)\cos(\Delta\tau_1+\Delta\tau_2)+\frac{u_{xo}}{u_{yo}}\left(\frac{\Delta u_{y2}}{u_{yo}}-\frac{\Delta u_{x2}}{u_{xo}}\right)2\sin(\Delta\tau_1+\Delta\tau_2) \\
&+\frac{\Delta u_{y2}}{u_{yo}}2\frac{\rho_o}{u_{yo}}\cos(\Delta\tau_1+\Delta\tau_2+\theta_o)+\frac{u_{xo}}{u_{yo}}\frac{\Delta u_{x2}}{u_{xo}}\frac{\rho_o}{u_{yo}}\sin(\Delta\tau_1+\Delta\tau_2+\theta_o) \\
&+\left(\frac{u_{x2}}{u_{xo}}\frac{\Delta u_{x1}}{u_{xo}}+\frac{u_{y2}}{u_{yo}}\frac{\Delta u_{y1}}{u_{yo}}4\right)\cos(\Delta\tau_2+\Delta\tau_3)+\frac{u_{xo}}{u_{yo}}\left(\frac{u_{x2}}{u_{xo}}\frac{\Delta u_{y1}}{u_{yo}}-\frac{u_{y2}}{u_{yo}}\frac{\Delta u_{x1}}{u_{xo}}\right)2\sin(\Delta\tau_2+\Delta\tau_3) \\
&-\left(\frac{u_{x2}}{u_{xo}}+\frac{u_{y2}}{u_{yo}}4\right)\cos(\Delta\tau_1+\Delta\tau_2+\Delta\tau_3)+\frac{u_{xo}}{u_{yo}}\left(\frac{u_{y2}}{u_{yo}}-\frac{u_{x2}}{u_{xo}}\right)2\sin(\Delta\tau_1+\Delta\tau_2+\Delta\tau_3) \\
&+\frac{u_{y2}}{u_{yo}}2\frac{\rho_o}{u_{yo}}\cos(\Delta\tau_1+\Delta\tau_2+\Delta\tau_3+\theta_o)+\frac{u_{xo}}{u_{yo}}\frac{u_{x2}}{u_{xo}}\frac{\rho_o}{u_{yo}}\sin(\Delta\tau_1+\Delta\tau_2+\Delta\tau_3+\theta_o) \qquad (5.44)
\end{aligned}
$$

This is a nonlinear function of a single variable, $\Delta\tau_1$, after substituting in equations (5.20) and (5.33). For the three subcases, a partial reduction is possible.

Subcase I. X-Control Switch Only

For this subcase, a quadratic function of $\cos\Delta\tau_1$ is obtained:

$$
\left(\beta^2+\gamma^2\right)\cos^2\Delta\tau_1-2\alpha\beta\cos\Delta\tau_1+\left(\alpha^2-\gamma^2\right)=0 \qquad (5.45)
$$

where some intermediate problem specific constants are defined,

$$\alpha = K_o - K_1 \tag{5.46}$$

$$\beta = \frac{u_{xo}}{u_{yo}} 2 \frac{\rho_o}{u_{yo}} \left[\sin\theta_o - \sin\left(K_3 + \theta_o\right)\right] + \frac{u_{xo}}{u_{yo}} 4 \left(\sin K_2 + \sin K_3 - \sin K_4\right) - 2\left(1 + \cos K_2 - \cos K_3 - \cos K_4\right) \tag{5.47}$$

$$\gamma = \frac{u_{xo}}{u_{yo}} 2 \frac{\rho_o}{u_{yo}} \left[\cos\theta_o - \cos\left(K_3 + \theta_o\right)\right] - \frac{u_{xo}}{u_{yo}} 4 \left(1 + \cos K_2 - \cos K_3 - \cos K_4\right) - 2\left(\sin K_2 + \sin K_3 - \sin K_4\right) \tag{5.48}$$

$$K_o = \frac{1}{2} \frac{1}{U_{max}^2} \left(\rho_f^2 - \rho_o^2\right) - 9 \tag{5.49}$$

$$K_1 = \frac{\rho_o}{u_{yo}} \left[2\cos\left(K_4 + \theta_o\right) + \frac{u_{xo}}{u_{yo}} \sin\left(K_4 + \theta_o\right) - 2\cos\theta_o - \frac{u_{xo}}{u_{yo}} \sin\theta_o\right] - 5\cos K_4 - 4\cos K_3 \tag{5.50}$$

$$K_2 = -\frac{3}{32} \frac{\Delta a}{u_{xo}} \frac{|\Delta a|}{U_{max}} + \frac{1}{4} \frac{\Delta b}{u_{yo}} + \frac{1}{4} \frac{|\Delta a|}{U_{max}} \tag{5.51}$$

$$K_3 = \frac{3}{32} \frac{\Delta a}{u_{xo}} \frac{|\Delta a|}{U_{max}} - \frac{1}{4} \frac{\Delta b}{u_{yo}} + \frac{1}{4} \frac{|\Delta a|}{U_{max}} \tag{5.52}$$

$$K_4 = \frac{1}{2} \frac{|\Delta a|}{U_{max}} \tag{5.53}$$

The solution is

$$\cos\Delta\tau_1 = \frac{1}{\left(\beta^2 + \gamma^2\right)} \left[\alpha\beta \pm \gamma\sqrt{\beta^2 + \gamma^2 - \alpha^2}\right] \tag{5.54}$$

Requiring the discriminant to be non-negative is equivalent to $\beta^2 + \gamma^2 \geq \alpha^2$. The magnitude of the right hand side must also be in the range of the arc-cosine function; i.e., the magnitude must be less than unity:

$$\left|\alpha\beta \pm \gamma\sqrt{\beta^2 + \gamma^2 - \alpha^2}\right| \leq \left(\beta^2 + \gamma^2\right) \tag{5.55}$$

Subcase II. X-Control Switch followed by Y-control Switch

For this subcase, Equation (5.44) reduces to

$$\begin{aligned} K_o = &-\frac{\rho_o}{u_{yo}} \sin\left(\Delta\tau_1 + \theta_o\right) - 2\left(\cos\Delta\tau_1 - 2\sin\Delta\tau_1\right) \\ &+ 8\sin\Delta\tau_2 - 5\cos\left(2\Delta\tau_1 + 2\Delta\tau_2 + \frac{1}{2}\frac{\Delta a}{u_{yo}}\right) \\ &- \frac{\rho_o}{u_{yo}}\left[2\cos\left(2\Delta\tau_1 + 2\Delta\tau_2 + \frac{1}{2}\frac{\Delta a}{u_{yo}} + \theta_o\right) - \sin\left(2\Delta\tau_1 + 2\Delta\tau_2 + \frac{1}{2}\frac{\Delta a}{u_{yo}} + \theta_o\right)\right] \\ &- 4\left[2\cos\left(\frac{1}{2}\frac{\Delta a}{u_{yo}} + \Delta\tau_1 + \Delta\tau_2\right) - \sin\left(\frac{1}{2}\frac{\Delta a}{u_{yo}} + \Delta\tau_1 + \Delta\tau_2\right)\right] \\ &- 4\left[2\cos\left(\Delta\tau_1 + \Delta\tau_2\right) - \sin\left(\Delta\tau_1 + \Delta\tau_2\right)\right] \\ &- 2\left[\cos\left(\frac{1}{2}\frac{\Delta a}{u_{yo}} + \Delta\tau_1 + 2\Delta\tau_2\right) - 2\sin\left(\frac{1}{2}\frac{\Delta a}{u_{yo}} + \Delta\tau_1 + 2\Delta\tau_2\right)\right] \\ &- 4\frac{\rho_o}{u_{yo}}\cos\left(\Delta\tau_1 + \Delta\tau_2 + \theta_o\right) \end{aligned} \tag{5.56}$$

where the intermediate constant is

$$K_o = \frac{1}{2}\frac{1}{U_{max}^2}\left(\rho_f^2 - \rho_o^2\right) - 15 + \frac{\rho_o}{u_{yo}}\left(2\cos\theta_o - \sin\theta_o\right) \tag{5.57}$$

This is really a function of only one variable, namely $\Delta\tau_1$, since $\Delta\tau_2$ is a quadratic in $\Delta\tau_1$. Analytical solution for this problem does not exist. Although it is nonlinear, the function is smooth and the solution could be found numerically.

Subcase III. Y-Control Switch followed by X-control Switch

For this subcase, Equation (5.44) reduces to:

$$
\begin{aligned}
K_o = 4\frac{\rho_o}{u_{yo}}\cos\left(\Delta\tau_1+\theta_o\right) + 4\left(2\cos\Delta\tau_1+\sin\Delta\tau_1\right) \\
+ 8\sin\Delta\tau_2 - 5\cos\left(2\Delta\tau_1+\frac{1}{2}\frac{\Delta a}{u_{yo}}\right) \\
- \frac{\rho_o}{u_{yo}}\left[2\cos\left(2\Delta\tau_1+\frac{1}{2}\frac{\Delta a}{u_{yo}}+\theta_o\right)+\sin\left(2\Delta\tau_1+\frac{1}{2}\frac{\Delta a}{u_{yo}}+\theta_o\right)\right] \\
- 2\left[\cos\left(\frac{1}{2}\frac{\Delta a}{u_{yo}}+\Delta\tau_1-\Delta\tau_2\right)+2\sin\left(\frac{1}{2}\frac{\Delta a}{u_{yo}}+\Delta\tau_1-\Delta\tau_2\right)\right] \\
- 2\left[\cos\left(\Delta\tau_1+\Delta\tau_2\right)+2\sin\left(\Delta\tau_1+\Delta\tau_2\right)\right] \\
+ 2\frac{\rho_o}{u_{yo}}\sin\left(\Delta\tau_1+\Delta\tau_2+\theta_o\right) \quad (5.58)
\end{aligned}
$$

where the left hand side is

$$
K_o = \frac{1}{2}\frac{1}{U_{max}^2}\left(\rho_f^2-\rho_o^2\right) - 15 + \frac{\rho_o}{u_{yo}}\left(2\cos\theta_o+\sin\theta_o\right) \quad (5.59)
$$

As it was for subcase II, this is also a function of only one variable $\Delta\tau_1$, since $\Delta\tau_2$ is function of $\Delta\tau_1$. Again, the analytical solution for this problem is not possible and must be found numerically.

The solution for the critical times cannot be obtained analytically for subcases II and III. This means that a numerical root solver must be used to calculate the control switching times.

5.3 Initial Costate

Once the critical times are solved, the initial costate can be found using the remaining necessary conditions. For the four unknowns, initial costate vector, four equations are required. The first equation is derived from the costate terminal condition. The second and third equations are derived from the control switching conditions, which are specific for each of the three subcases. The fourth equation is derived from the optimal theory

requiring that the Hamiltonian be zero. These four equations will be linear with respect to the costate vector, facilitating the calculation of the initial costate vector. They will now be presented in the order they were introduced.

The necessary condition in Chapter II provided the general terminal costate condition via Equation (2.14). Using the terminal state constraint in the form of Equation (5.13), the Jacobian with respect the terminal state was given in Equation (5.14). Therefore, the in-plane terminal costate condition becomes:

$$\boldsymbol{\lambda}^T(t_f) = \boldsymbol{\nu}^T \frac{\partial \boldsymbol{\Psi}\left(\mathbf{x}(t_f), t_f\right)}{\partial \mathbf{x}(t_f)} = \boldsymbol{\nu}^T \begin{bmatrix} 4 & 0 & 0 & 2 \\ 0 & 1 & -2 & 0 \\ 6\left(3x_f + 2\dot{y}_f\right) & 0 & 2\dot{x}_f & 4\left(3x_f + 2\dot{y}_f\right) \end{bmatrix}$$

$$\boldsymbol{\lambda}_f = \begin{bmatrix} \lambda_{xf} \\ \lambda_{yf} \\ \lambda_{\dot{x}f} \\ \lambda_{\dot{y}f} \end{bmatrix} = \begin{bmatrix} 4\nu_1 + 6(3x_f + 2\dot{y}_f)\nu_3 \\ \nu_2 \\ -2\nu_2 + 2\dot{x}_f\nu_3 \\ 2\nu_1 + 4(3x_f + 2\dot{y}_f)\nu_3 \end{bmatrix} \tag{5.60}$$

Taking advantage of the costate transition matrix, the final costate is transformed to a more suitable time; to one of the control switching times at which one of the velocity costates is known to be zero. The reason will be clear later when the initial costate is solved using a matrix inverse operator from linear algebra. So, the second switching time is chosen arbitrarily:

$$\boldsymbol{\lambda}_2 = \boldsymbol{\Phi}_\lambda^{-1}(t_f, t_2)\boldsymbol{\lambda}_f \tag{5.61}$$

This vector equation is manipulated through simple algebra, taking advantage of the costate corresponding to the in-track position being a constant. The resulting equation is linear with respect to $\boldsymbol{\lambda}_2$ and is one of the four equations required to solve for the initial costate:

$$\begin{bmatrix} \cos\left(\Delta\tau_3 - \theta(t_f)\right) & 2\sin\left(\Delta\tau_3 - \theta(t_f)\right) & \sin\left(\Delta\tau_3 - \theta(t_f)\right) & -2\cos\left(\Delta\tau_3 - \theta(t_f)\right) \end{bmatrix} \boldsymbol{\lambda}_2 = 0 \tag{5.62}$$

where $\theta(t_f)$ is not the desired final phase angle, but the resultant

$$\tan\theta(t_f) = -\frac{3x_f + 2\dot{y}_f}{\dot{x}_f} \tag{5.63}$$

The second and third equations are subcase specific and rely on the following observations about the velocity costate at the control switching time.

Subcase I. X-Control Switch Only

For this subcase, the $\lambda_{\dot{x}}(t)$ will be zero at each of the two control switching times. The costate vectors at these two times are:

$$\boldsymbol{\lambda}^T(t_1) = \begin{bmatrix} \lambda_{x1} & \lambda_{y1} & 0 & \lambda_{\dot{y}1} \end{bmatrix} \tag{5.64}$$

$$\boldsymbol{\lambda}^T(t_2) = \begin{bmatrix} \lambda_{x2} & \lambda_{y2} & 0 & \lambda_{\dot{y}2} \end{bmatrix} \tag{5.65}$$

Subcase II. X-Control Switch followed by Y-control Switch

For this subcase, the $\lambda_{\dot{x}}(t)$ will be zero at t_1 and $\lambda_{\dot{y}}(t)$ will be zero at t_2. The costate vectors at these two times are:

$$\boldsymbol{\lambda}^T(t_1) = \begin{bmatrix} \lambda_{x1} & \lambda_{y1} & 0 & \lambda_{\dot{y}1} \end{bmatrix} \tag{5.66}$$

$$\boldsymbol{\lambda}^T(t_2) = \begin{bmatrix} \lambda_{x2} & \lambda_{y2} & \lambda_{\dot{x}2} & 0 \end{bmatrix} \tag{5.67}$$

Subcase III. Y-Control Switch followed by X-control Switch

For this subcase, the $\lambda_{\dot{y}}(t)$ will be zero at t_1 and $\lambda_{\dot{x}}(t)$ will be zero at t_2. The costate

vectors at these two times are:

$$\boldsymbol{\lambda}^T(t_1) = \begin{bmatrix} \lambda_{x1} & \lambda_{y1} & \lambda_{\dot{x}1} & 0 \end{bmatrix} \tag{5.68}$$

$$\boldsymbol{\lambda}^T(t_2) = \begin{bmatrix} \lambda_{x2} & \lambda_{y2} & 0 & \lambda_{\dot{y}2} \end{bmatrix} \tag{5.69}$$

The costate vector at t_1 is transitioned to t_2 via the costate transition matrix,

$$\boldsymbol{\lambda}_1 = \boldsymbol{\Phi}_{\lambda}^{-1}(t_2, t_1)\boldsymbol{\lambda}_2 \tag{5.70}$$

The appropriate velocity costate at t_1 is then used to generate the second equation that is linear with respect to $\boldsymbol{\lambda}_2$. The third equation is either $\lambda_{\dot{x}}(t_2) = 0$ or $\lambda_{\dot{y}}(t_2) = 0$, depending on the subcase, which can also be considered linear with respect to $\boldsymbol{\lambda}_2$.

The fourth required equation comes from the Hamiltonian. The optimal theory for open final time dictates that the Hamiltonian will remain at zero, which can be readily shown. The Hamiltonian at four different times are all equivalent:

$$\begin{aligned} H_o &= 1 + \boldsymbol{\lambda}_o^T(\mathbf{A}\mathbf{x}_o + \mathbf{B}\mathbf{u}_o) = 0 \\ H_1 &= 1 + \boldsymbol{\lambda}_1^T(\mathbf{A}\mathbf{x}_1 + \mathbf{B}\mathbf{u}_1) = 0 \\ H_2 &= 1 + \boldsymbol{\lambda}_2^T(\mathbf{A}\mathbf{x}_2 + \mathbf{B}\mathbf{u}_2) = 0 \\ H_f &= 1 + \boldsymbol{\lambda}_f^T(\mathbf{A}\mathbf{x}_f + \mathbf{B}\mathbf{u}_2) = 0 \end{aligned} \tag{5.71}$$

where $\mathbf{u}_f = \mathbf{u}_2$ has been used. All of these equation are linear with respect to costate vector.[6] However, since the aim is to find an equation that in linear with respect to $\boldsymbol{\lambda}_2$, H_2 is chosen from above. When the H_2 is written out explicitly, the last required equation is obtained:

$$\dot{x}_2\lambda_{x2} + \dot{y}_2\lambda_{y2} + (3x_2 + 2\dot{y}_2 + u_{x2})\,\lambda_{\dot{x}2} + (-2\dot{x}_2 + u_{y2})\,\lambda_{\dot{y}2} = -1 \tag{5.72}$$

[6]For a scalar equation, $\boldsymbol{\lambda}^T(\mathbf{A}\mathbf{x} + \mathbf{B}\mathbf{u}) = (\mathbf{A}\mathbf{x} + \mathbf{B}\mathbf{u})^T\boldsymbol{\lambda}$.

All four equations needed to calculate the costate at t_2 have been derived. The four Equations (5.62), (5.70), (5.72), and the appropriate velocity costate at t_2 are put into a matrix form so that $\boldsymbol{\lambda}_2$ can be solved using linear algebra:

$$\boldsymbol{\Lambda} \begin{bmatrix} \lambda_{x2} \\ \lambda_{y2} \\ \lambda_{\dot{x}2} \\ \lambda_{\dot{y}2} \end{bmatrix} = \begin{bmatrix} -1 \\ \lambda_{\dot{x}1} \\ \lambda_{\dot{y}1} \\ 0 \end{bmatrix} \tag{5.73}$$

where $\boldsymbol{\Lambda}$ is

$$\begin{bmatrix} \dot{x}_2 & \dot{y}_2 & 3x_2 + 2\dot{y}_2 + u_{x2} & -2\dot{x}_2 + u_{y2} \\ \sin\Delta\tau_2 & 2\left(\cos\Delta\tau_2 - 1\right) & \cos\Delta\tau_2 & -2\sin\Delta\tau_2 \\ 2\left(1 - \cos\Delta\tau_2\right) & 4\sin\Delta\tau_2 - 3\Delta\tau_2 & 2\sin\Delta\tau_2 & 4\cos\Delta\tau_2 - 3 \\ \cos(\Delta\tau_3 - \theta(t_f)) & 2\sin(\Delta\tau_3 - \theta(t_f)) & \sin(\Delta\tau_3 - \theta(t_f)) & -2\cos(\Delta\tau_3 - \theta(t_f)) \end{bmatrix} \tag{5.74}$$

The reason for choosing to determine the costate at one of the switching times is now clear. Since one of the costates at t_2 is zero, the four equations can be reduced to three equations and three unknowns; i.e., a 3x3 matrix inversion is easier than a 4x4 matrix inversion. The results for the three subcases are now presented.

Subcase I. X-Control Switch Only

Using the transversality condition, setting the $\lambda_{\dot{x}1}$ equation to zero, and using the terminal boundary condition, along with $\lambda_{\dot{x}2} = 0$,

$$\begin{bmatrix} \dot{x}_2 & \dot{y}_2 & -2\dot{x}_2 + u_{y2} \\ \sin\Delta\tau_2 & 2\left(\cos\Delta\tau_2 - 1\right) & -2\sin\Delta\tau_2 \\ \cos(\Delta\tau_3 - \theta(t_f)) & 2\sin(\Delta\tau_3 - \theta(t_f)) & -2\cos(\Delta\tau_3 - \theta(t_f)) \end{bmatrix} \begin{bmatrix} \lambda_{x2} \\ \lambda_{y2} \\ \lambda_{\dot{y}2} \end{bmatrix} = \begin{bmatrix} -1 \\ 0 \\ 0 \end{bmatrix} \tag{5.75}$$

Performing the linear algebra,

$$\begin{bmatrix} \lambda_{x2} \\ \lambda_{y2} \\ \lambda_{\dot{y}2} \end{bmatrix} = -\frac{1}{u_{yo}} \begin{bmatrix} 2 \\ 0 \\ 1 \end{bmatrix} \tag{5.76}$$

This implies that $\lambda_y(t) = \lambda_{y2} = 0$ for all time. Consequently, $\lambda_{\dot{x}}(t)$ will be a pure sinusoid and $\lambda_{\dot{y}}(t)$ will not have a ramp term; i.e., it will be a pure sinusoid with a constant offset. So, in order for the y-control not to switch, the final time must be short enough that $\lambda_{\dot{y}}(t)$ does not cross zero for all $t \in [0, t_f]$, or the magnitude of the sinusoid be smaller than the offset. However, earlier in Section 3.2.2, the discussion made it clear that two consecutive x-control switchings cannot occur without a y-control switching between these two times when $\lambda_{\dot{y}}(t)$ does not have the ramp term. In other words, there must be a y-crossing between two x-crossings due to the phasing of $\lambda_{\dot{x}}(t)$ and $\lambda_{\dot{y}}(t)$. Therefore, this subcase is not a viable subcase for $N = 2$, even for $\Delta a \neq 0$.

Subcase II. X-Control Switch followed by Y-control Switch

Using the transversality condition, setting $\lambda_{\dot{x}1}$ to zero, and the terminal boundary condition, along with $\lambda_{\dot{y}2} = 0$,

$$\begin{bmatrix} \dot{x}_2 & \dot{y}_2 & 3x_2 + 2\dot{y}_2 + u_{x2} \\ \sin\Delta\tau_2 & 2\left(\cos\Delta\tau_2 - 1\right) & \cos\Delta\tau_2 \\ \cos(\Delta\tau_3 - \theta(t_f)) & 2\sin(\Delta\tau_3 - \theta(t_f)) & \sin(\Delta\tau_3 - \theta(t_f)) \end{bmatrix} \begin{bmatrix} \lambda_{x2} \\ \lambda_{y2} \\ \lambda_{\dot{x}2} \end{bmatrix} = \begin{bmatrix} -1 \\ 0 \\ 0 \end{bmatrix} \tag{5.77}$$

Performing the linear algebra,

$$\begin{bmatrix} \lambda_{x2} \\ \lambda_{y2} \\ \lambda_{\dot{x}2} \end{bmatrix} = \frac{1}{D} \begin{bmatrix} -2\sin\left(\Delta\tau_3 - \theta(t_f)\right) \\ \cos\left(\Delta\tau_2 + \Delta\tau_3 - \theta(t_f)\right) \\ 2\cos\left(\Delta\tau_3 - \theta(t_f)\right) - 2\cos\left(\Delta\tau_2 + \Delta\tau_3 - \theta(t_f)\right) \end{bmatrix} \tag{5.78}$$

where D is a modified determinant:

$$\begin{aligned} D &= 2\left(3x_2 + 2\dot{y}_2 - u_{xo}\right)\cos\left(\Delta\tau_3 - \theta(t_f)\right) - 2\dot{x}_2\sin\left(\Delta\tau_3 - \theta(t_f)\right) \\ &\quad - \left(6x_2 + 3\dot{y}_2 - 2u_{xo}\right)\cos\left(\Delta\tau_2 + \Delta\tau_3 - \theta(t_f)\right) \end{aligned} \tag{5.79}$$

$\boldsymbol{\lambda}_2$ is now known,

$$\boldsymbol{\lambda}_2^T = \frac{1}{D}\begin{bmatrix} -2\sin\left(\Delta\tau_3 - \theta(t_f)\right) \\ \cos\left(\Delta\tau_2 + \Delta\tau_3 - \theta(t_f)\right) \\ 2\cos\left(\Delta\tau_3 - \theta(t_f)\right) - 2\cos\left(\Delta\tau_2 + \Delta\tau_3 - \theta(t_f)\right) \\ 0 \end{bmatrix} \tag{5.80}$$

No other conclusion is made about this subcase.

Subcase III. Y-Control Switch followed by X-control Switch

Using the transversality condition, setting $\lambda_{\dot{y}1}$ equation to zero, and the terminal boundary condition, along with $\lambda_{\dot{x}2} = 0$,

$$\begin{bmatrix} \dot{x}_2 & \dot{y}_2 & -2\dot{x}_2 + u_{y2} \\ 2\left(1 - \cos\Delta\tau_2\right) & 4\sin\Delta\tau_2 - 3\Delta\tau_2 & 4\cos\Delta\tau_2 - 3 \\ \cos(\Delta\tau_3 - \theta(t_f)) & 2\sin(\Delta\tau_3 - \theta(t_f)) & -2\sin(\Delta\tau_3 - \theta(t_f)) \end{bmatrix}\begin{bmatrix} \lambda_{x2} \\ \lambda_{y2} \\ \lambda_{\dot{y}2} \end{bmatrix} = \begin{bmatrix} -1 \\ 0 \\ 0 \end{bmatrix} \tag{5.81}$$

Performing the linear algebra,

$$\begin{bmatrix} \lambda_{x2} \\ \lambda_{y2} \\ \lambda_{\dot{y}2} \end{bmatrix} = \frac{1}{D}\begin{bmatrix} -6\Delta\tau_2\cos\left(\Delta\tau_3 - \theta(t_f)\right) - 6\sin\left(\Delta\tau_3 - \theta(t_f)\right) + 8\sin\left(\Delta\tau_2 + \Delta\tau_3 - \theta(t_f)\right) \\ -\cos\left(\Delta\tau_3 - \theta(t_f)\right) \\ -3\Delta\tau_2\cos\left(\Delta\tau_3 - \theta(t_f)\right) - 4\sin\left(\Delta\tau_3 - \theta(t_f)\right) + 4\sin\left(\Delta\tau_2 + \Delta\tau_3 - \theta(t_f)\right) \end{bmatrix} \tag{5.82}$$

where D is the modified determinant:

$$\begin{aligned} D &= (2\dot{y}_2 - 3u_{yo}\Delta\tau_2)\cos(\Delta\tau_3 - \theta(t_f)) \\ &\quad -2(2u_{yo} + \dot{x}_2)\sin(\Delta\tau_3 - \theta(t_f)) + 4u_{yo}\sin(\Delta\tau_2 + \Delta\tau_3 - \theta(t_f)) \end{aligned} \tag{5.83}$$

$\boldsymbol{\lambda}_2$ is now known,

$$\boldsymbol{\lambda}_2^T = \frac{1}{D}\begin{bmatrix} -6\Delta\tau_2\cos(\Delta\tau_3 - \theta(t_f)) - 6\sin(\Delta\tau_3 - \theta(t_f)) + 8\sin(\Delta\tau_2 + \Delta\tau_3 - \theta(t_f)) \\ -\cos(\Delta\tau_3 - \theta(t_f)) \\ 0 \\ -3\Delta\tau_2\cos(\Delta\tau_3 - \theta(t_f)) - 4\sin(\Delta\tau_3 - \theta(t_f)) + 4\sin(\Delta\tau_2 + \Delta\tau_3 - \theta(t_f)) \end{bmatrix} \tag{5.84}$$

The calculation of initial costate then requires the use of the costate transition matrix one more time:

$$\boldsymbol{\lambda}_o = \boldsymbol{\Phi}_\lambda^{-1}(t_2, 0)\boldsymbol{\lambda}_2 \tag{5.85}$$

For the two viable subcases, the initial control pair can be either $+1$ or -1, but not both. This means the initial control options are reduced to two. Therefore, these calculations must be performed twice to ensure the signs correspond to

$$u_{xo} = -sgn\{\lambda_{\dot{x}o}\}U_{max} \tag{5.86a}$$

$$u_{yo} = -sgn\{\lambda_{\dot{y}o}\}U_{max} \tag{5.86b}$$

In Appendix D, a special $N = 2$ case is presented for the problem of maneuvering from one stable and centered orbit to another. When Δa and Δb are zero, all three subcases are not viable options. The solution did not exist for $\Delta a = 0 = \Delta b$. Therefore, to increase the solution space, initial coasting on a stable relative orbit is examined in Chapter VI.

5.4 Minimum Time XY-Motion: Generalization

In this section, the generalization for $N > 3$ for the in-plane problem is presented. For a general N, both the x-control and the y-control are switching alternatively ad infinitum (until t_f). Although there are $N + 1$ time intervals, the critical times can be reduced to just four. Remaining time intervals are functions of these first four due to regular periodicity. For example, the x-control switching times are periodic; $t_{x(i+2)} = t_{xi} + 2\pi$. Four general equations corresponding to the four relative orbit parameters are as follows:

– From the drifting equation,

$$0 = \frac{1}{2}\frac{\Delta a}{u_{yo}} + \sum_{i=1}^{N+1} \frac{u_{y(i-1)}}{u_{yo}} \Delta\tau_i \tag{5.87}$$

It is interesting to note the absence of u_x term. This make physical sense since the drift is in the in-track (or y) direction.

– From the centering equation,

$$\begin{aligned} 0 = \frac{\Delta b}{u_{yo}} - 2\frac{u_{xo}}{u_{yo}} \left(\sum_{i=1}^{N+1} \frac{u_{x(i-1)}}{u_{xo}} \Delta\tau_i \right) - \frac{3}{2}\frac{a_o}{u_{yo}} t_f \\ + \frac{3}{2} \left[\left(\sum_{i=1}^{N} \frac{\Delta u_{yi}}{u_{yo}} (t_f - t_i)^2 \right) - t_f^2 \right] \end{aligned} \tag{5.88}$$

where $t_f = \sum_{i=1}^{N+1} \Delta\tau_i$. After substituting in the drifting equation, this equation can be expressed as a quadratic in one of the remaining time intervals.

– From the phase angle equation,

$$\begin{aligned} \frac{\rho_o}{u_{yo}} \sin(t_f - \Delta_\theta) = -\frac{u_{xo}}{u_{yo}}\frac{u_{xN}}{u_{xo}} \cos\theta_f + 2\frac{u_{yN}}{u_{yo}} \sin\theta_f + \frac{u_{xo}}{u_{yo}} \cos(t_f - \theta_f) + 2\sin(t_f - \theta_f) \\ - \sum_{i=1}^{N} \left[\frac{u_{xo}}{u_{yo}}\frac{\Delta_{uxi}}{u_{xo}} \cos\left(\sum_{j=1}^{i} t_f - \Delta\tau_j - \theta_f \right) + 2\frac{\Delta_{uyi}}{u_{yo}} \sin\left(\sum_{j=1}^{i} t_f - \Delta\tau_j - \theta_f \right) \right] \end{aligned} \tag{5.89}$$

which, along with the relative size equation, must be solved numerically for the remaining two critical time intervals.

– From the relative size equation,

$$
\begin{aligned}
\frac{\rho_f^2 - \rho_o^2}{U_{max}^2} &= 10 + \sum_{i=1}^{N} \left[\left(\frac{\Delta_{uxi}}{u_{xo}} \right)^2 + 4 \left(\frac{\Delta_{uyi}}{u_{yo}} \right)^2 \right] \\
&\quad - 2\frac{\rho_o}{u_{yo}} \left(2\cos\theta_o + \frac{u_{xo}}{u_{yo}} \sin\theta_o \right) \\
&\quad + 2\frac{\rho_o}{u_{yo}} \sum_{i=1}^{N+1} \left[2\frac{\Delta_{uy(i-1)}}{u_{yo}} \cos\left(\sum_{j=1}^{i} \Delta\tau_j + \theta_o \right) + \frac{u_{xo}}{u_{yo}} \frac{\Delta_{ux(i-1)}}{u_{xo}} \sin\left(\sum_{j=1}^{i} \Delta\tau_j + \theta_o \right) \right] \\
&\quad - 2\sum_{i}^{N+1} \left(\frac{\Delta_{ux(i-1)}}{u_{xo}} + 4\frac{\Delta_{uy(i-1)}}{u_{yo}} \right) \cos\left(\sum_{j=1}^{i} \Delta\tau_j \right) \\
&\quad + 4\frac{u_{xo}}{u_{yo}} \left(\frac{\Delta_{uyi}}{u_{yo}} - \frac{\Delta_{uxi}}{u_{xo}} \right) \sin\left(\sum_{j=1}^{i} \Delta\tau_j \right) \\
&\quad + 2\sum_{k=2}^{N} \sum_{i=k}^{N+1} \left(\frac{\Delta_{ux(k-1)}}{u_{xo}} \frac{\Delta_{ux(i-1)}}{u_{xo}} + 4\frac{\Delta_{uy(k-1)}}{u_{yo}} \frac{\Delta_{uy(i-1)}}{u_{yo}} \right) \cos\left(\sum_{j=k}^{i} \Delta\tau_j \right) \\
&\quad + 4\frac{u_{xo}}{u_{yo}} \sum_{k=2}^{N} \sum_{i=k}^{N+1} \left(\frac{\Delta_{uy(k-1)}}{u_{yo}} \frac{\Delta_{ux(i-1)}}{u_{xo}} - \frac{\Delta_{ux(k-1)}}{u_{xo}} \frac{\Delta_{uy(i-1)}}{u_{yo}} \right) \sin\left(\sum_{j=k}^{i} \Delta\tau_j \right) \\
&\quad + 2\left(\frac{u_{xN}}{u_{xo}} \frac{\Delta_{uxN}}{u_{xo}} + 4\frac{u_{yN}}{u_{yo}} \frac{\Delta_{uyN}}{u_{yo}} \right) \cos\Delta\tau_{N+1} \\
&\quad + 4\frac{u_{xo}}{u_{yo}} \left(\frac{u_{xN}}{u_{xo}} \frac{\Delta_{uyN}}{u_{yo}} - \frac{u_{yN}}{u_{yo}} \frac{\Delta_{uxN}}{u_{xo}} \right) \sin\Delta\tau_{N+1}
\end{aligned}
\tag{5.90}
$$

The amount of relative orbit size change that can be achieved by N control switches can be estimated using the relative size equation. After substituting the phase angle equation into the relative size equation, all of the trigonometric sines and cosines can be bounded by unity. Then by use of the triangular inequality, an upper bound can be obtained [7] for the maximum relative size change that can be achieved with N control switches.

[7] The lower bound can be similarly found by using negative one for each of the sines and cosines.

Now, some general comments are summarized for the in-plane minimum time problem.

1. Finding the optimal control entails finding the critical switching times. These critical times are a function of initial and final relative orbit parameters. Existence of a solution is not guaranteed for arbitrary initial and final relative orbit parameters for a fixed value of N, especially when the target set is a fixed point (vector) in $\mathbb{R}^4$. The solution space is increased when the target set is the entire stable orbit of desired size. The solution is guaranteed to exist, however, for some optimal N^*. Now the question is, how is this N^* obtained for a given initial and final relative orbit parameters? The suggested approach is to chain together several reconfiguration problems ($N = 3$ case) until the final relative orbit can be reached. This approach relies on Bellman's "Optimality Principle" [51:pages 13 and 30].
2. This analytical approach transforms the original two point boundary value problem (TPBVP) into that of finding roots of simultaneous nonlinear equations. This approach still has a problem of the sensitivity of the solution to the initial guess. However, the analysis provides some insight. The range of valid time intervals is required to be non-negative. In addition, the upper bound on the time intervals is also known to be less than π. So, the initial guesses of the two time intervals should start with $\pi/2$.
3. When starting on a stable (non-drifting; i.e., $a_o = 0$) orbit, it may be possible to wait (coast) up to one orbit before maneuvering. Allowing this control-free coasting will increase the solution space, as was discussed for the out-of-plane motion. The difficulty with the in-plane motion is that the reachable set in $\mathbb{R}^4$ is difficult to visualize.

5.5 Summary

In this chapter the results for the in-plane minimum time problem was presented. Next chapter presents the solution to the same minimum-time problem in which the

satellite is initially on a stable orbit and is allowed to coast (control-free) up to 2π canonical units of time before the bang-bang control is applied.

VI. Optimal Time Control of Satellite Formation with Initial Coasting

In view of the previous chapters in which the control was applied at the initial time, waiting (or coasting) before maneuvering will increase the solution space. It is better known in the optimal theory as a corner condition [44]. In practical cases, maneuvers are from one stable orbit to another. In this scenario, there may be a better (in terms of fuel and time) initial phase angle to start the maneuver. In addition, allowing this new degree of freedom reduces the number of subcases required to incorporate all of the final relative orbit parameters. There are only three subcases when $N = 2$ for the problem admitting "initial coasting".

6.1 Necessary Conditions for the "Corner"

The additional state constraints are now placed at the corner or at $t = t_c$ where the coasting stops and enters the controlled arc. The corner constraint $\boldsymbol{\Theta}$ is

$$\boldsymbol{\Theta}(\mathbf{x}(t_c), t_c) = \begin{bmatrix} 4x(t_c) + 2\dot{y}(t_c) - a_o \\ y(t_c) - 2\dot{x}(t_c) - b_o \\ (3x(t_c) + 2\dot{y}(t_c))^2 + \dot{x}^2(t_c) - \rho_o^2 \end{bmatrix} = \mathbf{0} \tag{6.1}$$

where $a_c = a_o$, $b_c = b_o$, and $\rho_c = \rho_o$ since for a stable initial orbit, only the phase angle changes during the coasting arc. The addition of this constraint into the performance index generates two new necessary conditions:

$$H(t_{c+}) - H(t_{c-}) = \boldsymbol{\mu}^T \frac{\partial \boldsymbol{\Theta}\left(\mathbf{x}(t_c), t_c\right)}{\partial t_c} \tag{6.2}$$

$$\boldsymbol{\lambda}^T(t_{c+}) - \boldsymbol{\lambda}^T(t_{c-}) = -\boldsymbol{\mu}^T \frac{\partial \boldsymbol{\Theta}\left(\mathbf{x}(t_c), t_c\right)}{\partial \mathbf{x}(t_c)} \tag{6.3}$$

$\boldsymbol{\mu}$ is the constant Lagrange multiplier associated with corner state constraint. See Appendix F for details.

Closer examination of these two new conditions is warranted:

$$\frac{\partial \boldsymbol{\Theta}\left(\mathbf{x}(t_c), t_c\right)}{\partial t_c} = \begin{bmatrix} 0 \\ 0 \\ 0 \end{bmatrix} \tag{6.4}$$

since the initial orbit is assumed to be stable. This means the Hamiltonian will be continuous at t_c and $H(t) = 0 \; \forall \; t \in [t_o, t_f]$. However, the costate will not be continuous at t_c because

$$\frac{\partial \boldsymbol{\Theta}\left(\mathbf{x}(t_c), t_c\right)}{\partial \mathbf{x}(t_c)} = \begin{bmatrix} 4 & 0 & 0 & 2 \\ 0 & 1 & -2 & 0 \\ 6(3x(t_c) + 2\dot{y}(t_c)) & 0 & 2\dot{x}(t_c) & 3(3x(t_c) + 2\dot{y}(t_c)) \end{bmatrix} \tag{6.5}$$

is not a zero matrix. Then,

$$\boldsymbol{\lambda}^T(t_{c-}) = \boldsymbol{\lambda}^T(t_{c+}) + \boldsymbol{\mu}^T \frac{\partial \boldsymbol{\Theta}\left(\mathbf{x}(t_c), t_c\right)}{\partial \mathbf{x}(t_c)} \tag{6.6}$$

$$\boldsymbol{\lambda}(t_o) = \Phi_\lambda^{-1}(t_c, 0)\boldsymbol{\lambda}(t_{c-}) \tag{6.7}$$

The method/approach to calculate $\boldsymbol{\lambda}^T(t_{c+})$ is the same, but it now requires the calculation of $\boldsymbol{\mu}$ to get the initial costate. However, since $\mathbf{u}(t) = \mathbf{0}$ is assumed for $t \leq t_{c-}$, there is really no need to calculate $\boldsymbol{\lambda}_o$. Therefore the inability to calculate $\boldsymbol{\mu}$ does not hinder finding the optimal controller.

6.2 In-Plane Minimum Time Control with Initial Coasting for $N = 2$

The $N = 2$ case for the problem with initial coasting will be presented in this section. The analysis is very similar to that in Section 5.2 with slight modification of notation and introduction of a new time interval $\Delta\tau_o = t_c$.

The controls for the case of initial coasting are piecewise constant:

$$\mathbf{u}(t) = \begin{cases} \mathbf{0}, & 0 \le t \le t_{c-} \\ \mathbf{u}_c, & t_{c+} \le t < t_1 \\ \mathbf{u}_1, & t_1 \le t < t_2 \\ \mathbf{u}_2, & t_2 \le t \le t_f \end{cases} \tag{6.8}$$

where t_c is the end of initial coasting and t_1 and t_2 are control switching times. The four possible choices for the control at t_c are

$$\mathbf{u}_c = \begin{bmatrix} u_{xc} \\ u_{yc} \end{bmatrix} \in \left\{ \begin{bmatrix} U_{max} \\ U_{max} \end{bmatrix}, \begin{bmatrix} U_{max} \\ -U_{max} \end{bmatrix}, \begin{bmatrix} -U_{max} \\ U_{max} \end{bmatrix}, \begin{bmatrix} -U_{max} \\ -U_{max} \end{bmatrix} \right\} \tag{6.9}$$

The explicit state solution at time $t > t_2$ using the above control is

$$\begin{aligned} \mathbf{x}(t) = & \begin{bmatrix} \rho_o \sin(t+\theta_o) + a_o \\ 2\rho_o \cos(t+\theta_o) - \frac{3}{2}a_o t + b_o \\ \rho_o \cos(t+\theta_o) \\ -2\rho_o \sin(t+\theta_o) - \frac{3}{2}a_o \end{bmatrix} + \left[\int_{t_c}^{t_1} \mathbf{\Phi}_x(t,\tau)\mathbf{B}d\tau \right] \begin{bmatrix} u_{xc} \\ u_{yc} \end{bmatrix} \\ & + \left[\int_{t_1}^{t_2} \mathbf{\Phi}_x(t,\tau)\mathbf{B}d\tau \right] \begin{bmatrix} u_{x1} \\ u_{y1} \end{bmatrix} + \left[\int_{t_2}^{t} \mathbf{\Phi}_x(t,\tau)\mathbf{B}d\tau \right] \begin{bmatrix} u_{x2} \\ u_{y2} \end{bmatrix} \end{aligned} \tag{6.10}$$

6.3 Critical Times Calculations

An analysis similar to the problem without initial coasting is used to calculate the critical times using the relative orbit parameters a, b, and ρ. The four critical times are now t_c, t_1, t_2, and t_f.

First, the drifting parameter, $a(t)$, equation is solved at t_f:

$$a(t_f) = a_o + 2u_{yo}\Delta\tau_1 + 2u_{y1}\Delta\tau_2 + 2u_{y2}\Delta\tau_3 \tag{6.11}$$

where $\Delta\tau_o = t_c$, $\Delta\tau_1 = t_1 - t_c$, $\Delta\tau_2 = t_2 - t_1$, and $\Delta\tau_3 = t_f - t_2$, and $t_f = \Delta\tau_o + \Delta\tau_1 + \Delta\tau_2 + \Delta\tau_3$. Once again, the time intervals are used rather than the absolute times. Notice the lack of $\Delta\tau_o$ in the equation. This equation is identical to Equation (5.18). This means Equation (5.19), which was used to solve $\Delta\tau_3$ in terms of $\Delta\tau_1$ and $\Delta\tau_2$, remains valid. Furthermore, the analysis for each of the subcases is identical to those in Section 5.2, except that the statements regarding t_f is now for $(t_f - t_c)$. For example, the final time for Subcase I in Section 5.2 was given as

$$t_f = -\frac{1}{2}\frac{\Delta a}{u_{yo}} \tag{6.12}$$

which means for the problem with initial coasting:

$$t_f - t_c = -\frac{1}{2}\frac{\Delta a}{u_{yo}} \tag{6.13}$$

Analysis of the drifting parameter, similar to that in Section 5.2, provides the same insight into the possible initial y-control as a function of Δa. Subcase I is still not a viable option when $\Delta a = 0$.

Next, the centering parameter, $b(t)$, equation is examined at t_f:

$$b(t_f) = y(t_f) - 2\dot{x}(t_f) \tag{6.14}$$

which, after substituting in the Equation (5.20), allows $\Delta\tau_2$ to be solved in terms of $\Delta\tau_1$ (or, vice versa),

$$\begin{aligned}
& \left(\frac{u_{y2}}{u_{yo}} - \frac{u_{y1}}{u_{yo}}\right)\Delta\tau_2^2 \\
+ \; & \left[\frac{u_{xo}}{u_{yo}}\left(\frac{u_{x2}}{u_{xo}}\frac{u_{y1}}{u_{yo}}\frac{u_{y2}}{u_{yo}} - \frac{u_{x1}}{u_{xo}}\right)\frac{4}{3} + \left(\frac{u_{y1}}{u_{yo}}\frac{u_{y2}}{u_{yo}} - 1\right)\frac{a_o}{u_{yo}} + \left(\frac{u_{y1}}{u_{yo}}\frac{u_{y2}}{u_{yo}} - 1\right)2\Delta\tau_1\right]\Delta\tau_2 \\
+ \; & \left(\frac{u_{y2}}{u_{yo}} - 1\right)\Delta\tau_1^2 + \left[\frac{u_{xo}}{u_{yo}}\left(\frac{u_{x2}}{u_{xo}}\frac{u_{y2}}{u_{yo}} - 1\right)\frac{4}{3} + \frac{a_o}{u_{yo}}\left(\frac{u_{y2}}{u_{yo}} - 1\right)\right]\Delta\tau_1 - \frac{a_o}{u_{yo}}\Delta\tau_o \\
+ \; & \frac{2}{3}\frac{u_{y2}}{u_{yo}}\left(\frac{u_{xo}}{u_{yo}}\frac{u_{x2}}{u_{xo}} + \frac{3}{8}\frac{(a_o + a_f)}{u_{yo}}\right)\frac{\Delta a}{u_{yo}} + \frac{2}{3}\frac{\Delta b}{u_{yo}} = 0
\end{aligned} \tag{6.15}$$

where $\Delta b = b_o - b_f$. Notice the new term containing $\Delta\tau_o$. The analysis which parallels the one in Section 5.2 has been performed. The discriminant of this quadratic function must be non-negative in order for a physically meaningful time interval; i.e., no complex time intervals.

Next to be examined is the relative orbit size parameter, $\rho(t)$ at t_f:

$$\rho^2(t_f) = [x(t_f) - a(t_f)]^2 + \dot{x}^2(t_f) \tag{6.16}$$

Expressing this equation with $\rho(t_f) = \rho_f$,

$$\begin{aligned}
\frac{\rho_f^2 - \rho_o^2}{2U_{max}^2} = 5 &+ \frac{1}{2}\left(\frac{\Delta u_{x1}}{u_{xo}}\right)^2 + \frac{1}{2}\left(\frac{\Delta u_{x2}}{u_{xo}}\right)^2 + 2\left(\frac{\Delta u_{y1}}{u_{yo}}\right) + 2\left(\frac{\Delta u_{y2}}{u_{yo}}\right)^2 \\
&- 2\frac{\rho_o}{u_{yo}}\cos(\Delta\tau_o + \theta_o) - \frac{u_{xo}}{u_{yo}}\frac{\rho_o}{u_{yo}}\sin(\Delta\tau_o + \theta_o) \\
&+ \frac{\Delta u_{y1}}{u_{yo}}2\frac{\rho_o}{u_{yo}}\cos(\Delta\tau_o + \Delta\tau_1 + \theta_o) + \frac{u_{xo}}{u_{yo}}\frac{\Delta u_{x1}}{u_{xo}}\frac{\rho_o}{u_{yo}}\sin(\Delta\tau_o + \Delta\tau_1 + \theta_o) \\
&- \left(\frac{\Delta u_{x1}}{u_{xo}} + \frac{\Delta u_{y1}}{u_{yo}}4\right)\cos\Delta\tau_1 + \frac{u_{xo}}{u_{yo}}\left(\frac{\Delta u_{y1}}{u_{yo}} - \frac{\Delta u_{x1}}{u_{xo}}\right)2\sin\Delta\tau_1 \\
&+ \left(\frac{\Delta u_{x1}}{u_{xo}}\frac{\Delta u_{x2}}{u_{xo}} + \frac{\Delta u_{y1}}{u_{yo}}\frac{\Delta u_{y2}}{u_{yo}}4\right)\cos\Delta\tau_2 + \frac{u_{xo}}{u_{yo}}\left(\frac{\Delta u_{y1}}{u_{yo}}\frac{\Delta u_{x2}}{u_{xo}} - \frac{\Delta u_{x1}}{u_{xo}}\frac{\Delta u_{y2}}{u_{yo}}\right)2\sin\Delta\tau_2 \\
&+ \left(\frac{u_{x2}}{u_{xo}}\frac{\Delta u_{x2}}{u_{xo}} + \frac{u_{y2}}{u_{yo}}\frac{\Delta u_{y2}}{u_{yo}}4\right)\cos\Delta\tau_3 + \frac{u_{xo}}{u_{yo}}\left(\frac{u_{x2}}{u_{xo}}\frac{\Delta u_{y2}}{u_{yo}} - \frac{u_{y2}}{u_{yo}}\frac{\Delta u_{x2}}{u_{xo}}\right)2\sin\Delta\tau_3 \\
&- \left(\frac{\Delta u_{x2}}{u_{xo}} + \frac{\Delta u_{y2}}{u_{yo}}4\right)\cos(\Delta\tau_1 + \Delta\tau_2) + \frac{u_{xo}}{u_{yo}}\left(\frac{\Delta u_{y2}}{u_{yo}} - \frac{\Delta u_{x2}}{u_{xo}}\right)2\sin(\Delta\tau_1 + \Delta\tau_2) \\
&+ \frac{\Delta u_{y2}}{u_{yo}}2\frac{\rho_o}{u_{yo}}\cos(\Delta\tau_o + \Delta\tau_1 + \Delta\tau_2 + \theta_o) + \frac{u_{xo}}{u_{yo}}\frac{\Delta u_{x2}}{u_{xo}}\frac{\rho_o}{u_{yo}}\sin(\Delta\tau_o + \Delta\tau_1 + \Delta\tau_2 + \theta_o) \\
&+ \left(\frac{u_{x2}}{u_{xo}}\frac{\Delta u_{x1}}{u_{xo}} + \frac{u_{y2}}{u_{yo}}\frac{\Delta u_{y1}}{u_{yo}}4\right)\cos(\Delta\tau_2 + \Delta\tau_3) + \frac{u_{xo}}{u_{yo}}\left(\frac{u_{x2}}{u_{xo}}\frac{\Delta u_{y1}}{u_{yo}} - \frac{u_{y2}}{u_{yo}}\frac{\Delta u_{x1}}{u_{xo}}\right)2\sin(\Delta\tau_2 + \Delta\tau_3) \\
&- \left(\frac{u_{x2}}{u_{xo}} + \frac{u_{y2}}{u_{yo}}4\right)\cos(\Delta\tau_1 + \Delta\tau_2 + \Delta\tau_3) + \frac{u_{xo}}{u_{yo}}\left(\frac{u_{y2}}{u_{yo}} - \frac{u_{x2}}{u_{xo}}\right)2\sin(\Delta\tau_1 + \Delta\tau_2 + \Delta\tau_3) \\
&+ \frac{u_{y2}}{u_{yo}}2\frac{\rho_o}{u_{yo}}\cos(t_f + \theta_o) + \frac{u_{xo}}{u_{yo}}\frac{u_{x2}}{u_{xo}}\frac{\rho_o}{u_{yo}}\sin(t_f + \theta_o)
\end{aligned} \tag{6.17}$$

which becomes a nonlinear function of a variables, $\Delta\tau_o$ and $\Delta\tau_1$, after substituting in Equations (5.20) and (6.15) and does not lend itself to further reduction or analytical solution.

The calculation of the critical times requires slight modification. The assumption of stable initial orbit, $a_o = 0$, means that the first time interval, $\Delta\tau_o = t_c$, is limited to $[0, 2\pi]$ because the conditions are periodic. Equation (6.17) then becomes a function of $\Delta\tau_1$ only after substitution of the drifting and centering equations. The numerical solution is formed by sweeping $\Delta\tau_o$ from zero to 2π. For each $\Delta\tau_o$, determine $\Delta\tau_1$'s that satisfy Equation (6.17). Then, use the one that minimizes the overall final time.

Finally, the last relative orbit parameter, the phase angle parameter, $\theta(t_f)$, can be calculated using:

$$\tan\theta(t_f) = \frac{x(t_f) - a(t_f)}{\dot{x}(t_f)} = -\frac{3x(t_f) + 2\dot{y}(t_f)}{\dot{x}(t_f)} \tag{6.18}$$

6.4 Initial Costate Vector

The costate at t_2 is calculated using identical equations from Section 5.3. The analysis continues with the understanding that $\boldsymbol{\lambda}_2$ is known. The costate at t_{c+} is first calculated using

$$\boldsymbol{\lambda}_{c+} = \Phi_\lambda^{-1}(t_2, t_c)\boldsymbol{\lambda}_2 \tag{6.19}$$

In Equation (6.1),

$$\Delta H(t_c) \;=\; H(t_{c+}) - H(t_{c-}) = \boldsymbol{\mu}^T \frac{\partial \boldsymbol{\Theta}\left(\mathbf{x}(t_c), t_c\right)}{\partial t_c} = 0 \tag{6.20}$$

$$\Delta\boldsymbol{\lambda}^T(t_c) \;=\; \boldsymbol{\lambda}^T(t_{c+}) - \boldsymbol{\lambda}^T(t_{c-}) = -\boldsymbol{\mu}^T \frac{\partial \boldsymbol{\Theta}\left(\mathbf{x}(t_c), t_c\right)}{\partial \mathbf{x}(t_c)} \tag{6.21}$$

the second partial derivative, $\partial\boldsymbol{\Theta}(\mathbf{x}(t_c), t_c)/\partial\mathbf{x}(t_c)$, is not zero. Consequently, the costate will not be continuous across t_c.

$$\boldsymbol{\lambda}_{c-}^T = \boldsymbol{\lambda}_{c+}^T + \boldsymbol{\mu}^T \frac{\partial \boldsymbol{\Theta}\left(\mathbf{x}(t_c), t_c\right)}{\partial \mathbf{x}(t_c)}$$

However, the control Hamiltonian remains continuous at the corner:

$$\begin{aligned}
H(t_{c+}) &= H(t_{c-}) \\
1+\boldsymbol{\lambda}^T(t_{c+})[\mathbf{A}\mathbf{x}(t_{c+})+\mathbf{B}\mathbf{u}(t_{c+})] &= 1+\boldsymbol{\lambda}^T(t_{c-})[\mathbf{A}\mathbf{x}(t_{c-})+\mathbf{B}\mathbf{u}(t_{c-})] \\
\boldsymbol{\lambda}^T(t_{c+})[\mathbf{A}\mathbf{x}(t_c)+\mathbf{B}\mathbf{u}(t_{c+})] &= \boldsymbol{\lambda}^T(t_{c-})\mathbf{A}\mathbf{x}(t_c) \\
\boldsymbol{\lambda}^T(t_{c+})[\mathbf{A}\mathbf{x}(t_c)+\mathbf{B}\mathbf{u}(t_{c+})] &= \left[\boldsymbol{\lambda}^T(t_{c+})+\boldsymbol{\mu}^T\frac{\partial\boldsymbol{\Theta}\left(\mathbf{x}(t_c),t_c\right)}{\partial\mathbf{x}(t_c)}\right]\mathbf{A}\mathbf{x}(t_c) \\
\boldsymbol{\lambda}^T(t_{c+})\mathbf{B}\mathbf{u}_c &= \boldsymbol{\mu}^T\frac{\partial\boldsymbol{\Theta}\left(\mathbf{x}(t_c),t_c\right)}{\partial\mathbf{x}(t_c)}\mathbf{A}\mathbf{x}(t_c) \\
\boldsymbol{\lambda}_2^T\Phi_\lambda^{-T}(t_2,t_c)\mathbf{B}\mathbf{u}_c &= \boldsymbol{\mu}^T\frac{\partial\boldsymbol{\Theta}\left(\mathbf{x}(t_c),t_c\right)}{\partial\mathbf{x}(t_c)}\mathbf{A}\mathbf{x}(t_c) \\
\left[\frac{\partial\boldsymbol{\Theta}\left(\mathbf{x}(t_c),t_c\right)}{\partial\mathbf{x}(t_c)}\mathbf{A}\mathbf{x}(t_c)\right]^T\boldsymbol{\mu} &= \left[\boldsymbol{\lambda}_2^T\Phi_\lambda^{-T}(t_2,t_c)\mathbf{B}\mathbf{u}_c\right]^T
\end{aligned} \tag{6.22}$$

which is under-determined since $\boldsymbol{\mu}\in\mathbb{R}^3$ and there is only one scalar equation. There could be infinite $\boldsymbol{\mu}\in\mathbb{R}^3$ that would satisfy the above scalar equation. To solve for the costate at t_{c-}, the constant Lagrange multiplier, $\boldsymbol{\mu}$, needs to be first calculated:

$$\boldsymbol{\lambda}_{c-}^T=\boldsymbol{\lambda}_2^T\Phi_\lambda^{-T}(t_2,t_c)+\boldsymbol{\mu}^T\frac{\partial\boldsymbol{\Theta}\left(\mathbf{x}(t_c),t_c\right)}{\partial\mathbf{x}(t_c)} \tag{6.23}$$

However, as previously stated, since with the assumption that $\mathbf{u}(t)=\mathbf{0}$ for $t\le t_{c-}$, there is no need to calculate $\boldsymbol{\lambda}_o$ to know the optimal controller. Therefore, the inability to calculate $\boldsymbol{\mu}$ does not hinder finding the optimal control.

6.5 $N = 2$ for Stable Orbit to Stable Orbit Maneuver

In this section, a special $N = 2$ case is presented for the problem of maneuvering from one stable and centered orbit to another with initial coasting. The results follow directly from the previous Section 6.2 with the conditions

$$a_o = a_f = 0 \qquad b_o = b_f = 0 \tag{6.24}$$

which means $\Delta a = \Delta b = 0$.

Critical Times Calculations

Critical times are calculated using the relative orbit parameters a, b, and ρ as was done in Section 5.2. Beginning with the drifting equation $a(t_f) = 4x(t_f) + 2\dot{y}(t_f)$ with $\Delta a = 0$, the time intervals are related by

$$\Delta\tau_1 + \frac{u_{y1}}{u_{yo}}\Delta\tau_2 + \frac{u_{y2}}{u_{yo}}\Delta\tau_3 = 0 \tag{6.25}$$

Solving for $\Delta\tau_3$,

$$\Delta\tau_3 = -\frac{u_{y2}}{u_{yo}}\left(\Delta\tau_1 + \frac{u_{y1}}{u_{yo}}\Delta\tau_2\right) \tag{6.26}$$

where $u_{yo}/u_{y2} = u_{y2}/u_{yo}$ was used. This can be re-written as

$$t_f - t_c = \Delta\tau_1 + \Delta\tau_2 + \Delta\tau_3 = \left(1 - \frac{u_{y2}}{u_{yo}}\right)\Delta\tau_1 + \left(1 - \frac{u_{y1}}{u_{yo}}\frac{u_{y2}}{u_{yo}}\right)\Delta\tau_2 \tag{6.27}$$

providing an expression for the duration of active control. Table 6.1 provides the summary of the results for each subcases.

Next are the results from using the centering parameter $b(t_f)$ with $\Delta b = 0$,

$$b(t_f) = y(t_f) - 2\dot{x}(t_f) \tag{6.28}$$

Table 6.1 Three subcases of $N = 2$ with initial coasting for stable to stable orbit maneuver; active control time interval.

Subcase	Control Sequence	$t_f - t_c = \Delta\tau_1 + \Delta\tau_2 + \Delta\tau_3$
I.	X-X	$t_f - t_c = 0$
II.	X-Y	$t_f - t_c = 2(\Delta\tau_1 + \Delta\tau_2) = 2\Delta\tau_3$
III.	Y-X	$t_f - t_c = 2\Delta\tau_1$

which becomes, after substituting in the Equation (6.26),

$$\left(\frac{u_{y2}}{u_{yo}} - \frac{u_{y1}}{u_{yo}}\right)\Delta\tau_2^2 + \left[\frac{u_{xo}}{u_{yo}}\left(\frac{u_{x2}}{u_{xo}}\frac{u_{y1}}{u_{yo}}\frac{u_{y2}}{u_{yo}} - \frac{u_{x1}}{u_{xo}}\right)\frac{4}{3} + \left(\frac{u_{y1}}{u_{yo}}\frac{u_{y2}}{u_{yo}} - 1\right)2\Delta\tau_1\right]\Delta\tau_2 + \left(\frac{u_{y2}}{u_{yo}} - 1\right)\Delta\tau_1^2 + \frac{4}{3}\frac{u_{xo}}{u_{yo}}\left(\frac{u_{x2}}{u_{xo}}\frac{u_{y2}}{u_{yo}} - 1\right)\Delta\tau_1 = 0 \quad (6.29)$$

Performing the analysis for each subcases, the following observations are made:

1. Subcase I: This is not a viable option for this type of maneuver.

2. Subcase II: Solving the quadratic in $\Delta\tau_2$, the intermediate results are:

$$\Delta\tau_2 = -\frac{2}{3} - \Delta\tau_1 + \frac{2}{3}\sqrt{3\Delta\tau_1 + 1} \quad (6.30)$$

$$\Delta\tau_3 = \Delta\tau_1 + \Delta\tau_2 \quad (6.31)$$

For all positive $\Delta\tau_1$, $\Delta\tau_2$ and $\Delta\tau_3$ will be non-negative. However, if the equation is solved in terms of quadratic in $\Delta\tau_1$,

$$\Delta\tau_1 = -\Delta\tau_2 + \sqrt{-\frac{4}{3}\Delta\tau_2} \quad (6.32)$$

$$\Delta\tau_3 = \Delta\tau_1 + \Delta\tau_2 \quad (6.33)$$

This has the undesirable result of having negative determinant, unless $\Delta\tau_2$ is zero. If $\Delta\tau_2 = 0$, then $\Delta\tau_1 = \Delta\tau_3 = t_f = 0$, resulting in a trivial solution.

3. Subcase III: The roots of the quadratic equation results in:

$$\Delta\tau_2 = -\frac{3}{4}\Delta\tau_1^2 \tag{6.34}$$

$$\Delta\tau_3 = \Delta\tau_1 - \Delta\tau_2 \tag{6.35}$$

This has the similar undesirable result of having negative time intervals for $\Delta\tau_2$, unless $\Delta\tau_1$ is zero. If $\Delta\tau_1 = 0$, then $\Delta\tau_2 = \Delta\tau_3 = t_f = 0$, resulting in another trivial solution.

6.6 Summary

In this chapter, the results for minimum-time in-plane problem with initial coasting for $N = 2$ was examined. The analysis showed that there is no viable subcases for the stable to stable orbit maneuver using only two control switches; one for the radial controller and the second for the in-track controller. Next, the problem is reformulated by considering only one controllers. This reduces the possible control sequences to that of out-of-plane problem where the control switches from $+U_{max}$ to $-U_{max}$.

VII. In-Plane Solution with In-Track Controller Only

In the previous chapter, using both radial and in-track controllers did not generate a valid solution for the in-plane problem with $N = 2$. In this chapter, the problem is restated to allow only one controller to be active.

When both the radial and in-track thrusters is used, the system was found to be completely controllable through the use of the controllability matrix. Similarly, two new controllability matrix is generated; one for each thrusters entering the system independently.

$$\begin{aligned} \boldsymbol{G}_x &= \left[\boldsymbol{B}_x | \boldsymbol{A}\boldsymbol{B}_x | \boldsymbol{A}^{\boldsymbol{2}}\boldsymbol{B}_x | \boldsymbol{A}^{\boldsymbol{3}}\boldsymbol{B}_x\right] \\ \boldsymbol{G}_y &= \left[\boldsymbol{B}_y | \boldsymbol{A}\boldsymbol{B}_y | \boldsymbol{A}^{\boldsymbol{2}}\boldsymbol{B}_y | \boldsymbol{A}^{\boldsymbol{3}}\boldsymbol{B}_y\right] \end{aligned} \tag{7.1}$$

where $\boldsymbol{B}_x = \begin{bmatrix} 0 & 0 & 1 & 0 \end{bmatrix}^T$ and $\boldsymbol{B}_y = \begin{bmatrix} 0 & 0 & 0 & 1 \end{bmatrix}^T$. The rank of $\boldsymbol{G}_x$ is 3 and the rank of $\boldsymbol{G}_y$ is 4, full rank. So, while using the radial thruster alone, the in-plane system is not completely controllable, using the in-track thruster, the system is completely controllable. This makes some intuitive physical sense because the in-track thruster increases and decreases the satellite's specific energy. The change in the specific energy changes the satellites's orbital period as well the eccentricity generating in-track drifting, thus allowing the satellite to move ahead or behind the reference orbit. Therefore, in the remainder of this chapter, the minimum time solution is derived using only the in-track controller.

7.1 Critical Times Calculations

Earlier analysis in Chapter V showed that the centering equation did not involve the the radial controllers, coinciding with the non-controllability of the system using the x-controller alone. Therefore, the centering equation is unaffected by the absence of

radial controls; the valid equation repeated here for convenience.

$$0 = \frac{1}{2}\frac{\Delta a}{u_{yo}} + \Delta\tau_1 + \frac{u_{y1}}{u_{yo}}\Delta\tau_2 + \frac{u_{y2}}{u_{yo}}\Delta\tau_3 \tag{7.2}$$

For a single controller problem, there is only one subcase as it was for the out-plane problem. The optimal control sequence for $N = 2$ with in-track controller alone is now either $u_y^* = \{+U_{max}, -U_{max}, +U_{max}\}$ or $u_y^* = \{-U_{max}, +U_{max}, -U_{max}\}$. In either case, $u_{y1}/u_{yo} = -1$ and $u_{y2}/u_{yo} = +1$. Then, the drifting equation become:

$$0 = \frac{1}{2}\frac{\Delta a}{u_{yo}} + \Delta\tau_1 - \Delta\tau_2 + \Delta\tau_3 \tag{7.3}$$

and

$$t_f = \Delta\tau_1 + \Delta\tau_2 + \Delta\tau_3 = 2\Delta\tau_2 - \frac{1}{2}\frac{\Delta a}{u_{yo}} \tag{7.4}$$

The centering equation, after substituting in the expression for $\Delta\tau_3$ produces to an equation quadratic in $\Delta\tau_2$:

$$\Delta\tau_2^2 - \left(\frac{a_o}{u_{yo}} + 2\Delta\tau_1\right)\Delta\tau_2 + \frac{1}{3}\frac{\Delta b}{u_{yo}} + \frac{1}{8}\frac{(a_o + a_f)}{u_{yo}}\frac{\Delta a}{u_{yo}} \tag{7.5}$$

The relative orbit size equation is simpler in form but remains a non-linear function of $\Delta\tau_1$:

$$\begin{aligned}\frac{\rho_o}{u_{yo}}\cos\left(2\Delta\tau_2 - \frac{1}{2}\frac{\Delta a}{u_{yo}} + \theta_o\right) - 2\frac{\rho_o}{u_{yo}}\cos\left(\Delta\tau_1 + \Delta\tau_2 + \theta_o\right) - 2\cos\left(\Delta\tau_1 + \theta_o\right) \\ - 4\cos\Delta\tau_1 + 4\cos\left(\Delta\tau_1 + \Delta\tau_2\right) - 8\cos\Delta\tau_2 \\ + 4\cos\left(-\Delta\tau_1 + 2\Delta\tau_2 - \frac{1}{2}\frac{\Delta a}{u_{yo}}\right) - 4\cos\left(-\Delta\tau_1 + \Delta\tau_2 - \frac{1}{2}\frac{\Delta a}{u_{yo}}\right) \\ + 2\frac{\rho_o}{u_{yo}}\cos\left(\Delta\tau_1 + \theta_o\right) - \frac{\rho_o}{u_{yo}}\cos\theta_o + 10 - \left(\frac{\rho_f^2 - \rho_o^2}{4u_{yo}^2}\right) = 0\end{aligned} \tag{7.6}$$

The value of $\Delta\tau_1 \in [0, \pi]$ must be found numerically.

For a stable to stable orbit maneuver, the critical times equations become even simpler:

$$\begin{aligned} \Delta\tau_2 &= 2\Delta\tau_1 \\ \Delta\tau_3 &= \Delta\tau_1 \\ t_f &= 4\Delta\tau_1 \end{aligned} \tag{7.7}$$

The relative orbit size equation reduces to an eighth degree polynomial in $\cos\Delta\tau_1$ whose coefficients are:[1]

$$\begin{aligned} k_8 &= 16 - 16\cos\theta_o\frac{\rho_o}{u_{yo}} + 4\left(\frac{\rho_o}{u_{yo}}\right)^2 \\ k_7 &= -64 + 48\cos\theta_o\frac{\rho_o}{u_{yo}} - 8\left(\frac{\rho_o}{u_{yo}}\right)^2 \\ k_6 &= 64 - 16\cos\theta_o\frac{\rho_o}{u_{yo}} - 4\left(\frac{\rho_o}{u_{yo}}\right)^2 \\ k_5 &= 64 - 80\cos\theta_o\frac{\rho_o}{u_{yo}} + 16\left(\frac{\rho_o}{u_{yo}}\right)^2 \\ k_4 &= 8(\gamma_\rho - 80) + 4(20 - \gamma_\rho)\cos\theta_o\frac{\rho_o}{u_{yo}} - 3\left(\frac{\rho_o}{u_{yo}}\right)^2 - \cos^2\theta_o\left(\frac{\rho_o}{u_{yo}}\right)^2 \\ k_3 &= 16(4 - \gamma_\rho) + 4(\gamma_\rho + 4)\cos\theta_o\frac{\rho_o}{u_{yo}} - 8\left(\frac{\rho_o}{u_{yo}}\right)^2 - 2\sin^2\theta_o\left(\frac{\rho_o}{u_{yo}}\right)^2 \\ k_2 &= 64 + 4(\gamma_\rho - 12)\cos\theta_o\frac{\rho_o}{u_{yo}} + 4\left(\frac{\rho_o}{u_{yo}}\right)^2 \\ k_1 &= 16(\gamma_\rho - 4) - 4(4 - \gamma_\rho)\cos\theta_o\frac{\rho_o}{u_{yo}} + 2\sin^2\theta_o\left(\frac{\rho_o}{u_{yo}}\right)^2 \\ k_o &= \left(\frac{1}{4}\gamma_\rho - 4\right)^2 - \sin^2\theta_o\left(\frac{\rho_o}{u_{yo}}\right)^2 \\ \gamma_\rho &= \frac{1}{16}\left(\frac{\rho_f^2}{\rho_o^2} - 1\right)\left(\frac{\rho_o}{u_{yo}}\right)^2 \end{aligned} \tag{7.8}$$

[1] $k_8y^8 + k_7y^7 + k_6y^6 + k_5y^5 + k_4y^4 + k_3y^3 + k_2y^2 + k_1y + k_o = 0$, where $y \equiv \cos\Delta\tau_1$.

However, for two special initial phase angles ($\theta_o = 0$ and $\theta_o = \pi$), the equation reduces further to a quartic in $\cos\Delta\tau_1$ whose coefficients are:[2]

$$\begin{aligned}
k_4 &= 8\left(\cos\theta_o\frac{\rho_o}{u_{yo}} - 2\right) \\
k_3 &= 8\left(4 - \cos\theta_o\frac{\rho_o}{u_{yo}}\right) \\
k_2 &= -8\cos\theta_o\frac{\rho_o}{u_{yo}} \\
k_1 &= 8\left(\cos\theta_o\frac{\rho_o}{u_{yo}} - 4\right) \\
k_o &= \frac{1}{4}\left(1 - \frac{\rho_f^2}{\rho_o^2}\right)\left(\frac{\rho_o}{u_{yo}}\right)^2 + 16
\end{aligned} \tag{7.9}$$

The valid $\Delta\tau_1$ is the real root of these polynomials which minimized t_f while satisfying the final relative oribt parameters. The valid root must also be in the proper domain of the arccosine function; $[-1, +1]$.[3] Furthermore, in the case of multiple real roots, the largest root in the valid range generates the smallest $\Delta\tau_1$. However, the optimal $\Delta\tau_1$ (not necessarily the smallest) satisfies both the set of desired final relative orbit parameters and keeps the Hamiltonian at zero.

7.2 Initial Costate

The method of obtaining the four equations for the four unknowns of the initial costate is exactly the same as before. However, the Hamiltonian equation is slightly modified:

$$\begin{aligned}
H_o &= 1 + \boldsymbol{\lambda}_o^T\left[\boldsymbol{A}\boldsymbol{x}_o + \boldsymbol{B}_y u_{yo}\right] \\
-1 &= \left[\boldsymbol{A}\boldsymbol{x}_o + \boldsymbol{B}_y u_{yo}\right]^T \boldsymbol{\lambda}_o \\
-1 &= \begin{bmatrix}\dot{x}_o & \dot{y}_o & (3x_o + 2\dot{y}_o) & (-2\dot{x}_o + u_{yo})\end{bmatrix}\boldsymbol{\lambda}_o
\end{aligned} \tag{7.10}$$

[2] $k_4 y^4 + k_3 y^3 + k_2 y^2 + k_1 y + k_o = 0$, where $y \equiv \cos\Delta\tau_1$.
[3] The range of arccosine is in the proper range of $[0, \pi]$.

The natural boundary condition providing the terminal costate condition remains valid. However, this time the terminal condition is transitioned to the initial time.

$$\begin{aligned}
\boldsymbol{\lambda}_o &= \boldsymbol{\Phi}_\lambda^{-1}(t_f, 0)\boldsymbol{\lambda}(t_f) \\
\boldsymbol{\lambda}_o &= \boldsymbol{\Phi}_\lambda^{-1}(t_f, 0)\left[\boldsymbol{\nu}^T \frac{\partial \boldsymbol{\Psi}\left(\mathbf{x}(t_f), t_f\right)}{\partial \mathbf{x}(t_f)}\right]^T \\
\boldsymbol{\lambda}_o &= \boldsymbol{\Phi}_\lambda^{-1}(t_f, 0)\left[\frac{\partial \boldsymbol{\Psi}\left(\mathbf{x}(t_f), t_f\right)}{\partial \mathbf{x}(t_f)}\right]^T \boldsymbol{\nu}
\end{aligned} \tag{7.11}$$

This set of equations can be developed further as was done in previous chapters. The result is

$$\begin{aligned}
0 &= \begin{bmatrix} c_1 & c_2 & 2c_2 & -2c_1 \end{bmatrix} \boldsymbol{\lambda}_o \\
c_1 &= \cos\left(t_f - \theta(t_f)\right) \sin t_f \\
c_2 &= \cos\theta(t_f) - \cos\left(t_f - \theta(t_f)\right) \cos t_f \\
\tan\theta(t_f) &= \frac{x(t_f) - a(t_f)}{\dot{x}(t_f)}
\end{aligned} \tag{7.12}$$

The two remaining equations use the costate transition matrix in conjunction with the two switching conditions: $\lambda_{\dot{y}}(t_1) = \lambda_{\dot{y}}(t_2) = 0$.

$$\begin{aligned}
\boldsymbol{\lambda}(t_1) &= \boldsymbol{\Phi}_\lambda(t_1, 0)\boldsymbol{\lambda}_o \\
\boldsymbol{\lambda}(t_2) &= \boldsymbol{\Phi}_\lambda(t_2, 0)\boldsymbol{\lambda}_o
\end{aligned} \tag{7.13}$$

This represents two sets of four equations each. Since the switching function is $\lambda_{\dot{y}}(t)$, the fourth equations from these two sets are used to find the initial costate vector.

$$\begin{aligned}
\lambda_{\dot{y}}(t_1) &= \left[\boldsymbol{\Phi}_\lambda(t_1, 0)\right]_{(row\ 4)} \boldsymbol{\lambda}_o = 0 \\
\lambda_{\dot{y}}(t_2) &= \left[\boldsymbol{\Phi}_\lambda(t_2, 0)\right]_{(row\ 4)} \boldsymbol{\lambda}_o = 0
\end{aligned} \tag{7.14}$$

The four equation are again put into a large 4-by-4 matrix:

$$\begin{bmatrix} -1 \\ 0 \\ \lambda_{\dot{y}}(t_1) \\ \lambda_{\dot{y}}(t_2) \end{bmatrix} = \begin{bmatrix} [\boldsymbol{A}\boldsymbol{x}_o + \boldsymbol{B}_y u_{yo}]^T \\ \text{Natural Boundary Condition} \\ [\boldsymbol{\Phi}_\lambda(t_1, 0)]_{(row\ 4)} \\ [\boldsymbol{\Phi}_\lambda(t_2, 0)]_{(row\ 4)} \end{bmatrix} \boldsymbol{\lambda}_o$$

$$\begin{bmatrix} -1 \\ 0 \\ 0 \\ 0 \end{bmatrix} = \begin{bmatrix} \dot{x}_o & \dot{y}_o & 3x_o + 2\dot{y}_o & -2\dot{x}_o + u_{yo} \\ c_1 & c_2 & 2c_2 & -2c_1 \\ 2 - 2\cos t_1 & 3t_1 - 4\sin t_1 & -2\sin t_1 & 4\cos t_1 - 3 \\ 2 - 2\cos t_2 & 3t_2 - 4\sin t_2 & -2\sin t_2 & 4\cos t_2 - 3 \end{bmatrix} \boldsymbol{\lambda}_o \tag{7.15}$$

The initial costate vector is calculated by performing a matrix inverse operation.

7.3 Reconfiguration Example

A more physically realistic example is provided using the in-track controller alone. This illustrates how the non-dimensionalization is used. First assume some realistic spacecraft characteristics. A 50 kg satellite equipped with in-track electric ion propulsion system capable of producing maximum thrust of 10 mN is in a formation with initial relative orbit size of 2.0 km. The reference orbit is a low earth orbit with semi-major axis of 8000 km. The reconfiguration maneuver changes the relative orbit size from 2.0 km to 2.5 km while maintaining the stable and centered.

$$\begin{aligned} \omega &= \sqrt{\frac{\mu_\oplus}{R_o^3}} = \sqrt{\frac{3.986 \times 10^5\ km^3 s^{-2}}{(8000\ km)^3}} = 8.8234 \times 10^{-4}\ rad/sec \\ U_{max} &= \left(\frac{T_{max}}{mass}\right)\left(\frac{R_o^2}{\mu_\oplus}\right) = \frac{10 \times 10^{-3}\ N}{50\ kg}\left(\frac{R_o^2}{\mu_\oplus}\right) = 4.01 \times 10^{-6} \\ \rho_o &= \frac{2.0\ km}{R_o} = 0.00025 \\ \rho_f &= \frac{2.5\ km}{R_o} = 0.0003125 \end{aligned} \tag{7.16}$$

Therefore, the initial relative orbit parameters are: $a_o = b_o = 0$ and $\rho_o = 0.00025$. For convenience, the initial phase angle is zero, meaning the spacecraft is ahead of the center with no initial radial offset. In Figure 7.1, the initial position is marked with a circle on the inner orbit. The final relative orbit parameters are: $a_f = b_f = 0$ and $\rho_f = 0.0003125$. The final phase angle is not specified to provide larger solution space. For a stable to stable orbit maneuver, using only the in-track controller, two control switchings are required to satisfy the three final relative orbit parameters. Recall the results for stable

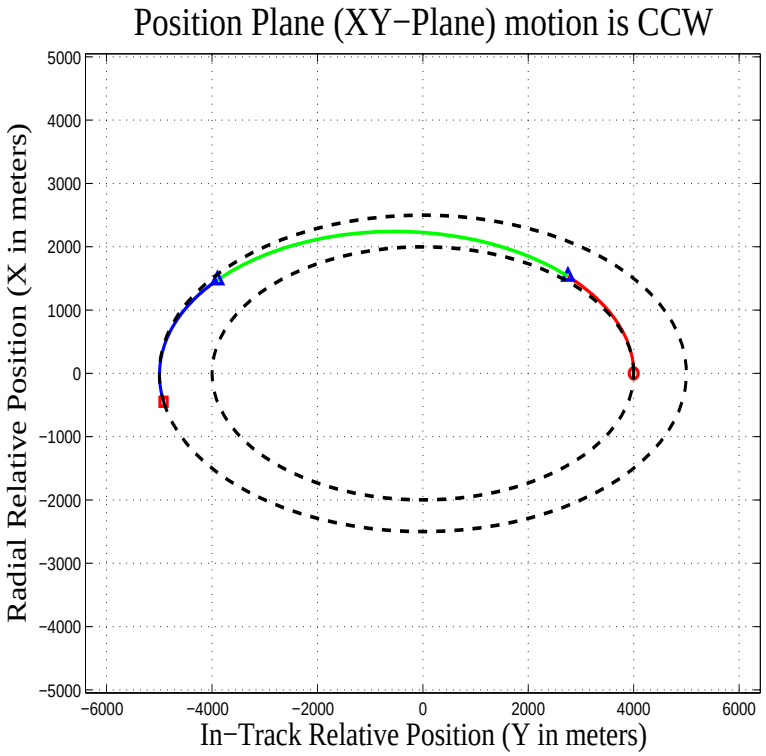

Figure 7.1 Position-plane state-phase space for reconfiguration example (N=2). Position-plane state-phase space for in-plane minimum-time, reconfiguration example (N=2) with in-track controller alone. The radial and in-track positions are plotted in physical units:$\rho_o = 2.0$ km and $\rho_f = 2.5$ km.

to stable orbit maneuver are $\Delta\tau_2 = 2\Delta\tau_1$, $\Delta\tau_3 = \Delta\tau_1$, and $t_f = \Delta\tau_1 + \Delta\tau_2 + \Delta\tau_3 = 4\Delta\tau_1$, where $\Delta\tau_1$ is solved numerically. The non-negative real root of the polynomial using initial control of $u_{yo} = +U_{max}$ result in $\Delta\tau_1 = 0.8356$ radians. The final time (minimum

time) is $t_f = 3.3427$ radians. The maneuver lasts approximately one-half orbit. The physical time is calculated by multiplying the canonical time by the mean motion,

$$t_f = 3.3427\omega = 3.3427\left(\sqrt{\frac{R_o^3}{\mu_\oplus}}\right) = 3788.5\ sec = 63.1\ min \tag{7.17}$$

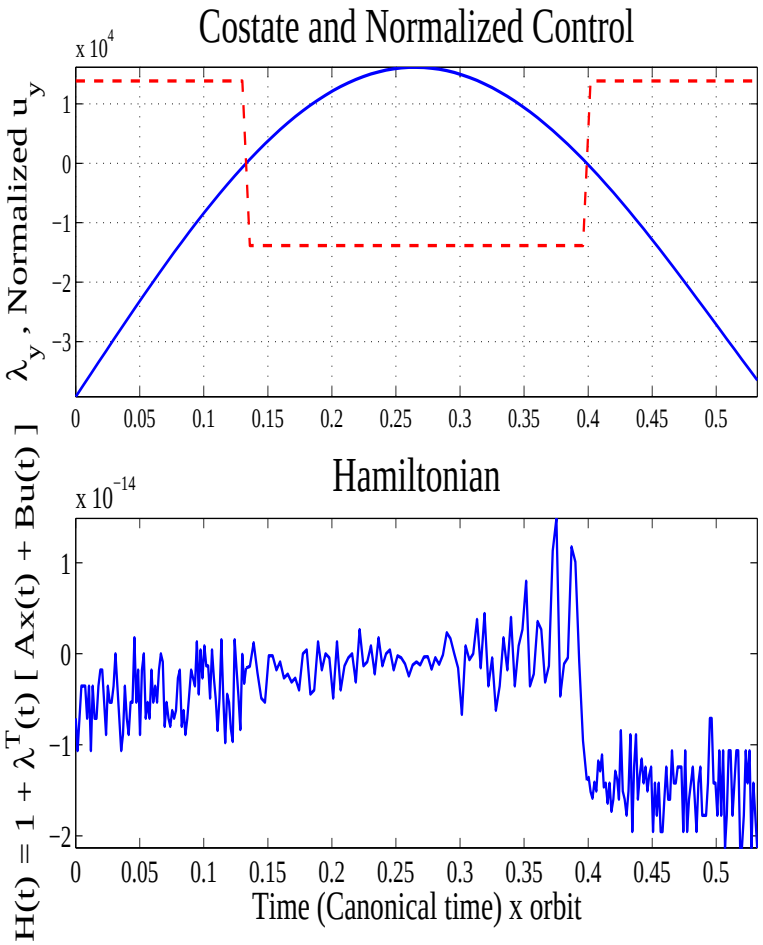

Figure 7.2 Costate, optimal control, and Hamiltonian time history, reconfiguration example (N=2).
Costate is in solid and the scaled optimal control is dashed. Notice the scale on the Hamiltonian.

A result of the second reconfiguration example is provided in Figure 7.3 for a satellite with the same physical properties as the previous example. This time the initial orbit relative radius is 1000 m and the desired final relative orbit radius is 2500 m.

The maximum acceleration is insufficient to get to the final orbit using a single $N = 2$ maneuver. Therefore, the first set of optimal control takes the satellite from $\rho_o = 1000$ m to $\rho_1 = 2000$ m, arriving at a point in the position phase-space labelled $\mathbf{x}_{f\,o}$ in Figure 7.3. Then the satellite coasts until the phase angle is π (a point labelled $\mathbf{x}_{o\,1}$) and performs another $N = 2$ optimal maneuver taking the satellite to a point labelled $\mathbf{x}_{f\,1}$. The first leg of the maneuver lasts 5.970 rad (0.95 reference orbit), the coasting is 2.241 rad (0.36 reference orbit), the second maneuver lasts for 3.343 rad (0.53 reference orbit).

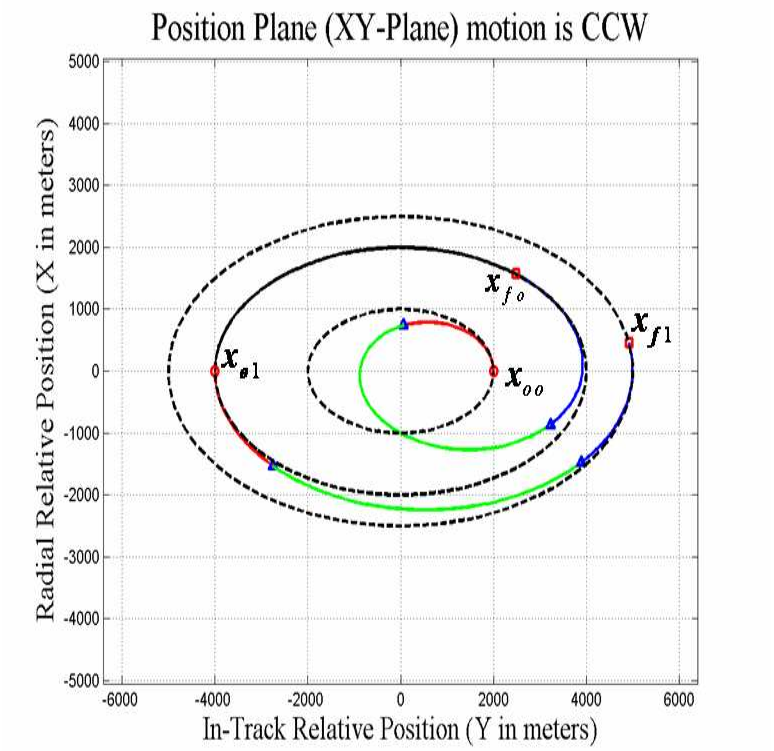

Figure 7.3 Position-plane state-phase space for in-plane minimum-time, Reconfiguration Example 2 (Multiple N=2).
The initial optimal control takes the satellite from $\mathbf{x}_{oo}$ to $\mathbf{x}_{f\,o}$, then it coasts to $\mathbf{x}_{o\,1}$ and another optimal control takes the satellite to the final orbit, arriving at $\mathbf{x}_{f\,1}$. from The radial and in-track positions are plotted in physical units:$\rho_o = 2.0$ km and $\rho_f = 2.5$ km.

7.4 General N

When there is only one subcase and the control switches ad infinitum, a general procedure can be obtained for $N > 2$ control switches. The state solution at $t = t_f$ become:

$$\mathbf{x}(t_f) = \begin{bmatrix} \rho_o \sin(t_f + \theta_f) + a_o \\ 2\rho_o \cos(t_f + \theta_o) + b_o - \frac{3}{2} a_o t_f \\ \rho_o \cos(t_f + \theta_o) \\ -2\rho_o \sin(t_f + \theta_o) - \frac{3}{2} a_o \end{bmatrix} + \int_0^{t_1} e^{\boldsymbol{A}(t_f - \tau)} \boldsymbol{B}_y u_{yo} d\tau - \int_{t_1}^{t_2} e^{\boldsymbol{A}(t_f - \tau)} \boldsymbol{B}_y u_{yo} d\tau$$
$$+ \sum_{i=2}^{N-1} \left((-1)^i \int_{t_i}^{t_{i+1}} e^{\boldsymbol{A}(t_f - \tau)} \boldsymbol{B}_y u_{yo} d\tau \right) + (-1)^N \int_{t_N}^{t_f} e^{\boldsymbol{A}(t_f - \tau)} \boldsymbol{B}_y u_{yo} d\tau \quad (7.18)$$

where $t_k = t_{k-2} + 2\pi$ for $k = \{3, 4, ...N\}$ and $\boldsymbol{B}_y = [0\ 0\ 0\ 1]^T$. Therefore, the only three unknowns remain t_1, t_2, and t_f. The above equation can be further reduced to two cases of general $N > 2$: even N and odd N.[4] These solutions are then applied to the three relative orbit parameters at the final time to obtain three equations required to solve for the unknown critical switching times.

Even N

[4] $t_{even\ N} = t_2 + (N-2)\pi$ and $t_{odd\ N} = t_1 + (N-1)\pi$.

For the general case of even N, the state at t_f is

$$\mathbf{x}(t_f) = \begin{bmatrix} \rho_o \sin(t_f + \theta_f) + a_o \\ 2\rho_o \cos(t_f + \theta_o) + b_o - \frac{3}{2} a_o t_f \\ \rho_o \cos(t_f + \theta_o) \\ -2\rho_o \sin(t_f + \theta_o) - \frac{3}{2} a_o \end{bmatrix} + u_{yo} \left(\int_0^{t_1} e^{\boldsymbol{A}(t_f - \tau)} d\tau - \int_{t_1}^{t_2} e^{\boldsymbol{A}(t_f - \tau)} d\tau + \int_{t_2 + (N-2)\pi}^{t_f} e^{\boldsymbol{A}(t_f - \tau)} d\tau \right) \boldsymbol{B}_y + u_{yo} \left(\sum_{k=2}^{N-1} (-1)^k \int_{t_k}^{t_{k+1}} e^{\boldsymbol{A}(t_f - \tau)} d\tau \right) \boldsymbol{B}_y \quad (7.19)$$

where the limits of integration are functions of k:

$$t_{k+1} = \left(\frac{1 - (-1)^{(k+1)}}{2} \right) (t_1 + k\pi) + \left(\frac{1 + (-1)^{(k+1)}}{2} \right) (t_2 + (k-1)\pi) \quad (7.20)$$

$$t_k = \left(\frac{1 - (-1)^{k}}{2} \right) (t_1 + (k-1)\pi) + \left(\frac{1 + (-1)^{k}}{2} \right) (t_2 + (k-2)\pi) \quad (7.21)$$

The explicit solution become function of t_1, t_2, t_f, and N:

$$\mathbf{x}(t_f) = \begin{bmatrix} \rho_o \sin(t_f + \theta_f) + a_o \\ 2\rho_o \cos(t_f + \theta_o) + b_o - \frac{3}{2} a_o t_f \\ \rho_o \cos(t_f + \theta_o) \\ -2\rho_o \sin(t_f + \theta_o) - \frac{3}{2} a_o \end{bmatrix} + u_{yo} \begin{bmatrix} 2N \sin(t_f - t_1) - 2N \sin(t_f - t_2) - 2 \sin t_f + 2t_f - 2N(t_2 - t_1) \\ y_p(t_f) \\ 2N \cos(t_f - t_1) - 2N \cos(t_f - t_2) - 2 \cos t_f + 2 \\ -4N \sin(t_f - t_1) + 4N \sin(t_f - t_2) + 4 \sin t_f - 3t_f + 3N(t_2 - t_1) \end{bmatrix} \quad (7.22)$$

where the particular solution for the in-track position is

$$y_p(t_f) = 4N\cos(t_f - t_1) - 4N\cos(t_f - t_2) - 4\cos t_f - 4 + \frac{3}{2}N\left((t_f - t_1)^2 - (t_f - t_2)^2\right) - \frac{3}{2}t_f^2 - 12\pi\left(\sum_{i=1}^{\frac{N}{2}}(i-1)\right)(t_2 - t_1) \quad (7.23)$$

Using this solution, the drifting equation for even N become:

$$\frac{a(t_f)}{u_{yo}} = \frac{a_o}{u_{yo}} - 2N(t_2 - t_1) + 2t_f \quad (7.24)$$

which can be solved for the final time in terms of the second time interval,

$$t_f = -\frac{1}{2}\frac{\Delta a}{u_{yo}} + 2N\Delta\tau_2 \quad (7.25)$$

For a stable to stable orbit maneuver, $t_f = 2N\Delta\tau_2$.

The centering equation is reduced again to a quadratic in $\Delta\tau_1$:

$$N(N-1)\Delta\tau_2^2 - 2\left(N\Delta\tau_1 + \frac{N}{2}\frac{a_o}{u_{yo}} + 4\pi\left(\sum_{i=1}^{\frac{N}{2}}(i-1)\right)\right)\Delta\tau_2 + \frac{1}{4}\frac{(a_o + a_f)}{u_{yo}}\frac{\Delta a}{u_{yo}} + \frac{2}{3}\frac{\Delta b}{u_{yo}} = 0 \quad (7.26)$$

For a stable to stable orbit maneuver, this greatly simplifies to:

$$N(N-1)\Delta\tau_2^2 - 2\left(N\Delta\tau_1 + 4\pi\left(\sum_{i=1}^{\frac{N}{2}}(i-1)\right)\right)\Delta\tau_2 = 0 \quad (7.27)$$

The two solutions are the trivial solution, $\Delta\tau_2 = 0$, and

$$\Delta\tau_2 = \frac{2}{N(N-1)}\left(N\Delta\tau_1 + 4\pi\left(\sum_{i=1}^{\frac{N}{2}}(i-1)\right)\right) \quad (7.28)$$

The relative orbit size equation become:

$$\left(\frac{\rho_f}{u_{yo}}\right)^2 = \left(\frac{\rho_o}{u_{yo}}\right)^2 + 8 - 4\frac{\rho_o}{u_{yo}}\cos\theta_o - 8\cos t_f + 8N\left(\cos(t_f - t_1) - \cos(t_f - t_2) + \cos t_2 - \cos t_1\right) + 8N^2\left(1 - \cos(t_2 - t_1)\right) + 4N\frac{\rho_o}{u_{yo}}\left(\cos(t_f + \theta_o) + \cos(t_1 + \theta_o) - \cos(t_2 + \theta_o)\right) \quad (7.29)$$

which is a function of only one unknown, $\Delta\tau_1$, when the intermediate results from the drifting and centering equations are used. A very conservative upper limit can be obtained by using triangular inequalities. If the final relative orbit size is expressed as a scale multiple of the initial size, $\rho_f = \alpha\rho_o$:

$$\alpha^2 < 1 + 8\frac{U_{max}^2}{\rho_o^2}\left(2(N+1)^2 + (N+1)\frac{U_{max}}{\rho_o}\right) \quad (7.30)$$

Odd N

For the general case of odd N, the state at t_f is

$$\mathbf{x}(t_f) = \begin{bmatrix} \rho_o\sin(t_f + \theta_f) + a_o \\ 2\rho_o\cos(t_f + \theta_o) + b_o - \frac{3}{2}a_o t_f \\ \rho_o\cos(t_f + \theta_o) \\ -2\rho_o\sin(t_f + \theta_o) - \frac{3}{2}a_o \end{bmatrix} + u_{yo}\left(\int_0^{t_1} e^{\boldsymbol{A}(t_f-\tau)}d\tau - \int_{t_1}^{t_2} e^{\boldsymbol{A}(t_f-\tau)}d\tau - \int_{t_1+(N-1)\pi}^{t_f} e^{\boldsymbol{A}(t_f-\tau)}d\tau\right)\boldsymbol{B}_y + u_{yo}\left(\sum_{k=2}^{N-1}(-1)^k\int_{t_k}^{t_{k+1}} e^{\boldsymbol{A}(t_f-\tau)}d\tau\right)\boldsymbol{B}_y \quad (7.31)$$

where the limits of integration are functions of k:

$$t_{k+1} = \left(\frac{1-(-1)^{(k+1)}}{2}\right)(t_1 + k\pi) + \left(\frac{1+(-1)^{(k+1)}}{2}\right)(t_2 + (k-1)\pi) \quad (7.32)$$

$$t_k = \left(\frac{1-(-1)^{k}}{2}\right)(t_1 + (k-1)\pi) + \left(\frac{1+(-1)^{k}}{2}\right)(t_2 + (k-2)\pi) \quad (7.33)$$

The explicit solution become function of t_1, t_2, t_f, and N:

$$\mathbf{x}(t_f) = \begin{bmatrix} \rho_o \sin(t_f + \theta_f) + a_o \\ 2\rho_o \cos(t_f + \theta_o) + b_o - \frac{3}{2}a_o t_f \\ \rho_o \cos(t_f + \theta_o) \\ -2\rho_o \sin(t_f + \theta_o) - \frac{3}{2}a_o \end{bmatrix} + \begin{bmatrix} x_p(t_f) \\ y_p(t_f) \\ 2(N+1)\cos(t_f - t_1) - 2(N-1)\cos(t_f - t_2) - 2\cos t_f + 2 \\ \dot{y}_p(t_f) \end{bmatrix} \quad (7.34)$$

where the particular solutions are:

$$\begin{aligned} x_p(t_f) &= 2(N+1)\sin(t_f - t_1) - 2(N-1)\sin(t_f - t_2) - 2(N-1)(t_2 - t_1) \\ &\quad + 4t_1 + 4(N-1)\pi - 2\sin t_f - 2t_f \end{aligned} \quad (7.35)$$

$$\begin{aligned} y_p(t_f) &= 4(N+1)\cos(t_f - t_1) - 4(N-1)\cos(t_f - t_2) - 4\cos t_f - 4 \\ &\quad - \frac{3}{2}(N-1)\left((t_f - t_2)^2 - (t_f - t_1)^2\right) + 3(t_f - t_1)^2 - \frac{3}{2}t_f^2 \\ &\quad + 6(N-1)\pi(t_f - t_1) - 12\pi\left(\sum_{i=1}^{\frac{(N-1)}{2}}(i-1)\right)(t_2 - t_1) + 3(N-1)^2\pi^2 \end{aligned} \quad (7.36)$$

$$\begin{aligned} \dot{y}_p(t_f) &= -4(N+1)\sin(t_f - t_1) + 4(N-1)\sin(t_f - t_2) + 4\sin t_f + 3t_f \\ &\quad + 3(N-1)(t_2 - t_1) - 6t_1 - 6(N-1)\pi \end{aligned} \quad (7.37)$$

Using this solution, the drifting equation for odd N become:

$$\frac{a(t_f)}{u_{yo}} = \frac{a_o}{u_{yo}} - 2(N-1)(t_2 - t_1) + 4t_1 + 4(N-1)\pi - 2t_f \tag{7.38}$$

which can be solved for the final time in terms of the second time interval,

$$t_f = \frac{1}{2}\frac{\Delta a}{u_{yo}} + 2(N-1)\pi - (N-1)\Delta\tau_2 + 2\Delta\tau_1 \tag{7.39}$$

The centering equation is reduced again to a quadratic in $\Delta\tau_1$:

$$\begin{aligned} -N(N-1)\Delta\tau_2^2 + 2\left((N-1)\left(\frac{1}{2}\frac{a_o}{u_{yo}}\Delta\tau_1\right) - 4\pi\left(\sum_{i=1}^{\frac{N}{2}}(i-1)\right) - 2(N-2)^2\pi\right)\Delta\tau_2 \\ -2\Delta\tau_1^2 + 2\left(2(N-1)\pi - \frac{a_o}{u_{yo}}\right)\Delta\tau_1 \\ -\frac{1}{4}\frac{(a_o + a_f)}{u_{yo}}\frac{\Delta a}{u_{yo}} + \frac{2}{3}\frac{\Delta b}{u_{yo}} + 14(N-2)^2\pi^2 + 2\frac{(a_o - 2a_f)}{u_{yo}}(N-1)\pi = 0 \end{aligned} \tag{7.40}$$

The relative orbit size equation become:

$$\begin{aligned} \left(\frac{\rho_f}{u_{yo}}\right)^2 = \left(\frac{\rho_o}{u_{yo}}\right)^2 + 16 - 4\frac{\rho_o}{u_{yo}}\cos\theta_o + 8\cos t_f + 8\cos(t_2 - t_1) \\ -8(N+1)\left(\cos(t_f - t_1) + \cos t_1\right) + 8(N-1)\left(\cos(t_f - t_2) + \cos t_2\right) + 8N^2\left(1 - \cos(t_2 - t_1)\right) \\ + 4\frac{\rho_o}{u_{yo}}\left(-\cos(t_f + \theta_o) + (N+1)\cos(t_1 + \theta_o) - (N-1)\cos(t_2 + \theta_o)\right) \end{aligned} \tag{7.41}$$

which is a function of only one unknown, $\Delta\tau_1$, when the intermediate results from the drifting and centering equations are used. A very conservative upper limit can be obtained by using triangular inequalities. If the final relative orbit size is expressed as a scale multiple of the initial size, $\rho_f = \alpha\rho_o$:

$$\alpha^2 < 1 + 8\frac{U_{max}^2}{\rho_o^2}\left(2(N+1)^2 + 2 + (N+2)\frac{U_{max}}{\rho_o}\right) \tag{7.42}$$

Initial Costate Vector Calculation

Recall λ_{yo} was the coefficient in $\lambda_{\dot{y}}(t)$ equation which generated the ramp term. Therefore, for a general N control switching, $\lambda_{\dot{y}}(t)$ must be periodic without a ramp term; i.e., λ_{yo} must be zero. Then, for the calculations of the initial costate vector, there are only three unknowns: λ_{xo}, $\lambda_{\dot{x}o}$, and $\lambda_{\dot{y}o}$. These three are solved for using the Hamiltonian condition and the two control switching conditions:

$$[\boldsymbol{A}\mathbf{x}_o + \boldsymbol{B}_y u_{yo}]^T \tilde{\boldsymbol{\lambda}}_o = -1 \tag{7.43}$$

$$[\boldsymbol{\Phi}_\lambda(t_1, 0)]_{row\ 4} \tilde{\boldsymbol{\lambda}}_o = \lambda_{\dot{y}}(t_1) = 0 \tag{7.44}$$

$$[\boldsymbol{\Phi}_\lambda(t_2, 0)]_{row\ 4} \tilde{\boldsymbol{\lambda}}_o = \lambda_{\dot{y}}(t_2) = 0 \tag{7.45}$$

where $\tilde{\boldsymbol{\lambda}}_o = [\lambda_{xo}\ \lambda_{\dot{x}o}\ \lambda_{\dot{y}o}]^T$ since $\lambda_{yo} = 0$. The initial costate is determined by the use of inverse matrix operation.

7.5 Summary

In this chapter, the solution for the in-plane maneuver in minimum time using only the in-track controller was presented. The solution was simpler in form then the problem involving both the radial and in-track thrusters. The reconfiguration example showed the accuracy of the solution. The next chapter is the last chapter in this dissertation and will present the conclusion of this research as well as recommendations for future work.

VIII. Conclusions and Recommendation for Future Research

This dissertation presented a semi-analytical method of determining optimal-time control of satellite formations as well as the optimal-fuel control for the out-of-plane motion.

8.1 Concluding Remarks

1. The problem of minimum-time is complex. Determination of the optimal number of control switches for an arbitrary initial and final state is difficult to determine. By excluding the final phase angles (both for out-of-plane and in-plane) from the constraints, the solution space is increased. By including initial coasting, the solution space is increased even further.

2. The in-track controller (y-controls) must be employed for any time-optimal control. To move from one stable orbit to another, the drift must be introduced and then removed. This can only be accomplished with a change in the y-controls. The y-control increases and decreases the specific energy of the orbit and hence affects the eccentricity. Control schemes using only the radial control has no effect on the drifting term and therefore cannot be used to change the stability of the relative orbit.

3. Understanding the costate dynamics was key. For the in-plane motion, the number of y-control switches was sensitive to the y-position costate, λ_y, which is constant. It introduces the offset in the $\lambda_{\dot{x}}(t)$ as well as the ramp term in the $\lambda_{\dot{y}}(t)$, which are the switching functions of the x- and y-controllers, respectively. A non-zero λ_y means the number of y-control switchings is limited to some finite number. If, in addition to $\lambda_y = 0$, we have $\lambda_{xo} = 1.5\lambda_{\dot{y}o}$, then the y-control can switch periodically without limit. Similarly, in general, the x-controls can switch without limit as long as the magnitude of the offset ($|2\lambda_y|$) is less than the amplitude of the the sinusoidal $\lambda_{\dot{x}}(t)$ function. For the most general case, only one control series is viable; that of

alternating between x-control switch and the y-control switch. Only this control can be repeated ad infinitum for a general number, N, of control switches.

4. The initial costate, hence the optimal control, found in this dissertation could serve as the initial guess for a numerical solution employing higher fidelity nonlinear models.

5. Although the optimal control theory is mature and many have used it to solve minimum time problems, none have performed fully analytical studies with satellite formation dynamics. Most relied on the numerical solutions, using the satisfaction of the Hamiltonian condition as their validation method. This research performed an analytical study of this problem. The specific contributions stemming from this research include:

    i. A costate analysis that was not seen in the literature providing insight to possible optimal control sequences.

    ii. Use of relative orbit parameters for critical time calculations.

    iii. A fully analytical solution for the out-of-plane motion, which is a general harmonic motion having wide applicability.

    These contributions provide an alternative methods to determine the minimum time control of a satellite formation as well as an independent means to verify the optimality of the numerical solutions. For the in-plane problem, the TPBV problem requiring a search in eight-dimensional space was reduced to solving for a root of a single nonlinear equation where the valid range of solution is limited to small subset of the positive real line. This reduction provides a means for possible real-time (and possibly automated) application of minimum time control of satellites in a formation.

8.2 Recommendation for Future Research

Future research in this optimal control problem of satellite formation may include:

1. Investigate fully, the general N solution for the in-plane problem using only the in-track control. This solution does not require coasting arcs in between chains of optimal $N = 2$ solutions.

2. Investigate whether the radial thruster alone can be used for in-plane phasing maneuvers where $rho_f = \rho_o$. The requirement of radial thrusters should be examined if the investigation reveal that x-controllers cannot be used by themselves for practical formation control maneuvers.

3. Complete the analytical work on minimum-fuel problem for the in-plane maneuver. More than the minimum-time cases, the minimum-fuel solutions will be practical for application. The minimum-time solution provided the lower limit on the time that can be required for the minimum-fuel problem. It is also possible to examine the combination of minimum-time and minimum-fuel by incorporating both in the performance index functional. The performance index might be:

$$J = \int_{t_o}^{t_f} [1 + |\mathbf{u}(t)|] \, dt \tag{8.1}$$

   where t_f is free.

4. Instead of minimum-fuel, it may be useful to study the case of minimum-energy, since the low-thrust propulsion systems are electric powered. With these electric propulsion systems, the fuel usage is minimum and its usage is less important than the power consumption. The performance index might be,

$$J = \int_{t_o}^{t_f} \frac{1}{2} \mathbf{u}^T(t) \mathbf{u}(t) dt \tag{8.2}$$

   where t_f is fixed.

5. Generalize the dynamics to include a non-circular reference orbit. Then the analysis performed in this dissertation will be a special case with zero eccentricity.

6. The approach taken in this dissertation could again be applied to Wiesel's Floquet model [25] of the satellite formation. By introducing his Floquet modal variables, $\mathbf{z}(t) = \boldsymbol{F}^{-1}(t)\mathbf{x}(t)$, the time-periodic relative orbit is transformed to a constant coefficient system:

$$\dot{\mathbf{z}}(t) = \boldsymbol{\mathcal{J}}\mathbf{z}(t) + \boldsymbol{F}^{-1}(t)\mathbf{B}\mathbf{u}(t) \tag{8.3}$$

where $\boldsymbol{\mathcal{J}}$ satisfies $\dot{\boldsymbol{F}}(t) = \mathbf{A}(t)\mathbf{F}(t) - \boldsymbol{F}(t)\boldsymbol{\mathcal{J}}$ and is the constant matrix in Jordan canonical form. Applying optimization theory, the costate is fully analytic:

$$\begin{aligned}\boldsymbol{\lambda}(t) &= \boldsymbol{\Phi}_\lambda(t, t_o)\boldsymbol{\lambda}(t_o) = e^{-\boldsymbol{\mathcal{J}}^T(\delta t = t - t_o)}\boldsymbol{\lambda}(t_o) \\ &= \begin{bmatrix} \cos\omega\delta t & \sin\omega\delta t & 0 & 0 & 0 & 0 \\ -\sin\omega\delta t & \cos\omega\delta t & 0 & 0 & 0 & 0 \\ 0 & 0 & 1 & 0 & 0 & 0 \\ 0 & 0 & \delta t & 1 & 0 & 0 \\ 0 & 0 & 0 & 0 & 1 & 0 \\ 0 & 0 & 0 & 0 & \delta t & 1 \end{bmatrix} \boldsymbol{\lambda}(t_o)\end{aligned} \tag{8.4}$$

and the resulting bang-bang controller (because the control enters the control Hamiltonian linearly) will be

$$u_i^*(t) = \begin{cases} +U_{max}, & S_i(t) < 0 \\ -U_{max}, & S_i(t) > 0 \end{cases} \tag{8.5}$$

where $\boldsymbol{S}(t) = \boldsymbol{\lambda}^T\boldsymbol{F}^{-1}(t)\mathbf{B}$ is the switching function and

$$\begin{aligned} S_i(t) &= [\boldsymbol{\lambda}^T(t)\boldsymbol{F}^{-1}(t)\mathbf{B}]_{\text{row } i+3} \\ &= \sum_{\alpha=1}^{6} \lambda_\alpha(t) \left(\boldsymbol{F}^{-1}(t)\right)_{(\alpha, i+3)} \end{aligned} \tag{8.6}$$

Notice that $S_i(t)$ will be sinusoidal with offset and a ramp, much like the C-W system.[1] The advantage here is that the dynamic system contains all of the zonal harmonics.

7. The same approach/algorithm may be useful for any constant coefficient linear system, including the linear system for the satellite formation developed by Schweighart and Sedwick of MIT [13] which includes the J_2 terms and has position error less than 4%.

8. Develop an algorithm to incorporate the optimal controller based on the CW model into the high fidelity models for orbit prediction.

9. Perform an analysis and develop an algorithm for minimum-time and minimum-fuel control strategies for simultaneous reconfiguration of multiple satellites.

[1]The subscript $_{i+3}$ corresponds to the velocity costates as was the case for the C-W system. For example, the switching function for the first state (i=1) was governed by the x-velocity costate (i=4).

Appendix A. The Classical Clohessy-Wiltshire Equations

This Appendix is adopted from Parker's Dissertation [52] with minor modifications and addition of section A.6.

A.1 Hill's Rotating Coordinate Frame

The Clohessy-Wiltshire approach to describing the dynamics of clustered satellites in a local coordinate frame began with choosing a circular orbit of radius R_o as the local origin, with mean motion $\omega = \sqrt{\frac{\mu_\oplus}{R_o^3}}$. Though Clohessy and Wiltshire originally chose the y axis in the radial direction and the x axis in the negative velocity direction [1], the more conventional approach sets x in the radial, y in the velocity direction, and z normal to the orbit plane [48]. (The details of algebra which follow is worthwhile to see the extensive approximations necessary to yield a linear system.)

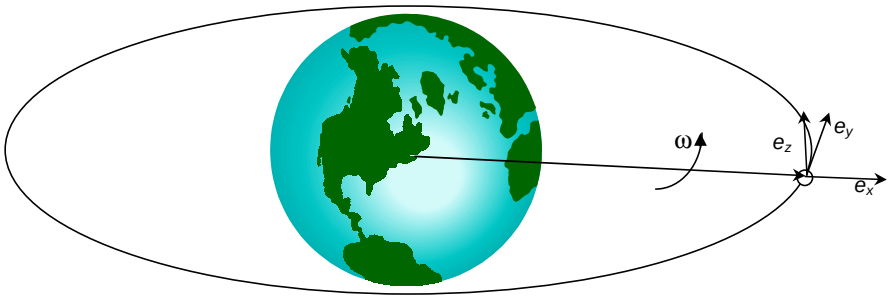

Figure A.1 The Clohessy and Wiltshire coordinate frame with x in the radial direction and y in the velocity direction.

A.2 Kinematics

In this rotating reference frame, the radius vector to a cluster satellite at some location (x, y, z) in the local frame is

$$\vec{\boldsymbol{r}} = (x + R_o)\hat{e}_x + y\hat{e}_y + z\hat{e}_z \tag{A.1}$$

Since the local reference frame rotates with a constant angular velocity of $\omega = n = \sqrt{\frac{\mu_\oplus}{R_o^3}}$, the inertial velocity vector expressed in the rotating coordinate frame is

$$\begin{aligned}\dot{\vec{\boldsymbol{r}}} &= \left[\tfrac{d}{dt}\vec{\boldsymbol{r}}\right]_{xyz} + [\vec{\omega} \times \vec{\boldsymbol{r}}] \\ &= [\dot{x}\hat{e}_x + \dot{y}\hat{e}_y + \dot{z}\hat{e}_z] + [\omega(x + R_o)\hat{e}_y - \omega y\hat{e}_x] \\ &= (\dot{x} - \omega y)\hat{e}_x + [\dot{y} + \omega(x + R_o)]\,\hat{e}_y + \dot{z}\hat{e}_z\end{aligned} \tag{A.2}$$

where $\vec{\omega} = \omega\hat{e}_z$ and the inertial acceleration vector expressed in this rotating coordinate frame is

$$\begin{aligned}\ddot{\vec{\boldsymbol{r}}} &= \left[\tfrac{d}{dt}\dot{\vec{\boldsymbol{r}}}\right]_{xyz} + \left[\vec{\omega} \times \dot{\vec{\boldsymbol{r}}}\right] \\ &= [(\ddot{x} - \omega\dot{y})\hat{e}_x + (\ddot{y} + \omega\dot{x})\hat{e}_y + \ddot{z}\hat{e}_z] + [\omega(\dot{x} - \omega y)\hat{e}_y - \omega\,(\dot{y} + \omega(x + R_o))\,\hat{e}_x] \\ &= [\ddot{x} - 2\omega\dot{y} - \omega^2(x + R_o)]\,\hat{e}_x + (\ddot{y} + 2\omega\dot{x} - \omega^2 y)\hat{e}_y + \ddot{z}\hat{e}_z\end{aligned} \tag{A.3}$$

A.3 Linearization of Central Gravity

In the absence of control forces, gravity is the only acceleration. Therefore, assuming a point source of this central gravity,

$$\begin{aligned}\ddot{\vec{\boldsymbol{r}}} &= \tfrac{-\mu\vec{\boldsymbol{r}}}{|\vec{\boldsymbol{r}}|^3} \\ &= \tfrac{-\mu((x+R_o)\hat{e}_x + y\hat{e}_y + z\hat{e}_z)}{((x+R_o)^2+y^2+z^2)^{\frac{3}{2}}}\end{aligned} \tag{A.4}$$

The denominator may be expanded using the binomial theorem after a few algebraic steps.

$$\begin{aligned}[(x + R_o)^2 + y^2 + z^2]^{\frac{3}{2}} &= (R_o^2 + 2R_o x + x^2 + y^2 + z^2)^{\frac{3}{2}} \\ &= \left[R_o^2\left(1 + \left(\tfrac{2x}{R_o} + \tfrac{x^2}{R_o^2} + \tfrac{y^2}{R_o^2} + \tfrac{z^2}{R_o^2}\right)\right)\right]^{\frac{3}{2}} \\ &= R_o^3\left[1 + \left(\tfrac{2x}{R_o} + \tfrac{x^2}{R_o^2} + \tfrac{y^2}{R_o^2} + \tfrac{z^2}{R_o^2}\right)\right]^{\frac{3}{2}} \text{ using the binomial theorem,} \\ &= R_o^3\left[1 + \tfrac{3}{2}\left(\tfrac{2x}{R_o} + \tfrac{x^2}{R_o^2} + \tfrac{y^2}{R_o^2} + \tfrac{z^2}{R_o^2}\right) + H.O.T.\right]\end{aligned} \tag{A.5}$$

Assuming small components in the local coordinate system, $\frac{x^2}{R_o^2}$, $\frac{y^2}{R_o^2}$, and $\frac{z^2}{R_o^2}$ may be assumed ≈ 0. For a reference orbit of 7000 km and relative distance of 1 km, $(\frac{1}{7000})^2 \approx 2 \times 10^{-8}$. This reduces to

$$\left[(x+R_o)^2+y^2+z^2\right]^{\frac{3}{2}} \approx R_o^3\left[1+\frac{3x}{R_o}\right] = R_o^3 + 3R_o^2 x \tag{A.6}$$

to first order. Inserting this into the $\ddot{\vec{r}}$ expression,

$$\ddot{\vec{r}} \approx \frac{-\mu\left[(x+R_o)\hat{e}_x + y\hat{e}_y + z\hat{e}_z\right]}{R_o^3 + 3R_o^2 x} \tag{A.7}$$

A.4 Linearization of the Dynamics

This expression for the linearized acceleration due to a point source gravity can be equated component by component with the kinematic Equation (A.3) to yield the equations of motion.

$$\begin{aligned} \hat{e}_x: &\quad \tfrac{-\mu(x+R_o)}{R_o^3+3R_o^2x} = \ddot{x} - 2\omega\dot{y} - \omega^2(x+R_o) \\ \hat{e}_y: &\quad \tfrac{-\mu y}{R_o^3+3R_o^2x} = \ddot{y} + 2\omega\dot{x} - \omega^2 y \\ \hat{e}_z: &\quad \tfrac{-\mu z}{R_o^3+3R_o^2x} = \ddot{z} \end{aligned} \tag{A.8}$$

Substituting in $\mu = \omega^2 R_o^3$ and a few steps of algebra yields

$$\begin{aligned} \ddot{x} &= 2\omega\dot{y} + \omega^2(x+R_o) - \tfrac{\omega^2 R_o^3(x+R_o)}{R_o^3(\frac{R_o+3x}{R_o})} \\ \ddot{y} &= -2\omega\dot{x} + \omega^2 y - \tfrac{\omega^2 R_o^3 y}{R_o^3(\frac{R_o+3x}{R_o})} \\ \ddot{z} &= -\tfrac{\omega^2 R_o^3 z}{R_o^3(\frac{R_o+3x}{R_o})} \end{aligned} \tag{A.9}$$

$$\begin{aligned} \ddot{x} &= 2\omega\dot{y} + \omega^2(x+R_o)\left(1-\tfrac{R_o}{R_o+3x}\right) = 2\omega\dot{y} + \omega^2(x+R_o)\left(\tfrac{3x}{R_o+3x}\right) \\ \ddot{y} &= -2\omega\dot{x} + \omega^2 y\left(1-\tfrac{R_o}{R_o+3x}\right) = -2\omega\dot{x} + \omega^2 y\left(\tfrac{3x}{R_o+3x}\right) \\ \ddot{z} &= -\omega^2 z\left(\tfrac{R_o}{R_o+3x}\right) \end{aligned} \tag{A.10}$$

For small displacements in the local coordinate frame, it is possible to linearize further. Assuming $x + R_o \approx R_o$, and $3x + R_o \approx R_o$,

$$\ddot{x} = 2\omega\dot{y} + 3\omega^2 x \tag{A.11a}$$

$$\ddot{y} = -2\omega\dot{x} \tag{A.11b}$$

$$\ddot{z} = -\omega^2 z \tag{A.11c}$$

which are the classical linearized Clohessy-Wiltshire equations of motion (C-W Equation) in relative coordinates.

A.5 State-Space Representation

By employing normalized, canonical units, ($\omega = 1$, $\mu_\oplus = 1$) it is possible to set up a linear system using the state-space form. Adding in thrusts along each axis as T_x, T_y, and T_z,

$$\begin{bmatrix} \dot{x} \\ \dot{y} \\ \dot{z} \\ \ddot{x} \\ \ddot{y} \\ \ddot{z} \end{bmatrix} = \begin{bmatrix} 0 & 0 & 0 & 1 & 0 & 0 \\ 0 & 0 & 0 & 0 & 1 & 0 \\ 0 & 0 & 0 & 0 & 0 & 1 \\ 3 & 0 & 0 & 0 & 2 & 0 \\ 0 & 0 & 0 & -2 & 0 & 0 \\ 0 & 0 & -1 & 0 & 0 & 0 \end{bmatrix} \begin{bmatrix} x \\ y \\ z \\ \dot{x} \\ \dot{y} \\ \dot{z} \end{bmatrix} + \begin{bmatrix} 0 & 0 & 0 \\ 0 & 0 & 0 \\ 0 & 0 & 0 \\ 1 & 0 & 0 \\ 0 & 1 & 0 \\ 0 & 0 & 1 \end{bmatrix} \begin{bmatrix} u_x \\ u_y \\ u_z \end{bmatrix} \tag{A.12}$$

where,

$$\begin{bmatrix} u_x \\ u_y \\ u_z \end{bmatrix} = \begin{bmatrix} \frac{T_x}{m} \\ \frac{T_y}{m} \\ \frac{T_z}{m} \end{bmatrix} \tag{A.13}$$

and $\mathbf{u}^T = [u_x, u_y, u_z]$ is the net/effective acceleration between the member satellite and the reference orbit. This has the familiar form of a linear, constant-coefficient dynamic

system[46].

$$\dot{\mathbf{x}}(t) = \mathbf{A}\mathbf{x}(t) + \mathbf{B}\mathbf{u}(t) \tag{A.14}$$

A.6 Closed Form Solution with Constant Forcing

The z-equations decouples to

$$\begin{bmatrix} \dot{z}(t) \\ \ddot{z}(t) \end{bmatrix} = \begin{bmatrix} 0 & 1 \\ -1 & 0 \end{bmatrix} \begin{bmatrix} z(t) \\ \dot{z}(t) \end{bmatrix} + \begin{bmatrix} 0 \\ u_z(t) \end{bmatrix} \tag{A.15}$$

which can be solved easily for $u_z(t) = \text{constant } \forall\ t \in [t_{on}, t_{off}]$ given $z(t = t_{on}) = z_o$ and $\dot{z}(t = t_{on}) = \dot{z}_o$.

$$z(t) = \frac{\dot{z}_o}{\omega} \sin(\omega(t - t_{on})) + \left(z_o - \frac{u_z}{\omega^2}\right) \cos(\omega(t - t_{on})) + \frac{u_z}{\omega^2} \tag{A.16}$$

and for $\omega = 1$ for canonical units,

$$z(t) = \dot{z}_o \sin(t - t_{on}) + (z_o - u_z) \cos(t - t_{on}) + u_z \tag{A.17}$$

Now, for the x and y equations, Equation (A.12) can be reduced to,

$$\begin{bmatrix} \dot{x}(t) \\ \dot{y}(t) \\ \ddot{x}(t) \\ \ddot{y}(t) \end{bmatrix} = \begin{bmatrix} 0 & 0 & 1 & 0 \\ 0 & 0 & 0 & 1 \\ 3 & 0 & 0 & 2 \\ 0 & 0 & -2 & 0 \end{bmatrix} \begin{bmatrix} x(t) \\ y(t) \\ \dot{x}(t) \\ \dot{y}(t) \end{bmatrix} + \begin{bmatrix} 0 & 0 \\ 0 & 0 \\ 1 & 0 \\ 0 & 1 \end{bmatrix} \begin{bmatrix} u_x(t) \\ u_y(t) \end{bmatrix} \tag{A.18}$$

which can be solved by [46],

$$\mathbf{x}(t) = \mathbf{\Phi}_x(t, t_o)\mathbf{x}_o + \int_{t_o}^{t} \mathbf{\Phi}_x(t, \tau)\mathbf{B}\mathbf{u}(t)d\tau \tag{A.19}$$

where $\mathbf{\Phi}_x(t, t_o)$ is the transition matrix, $e^{\mathbf{A}(t-t_o)}$ and $\mathbf{x}_o$ is the state vector at $t = t_o$.

$$\mathbf{\Phi}_x(t,t_o) = \begin{bmatrix} 4-3\cos(\omega(t-t_{on})) & 0 & \frac{\sin(\omega(t-t_{on}))}{\omega} & \frac{-2\cos(\omega(t-t_{on}))+2}{\omega} \\ 6\sin(\omega(t-t_{on}))-6\omega(t-t_{on}) & 1 & \frac{2\cos(\omega(t-t_{on}))-2}{\omega} & \frac{-3\omega(t-t_{on})+4\sin(\omega(t-t_{on}))}{\omega} \\ 3\omega\sin(\omega(t-t_{on})) & 0 & \cos(\omega(t-t_{on})) & 2\sin(\omega(t-t_{on})) \\ 6\omega\cos(\omega(t-t_{on}))-6\omega & 0 & -2sin(\omega(t-t_{on})) & -3+4\cos(\omega(t-t_{on})) \end{bmatrix} \tag{A.20}$$

After carrying out the multiplication and the integration with constant controls, the $x(t)$ and $y(t)$ solutions for $t \in [t_o, t_{off}]$ becomes,

$$\begin{aligned} x(t) &= (4-3\cos(\omega(t-t_{on})))\,x_o + \frac{\dot{x}_o}{\omega}\sin(\omega(t-t_{on})) + \frac{2\dot{y}_o}{\omega}(1-\cos(\omega(t-t_{on}))) \\ &\quad + \frac{u_x}{\omega^2}(1-\cos(\omega(t-t_{on}))) + \frac{2u_y}{\omega^2}(\omega(t-t_{on}) - sin(\omega(t-t_{on}))) \end{aligned} \tag{A.21}$$

$$\begin{aligned} y(t) &= 6(\sin(\omega(t-t_{on})) - \omega t)\,x_o + y_o + \frac{2\dot{x}_o}{\omega}(\cos(\omega(t-t_{on})) - 1) \\ &\quad + \frac{\dot{y}_o}{\omega}(-3\omega(t-t_{on}) + 4\sin(\omega(t-t_{on}))) \\ &\quad + \frac{2u_x}{\omega^2}\sin(\omega(t-t_{on})) - \frac{2u_x}{\omega}t - \frac{3u_y}{2}t^2 + \frac{4u_y}{\omega^2}(1-\cos(\omega(t-t_{on}))) \end{aligned} \tag{A.22}$$

In summary, for $\omega = 1$, we have

$$\begin{aligned} x(t) &= [\dot{x}_o - 2u_y]\sin(t-t_{on}) - [3x_o + 2\dot{y}_o + u_x]\cos(t-t_{on}) \\ &\quad + 2u_y(t-t_{on}) + [4x_o + 2\dot{y}_o + u_x] \end{aligned} \tag{A.23}$$

$$\begin{aligned} y(t) &= 2[3x_o + 2\dot{y}_o + u_x]\sin(t-t_{on}) + 2[\dot{x}_o - 2u_y]\cos(t-t_{on}) \\ &\quad - \frac{3}{2}u_y(t-t_{on})^2 - 3\left[2x_o + \dot{y}_o + \frac{2}{3}u_x\right](t-t_{on}) + [y_o - 2(\dot{x}_o - 2u_y)] \end{aligned} \tag{A.24}$$

$$z(t) = \dot{z}_o\sin(t-t_{on}) + (z_o - u_z)\cos(t-t_{on}) + u_z \tag{A.25}$$

Appendix B. Hill's Equations, Solution, and Parameterizations

This Appendix is also adopted from Parker's Dissertation [52] with enhancement of section B.2 and addition of sections B.3 and B.4.

B.1 Solution

As derived in Appendix A, the linearized equations of motion for a satellite formation in a localized coordinate system are

$$\ddot{x} = 2\omega\dot{y} + 3\omega^2 x \tag{B.1a}$$

$$\ddot{y} = -2\omega\dot{x} \tag{B.1b}$$

$$\ddot{z} = -\omega^2 z \tag{B.1c}$$

Summarizing the derivation by Irvin [41], these equations can be solved in terms of these constants by first performing the Laplace transformation

$$\begin{aligned} s^2X(s) - sx_o - \dot{x}_o &= 2\omega[sY(s) - y_o] + 3\omega^2 X(s) \\ s^2Y(s) - sy_o - \dot{y}_o &= -2\omega[sX(s) - x_o] \\ s^2Z(s) - sz_o - \dot{z}_o &= \omega^2 Z(s) \end{aligned} \tag{B.2}$$

where the subscripted "$_o$" values are the components of initial position and velocity. Collecting these initial conditions, these equations may be expressed in matrix form as

$$\begin{bmatrix} s^2 - 3\omega^2 & -2\omega s & 0 \\ 2\omega s & s^2 & 0 \\ 0 & 0 & s^2 + \omega^2 \end{bmatrix} \begin{bmatrix} X(s) \\ Y(s) \\ Z(s) \end{bmatrix} = \begin{bmatrix} sx_o + \dot{x}_o - 2\omega y_o \\ sy_o + \dot{y}_o - 2\omega x_o \\ sz_o + \dot{z}_o \end{bmatrix} \tag{B.3}$$

Solving for $X(s)$, $Y(s)$, and $Z(s)$

$$\begin{aligned}\begin{bmatrix} X(s) \\ Y(s) \\ Z(s) \end{bmatrix} &= \begin{bmatrix} \frac{1}{s^2+\omega^2} & \frac{2\omega}{s(s^2+\omega^2)} & 0 \\ \frac{-2\omega}{s(s^2+\omega^2)} & \frac{s^2-3\omega^2}{s^s(s^2+\omega^2)} & 0 \\ 0 & 0 & \frac{1}{s^2+\omega^2} \end{bmatrix} \begin{bmatrix} sx_o + \dot{x}_o - 2\omega y_o \\ sy_o + \dot{y}_o - 2\omega x_o \\ sz_o + \dot{z}_o \end{bmatrix} \\ &= \begin{bmatrix} \frac{sx_o+\dot{x}_o-2\omega y_o}{s^2+\omega^2} + \frac{2\omega(sy_o+\dot{y}_o)+2\omega x_o}{s(s^2+\omega^2)} \\ \frac{-2\omega(sx_o+\dot{x}_o-2\omega y_o)}{s(s^2+\omega^2)} + \frac{(s^2-3\omega^2)(sy_o+\dot{y}_o+2\omega x_o)}{s^2(s^2+\omega^2)} \\ \frac{sz_o+\dot{z}_o}{s^2+\omega^2} \end{bmatrix}\end{aligned} \tag{B.4}$$

Performing the partial fraction expansion and setting up for the inverse Laplace transform by collecting terms,

$$\begin{aligned}\begin{bmatrix} X(s) \\ Y(s) \\ Z(s) \end{bmatrix} &= \begin{bmatrix} \frac{sx_o+\dot{x}_o-2\omega y_o}{s^2+\omega^2} + \frac{2\omega^2 y_o-2s\dot{y}_o-4s\omega x_o}{\omega(s^2+\omega^2)} + \frac{2\dot{y}_o+4\omega x_o}{\omega}\frac{1}{s} \\ \frac{4sy_o+4\dot{y}_o+8\omega x_o}{s^2+\omega^2} + \frac{-2\omega^2 x_o+2s\dot{x}_o-4sy_o\omega}{\omega(s^2+\omega^2)} + \frac{-3\dot{y}_o-6\omega x_o}{s^2} + \frac{\omega y_o-2\dot{x}_o}{\omega}\frac{1}{s} \\ \frac{sz_o+\dot{z}_o}{s^2+\omega^2} \end{bmatrix} \\ &= \begin{bmatrix} \frac{\left(x_o-\frac{2\dot{y}_o+4\omega x_o}{\omega}\right)s}{s^2+\omega^2} + \frac{\left(\frac{\dot{x}_o}{\omega}\right)\omega}{s^2+\omega^2} + \frac{2\dot{y}_o+4\omega x_o}{\omega}\frac{1}{s} \\ \frac{2\left(\frac{\dot{x}_o}{\omega}\right)s}{s^2+\omega^2} + \frac{2\left(\frac{2\dot{y}_o+4\omega x_o}{\omega}-x_o\right)\omega}{s^2+\omega^2} - \frac{3\omega}{2}\frac{2\dot{y}_o+4\omega x_o}{\omega}\frac{1}{s^2} + \frac{\omega y_o-2\dot{x}_o}{\omega}\frac{1}{s} \\ \frac{sz_o}{s^2+\omega^2} + \frac{\left(\frac{\dot{z}_o}{\omega}\right)\omega}{s^2+\omega^2} \end{bmatrix}\end{aligned} \tag{B.5}$$

and perform the inverse transform [41]

$$x(t) = \left(-3x_o - \frac{2\dot{y}_o}{\omega}\right)\cos(\omega t + \theta_o) + \frac{\dot{x}_o}{\omega}\sin(\omega t + \theta_o) + \frac{2\dot{y}_o}{\omega} + 4x_o \tag{B.6a}$$

$$\begin{aligned} y(t) &= 2\left(\frac{\dot{x}_o}{\omega}\right)\cos(\omega t + \theta_o) + 2\left(\frac{2\dot{y}_o}{\omega} + 3x_o\right)\sin(\omega t + \theta_o) \\ &\quad - \frac{3\omega t}{2}\left(\frac{2\dot{y}_o}{\omega} + 4x_o\right) + \frac{\omega y_o - 2\dot{x}_o}{\omega} \end{aligned} \tag{B.6b}$$

$$z(t) = z_o\cos(\omega t + \theta_o) + \frac{\dot{z}_o}{\omega}\sin(\omega t + \theta_o) \tag{B.6c}$$

Note that θ_o is just an initial phase angle. This is equivalent to homogeneous part of the solutions in Appendix A, equations (A.16) and (A.21).

B.2 Parameterizations

As presented by Yeh and Sparks [49], these equations can be parameterized in terms of six arbitrary constants: a, b, ρ, m, n, and θ_o. Since the initial conditions are not time-dependent, and ω is a constant for the system, it is possible to define the following constants,

$$a = \frac{2\dot{y}_o + 4\omega x_o}{\omega} \tag{B.7a}$$

$$b = \frac{\omega y_o - 2\dot{x}_o}{\omega} \tag{B.7b}$$

$$\rho^2 = (x_o - a)^2 + \left(\frac{\dot{x}_o}{\omega}\right)^2 \tag{B.7c}$$

$$m = \frac{\dot{z}_o\dot{x}_o - z_o\omega^2(a - x_o)}{\dot{x}_o^2 + \omega^2(a - x_o)^2} \tag{B.7d}$$

$$n = \frac{z_o\dot{x}_o\omega + \dot{z}_o\omega(a - x_o)}{2\left[\dot{x}_o^2 + \omega^2(a - x_o)^2\right]} \tag{B.7e}$$

$$\tan\theta_o = \frac{\omega(x_o - a)}{\dot{x}_o} \tag{B.7f}$$

These constants describe the size, shape, location, and phase of the formation elements' relative orbits in the local coordinate system. Their physical interpretation within the x-y plane is shown in Figure B.1. The parameter m is the tangent of the angle between the minor axis and $\hat{e}_x$, and n is the tangent of the angle between the major axis and $\hat{e}_y$.

Using these parameters, Clohessy and Wiltshire's solutions may be written as

$$x(t) = \rho\sin(\omega t + \theta_o) + a \tag{B.8a}$$

$$y(t) = 2\rho\cos(\omega t + \theta_o) - \frac{3\omega}{2}at + b \tag{B.8b}$$

$$z(t) = m\rho\sin(\omega t + \theta_o) + 2n\rho\cos(\omega t + \theta_o) \tag{B.8c}$$

Obviously, the secular term in $y(t)$ causes a problem for maintaining a closed path in the local coordinate system. Therefore, keeping a formation together requires $a = 0$. This yields the initial constraint of $\dot{y}_o = -2\omega x_o$. From Yeh and Sparks [49], the parameteri-

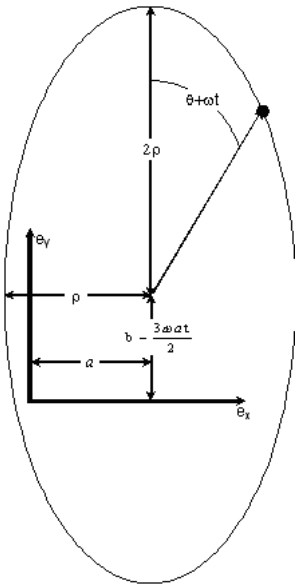

Figure B.1 The constants defined to parameterize the C-W solution define the relative orbit size (ρ), location (a and b), and phase (θ) .

zations yields the identities:

$$\begin{aligned} &\tfrac{(x-a)^2}{\rho^2} + \tfrac{\left(y+\frac{3\omega}{2}at-b\right)^2}{(2\rho)^2} = 1 \\ &z(t) = m(x-a) + n(y+\tfrac{3\omega}{2}at - b) \end{aligned} \tag{B.9}$$

For a non-dispersing formation, these become:

$$\begin{aligned} &\tfrac{x^2}{\rho^2} + \tfrac{(y-b)^2}{(2\rho)^2} = 1 \\ &z = mx + n(y-b) \end{aligned} \tag{B.10}$$

and b becomes simply an offset of the relative orbit along the velocity direction. Since Hill's equations have a limited range of validity, there is no immediate reason to offset the origin from the ellipse center, so formations also set $b = 0$. Thus the degrees of freedom for the orbit of each allowable element of a formation have been reduced from six to four, in agreement with Schaub and Alfriend [14].

For better visualization, examine the special orbit with no cross-track motion; i.e., $z(t) = 0\ \forall t$. The non-dispersing relative elliptic motion is achieved due to the period

matching of the reference orbit and the relative orbit. While the reference orbit is circular (dashed line), the relative orbit is slightly elliptic (bold line); see figure B.2. At point A($y = 0,\ x = \rho$), the member spacecraft is at the apogee of the relative orbit hence is slower than the reference orbit. At point B($y = -2\rho,\ x = 0$), the member spacecraft is at the same altitude as the reference orbit, but have lagged behind. At point C($y = 0,\ x = -\rho$), the member spacecraft has reached perigee on the reference orbit and is lower and faster than the reference orbit. At point D($y = 2\rho,\ x = 0$), the member spacecraft is again at the same altitude, but have moved ahead.

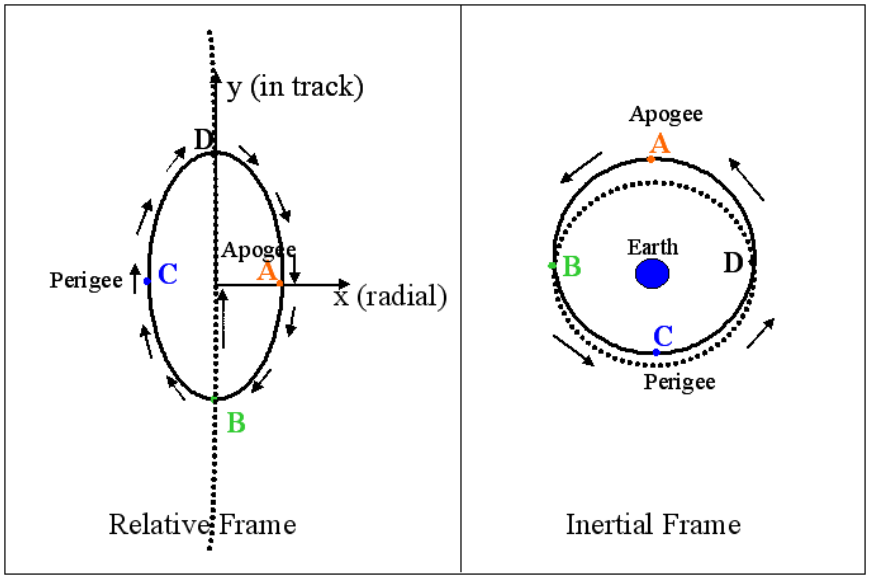

Figure B.2 2:1 Relative Ellipse

The phase angle $\omega t + \theta_o$ is not a physical angle on the relative ellipse. Rather it is the angle on the larger circumscribed circle with radius of 2ρ (or on the smaller inscribed circle with radius of ρ); see figure B.3. The relationship between the phase angle, $\omega t + \theta_o$, and the physical angle, γ, is given by

$$\begin{aligned} \tan(\gamma) &= \frac{x}{y} \\ &= \frac{\rho \sin(\omega t + \theta_o)}{2\rho \cos(\omega t + \theta_o)} \\ &= \frac{1}{2} \tan(\omega t + \theta_o) \end{aligned} \tag{B.11}$$

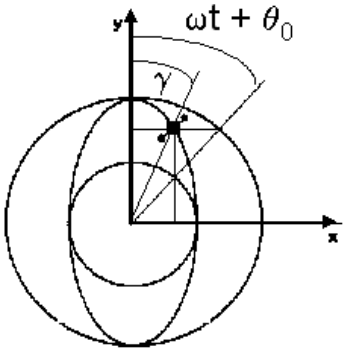

Phase Angle

Figure B.3 Phase Angle on the Relative Ellipse

The motion on the circumscribed circle (or the inscribed circle) is uniform with angular velocity of ω, however, the motion on the relative ellipse is not. By taking derivative of Eqn. (B.11),

$$\begin{aligned}
\dot{\gamma} &= \frac{\omega \sec^2(\omega t + \theta_o)}{2 \sec^2 \gamma} \\
&= \frac{\omega}{2} \frac{\sec^2(\omega t + \theta_o)}{(1 + \tan^2 \gamma)} \\
&= \frac{\omega}{2} \frac{\sec^2(\omega t + \theta_o)}{\left(1 + \frac{1}{4} \tan^2(\omega t + \theta_o)\right)} \\
&= \frac{2\omega}{4 \cos^2(\omega t + \theta_o) + \sin^2(\omega t + \theta_o)} \\
&= \frac{2\omega}{1 + 3 \cos^2(\omega t + \theta_o)}
\end{aligned} \tag{B.12}$$

B.3 Inverse Parameterization

The inverse mapping from the parameters describing the relative orbit to initial conditions cab be obtained from Eq(B.8) and its derivatives

$$\dot{x}(t) = \rho\omega\cos(\omega t + \theta_o) \tag{B.13a}$$

$$\dot{y}(t) = -2\rho\omega\sin(\omega t + \theta_o) - \frac{3\omega}{2}a \tag{B.13b}$$

$$\dot{z}(t) = m\rho\omega\cos(\omega t + \theta_o) - 2n\rho\omega\sin(\omega t + \theta_o) \tag{B.13c}$$

By solving both Equations (B.8) and (B.13) at $t = 0$:

$$x_o = x(t=0) = \rho\sin(\theta_o) + a \tag{B.14a}$$

$$y_o = y(t=0) = 2\rho\cos(\theta_o) + b \tag{B.14b}$$

$$z_o = z(t=0) = m\rho\sin(\theta_o) + 2n\rho\cos(\theta_o) \tag{B.14c}$$

$$\dot{x}_o = \dot{x}(t=0) = \rho\omega\cos(\theta_o) \tag{B.14d}$$

$$\dot{y}_o = \dot{y}(t=0) = -2\rho\omega\sin(\theta_o) - \frac{3\omega}{2}a \tag{B.14e}$$

$$\dot{z}_o = \dot{z}(t=0) = m\rho\omega\cos(\theta_o) - 2n\rho\omega\sin(\theta_o) \tag{B.14f}$$

Now for a non-dispersing formation centered on the reference orbit ($a = b = 0$), this simply reduces to:

$$x_o = \rho\sin\theta_o \tag{B.15a}$$

$$y_o = 2\rho\cos\theta_o \tag{B.15b}$$

$$z_o = m\rho\sin\theta_o + 2n\rho\cos\theta_o \tag{B.15c}$$

$$\dot{x}_o = \rho\omega\cos\theta_o \tag{B.15d}$$

$$\dot{y}_o = -2\rho\omega\sin\theta_o \tag{B.15e}$$

$$\dot{z}_o = m\rho\omega\cos\theta_o - 2n\rho\omega\sin\theta_o \tag{B.15f}$$

These transformation will allow easy specification of natural orbits as the desired terminal state. Only difficulty would be to specify which point on the natural orbit to target.

B.4 Time Variation of In-Plane Relative Orbit Parameters

In this appendix, up to now, the parameters were considered constants, except for the phase angle θ. However, this is only true if the drifting parameter, a, is exactly zero. There are two situations in which a will not be zero; i.e., there will be in-track drift. In the first case, the satellite member is not on a stable relative orbit. The second situation occurs when the satellite member is on a stable orbit initially, but once control is activated, the satellite will immediately move off of the stable orbit. So, these parameters need to be considered time varying during active control. Then, at any instant in time, the in-plane states are transformed into the instantaneous in-plane relative orbit parameters:

$$a(t) = 4x(t) + 2\frac{\dot{y}(t)}{\omega} \tag{B.16a}$$

$$b(t) = y(t) - 2\frac{\dot{x}(t)}{\omega} \tag{B.16b}$$

$$\rho^2(t) = (x(t) - a(t))^2 + \left(\frac{\dot{x}(t)}{\omega}\right)^2 \tag{B.16c}$$

$$\tan\theta(t) = = \omega\frac{x(t) - a(t)}{\dot{x}(t)} \tag{B.16d}$$

Appendix C. The First Order Variation for Minimum Time Problem

This appendix describes the first order necessary condition for minimum time problem. The derivation is a well known results from the optimal control theory using calculus of variation.

Performance Index:

$$J[\mathbf{u}(t)] = t_f - t_o = \int_{t_o}^{t_f} dt \tag{C.1}$$

where t_o is fixed, but t_f is free.

Dynamic Constraint:

$$\dot{\mathbf{x}}(t) = \mathbf{A}\mathbf{x}(t) + \mathbf{B}\mathbf{u}(t) \tag{C.2}$$

Terminal State Constraint:

$$\mathbf{\Psi}(\mathbf{x}(t_f), t_f) = 0 \tag{C.3}$$

Control Constraint:

$$|u_i(t)| \leq U_{max} \qquad i = x, y, z \tag{C.4}$$

Augmenting the Performance Index with constant lagrange multipliers for the terminal state constraint and dynamic lagrange multipliers (also known as the Adjoint or Costate) for the dynamic constraint:

$$\widetilde{J}[\mathbf{u}(t)] = \boldsymbol{\nu}^T \mathbf{\Psi}(\mathbf{x}(t_f), t_f) + \int_{t_o}^{t_f} \left(1 + \boldsymbol{\lambda}^T(t) \left[\mathbf{A}\mathbf{x}(t) + \mathbf{B}\mathbf{u}(t) - \dot{\mathbf{x}}(t)\right]\right) dt \tag{C.5}$$

Define the control or variational Hamiltonian: $H(\mathbf{x}(t), \mathbf{u}(t), \boldsymbol{\lambda}(t), t) = H(\mathbf{x}(t), \mathbf{u}(t), \boldsymbol{\lambda}(t)) = 1 + \boldsymbol{\lambda}^T(t) \left[\mathbf{A}\mathbf{x}(t) + \mathbf{B}\mathbf{u}(t)\right]$ Then,

$$\widetilde{J}[\mathbf{u}(t)] = \boldsymbol{\nu}^T \mathbf{\Psi}(\mathbf{x}(t_f), t_f) + \int_{t_o}^{t_f} \left[H(\mathbf{x}(t), \mathbf{u}(t), \boldsymbol{\lambda}(t)) - \boldsymbol{\lambda}^T(t)\dot{\mathbf{x}}(t)\right] dt \tag{C.6}$$

C.1 First Variation

Now, taking the first variation,

$$\begin{aligned}\delta\widetilde{J} &= \boldsymbol{\nu}^T\frac{\partial\boldsymbol{\Psi}\left(\mathbf{x}(t_f),t_f\right)}{\partial t_f}\delta t_f+\boldsymbol{\nu}^T\frac{\partial\boldsymbol{\Psi}\left(\mathbf{x}(t_f),t_f\right)}{\partial\mathbf{x}(t_f)}\delta\mathbf{x}(t_f)+\left[\left(H-\boldsymbol{\lambda}^T(t)\dot{\mathbf{x}}(t)\right)\delta t\right]\Big|_{t_o}^{t_f}\\ &\quad+\int_{t_o}^{t_f}\left[\frac{\partial H}{\partial\mathbf{x}(t)}\widetilde{\delta}\mathbf{x}(t)+\frac{\partial H}{\partial\mathbf{u}(t)}\widetilde{\delta}\mathbf{u}(t)-\boldsymbol{\lambda}^T(t)\widetilde{\delta}\dot{\mathbf{x}}(t)\right]dt \qquad \text{(C.7)}\end{aligned}$$

where $\delta(\cdot)$ is a total variation and $\widetilde{\delta}(\cdot)$is a partial variation. Since $\mathbf{x}(t)$ is continuous,

$$\widetilde{\delta}\dot{\mathbf{x}}(t)=\widetilde{\delta}\left(\frac{d\mathbf{x}(t)}{dt}\right)=\frac{d\left(\widetilde{\delta}\mathbf{x}(t)\right)}{dt} \qquad \text{(C.8)}$$

Now, integrating the last term in the integral by parts,

$$-\int_{t_o}^{t_f}\boldsymbol{\lambda}^T(t)\widetilde{\delta}\dot{\mathbf{x}}(t)dt=-\int_{t_o}^{t_f}\boldsymbol{\lambda}^T(t)d\left(\widetilde{\delta}\mathbf{x}(t)\right)=-\left[\boldsymbol{\lambda}^T(t)\widetilde{\delta}\mathbf{x}(t)\right]\Big|_{t_o}^{t_f}+\int_{t_o}^{t_f}\dot{\boldsymbol{\lambda}}^T(t)\widetilde{\delta}\mathbf{x}(t)dt \qquad \text{(C.9)}$$

and we note that $\delta\mathbf{x}(t)=\widetilde{\delta}\mathbf{x}(t)+\dot{\mathbf{x}}(t)\delta t\ \rightarrow\ \widetilde{\delta}\mathbf{x}(t)=\delta\mathbf{x}(t)-\dot{\mathbf{x}}(t)\delta t$. So,

$$\begin{aligned}-\int_{t_o}^{t_f}\boldsymbol{\lambda}^T(t)\widetilde{\delta}\dot{\mathbf{x}}(t)dt &= -\left[\boldsymbol{\lambda}^T(t)\delta\mathbf{x}(t)-\boldsymbol{\lambda}^T(t)\dot{\mathbf{x}}(t)\delta t\right]\Big|_{t_o}^{t_f}+\int_{t_o}^{t_f}\dot{\boldsymbol{\lambda}}^T(t)\widetilde{\delta}\mathbf{x}(t)dt\\ &= -\left[\boldsymbol{\lambda}^T(t)\delta\mathbf{x}(t)\right]\Big|_{t_o}^{t_f}+\left[\boldsymbol{\lambda}^T(t)\dot{\mathbf{x}}(t)\delta t\right]\Big|_{t_o}^{t_f}+\int_{t_o}^{t_f}\dot{\boldsymbol{\lambda}}^T(t)\widetilde{\delta}\mathbf{x}(t)dt\\ &= -\boldsymbol{\lambda}^T(t_f)\delta\mathbf{x}(t_f)+\boldsymbol{\lambda}^T(t_o)\delta t_o+\left[\boldsymbol{\lambda}^T(t)\dot{\mathbf{x}}(t)\right]\Big|_{t_f}\delta t_f-\left[\boldsymbol{\lambda}^T(t)\dot{\mathbf{x}}(t)\right]\Big|_{t_o}\delta t_o\\ &\quad+\int_{t_o}^{t_f}\dot{\boldsymbol{\lambda}}^T(t)\widetilde{\delta}\mathbf{x}(t)dt \qquad \text{(C.10)}\end{aligned}$$

The first variation now becomes,

$$\begin{aligned}
\delta\widetilde{J} &= \nu\frac{\partial\boldsymbol{\Psi}\left(\mathbf{x}(t_f),t_f\right)}{\partial t_f}\delta t_f + \boldsymbol{\nu}^T\frac{\partial\boldsymbol{\Psi}\left(\mathbf{x}(t_f),t_f\right)}{\partial\mathbf{x}(t_f)}\delta\mathbf{x}(t_f) + \left(H-\boldsymbol{\lambda}^T(t)\dot{\mathbf{x}}(t)\right)|_{t_f}\delta t_f \\
&\quad - \left(H-\boldsymbol{\lambda}^T(t)\dot{\mathbf{x}}(t)\right)|_{t_o}\delta t_o + \int_{t_o}^{t_f}\left[\frac{\partial H}{\partial\mathbf{x}(t)}\widetilde{\delta}\mathbf{x}(t) + \frac{\partial H}{\partial\mathbf{u}(t)}\widetilde{\delta}\mathbf{u}(t)\right]dt \\
&\quad -\boldsymbol{\lambda}^T(t_f)\delta\mathbf{x}(t_f) + \boldsymbol{\lambda}^T(t_o)\delta t_o + \left[\boldsymbol{\lambda}^T(t)\dot{\mathbf{x}}(t)\right]|_{t_f}\delta t_f - \left[\boldsymbol{\lambda}^T(t)\dot{\mathbf{x}}(t)\right]|_{t_o}\delta t_o \\
&\quad + \int_{t_o}^{t_f}\dot{\boldsymbol{\lambda}}^T(t)\widetilde{\delta}\mathbf{x}(t)dt \\
&= \nu\frac{\partial\boldsymbol{\Psi}\left(\mathbf{x}(t_f),t_f\right)}{\partial t_f}\delta t_f + \boldsymbol{\nu}^T\frac{\partial\boldsymbol{\Psi}\left(\mathbf{x}(t_f),t_f\right)}{\partial\mathbf{x}(t_f)}\delta\mathbf{x}(t_f) + (H)|_{t_f}\delta t_f - (H)|_{t_o}\delta t_o \\
&\quad + \int_{t_o}^{t_f}\left[\left(\frac{\partial H}{\partial\mathbf{x}(t)} + \dot{\boldsymbol{\lambda}}^T(t)\right)\widetilde{\delta}\mathbf{x}(t) + \frac{\partial H}{\partial\mathbf{u}(t)}\widetilde{\delta}\mathbf{u}(t)\right]dt \\
&\quad -\boldsymbol{\lambda}^T(t_f)\delta\mathbf{x}(t_f) + \boldsymbol{\lambda}^T(t_o)\delta\mathbf{x}(t_o)
\end{aligned} \tag{C.11}$$

We also have fixed initial time and initial state ($\delta t_o = \delta\mathbf{x}(t_o) = 0$), then

$$\begin{aligned}
\delta\widetilde{J} &= \left[\boldsymbol{\nu}^T\frac{\partial\boldsymbol{\Psi}\left(\mathbf{x}(t_f),t_f\right)}{\partial t_f} + H\left(t_f\right)\right]\delta t_f + \left[\boldsymbol{\nu}^T\frac{\partial\boldsymbol{\Psi}\left(\mathbf{x}(t_f),t_f\right)}{\partial\mathbf{x}(t_f)} - \boldsymbol{\lambda}^T(t_f)\right]\delta\mathbf{x}(t_f) \\
&\quad + \int_{t_o}^{t_f}\left[\left(\frac{\partial H}{\partial\mathbf{x}(t)} + \dot{\boldsymbol{\lambda}}^T(t)\right)\widetilde{\delta}\mathbf{x}(t) + \frac{\partial H}{\partial\mathbf{u}(t)}\widetilde{\delta}\mathbf{u}(t)\right]dt
\end{aligned} \tag{C.12}$$

Now we choose the costate such that:

1. Costate/Adjoint Equation

$$\frac{\partial H}{\partial\mathbf{x}(t)} + \dot{\boldsymbol{\lambda}}^T(t) = 0 \qquad \rightarrow \qquad \dot{\boldsymbol{\lambda}}^T(t) = -\frac{\partial H}{\partial\mathbf{x}(t)} = -\boldsymbol{\lambda}^T(t)\mathbf{A} \tag{C.13}$$

   This equation along with $\dot{\mathbf{x}}(t) = \mathbf{A}\mathbf{x}(t) + \mathbf{B}\mathbf{u}(t)$ are known as the Euler-Lagrange equations.

2. Natural Boundary Condition

$$\boldsymbol{\nu}^T\frac{\partial\boldsymbol{\Psi}\left(\mathbf{x}(t_f),t_f\right)}{\partial\mathbf{x}(t_f)} - \boldsymbol{\lambda}^T(t_f) = 0 \qquad \rightarrow \qquad \boldsymbol{\lambda}^T(t_f) = \boldsymbol{\nu}^T\frac{\partial\boldsymbol{\Psi}\left(\mathbf{x}(t_f),t_f\right)}{\partial\mathbf{x}(t_f)} \tag{C.14}$$

Then, the first variation is reduced to,

$$\delta\widetilde{J} = \left[\boldsymbol{\nu}^T \frac{\partial \boldsymbol{\Psi}\left(\mathbf{x}(t_f), t_f\right)}{\partial t_f} + H\left(t_f\right)\right] \delta t_f + \int_{t_o}^{t_f} \frac{\partial H}{\partial \mathbf{u}(t)} \widetilde{\delta}\mathbf{u}(t) dt \tag{C.15}$$

For an extremum, the first variation must necessarily be zero. The two remaining variations are independent and we must now require these additional necessary conditions:

3. Optimality Condition

$$\frac{\partial H}{\partial \mathbf{u}(t)} = 0 \qquad \rightarrow \qquad \boldsymbol{\lambda}^T(t)\mathbf{B} = 0 \tag{C.16}$$

   Notice this equation does not provide the optimal control directly because the control Hamiltonian is linear in $\mathbf{u}$. We must rely on Pontryagin's Minimum Principle which examined the second variation. The resulting optimal control minimizes the Hamiltonian and leads to a Bang-Bang controller. We shall see that $\boldsymbol{\lambda}^T(t)\mathbf{B}$ is the switching function for the Bang-Bang controller and that $\boldsymbol{\lambda}^T(t_i)\mathbf{B} = 0$ where t_i are the control switch times.

4. Transversality Condition

$$\begin{aligned} \boldsymbol{\nu}^T \frac{\partial \boldsymbol{\Psi}\left(\mathbf{x}(t_f), t_f\right)}{\partial t_f} &+ H(t_f) = 0 \\ \boldsymbol{\nu}^T \frac{\partial \boldsymbol{\Psi}\left(\mathbf{x}(t_f), t_f\right)}{\partial t_f} &+ \boldsymbol{\lambda}^T(t_f)\left[\mathbf{A}\mathbf{x}(t_f) + \mathbf{B}\mathbf{u}(t_f)\right] = -1 \end{aligned} \tag{C.17}$$

Any control within the admissible set of controls (bounded by U_{max}) that satisfy these four enumerated first order conditions are extremum of this performance index.

C.2 Second Variation

Now we examine the second variation of the augmented performance index

$$\begin{aligned}
\delta\left(\delta\widetilde{J}\right) &= \delta\left[\begin{array}{r}\left[\boldsymbol{\nu}^T\frac{\partial\boldsymbol{\Psi}\left(\mathbf{x}(t_f),t_f\right)}{\partial t_f}+H(t_f)\right]\delta t_f+\left[\boldsymbol{\nu}^T\frac{\partial\boldsymbol{\Psi}\left(\mathbf{x}(t_f),t_f\right)}{\partial\mathbf{x}(t_f)}-\boldsymbol{\lambda}^T(t_f)\right]\delta\mathbf{x}(t_f)\\ +\int_{t_o}^{t_f}\left[\left(\frac{\partial H}{\partial\mathbf{x}(t)}+\dot{\boldsymbol{\lambda}}^T(t)\right)\widetilde{\delta}\mathbf{x}(t)+\frac{\partial H}{\partial\mathbf{u}(t)}\widetilde{\delta}\mathbf{u}(t)\right]dt\end{array}\right]\\
&= \delta\left\{\left[\boldsymbol{\nu}^T\frac{\partial\boldsymbol{\Psi}\left(\mathbf{x}(t_f),t_f\right)}{\partial t_f}+H(t_f)\right]\delta t_f\right\}\\
&\quad+\delta\left\{\left[\boldsymbol{\nu}^T\frac{\partial\boldsymbol{\Psi}\left(\mathbf{x}(t_f),t_f\right)}{\partial\mathbf{x}(t_f)}-\boldsymbol{\lambda}^T(t_f)\right]\delta\mathbf{x}(t_f)\right\}\\
&\quad+\delta\left\{\int_{t_o}^{t_f}\left[\left(\frac{\partial H}{\partial\mathbf{x}(t)}+\dot{\boldsymbol{\lambda}}^T(t)\right)\widetilde{\delta}\mathbf{x}(t)+\frac{\partial H}{\partial\mathbf{u}(t)}\widetilde{\delta}\mathbf{u}(t)\right]dt\right\} \qquad \text{(C.18)}
\end{aligned}$$

Taking each of the three variations separately,

$$\begin{aligned}
\delta\left\{\left[\boldsymbol{\nu}^T\frac{\partial\boldsymbol{\Psi}\left(\mathbf{x}(t_f),t_f\right)}{\partial t_f}+H(t_f)\right]\delta t_f\right\} &= \frac{\partial}{\partial\mathbf{x}(t_f)}\left[\boldsymbol{\nu}^T\frac{\partial\boldsymbol{\Psi}\left(\mathbf{x}(t_f),t_f\right)}{\partial t_f}+H(t_f)\right]\delta t_f\delta\mathbf{x}(t_f)\\
&\quad+\frac{\partial}{\partial t_f}\left[\boldsymbol{\nu}^T\frac{\partial\boldsymbol{\Psi}\left(\mathbf{x}(t_f),t_f\right)}{\partial t_f}+H(t_f)\right]\delta^2 t_f\\
&= \left[\boldsymbol{\nu}^T\frac{\partial^2\boldsymbol{\Psi}\left(\mathbf{x}(t_f),t_f\right)}{\partial\mathbf{x}(t_f)\partial t_f}+\frac{\partial H(t_f)}{\partial\mathbf{x}(t_f)}\right]\delta t_f\delta\mathbf{x}(t_f)\\
&\quad+\left[\boldsymbol{\nu}^T\frac{\partial^2\boldsymbol{\Psi}\left(\mathbf{x}(t_f),t_f\right)}{\partial^2 t_f}+\frac{\partial H(t_f)}{\partial t_f}\right]\delta^2 t_f \qquad \text{(C.19)}
\end{aligned}$$

$$\begin{aligned}
\delta\left\{\left[\boldsymbol{\nu}^T\frac{\partial\boldsymbol{\Psi}\left(\mathbf{x}(t_f),t_f\right)}{\partial\mathbf{x}(t_f)}-\boldsymbol{\lambda}^T(t_f)\right]\delta\mathbf{x}(t_f)\right\} &= \frac{\partial}{\partial\mathbf{x}(t_f)}\left[\boldsymbol{\nu}^T\frac{\partial\boldsymbol{\Psi}\left(\mathbf{x}(t_f),t_f\right)}{\partial\mathbf{x}(t_f)}-\boldsymbol{\lambda}^T(t_f)\right]\delta^2\mathbf{x}(t_f)\\
&\quad+\frac{\partial}{\partial t_f}\left[\boldsymbol{\nu}^T\frac{\partial\boldsymbol{\Psi}\left(\mathbf{x}(t_f),t_f\right)}{\partial\mathbf{x}(t_f)}-\boldsymbol{\lambda}^T(t_f)\right]\delta\mathbf{x}(t_f)\delta t_f\\
&= \left[\boldsymbol{\nu}^T\frac{\partial^2\boldsymbol{\Psi}\left(\mathbf{x}(t_f),t_f\right)}{\partial^2\mathbf{x}(t_f)}\right]\delta^2\mathbf{x}(t_f)\\
&\quad+\left[\boldsymbol{\nu}^T\frac{\partial^2\boldsymbol{\Psi}\left(\mathbf{x}(t_f),t_f\right)}{\partial t_f\partial\mathbf{x}(t_f)}\right]\delta\mathbf{x}(t_f)\delta t_f \qquad \text{(C.20)}
\end{aligned}$$

$$
\begin{aligned}
\delta \left\{ \int_{t_o}^{t_f} \left[\left(\frac{\partial H}{\partial \mathbf{x}(t)} + \dot{\boldsymbol{\lambda}}^T(t) \right) \widetilde{\delta}\mathbf{x}(t) + \frac{\partial H}{\partial \mathbf{u}(t)} \widetilde{\delta}\mathbf{u}(t) \right] dt \right\} & \\
= & \left[\left(\frac{\partial H}{\partial \mathbf{x}(t)} + \dot{\boldsymbol{\lambda}}^T(t) \right) \widetilde{\delta}\mathbf{x}(t) + \frac{\partial H}{\partial \mathbf{u}(t)} \widetilde{\delta}\mathbf{u}(t) \right] \delta t |_{t_o}^{t_f} \\
& + \int_{t_o}^{t_f} \frac{\partial}{\partial x(t)} \left[\left(\frac{\partial H}{\partial \mathbf{x}(t)} + \dot{\boldsymbol{\lambda}}^T(t) \right) \widetilde{\delta}\mathbf{x}(t) + \frac{\partial H}{\partial \mathbf{u}(t)} \widetilde{\delta}\mathbf{u}(t) \right] \widetilde{\delta}\mathbf{x}(t) dt \\
& + \int_{t_o}^{t_f} \frac{\partial}{\partial u(t)} \left[\left(\frac{\partial H}{\partial \mathbf{x}(t)} + \dot{\boldsymbol{\lambda}}^T(t) \right) \widetilde{\delta}\mathbf{x}(t) + \frac{\partial H}{\partial \mathbf{u}(t)} \widetilde{\delta}\mathbf{u}(t) \right] \widetilde{\delta}\mathbf{u}(t) dt \\
= & \left[\left(\frac{\partial H}{\partial \mathbf{x}(t)} + \dot{\boldsymbol{\lambda}}^T(t) \right) \widetilde{\delta}\mathbf{x}(t) + \frac{\partial H}{\partial \mathbf{u}(t)} \widetilde{\delta}\mathbf{u}(t) \right] |_{t_f} \delta t_f \\
& - \left[\left(\frac{\partial H}{\partial \mathbf{x}(t)} + \dot{\boldsymbol{\lambda}}^T(t) \right) \widetilde{\delta}\mathbf{x}(t) + \frac{\partial H}{\partial \mathbf{u}(t)} \widetilde{\delta}\mathbf{u}(t) \right] |_{t_o} \delta t_o \\
& + \int_{t_o}^{t_f} \left[\left(\frac{\partial^2 H}{\partial^2 \mathbf{x}(t_f)} + \frac{\partial \dot{\boldsymbol{\lambda}}^T(t)}{\partial x(t)} \right) \widetilde{\delta}\mathbf{x}(t) + \frac{\partial^2 H}{\partial \mathbf{x}(t_f) \partial \mathbf{u}(t)} \widetilde{\delta}\mathbf{u}(t) \right] \widetilde{\delta}\mathbf{x}(t) dt \\
& + \int_{t_o}^{t_f} \left[\frac{\partial^2 H}{\partial \mathbf{u}(t) \partial \mathbf{x}(t_f)} \widetilde{\delta}\mathbf{x}(t) + \frac{\partial^2 H}{\partial^2 \mathbf{u}(t)} \widetilde{\delta}\mathbf{u}(t) \right] \widetilde{\delta}\mathbf{u}(t) dt
\end{aligned} \tag{C.21}
$$

but, the first two terms are zero due to the first order necessary condition and fixed initial time, so,

$$
\begin{aligned}
\delta \left\{ \int_{t_o}^{t_f} \left[\left(\frac{\partial H}{\partial \mathbf{x}(t)} + \dot{\boldsymbol{\lambda}}^T(t) \right) \widetilde{\delta}\mathbf{x}(t) + \frac{\partial H}{\partial \mathbf{u}(t)} \widetilde{\delta}\mathbf{u}(t) \right] dt \right\} & \\
= & \int_{t_o}^{t_f} \left[\left(\frac{\partial^2 H}{\partial^2 \mathbf{x}(t_f)} + \frac{\partial \dot{\boldsymbol{\lambda}}^T(t)}{\partial x(t)} \right) \widetilde{\delta}\mathbf{x}(t) + \frac{\partial^2 H}{\partial \mathbf{x}(t_f) \partial \mathbf{u}(t)} \widetilde{\delta}\mathbf{u}(t) \right] \widetilde{\delta}\mathbf{x}(t) dt \\
& + \int_{t_o}^{t_f} \left[\frac{\partial^2 H}{\partial \mathbf{u}(t) \partial \mathbf{x}(t_f)} \widetilde{\delta}\mathbf{x}(t) + \frac{\partial^2 H}{\partial^2 \mathbf{u}(t)} \widetilde{\delta}\mathbf{u}(t) \right] \widetilde{\delta}\mathbf{u}(t) dt
\end{aligned} \tag{C.22}
$$

Combining,

$$\begin{aligned}\delta^2\widetilde{J} = & \left[\boldsymbol{\nu}^T\frac{\partial^2\boldsymbol{\Psi}\left(\mathbf{x}(t_f),t_f\right)}{\partial\mathbf{x}(t_f)\partial t_f}+\boldsymbol{\nu}^T\frac{\partial^2\boldsymbol{\Psi}\left(\mathbf{x}(t_f),t_f\right)}{\partial t_f\partial\mathbf{x}(t_f)}+\frac{\partial H(t_f)}{\partial\mathbf{x}(t_f)}\right]\delta t_f\delta\mathbf{x}(t_f)\\ &+\left[\boldsymbol{\nu}^T\frac{\partial^2\boldsymbol{\Psi}\left(\mathbf{x}(t_f),t_f\right)}{\partial^2\mathbf{x}(t_f)}\right]\delta^2\mathbf{x}(t_f)+\left[\boldsymbol{\nu}^T\frac{\partial^2\boldsymbol{\Psi}\left(\mathbf{x}(t_f),t_f\right)}{\partial^2 t_f}+\frac{\partial H(t_f)}{\partial t_f}\right]\delta^2 t_f\\ &+\int_{t_o}^{t_f}\left[\left(\frac{\partial^2 H}{\partial^2\mathbf{x}(t_f)}+\frac{\partial\dot{\boldsymbol{\lambda}}^T(t)}{\partial\mathbf{x}(t)}\right)\widetilde{\delta}^2\mathbf{x}(t)+\frac{\partial^2 H}{\partial^2\mathbf{u}(t)}\widetilde{\delta}^2\mathbf{u}(t)\right]dt\\ &+\int_{t_o}^{t_f}\left[\frac{\partial^2 H}{\partial\mathbf{x}(t_f)\partial\mathbf{u}(t)}\widetilde{\delta}\mathbf{u}(t)\widetilde{\delta}\mathbf{x}(t)+\frac{\partial^2 H}{\partial\mathbf{u}(t)\partial\mathbf{x}(t_f)}\widetilde{\delta}\mathbf{x}(t)\widetilde{\delta}\mathbf{u}(t)\right]dt \qquad \text{(C.23)}\end{aligned}$$

We note the following from the first order necessary condition:

1. $\delta t_f\delta\mathbf{x}(t_f)$ variation

$$\boldsymbol{\nu}^T\frac{\partial^2\boldsymbol{\Psi}\left(\mathbf{x}(t_f),t_f\right)}{\partial\mathbf{x}(t_f)\partial t_f}+\frac{\partial H(t_f)}{\partial\mathbf{x}(t_f)}=\frac{\partial}{\partial\mathbf{x}(t_f)}\left[\boldsymbol{\nu}^T\frac{\partial\boldsymbol{\Psi}\left(\mathbf{x}(t_f),t_f\right)}{\partial t_f}+H\left(t_f\right)\right]=0 \qquad \text{(C.24)}$$

   from the first order Transversality condition, we have the bracketed term identically equal to zero.

2. $\delta^2 t_f$ variation

   Similarly,

$$\boldsymbol{\nu}^T\frac{\partial^2\boldsymbol{\Psi}\left(\mathbf{x}(t_f),t_f\right)}{\partial^2 t_f}+\frac{\partial H(t_f)}{\partial t_f}=\frac{\partial}{\partial t_f}\left[\boldsymbol{\nu}^T\frac{\partial\boldsymbol{\Psi}\left(\mathbf{x}(t_f),t_f\right)}{\partial t_f}+H(t_f)\right]=0 \qquad \text{(C.25)}$$

3. $\widetilde{\delta}^2\mathbf{x}(t)$ variation

$$\frac{\partial^2 H}{\partial^2\mathbf{x}(t_f)}+\frac{\partial\dot{\boldsymbol{\lambda}}^T(t)}{\partial\mathbf{x}(t)}=\frac{\partial^2 H}{\partial^2\mathbf{x}(t_f)}+\frac{\partial}{\partial\mathbf{x}(t)}\left(-\frac{\partial H}{\partial\mathbf{x}(t)}\right)=\frac{\partial^2 H}{\partial^2\mathbf{x}(t_f)}-\frac{\partial^2 H}{\partial^2\mathbf{x}(t_f)}=0 \qquad \text{(C.26)}$$

4. $\widetilde{\delta}\mathbf{u}(t)\widetilde{\delta}\mathbf{x}(t)$ and $\widetilde{\delta}\mathbf{x}(t)\widetilde{\delta}\mathbf{u}(t)$ variations

$$\frac{\partial^2 H}{\partial\mathbf{x}(t_f)\partial\mathbf{u}(t)}=0 \qquad \frac{\partial^2 H}{\partial\mathbf{u}(t)\partial\mathbf{x}(t_f)}=0 \qquad \text{(C.27)}$$

These are also satisfied because we have $\frac{\partial H}{\partial \mathbf{x}(t)} = \boldsymbol{\lambda}^T \mathbf{A}$ is not a function of $\mathbf{u}$ and $\frac{\partial H}{\partial \mathbf{u}(t)} = \boldsymbol{\lambda}^T \mathbf{B}$ is not a function of $\mathbf{x}$; i.e. H is linear in both $\mathbf{x}$ and $\mathbf{u}$.

5. $\widetilde{\delta}^2 \mathbf{u}(t)$ variation

$$\frac{\partial^2 H}{\partial^2 \mathbf{u}(t)} = \frac{\partial}{\partial \mathbf{u}(t)} \left(\frac{\partial H}{\partial \mathbf{u}(t)} \right) = 0 \tag{C.28}$$

This is satisfied again because H is only linear in $\mathbf{u}$.

Now we have, for the second variation,

$$\delta^2 \widetilde{J} = \left[\boldsymbol{\nu}^T \frac{\partial^2 \boldsymbol{\Psi} \left(\mathbf{x}(t_f), t_f \right)}{\partial t_f \partial \mathbf{x}(t_f)} \right] \delta t_f \delta \mathbf{x}(t_f) + \left[\boldsymbol{\nu}^T \frac{\partial^2 \boldsymbol{\Psi} \left(\mathbf{x}(t_f), t_f \right)}{\partial^2 \mathbf{x}(t_f)} \right] \delta^2 \mathbf{x}(t_f) \tag{C.29}$$

The second order necessary condition is then

$$\left[\boldsymbol{\nu}^T \frac{\partial^2 \boldsymbol{\Psi} \left(\mathbf{x}(t_f), t_f \right)}{\partial t_f \partial \mathbf{x}(t_f)} \right] \delta t_f \delta \mathbf{x}(t_f) + \left[\boldsymbol{\nu}^T \frac{\partial^2 \boldsymbol{\Psi} \left(\mathbf{x}(t_f), t_f \right)}{\partial^2 \mathbf{x}(t_f)} \right] \delta^2 \mathbf{x}(t_f) \geq 0 \tag{C.30}$$

and the sufficient condition is

$$\left[\boldsymbol{\nu}^T \frac{\partial^2 \boldsymbol{\Psi} \left(\mathbf{x}(t_f), t_f \right)}{\partial t_f \partial \mathbf{x}(t_f)} \right] \delta t_f \delta \mathbf{x}(t_f) + \left[\boldsymbol{\nu}^T \frac{\partial^2 \boldsymbol{\Psi} \left(\mathbf{x}(t_f), t_f \right)}{\partial^2 \mathbf{x}(t_f)} \right] \delta^2 \mathbf{x}(t_f) > 0 \tag{C.31}$$

C.3 Pontryagin's Minimum Principle Summary

A second order strong variation condition is known as the Weirstrauss condition. In Pontryagin's minimum principle, this condition was used, namely that the optimal control will be Hamiltonian-minimizer:

$$H(\mathbf{x}(t), \mathbf{u}^*(t), \boldsymbol{\lambda}(t)) \leq H(\mathbf{x}(t), \mathbf{u}(t), \boldsymbol{\lambda}(t)) \tag{C.32}$$

where $\mathbf{u}^*(t)$ is the optimal control and $\forall$ $\mathbf{u}(t)$ in the admissible set of controls. Then it is easy to see that only $\mathbf{u}^*(t) = -sgn \left\{ \boldsymbol{\lambda}^T(t) \mathbf{B} \right\} U_{max}$ will make the inequality hold.

$$
\begin{aligned}
1 + \boldsymbol{\lambda}^T(t)\left[\mathbf{A}\mathbf{x}(t) + \mathbf{B}\mathbf{u}^*(t)\right] &\leq 1 + \boldsymbol{\lambda}^T(t)\left[\mathbf{A}\mathbf{x}(t) + \mathbf{B}\mathbf{u}(t)\right] \\
\boldsymbol{\lambda}^T(t)\left[\mathbf{A}\mathbf{x}(t) + \mathbf{B}\mathbf{u}^*(t)\right] &\leq \boldsymbol{\lambda}^T(t)\left[\mathbf{A}\mathbf{x}(t) + \mathbf{B}\mathbf{u}(t)\right] \\
\boldsymbol{\lambda}^T(t)\mathbf{B}\mathbf{u}^*(t) &\leq \boldsymbol{\lambda}^T(t)\mathbf{B}\mathbf{u}(t) \\
-\left|\boldsymbol{\lambda}^T(t)\mathbf{B}\right| U_{max} &\leq \boldsymbol{\lambda}^T(t)\mathbf{B}\mathbf{u}(t) \qquad \text{(C.33)}
\end{aligned}
$$

Furthermore, in a conference paper by Chang [47], the necessary condition for the Pontryagin's Maximum Principle also becomes the sufficient condition for the optimal control to be the global solution. The required condition is that the state not be constrained during the maneuver and that the either the end point be fixed or be bounded within a convex set. Our minimum-time problem satisfies these conditions and hence the minimum-time solution is globally optimal.

Appendix D. $N = 2$ for Stable Orbit to Stable Orbit Maneuver

In this appendix, a special case of the $N = 2$ case is presented for the problem of maneuvering from one stable and centered orbit to another; a reconfiguration maneuver. The results follow directly from the previous Section 5.2 with the conditions

$$a_o = a_f = 0 \qquad b_o = b_f = 0 \tag{D.1}$$

which means $\Delta a = \Delta b = 0$.

Critical Times Calculations

The critical times are now calculated based on the equations developed in the previous section with $\Delta a = \Delta b = 0$.

Equation (5.20) becomes

$$\Delta\tau_3 = -\frac{u_{y2}}{u_{yo}}\left[\Delta\tau_1 + \frac{u_{y1}}{u_{yo}}\Delta\tau_2\right] \tag{D.2}$$

The intermediate results for the two viable subcases of $N = 2$ are summarized in Table D.1 below. Subcase I of x-control switch only was eliminated from the pool of viable control sequences based on the analysis from Section 5.3.

Table D.1 Final times for two viable subcases of $N = 3$ for stable to stable orbit maneuver.

Subcase	Control Sequence	$t_f = \Delta\tau_1 + \Delta\tau_2 + \Delta\tau_3$
II.	X-Y	$t_f = 2\Delta\tau_3$
III.	Y-X	$t_f = 2\Delta\tau_1$

Equation (5.33) with $\Delta a = \Delta b = 0$ becomes

$$\left(-\frac{u_{y1}}{u_{yo}} + \frac{u_{y2}}{u_{yo}}\right)\Delta\tau_2^2 + \left[\frac{u_{xo}}{u_{yo}}\left(\frac{u_{x2}}{u_{xo}}\frac{u_{y1}}{u_{yo}}\frac{u_{y2}}{u_{yo}} - \frac{u_{x1}}{u_{xo}}\right)\frac{4}{3} + \left(\frac{u_{y1}}{u_{yo}}\frac{u_{y2}}{u_{yo}} - 1\right)2\Delta\tau_1\right]\Delta\tau_2 + \left(\frac{u_{y2}}{u_{yo}} - 1\right)\Delta\tau_1^2 + \left[\frac{u_{xo}}{u_{yo}}\left(\frac{u_{x2}}{u_{xo}}\frac{u_{y2}}{u_{yo}} - 1\right)\frac{4}{3}\right]\Delta\tau_1 = 0 \quad \text{(D.3)}$$

Details for the intermediate results using these equations for the four subcases of $N = 2$ are as follows:

Subcase I. (X-X)

This subcase is no longer a viable option for $N = 2$. *Subcase II. (X-Y)*

Equation (D.3) reduces to

$$\Delta\tau_2^2 + \left(2\Delta\tau_1 + \frac{4}{3}\right)\Delta\tau_2 + \Delta\tau_1^2 = 0 \quad \text{(D.4)}$$

and the intermediate results are

$$\Delta\tau_2 = -\frac{2}{3} - \Delta\tau_1 + \frac{2}{3}\sqrt{1 + 3\Delta\tau_1} \quad \text{(D.5)}$$

$$\Delta\tau_3 = \Delta\tau_1 + \Delta\tau_2 = -\frac{2}{3} + \frac{2}{3}\sqrt{1 + 3\Delta\tau_1} \quad \text{(D.6)}$$

$$t_f = \Delta\tau_1 + \Delta\tau_2 + \Delta\tau_3 = -\frac{4}{3} + \frac{4}{3}\sqrt{1 + 3\Delta\tau_1} \quad \text{(D.7)}$$

where only the positive roots were taken due to the restrictions on non-negativity of time intervals.

Subcase III. (Y-X)

For this subcase, a quadratic function of $\Delta\tau_1$ in terms of $\Delta\tau_2$ is obtained,

$$\Delta\tau_1^2 + \frac{4}{3}\Delta\tau_2 = 0 \quad \text{(D.8)}$$

However, this means that

$$\Delta\tau_2 = -\frac{3}{4}\Delta\tau_1^2 \tag{D.9}$$

and the only way $\Delta\tau_2 \geq 0$ can be achieved is when $\Delta\tau_1 = 0$. So, this subcase is not viable for stable-to-stable maneuver.

$$\Delta\tau_3 = \Delta\tau_1 - \Delta\tau_2 = \frac{3}{4}\Delta\tau_1^2 \tag{D.10}$$

These results are summarized in Table D.2. The analysis has further eliminated the subcases down to one.

Table D.2 Time intervals for $N = 2$: stable-to-stable orbit maneuver

Subcase	Cntrl Seq.	$\Delta\tau_2$	$\Delta\tau_3$
II.	X-Y-X	$-\frac{2}{3} - \Delta\tau_1 + \frac{2}{3}\sqrt{1+3\Delta\tau_1}$	$-\frac{2}{3} + \frac{2}{3}\sqrt{1+3\Delta\tau_1}$
III.[a]	Y-X-X	$-\frac{3}{4}\Delta\tau_1^2$	$\frac{3}{4}\Delta\tau_1^2$

[a] $\Delta\tau_1 = \Delta\tau_2 = \Delta\tau_3 = t_f = 0$

Finally, the relative orbit size parameter, $\rho(t)$was examined. Equation (5.44) for the only viable subcase become,

$$\begin{aligned} K_o = &-2\frac{\rho_o}{u_{yo}}\sin\left(\Delta\tau_1 + \theta_o\right) - 2\left(\cos\Delta\tau_1 - 2\sin\Delta\tau_1\right) \\ &+8\sin\Delta\tau_2 - 5\cos\left(2\Delta\tau_1 + 2\Delta\tau_2\right) - \frac{\rho_o}{u_{yo}}\left[2\cos\left(2\Delta\tau_1 + 2\Delta\tau_2 + \theta_o\right) - \sin\left(2\Delta\tau_1 + 2\Delta\tau_2 + \theta_o\right)\right] \\ &- 8\left[2\cos\left(\Delta\tau_1 + \Delta\tau_2\right) - \sin\left(\Delta\tau_1 + \Delta\tau_2\right)\right] - 2\left[\cos\left(\Delta\tau_1 + 2\Delta\tau_2\right) - 2\sin\left(\Delta\tau_1 + 2\Delta\tau_2\right)\right] \\ &- 4\frac{\rho_o}{u_{yo}}\cos\left(\Delta\tau_1 + \Delta\tau_2 + \theta_o\right) \end{aligned} \tag{D.11}$$

where the intermediate constant is

$$K_o = \frac{1}{2U_{max}^2}\left(\rho_f^2 - \rho_o^2\right) - 15 + \frac{\rho_o}{u_{yo}}\left(2\cos\theta_o - \sin\theta_o\right) \tag{D.12}$$

The solution to the critical times will require solving this equation numerically.

Initial Costate

The analysis for both the costate terminal condition and the Hamiltonian are exactly the same as for the general $N = 2$ case. Therefore Equations (5.62) and (5.72) are still valid. Equation (5.73) is still valid. The remainder of the analysis is identical to the general $N = 2$ case as per Section 5.3. Stable orbit to stable orbit maneuver has no effect on the initial costate vector determination; the effect is carried in indirectly through the critical times. $\boldsymbol{\lambda}_2$ in terms of the time intervals for the only viable subcase is:

$$\boldsymbol{\lambda}_2^T = \frac{1}{D} \begin{bmatrix} -2\sin\left(\Delta\tau_3 - \theta(t_f)\right) \\ \cos\left(\Delta\tau_2 + \Delta\tau_3 - \theta(t_f)\right) \\ 2\cos\left(\Delta\tau_3 - \theta(t_f)\right) - 2\cos\left(\Delta\tau_2 + \Delta\tau_3 - \theta(t_f)\right) \\ 0 \end{bmatrix} \tag{D.13}$$

where D is a modified determinant:

$$\begin{aligned} D &= 2\left(3x_2 + 2\dot{y}_2 + u_{yo}\right)\cos\left(\Delta\tau_3 - \theta(t_f)\right) - 2\dot{x}_2\sin\left(\Delta\tau_3 - \theta(t_f)\right) \\ &\quad - \left(6x_2 + 3\dot{y}_2 + 2u_{yo}\right)\cos\left(\Delta\tau_2 + \Delta\tau_3 - \theta(t_f)\right) \end{aligned} \tag{D.14}$$

Finally, the initial costate is given by:

$$\boldsymbol{\lambda}_o = \boldsymbol{\Phi}_\lambda^{-1}(t_2, 0)\boldsymbol{\lambda}_2 \tag{D.15}$$

Appendix E. Minimum Time XY-Motion for $N = 3$

This appendix presents the derivation of the initial costate vector for the in-plane minimum-time problem with three control switches. Compared to all of the $N < 3$ cases, the $N = 3$ case is more complex and does not have an analytical solution for the critical times. For this analysis, the final state $\mathbf{x}_f$ is assumed to be "close" enough to the initial state $\mathbf{x}_o$ to require only three control switches. That is, three is the minimum number of switching required to meet the four terminal constraint. $N = 3$ means there are four critical times: t_1, t_2, t_3, t_f; the first control switch, the second control switch, the third control switch, and the final times respectively. For $N < 3$ not all of the relative orbit parameters could be satisfied. However, now for $N = 3$ all of the final relative orbit parameters could be satisfied, provided the solution exists. The target set is a single point is $\mathbb{R}^4$.

E.1 Control and State Solution

The controls for $N = 3$ are piecewise constants

$$\mathbf{u}(t) = \begin{cases} \mathbf{u}_o, & 0 \leq t < t_1 \\ \mathbf{u}_1, & t_1 \leq t < t_2 \\ \mathbf{u}_2, & t_2 \leq t < t_3 \\ \mathbf{u}_3, & t_3 \leq t \leq t_f \end{cases} \tag{E.1}$$

where t_1, t_2, and t_3 are control switching times. The explicit state solution at time $t > t_3$ using the above control is

$$\begin{aligned}
\mathbf{x}(t) &= \mathbf{\Phi}_x(t,0)\mathbf{x}_o + \left[\int_0^{t_1} \mathbf{\Phi}_x(t,\tau)\mathbf{B}d\tau\right]\mathbf{u}_o + \left[\int_{t_1}^{t_2} \mathbf{\Phi}_x(t,\tau)\mathbf{B}d\tau\right]\mathbf{u}_1 \\
&+ \left[\int_{t_2}^{t_3} \mathbf{\Phi}_x(t,\tau)\mathbf{B}d\tau\right]\mathbf{u}_2 + \left[\int_{t_3}^{t} \mathbf{\Phi}_x(t,\tau)\mathbf{B}d\tau\right]\mathbf{u}_3
\end{aligned}$$

$$\begin{bmatrix} x(t) \\ y(t) \\ \dot{x}(t) \\ \dot{y}(t) \end{bmatrix} = \begin{bmatrix} \rho_o \sin(t+\theta_o) + a_o \\ 2\rho_o \cos(t+\theta_o) - \frac{3}{2}a_o t + b_o \\ \rho_o \cos(t+\theta_o) \\ -2\rho_o \sin(t+\theta_o) - \frac{3}{2}a_o \end{bmatrix}$$

$$+ \begin{bmatrix} \cos(t-t_1) - \cos t & -2\sin t + 2t_1 + 2\sin(t-t_1) \\ -2\sin(t-t_1) - 2t_1 + 2\sin t & -4\cos t + \frac{3}{2}t_1^2 - 3t_1 t + 4\cos(t-t_1) \\ -\sin(t-t_1) + \sin t & 2\cos(t-t_1) - 2\cos t \\ -2\cos(t-t_1) + 2\cos t & 4\sin t - 3t_1 - 4\sin(t-t_1) \end{bmatrix} \begin{bmatrix} u_{xo} \\ u_{yo} \end{bmatrix}$$

$$+ \begin{bmatrix} \cos(t-t_2) - \cos(t-t_1) \\ -2(\sin(t-t_1) - \sin(t-t_2)) - 2(t_2 - t_1) \\ \sin(t-t_1) - \sin(t-t_2) \\ -2 + 2(\cos(t-t_1) - \cos(t-t_2)) \end{bmatrix} u_{x1}$$

$$+ \begin{bmatrix} 2(\sin(t-t_2) - \sin(t-t_1)) + 2(t_2 - t_1) \\ 4(1 + \cos(t-t_2) - \cos(t-t_1)) - \frac{3}{2}t_1^2 - \frac{3}{2}t_2^2 - 3t_1 t \\ 2 - 2\cos(t-t_1) + 2\cos(t-t_2) \\ 4\sin(t-t_1) - 4\sin(t-t_2) - 3(t_2 - t_1) \end{bmatrix} u_{y1}$$

$$+ \begin{bmatrix} \cos(t-t_3) - \cos(t-t_2) \\ -2(\sin(t-t_2) - \sin(t-t_3)) - 2(t_3 - t_2) \\ \sin(t-t_2) - \sin(t-t_3) \\ -2 + 2(\cos(t-t_2) - \cos(t-t_3)) \end{bmatrix} u_{x2}$$

$$+\begin{bmatrix} 2(\sin(t-t_3)-\sin(t-t_2))+2(t_3-t_2) \\ 4(1+\cos(t-t_3)-\cos(t-t_2))-\frac{3}{2}t_2^2-\frac{3}{2}t_3^2-3t_2t \\ 2-2\cos(t-t_2)+2\cos(t-t_3) \\ 4\sin(t-t_2)-4\sin(t-t_3)-3(t_3-t_2) \end{bmatrix} u_{y2}$$

$$+\begin{bmatrix} 1-\cos(t-t_3) & -2\sin(t-t_3)+2(t-t_3) \\ 2\sin(t-t_3)-2(t-t_3) & 4-4\cos(t-t_3)-\frac{3}{2}t_3^2-\frac{3}{2}t^2-3t_3t \\ \sin(t-t_3) & 2-2\cos(t-t_3) \\ -2+2\cos(t-t_3) & 4\sin(t-t_3)-3(t-t_3) \end{bmatrix} \begin{bmatrix} u_{x3} \\ u_{y3} \end{bmatrix} \tag{E.2}$$

The four possible choices for the initial control are:

$$\mathbf{u}_o = \begin{bmatrix} u_{xo} \\ u_{yo} \end{bmatrix} \in \left\{ \begin{bmatrix} U_{max} \\ U_{max} \end{bmatrix}, \begin{bmatrix} U_{max} \\ -U_{max} \end{bmatrix}, \begin{bmatrix} -U_{max} \\ U_{max} \end{bmatrix}, \begin{bmatrix} -U_{max} \\ -U_{max} \end{bmatrix} \right\} \tag{E.3}$$

In Section 3.2.2 a total of five possible series of control switches for $N = 3$ was presented.

E.2 Critical Times Calculations

An analysis similar to earlier cases ($N < 3$) is performed for the $N = 3$ case to determine the switching times and the final time. The four critical times for $N = 3$ are t_1, t_2, t_3, and t_f. These four times are found using all four relative orbit parameters.

First the drifting parameter, $a(t)$, is examined,

$$\begin{aligned} a(t) &= 4x(t) + 2\dot{y}(t) \\ &= a_o + 2u_{yo}\Delta\tau_1 + 2u_{y1}\Delta\tau_2 + 2u_{y2}\Delta\tau_3 + 2u_{y3}\Delta\tau_4 \end{aligned} \tag{E.4}$$

where, $\Delta\tau_1 = t_1$, $\Delta\tau_2 = t_2 - t_1$, and $\Delta\tau_3 = t_3 - t_2$, $\Delta\tau_4 = t_f - t_3$. Also, $t_f = \Delta\tau_1 + \Delta\tau_2 + \Delta\tau_3 + \Delta\tau_4$. As noted earlier, these time intervals are more useful than the absolute

times. Now, with $a(t_f) = a_f$ and defining $\Delta a = a_f - a_o$:

$$\frac{\Delta a}{2u_{yo}} + \Delta\tau_1 + \frac{u_{y1}}{u_{yo}}\Delta\tau_2 + \frac{u_{y2}}{u_{yo}}\Delta\tau_3 + \frac{u_{y3}}{u_{yo}}\Delta\tau_4 = 0 \tag{E.5}$$

Equation (E.5) reduces the number of unknowns from four to three; i.e., one of the four time intervals can be expressed in terms of the other three:

$$\Delta\tau_4 = -\frac{u_{y3}}{u_{yo}}\left[\frac{\Delta a}{2u_{yo}} + \Delta\tau_1 + \frac{u_{y1}}{u_{yo}}\Delta\tau_2 + \frac{u_{y2}}{u_{yo}}\Delta\tau_3\right] \tag{E.6}$$

where $u_{yo}/u_{y3} = u_{y3}/u_{yo} = \pm 1$ is used. [1] For the five subcases of $N = 3$, the time intervals and their combinations must be non-negative. This leads to constraints on the time intervals that could be used as a test of existence of solution.

Subcase I. (Y-X-Y)

The control switching sequence for this subcase is y at t_1, then x at t_2, followed by y-control switches at t_3. By adding $\Delta\tau_1 + \Delta\tau_2 + \Delta\tau_3 + \Delta\tau_4 = t_f$ to Equation (E.5), along with $u_{y1} = u_{y2} = -u_{yo}$ and $u_{y3} = +u_{yo}$, the final time becomes,

$$t_f = \frac{1}{2}\frac{\Delta a}{u_{yo}} + 2\left(\Delta\tau_1 + \Delta\tau_4\right) \tag{E.7}$$

Rewriting this as,

$$2\left(\Delta\tau_1 + \Delta\tau_4\right) = t_f - \frac{1}{2}\frac{\Delta a}{u_{yo}} \tag{E.8}$$

and noting that the sum of time intervals $\Delta\tau_1 + \Delta\tau_4 \geq 0$, t_f is restricted to

$$t_f \geq \max\left\{0, \frac{1}{2}\frac{\Delta a}{u_{yo}}\right\} \tag{E.9}$$

[1] In fact, any control ratios are always ± 1, which means the reciprocal is the same as the original ratio.

Furthermore, if the y-control is $u_{yo} = sgn\{\Delta a\}U_{max}$ then,

$$t_f \geq \frac{1}{2}\frac{|\Delta a|}{U_{max}} \tag{E.10}$$

Conversely, if the y-control had the opposite sign,$u_{yo} = -sgn\{\Delta a\}U_{max}$, $t_f \geq 0$.

Subcase II. (X-Y-X)

In this subcase, we alternate the control switches: x followed by y, followed by x at t_1, t_2, and t_3 respectively. The final time is given by,

$$t_f = \frac{1}{2}\frac{\Delta a}{u_{yo}} + 2\left(\Delta\tau_1 + \Delta\tau_2\right) \tag{E.11}$$

which can be written as

$$2\left(\Delta\tau_1 + \Delta\tau_2\right) = t_f - \frac{1}{2}\frac{\Delta a}{u_{yo}} \tag{E.12}$$

When non-negative time interval is required, $\Delta\tau_1 + \Delta\tau_2 \geq 0$,

$$t_f \geq \max\left\{0, \frac{1}{2}\frac{\Delta a}{u_{yo}}\right\} \tag{E.13}$$

Now if the y-control is set to $u_{yo} = sgn\{\Delta a\}U_{max}$ then,

$$t_f \geq \frac{1}{2}\frac{|\Delta a|}{U_{max}} \tag{E.14}$$

However, if y-control is set to $u_{yo} = -sgn\{\Delta a\}U_{max}$, $t_f \geq 0$.

Subcase III. (Y-X-X)

In this subcase, the y-control switches first at t_1 and then the x-control switches at t_2 and at t_3. The final time is given by

$$t_f = \frac{1}{2}\frac{\Delta a}{u_{yo}} + 2\Delta\tau_1 \tag{E.15}$$

which can be written as

$$2\Delta\tau_1 = t_f - \frac{1}{2}\frac{\Delta a}{u_{yo}} \tag{E.16}$$

Restraining $\Delta\tau_1 \geq 0$,

$$t_f \geq \max\left\{0, \frac{1}{2}\frac{\Delta a}{u_{yo}}\right\} \tag{E.17}$$

Now if the y-control is set to $u_{yo} = sgn\{\Delta a\}U_{max}$ then,

$$t_f \geq \frac{1}{2}\frac{|\Delta a|}{U_{max}} \tag{E.18}$$

However, if y-control is set to $u_{yo} = -sgn\{\Delta a\}U_{max}$, $t_f \geq 0$.

Subcase IV. (X-X-Y)

In this subcase, the x-control switches at the first two times and the y-control switches at t_3. The final time is given by,

$$t_f = -\frac{1}{2}\frac{\Delta a}{u_{yo}} + 2\Delta\tau_4 \tag{E.19}$$

which can be written as

$$2\Delta\tau_4 = t_f + \frac{1}{2}\frac{\Delta a}{u_{yo}} \tag{E.20}$$

Restraining $\Delta\tau_4 \geq 0$,

$$t_f \geq \max\left\{0, -\frac{1}{2}\frac{\Delta a}{u_{yo}}\right\} \tag{E.21}$$

Now if the y-control is set to $u_{yo} = -sgn\{\Delta a\}U_{max}$ then,

$$t_f \geq \frac{1}{2}\frac{|\Delta a|}{U_{max}} \tag{E.22}$$

However, if y-control is set to $u_{yo} = sign\{\Delta a\}U_{max}$, $t_f \geq 0$.

Subcase V. (X-X-X)

In this subcase, only the x-control switches at all three times. The final time is given by

$$t_f = -\frac{1}{2}\frac{\Delta a}{u_{yo}} \tag{E.23}$$

then, non-negative final time constraint leads to

$$u_{yo} = -sgn\{\Delta a\}U_{max} \tag{E.24}$$

Then, each of the time intervals are bounded by

$$0 \leq \{\Delta\tau_1, \Delta\tau_2, \Delta\tau_3, \Delta\tau_4\} \leq \frac{1}{2}\frac{|\Delta a|}{U_{max}} \tag{E.25}$$

since their sum $t_f = \Delta\tau_1 + \Delta\tau_2 + \Delta\tau_3 + \Delta\tau_4 = \frac{1}{2}|\Delta a|/U_{max}$. Notice also that if the maneuver is from one non-drifting orbit to another ($a_o = a_f = 0$) then $\Delta a = 0$ and $t_f = 0$ implying that this subcase is not suitable for this type of maneuver. Practical use of formation control is from one stable orbit to another, and in these cases the number of subcases are reduced from five to four.

The drifting parameter analysis revealed that the initial y-control as a function of Δa has influence on the positivity of the time intervals (and their combinations). The fact the y-control is a function of the change in drift term makes physical sense since the drift is in the y-direction (in-track direction).

Next, the centering parameter $b(t)$ is examined,

$$b(t) = y(t) - 2\dot{x}(t) \tag{E.26}$$

At $t = t_f$ and $b(t_f) = b_f$, after a bit of algebra,

$$\begin{aligned} 0 =& \frac{\Delta b}{u_{yo}} + 3\left(\Delta\tau_1 + \frac{u_{y1}}{u_{yo}}\Delta\tau_2 + \frac{u_{y2}}{u_{yo}}\Delta\tau_3 + \frac{u_{y3}}{u_{yo}}\Delta\tau_4\right) t_f \\ &+ \frac{3}{2}\left(\frac{\Delta u_{y1}}{u_{yo}}\left(t_f - t_1\right)^2 + \frac{\Delta u_{y2}}{u_{yo}}\left(t_f - t_2\right)^2 + \frac{\Delta u_{y3}}{u_{yo}}\left(t_f - t_3\right)^2 - t_f^2\right) \\ &- 2\frac{u_{xo}}{u_{yo}}\left(\Delta\tau_1 + \frac{u_{x1}}{u_{xo}}\Delta\tau_2 + \frac{u_{x2}}{u_{xo}}\Delta\tau_3 + \frac{u_{x3}}{u_{xo}}\Delta\tau_4\right) \end{aligned} \tag{E.27}$$

Now, substituting in the Equation (E.6), the the fourth time interval is eliminated,

$$\begin{aligned} &\frac{3}{2}\boldsymbol{\Delta T}^T \begin{bmatrix} \frac{u_{y3}}{u_{yo}} - 1 & \frac{u_{y1}}{u_{yo}}\frac{u_{y3}}{u_{yo}} - 1 & \frac{u_{y2}}{u_{yo}}\frac{u_{y3}}{u_{yo}} - 1 \\ \frac{u_{y1}}{u_{yo}}\frac{u_{y3}}{u_{yo}} - 1 & \frac{u_{y3}}{u_{yo}} - \frac{u_{y1}}{u_{yo}} & \frac{u_{y1}}{u_{yo}}\left(\frac{u_{y2}}{u_{yo}}\frac{u_{y3}}{u_{yo}} - 1\right) \\ \frac{u_{y2}}{u_{yo}}\frac{u_{y3}}{u_{yo}} - 1 & \frac{u_{y1}}{u_{yo}}\left(\frac{u_{y2}}{u_{yo}}\frac{u_{y3}}{u_{yo}} - 1\right) & \frac{u_{y3}}{u_{yo}} - \frac{u_{y2}}{u_{yo}} \end{bmatrix} \boldsymbol{\Delta T} \\ &+\boldsymbol{\Delta T}^T \begin{bmatrix} \frac{3}{2}\left(\frac{u_{y3}}{u_{yo}} - 1\right)\frac{\Delta a}{u_{yo}} + 2\left(\frac{u_{x3}}{u_{y3}} - \frac{u_{xo}}{u_{yo}}\right) \\ \frac{3}{2}\left(\frac{u_{y1}}{u_{yo}}\frac{u_{y3}}{u_{yo}} - 1\right)\frac{\Delta a}{u_{yo}} + 2\left(\frac{u_{x3}}{u_{y3}}\frac{u_{y1}}{u_{yo}} - \frac{u_{xo}}{u_{yo}}\frac{u_{x1}}{u_{xo}}\right) \\ \frac{3}{2}\left(\frac{u_{y2}}{u_{yo}}\frac{u_{y3}}{u_{yo}} - 1\right)\frac{\Delta a}{u_{yo}} + 2\left(\frac{u_{x3}}{u_{y3}}\frac{u_{y2}}{u_{yo}} - \frac{u_{xo}}{u_{yo}}\frac{u_{x2}}{u_{xo}}\right) \end{bmatrix} \\ &+ \left[\frac{\Delta b}{u_{yo}} + \frac{u_{y3}}{u_{yo}}\frac{3}{8}\left(\frac{\Delta a}{u_{yo}}\right)^2 + \frac{u_{x3}}{u_{y3}}\frac{\Delta a}{u_{yo}}\right] = 0 \end{aligned} \tag{E.28}$$

where, this equation is a quadratic function of the time interval vector,

$\boldsymbol{\Delta T}^T = \begin{bmatrix} \Delta\tau_1 & \Delta\tau_2 & \Delta\tau_3 \end{bmatrix}$. For the five subcases of $N = 3$, the intermediate results are:

Subcase I. (Y-X-Y)

For this subcase, we get

$$\frac{3}{2}\boldsymbol{\Delta T}^T\begin{bmatrix}0 & -2 & -2\\ -2 & 2 & 2\\ -2 & 2 & 2\end{bmatrix}\boldsymbol{\Delta T} - 4\frac{u_{xo}}{u_{yo}}\Delta\tau_1 - 3\frac{\Delta a}{u_{yo}}\Delta\tau_2 - \left(3\frac{\Delta a}{u_{yo}} - 4\frac{u_{xo}}{u_{yo}}\right)\Delta\tau_3 + \left[\frac{\Delta b}{u_{yo}} + \frac{3}{8}\left(\frac{\Delta a}{u_{yo}}\right)^2 - \frac{u_{xo}}{u_{yo}}\frac{\Delta a}{u_{yo}}\right] = 0 \quad \text{(E.29)}$$

and for this subcase $u_{xo}/u_{yo} = +1$, so

$$\frac{3}{2}\boldsymbol{\Delta T}^T\begin{bmatrix}0 & -2 & -2\\ -2 & 2 & 2\\ -2 & 2 & 2\end{bmatrix}\boldsymbol{\Delta T} - 4\Delta\tau_1 - 3\frac{\Delta a}{u_{yo}}\Delta\tau_2 - \left(3\frac{\Delta a}{u_{yo}} - 4\right)\Delta\tau_3 + \left[\frac{\Delta b}{u_{yo}} + \frac{3}{8}\left(\frac{\Delta a}{u_{yo}}\right)^2 - \frac{\Delta a}{u_{yo}}\right] = 0 \quad \text{(E.30)}$$

which is a quadratic in $\Delta\tau_2$ and $\Delta\tau_3$, but linear in $\Delta\tau_1$. Solving for $\Delta\tau_1$ directly,

$$\begin{aligned}\Delta\tau_1 =& \frac{3}{6\left(\Delta\tau_2 + \Delta\tau_3\right) + 4}\left(\Delta\tau_2 + \Delta\tau_3 - \frac{\Delta a}{u_{yo}}\right)\left(\Delta\tau_2 + \Delta\tau_3\right)\\ &+ \frac{1}{6\left(\Delta\tau_2 + \Delta\tau_3\right) + 4}\left[\frac{\Delta b}{u_{yo}} + \frac{3}{8}\left(\frac{\Delta a}{u_{yo}}\right)^2 - \frac{\Delta a}{u_{yo}}\right]\\ &+ \frac{2}{3\left(\Delta\tau_2 + \Delta\tau_3\right) + 2}\Delta\tau_3\end{aligned} \quad \text{(E.31)}$$

which can be substituted back into Equation (E.6),

$$\begin{aligned}\Delta\tau_4 =& -\frac{1}{2}\frac{\Delta a}{u_{yo}} + \left[1 - \frac{3}{6\left(\Delta\tau_2 + \Delta\tau_3\right) + 4}\left(\Delta\tau_2 + \Delta\tau_3 - \frac{\Delta a}{u_{yo}}\right)\right]\left(\Delta\tau_2 + \Delta\tau_3\right)\\ &- \frac{1}{6\left(\Delta\tau_2 + \Delta\tau_3\right) + 4}\left[\frac{\Delta b}{u_{yo}} + \frac{3}{8}\left(\frac{\Delta a}{u_{yo}}\right)^2 - \frac{\Delta a}{u_{yo}}\right]\\ &- \frac{2}{3\left(\Delta\tau_2 + \Delta\tau_3\right) + 2}\Delta\tau_3\end{aligned} \quad \text{(E.32)}$$

At this point both $\Delta\tau_1$ and $\Delta\tau_4$ are considered to be functions of only $\Delta\tau_2$ and $\Delta\tau_3$.

Subcase II. (X-Y-X)

For this subcase, we get

$$\frac{3}{2}\boldsymbol{\Delta T}^T\begin{bmatrix}-2 & -2 & 0\\ -2 & -2 & 0\\ 0 & 0 & 0\end{bmatrix}\boldsymbol{\Delta T} - \left(3\frac{\Delta a}{u_{yo}} + 4\frac{u_{xo}}{u_{yo}}\right)\Delta\tau_1 - 3\frac{\Delta a}{u_{yo}}\Delta\tau_2 + 4\frac{u_{xo}}{u_{yo}}\Delta\tau_3 + \left[\frac{\Delta b}{u_{yo}} - \frac{3}{8}\left(\frac{\Delta a}{u_{yo}}\right)^2 - \frac{u_{xo}}{u_{yo}}\frac{\Delta a}{u_{yo}}\right] = 0 \quad \text{(E.33)}$$

and for this subcase, $u_{xo}/u_{yo} = -1$, so,

$$\frac{3}{2}\boldsymbol{\Delta T}^T\begin{bmatrix}-2 & -2 & 0\\ -2 & -2 & 0\\ 0 & 0 & 0\end{bmatrix}\boldsymbol{\Delta T} - \left(3\frac{\Delta a}{u_{yo}} - 4\right)\Delta\tau_1 - 3\frac{\Delta a}{u_{yo}}\Delta\tau_2 - 4\Delta\tau_3 + \left[\frac{\Delta b}{u_{yo}} - \frac{3}{8}\left(\frac{\Delta a}{u_{yo}}\right)^2 + \frac{\Delta a}{u_{yo}}\right] = 0 \quad \text{(E.34)}$$

which is quadratic in $\Delta\tau_1$ and $\Delta\tau_2$, but linear in $\Delta\tau_3$. Solving for $\Delta\tau_3$ directly,

$$\Delta\tau_3 = \frac{1}{4}\frac{\Delta a}{u_{yo}} + \Delta\tau_1 - \frac{3}{4}\left[\Delta\tau_1 + \Delta\tau_2 + \frac{\Delta a}{u_{yo}}\right](\Delta\tau_1 + \Delta\tau_2) + \frac{1}{4}\left[\frac{\Delta b}{u_{yo}} - \frac{3}{8}\left(\frac{\Delta a}{u_{yo}}\right)^2\right] \quad \text{(E.35)}$$

which can be substituted into Equation (E.28),

$$\Delta\tau_4 = \frac{1}{4}\frac{\Delta a}{u_{yo}} + \Delta\tau_2 + \frac{3}{4}\left[\Delta\tau_1 + \Delta\tau_2 + \frac{\Delta a}{u_{yo}}\right](\Delta\tau_1 + \Delta\tau_2) - \frac{1}{4}\left[\frac{\Delta b}{u_{yo}} - \frac{3}{8}\left(\frac{\Delta a}{u_{yo}}\right)^2\right] \quad \text{(E.36)}$$

Now $\Delta\tau_3$ and $\Delta\tau_4$ are considered functions of $\Delta\tau_1$ and $\Delta\tau_2$.

Subcase III. (Y-X-X)

For this subcase, Equation (E.28) reduces to

$$\frac{3}{2}\boldsymbol{\Delta T}^T \begin{bmatrix} -2 & 0 & 0 \\ 0 & 0 & 0 \\ 0 & 0 & 0 \end{bmatrix} \boldsymbol{\Delta T} - \left(3\frac{\Delta a}{u_{yo}} + 4\frac{u_{xo}}{u_{yo}}\right)\Delta\tau_1 + 4\frac{u_{xo}}{u_{yo}}\Delta\tau_3 + \left[\frac{\Delta b}{u_{yo}} - \frac{3}{8}\left(\frac{\Delta a}{u_{yo}}\right)^2 - \frac{u_{xo}}{u_{yo}}\frac{\Delta a}{u_{yo}}\right] = 0 \quad \text{(E.37)}$$

and for this subcase $u_{xo}/u_{yo} = +1$,

$$\frac{3}{2}\boldsymbol{\Delta T}^T \begin{bmatrix} -2 & 0 & 0 \\ 0 & 0 & 0 \\ 0 & 0 & 0 \end{bmatrix} \boldsymbol{\Delta T} - \left(3\frac{\Delta a}{u_{yo}} + 4\right)\Delta\tau_1 + 4\Delta\tau_3 + \left[\frac{\Delta b}{u_{yo}} - \frac{3}{8}\left(\frac{\Delta a}{u_{yo}}\right)^2 - \frac{\Delta a}{u_{yo}}\right] = 0 \quad \text{(E.38)}$$

which is a quadratic in $\Delta\tau_1$ and linear in both $\Delta\tau_2$ and $\Delta\tau_3$. We Solving for $\Delta\tau_3$ directly,

$$\Delta\tau_3 = \frac{1}{4}\frac{\Delta a}{u_{yo}} + \Delta\tau_1 + \frac{3}{4}\left(\Delta\tau_1 + \frac{\Delta a}{u_{yo}}\right)\Delta\tau_1 - \frac{1}{4}\left[\frac{\Delta b}{u_{yo}} - \frac{3}{8}\left(\frac{\Delta a}{u_{yo}}\right)^2\right] \quad \text{(E.39)}$$

which can be substituted back into Equation (E.6),

$$\Delta\tau_4 = \frac{1}{4}\frac{\Delta a}{u_{yo}} - \Delta\tau_2 - \frac{3}{4}\left(\Delta\tau_1 + \frac{\Delta a}{u_{yo}}\right)\Delta\tau_1 + \frac{1}{4}\left[\frac{\Delta b}{u_{yo}} - \frac{3}{8}\left(\frac{\Delta a}{u_{yo}}\right)^2\right] \quad \text{(E.40)}$$

At this point both $\Delta\tau_3$ and $\Delta\tau_4$ are considered to be functions of only $\Delta\tau_1$ and $\Delta\tau_2$.

Subcase IV. (X-X-Y)

For this subcase,

$$\frac{3}{2}\boldsymbol{\Delta T}^T\begin{bmatrix}-2 & -2 & -2\\ -2 & -2 & -2\\ -2 & -2 & -2\end{bmatrix}\boldsymbol{\Delta T} - \left(3\frac{\Delta a}{u_{yo}} + 4\frac{u_{xo}}{u_{yo}}\right)(\Delta\tau_1 + \Delta\tau_3) - 3\frac{\Delta a}{u_{yo}}\Delta\tau_2 + \left[\frac{\Delta b}{u_{yo}} - \frac{3}{8}\left(\frac{\Delta a}{u_{yo}}\right)^2 - \frac{u_{xo}}{u_{yo}}\frac{\Delta a}{u_{yo}}\right] = 0 \quad \text{(E.41)}$$

and for this subcase $u_{xo}/u_{yo} = +1$,

$$\frac{3}{2}\boldsymbol{\Delta T}^T\begin{bmatrix}-2 & -2 & -2\\ -2 & -2 & -2\\ -2 & -2 & -2\end{bmatrix}\boldsymbol{\Delta T} - \left(3\frac{\Delta a}{u_{yo}} + 4\right)(\Delta\tau_1 + \Delta\tau_3) - 3\frac{\Delta a}{u_{yo}}\Delta\tau_2 + \left[\frac{\Delta b}{u_{yo}} - \frac{3}{8}\left(\frac{\Delta a}{u_{yo}}\right)^2 - \frac{\Delta a}{u_{yo}}\right] = 0 \quad \text{(E.42)}$$

which is quadratic in all three time intervals. Choosing $\Delta\tau_3$ to be expressed as a quadratic in terms of $\Delta\tau_1$ and $\Delta\tau_2$, the discriminant must be non-negative

$$\begin{aligned}&\left(5\frac{\Delta a}{u_{yo}} + \frac{20}{3}\right)\Delta\tau_1 + \left(5\frac{\Delta a}{u_{yo}} + 8\right)\Delta\tau_2\\ &+ \frac{71}{8}\left(\frac{\Delta a}{u_{yo}}\right)^2 + \frac{83}{3}\frac{\Delta a}{u_{yo}} + 16 + \frac{1}{3}\frac{\Delta b}{u_{yo}} \geq 0\end{aligned} \quad \text{(E.43)}$$

which can be used as an affine inequality constraint on $\Delta\tau_1$ and $\Delta\tau_2$.
For a special case where $\Delta a = 0$, the inequality becomes,

$$\Delta\tau_2 \geq -\frac{5}{6}\Delta\tau_1 - \frac{1}{24}\frac{\Delta b}{u_{yo}} - 2 \quad \text{(E.44)}$$

which implies that if $\frac{\Delta b}{u_{yo}} > -48$, there is no positive range for $\Delta\tau_2$; i.e., the inequality cannot be satisfied with this subcase. If, however, $\Delta a = 0$ and $\frac{\Delta b}{u_{yo}} < -48$ this subcase could be a viable option. In this situation, the inequality places a lower limit on $\Delta\tau_1$

that will result in non-negative $\Delta\tau_2$.

$$\Delta\tau_1 \geq -\frac{1}{20}\frac{\Delta b}{u_{yo}} - \frac{12}{5} \tag{E.45}$$

Only positive-real roots of the quadratic equations are valid for non-negative time intervals. No additional reduction is possible by substituting this quadratic into Equation (E.28), but at this time, $\Delta\tau_3$ and $\Delta\tau_4$ are considered as functions of $\Delta\tau_1$ and $\Delta\tau_2$.

Subcase V. (X-X-X)

For this subcase,

$$\frac{3}{2}\boldsymbol{\Delta T}^T \begin{bmatrix} 0 & 0 & 0 \\ 0 & 0 & 0 \\ 0 & 0 & 0 \end{bmatrix} \boldsymbol{\Delta T} - 4\frac{u_{xo}}{u_{yo}}\left(\Delta\tau_1 + \Delta\tau_3\right) + \left[\frac{\Delta b}{u_{yo}} + \frac{3}{8}\left(\frac{\Delta a}{u_{yo}}\right)^2 - \frac{u_{xo}}{u_{yo}}\frac{\Delta a}{u_{yo}}\right] = 0 \tag{E.46}$$

which is not a quadratic in any time interval variables, but linear in $\Delta\tau_1$ and $\Delta\tau_3$. Solving for the sum $\Delta\tau_1 + \Delta\tau_3$ directly, recalling that for this subcase only $u_{xo}/u_{yo} = +1$ is allowed,

$$\Delta\tau_1 + \Delta\tau_3 = \frac{1}{4}\left[\frac{\Delta b}{u_{yo}} + \frac{3}{8}\left(\frac{\Delta a}{u_{yo}}\right)^2\right] - \frac{1}{4}\frac{\Delta a}{u_{yo}} \tag{E.47}$$

which can be substituted back into Equation (E.6),

$$\Delta\tau_2 + \Delta\tau_4 = -\frac{1}{4}\left[\frac{\Delta b}{u_{yo}} + \frac{3}{8}\left(\frac{\Delta a}{u_{yo}}\right)^2\right] - \frac{1}{4}\frac{\Delta a}{u_{yo}} \tag{E.48}$$

Closer examination of these two equations show that requiring both the $\Delta\tau_1 + \Delta\tau_3 \geq 0$ and $\Delta\tau_2 + \Delta\tau_4 \geq 0$ results in

$$\frac{\Delta a}{\Delta b - \frac{3}{8}\frac{|\Delta a|}{U_{max}}\Delta a} = 1 \tag{E.49}$$

which only confirms earlier analysis of this subcase when $\Delta a = 0$, $t_f = 0$. Now, for $\Delta a = 0$, this equation cannot be satisfied for any value of Δb; $\frac{0}{\Delta b} \neq 1$. In addition, for $\Delta a \neq 0$, only when Δb has the following values, can this subcase result in positive time intervals:

$$\Delta b = \left(\frac{3}{8} \frac{|\Delta a|}{U_{max}} + 1 \right) \Delta a \tag{E.50}$$

Now, substituting this back into the $\Delta\tau_1 + \Delta\tau_3$ and $\Delta\tau_2 + \Delta\tau_4$ equations,

$$\Delta\tau_1 + \Delta\tau_3 = -\frac{1}{2} \frac{\Delta a}{u_{yo}} = \frac{1}{2} \frac{|\Delta a|}{U_{max}} = t_f \tag{E.51a}$$

$$\Delta\tau_2 + \Delta\tau_4 = 0 \tag{E.51b}$$

which is a very strange result. This says that only one x-control switch at t_1 is needed, which is like the $N = 1$ case. Therefore, this subcase is eliminated as a viable option for $N = 3$ case; changing only the x-control will not result in the desired final relative orbit parameters for any values of Δa and Δb.

Next, the relative orbit size parameter, $\rho(t)$, is examined

$$\rho^2(t) = [x(t) - a(t)]^2 + \dot{x}^2(t) \tag{E.52}$$

Expressing this equation at $t = t_f$ with $\rho(t_f) = \rho_f$,

$$\frac{\rho_f^2 - \rho_o^2}{U_{max}^2} = \left[\begin{array}{l}
10 + \left(\frac{\Delta u_{x1}}{u_{xo}}\right)^2 + \left(\frac{\Delta u_{x2}}{u_{xo}}\right)^2 + \left(\frac{\Delta u_{x3}}{u_{xo}}\right)^2 + 4\left(\frac{\Delta u_{y1}}{u_{yo}}\right)^2 + 4\left(\frac{\Delta u_{y2}}{u_{yo}}\right)^2 + 4\left(\frac{\Delta u_{y3}}{u_{yo}}\right)^2 \\
-2\frac{\rho_o}{u_{yo}}\left(2\cos\theta_o + \frac{u_{xo}}{u_{yo}}\sin\theta_o\right) \\
+2\frac{\rho_o}{u_{yo}}\left[2\frac{\Delta u_{y1}}{u_{yo}}\cos\left(\Delta\tau_1 + \theta_o\right) + \frac{u_{xo}}{u_{yo}}\frac{\Delta u_{x1}}{u_{xo}}\sin\left(\Delta\tau_1 + \theta_o\right)\right] \\
+2\frac{\rho_o}{u_{yo}}\left[2\frac{\Delta u_{y2}}{u_{yo}}\cos\left(\Delta\tau_1 + \Delta\tau_2 + \theta_o\right) + \frac{u_{xo}}{u_{yo}}\frac{\Delta u_{x2}}{u_{xo}}\sin\left(\Delta\tau_1 + \Delta\tau_2 + \theta_o\right)\right] \\
+2\frac{\rho_o}{u_{yo}}\left[2\frac{\Delta u_{y3}}{u_{yo}}\cos\left(\Delta\tau_1 + \Delta\tau_2 + \Delta\tau_3 + \theta_o\right) + \frac{u_{xo}}{u_{yo}}\frac{\Delta u_{x3}}{u_{xo}}\sin\left(\Delta\tau_1 + \Delta\tau_2 + +\Delta\tau_3\theta_o\right)\right] \\
+2\frac{\rho_o}{u_{yo}}\left[2\frac{u_{y3}}{u_{yo}}\cos\left(t_f + \theta_o\right) + \frac{u_{xo}}{u_{yo}}\frac{u_{x3}}{u_{xo}}\sin\left(t_f + \theta_o\right)\right] \\
-2\left(\frac{\Delta u_{x1}}{u_{xo}} + 4\frac{\Delta u_{y1}}{u_{yo}}\right)\cos\Delta\tau_1 + 4\frac{u_{xo}}{u_{yo}}\left(\frac{\Delta u_{y1}}{u_{yo}} - \frac{\Delta u_{x1}}{u_{xo}}\right)\sin\Delta\tau_1 \\
-2\left(\frac{\Delta u_{x2}}{u_{xo}} + 4\frac{\Delta u_{y2}}{u_{yo}}\right)\cos\left(\Delta\tau_1 + \Delta\tau_2\right) + 4\frac{u_{xo}}{u_{yo}}\left(\frac{\Delta u_{y2}}{u_{yo}} - \frac{\Delta u_{x2}}{u_{xo}}\right)\sin\left(\Delta\tau_1 + \Delta\tau_2\right) \\
-2\left(\frac{\Delta u_{x3}}{u_{xo}} + 4\frac{\Delta u_{y3}}{u_{yo}}\right)\cos\left(\Delta\tau_1 + \Delta\tau_2 + \Delta\tau_3\right) \\
+4\frac{u_{xo}}{u_{yo}}\left(\frac{\Delta u_{y3}}{u_{yo}} - \frac{\Delta u_{x3}}{u_{xo}}\right)\sin\left(\Delta\tau_1 + \Delta\tau_2 + \Delta\tau_3\right) \\
-2\left(\frac{u_{x3}}{u_{xo}} + 4\frac{u_{y3}}{u_{yo}}\right)\cos t_f + 4\frac{u_{xo}}{u_{yo}}\left(\frac{u_{y3}}{u_{yo}} - \frac{u_{x3}}{u_{xo}}\right)\sin t_f \\
+2\left(\frac{\Delta u_{x1}}{u_{xo}}\frac{\Delta u_{x2}}{u_{xo}} + 4\frac{\Delta u_{y1}}{u_{yo}}\frac{\Delta u_{y2}}{u_{yo}}\right)\cos\Delta\tau_2 + 4\frac{u_{xo}}{u_{yo}}\left(\frac{\Delta u_{x2}}{u_{xo}}\frac{\Delta u_{y1}}{u_{yo}} - \frac{\Delta u_{x1}}{u_{xo}}\frac{\Delta u_{y2}}{u_{yo}}\right)\sin\Delta\tau_2 \\
+2\left(\frac{\Delta u_{x1}}{u_{xo}}\frac{\Delta u_{x3}}{u_{xo}} + 4\frac{\Delta u_{y1}}{u_{yo}}\frac{\Delta u_{y3}}{u_{yo}}\right)\cos\left(\Delta\tau_2 + \Delta\tau_3\right) \\
+4\frac{u_{xo}}{u_{yo}}\left(\frac{\Delta u_{x3}}{u_{xo}}\frac{\Delta u_{y1}}{u_{yo}} - \frac{\Delta u_{x1}}{u_{xo}}\frac{\Delta u_{y3}}{u_{yo}}\right)\sin\left(\Delta\tau_2 + \Delta\tau_3\right) \\
+2\left(\frac{u_{x3}}{u_{xo}}\frac{\Delta u_{x1}}{u_{xo}} + 4\frac{u_{y3}}{u_{yo}}\frac{\Delta u_{y1}}{u_{yo}}\right)\cos\left(\Delta\tau_2 + \Delta\tau_3 + \Delta\tau_4\right) \\
+4\frac{u_{xo}}{u_{yo}}\left(\frac{\Delta u_{y1}}{u_{yo}}\frac{u_{x3}}{u_{xo}} - \frac{\Delta u_{x1}}{u_{xo}}\frac{u_{y3}}{u_{yo}}\right)\sin\left(\Delta\tau_2 + \Delta\tau_3 + \Delta\tau_4\right) \\
+2\left(\frac{\Delta u_{x2}}{u_{xo}}\frac{\Delta u_{x3}}{u_{xo}} + 4\frac{\Delta u_{y2}}{u_{yo}}\frac{\Delta u_{y3}}{u_{yo}}\right)\cos\Delta\tau_3 + 4\frac{u_{xo}}{u_{yo}}\left(\frac{\Delta u_{x3}}{u_{xo}}\frac{\Delta u_{y2}}{u_{yo}} - \frac{\Delta u_{x2}}{u_{xo}}\frac{\Delta u_{y3}}{u_{yo}}\right)\sin\Delta\tau_3 \\
+2\left(\frac{u_{x3}}{u_{xo}}\frac{\Delta u_{x2}}{u_{xo}} + 4\frac{u_{y3}}{u_{yo}}\frac{\Delta u_{y2}}{u_{yo}}\right)\cos\left(\Delta\tau_3 + \Delta\tau_4\right) \\
+4\frac{u_{xo}}{u_{yo}}\left(\frac{\Delta u_{y2}}{u_{yo}}\frac{u_{x3}}{u_{xo}} - \frac{\Delta u_{x2}}{u_{xo}}\frac{u_{y3}}{u_{yo}}\right)\sin\left(\Delta\tau_3 + \Delta\tau_4\right) \\
+2\left(\frac{u_{x3}}{u_{xo}}\frac{\Delta u_{x3}}{u_{xo}} + 4\frac{u_{y3}}{u_{yo}}\right)\cos\Delta\tau_4 + 4\frac{u_{xo}}{u_{yo}}\left(\frac{u_{x3}}{u_{xo}}\frac{\Delta u_{y3}}{u_{yo}} - \frac{u_{y3}}{u_{yo}}\frac{\Delta u_{x3}}{u_{xo}}\right)\sin\Delta\tau_4
\end{array}\right] \tag{E.53}$$

which becomes a nonlinear function of two variables, after the substituting in Equations (E.6) and the reduced form of (E.28). Therefore, no analytical solution can be found to solve for the critical times; numerical root solver must be employed. The resulting equations for each subcases will be provided along with the phase angle parameter equation.

Finally, the last relative orbit parameter, the phase angle parameter, $\theta(t)$, is examined.

$$\tan\theta(t) = \frac{x(t) - a(t)}{\dot{x}(t)} = -\frac{3x(t) + 2\dot{y}(t)}{\dot{x}(t)} \tag{E.54}$$

Expressing this equation at $t = t_f$ with $\theta(t_f) = \theta_f$,

$$\frac{\rho_o}{u_{yo}}\sin(t_f + \theta_o - \theta_f) = \begin{bmatrix} -\frac{u_{xo}}{u_{yo}}\frac{u_{x3}}{u_{xo}}\cos\theta_f + 2\frac{u_{y3}}{u_{yo}}\sin\theta_f \\ -\frac{u_{xo}}{u_{yo}}\frac{\Delta u_{x3}}{u_{xo}}\cos(\Delta\tau_4 - \theta_f) - 2\frac{\Delta u_{y3}}{u_{yo}}\sin(\Delta\tau_4 - \theta_f) \\ -\frac{u_{xo}}{u_{yo}}\frac{\Delta u_{x2}}{u_{xo}}\cos(\Delta\tau_3 + \Delta\tau_4 - \theta_f) \\ -2\frac{\Delta u_{y2}}{u_{yo}}\sin(\Delta\tau_3 + \Delta\tau_4 - \theta_f) \\ -\frac{u_{xo}}{u_{yo}}\frac{\Delta u_{x1}}{u_{xo}}\cos(\Delta\tau_2 + \Delta\tau_3 + \Delta\tau_4 - \theta_f) \\ -2\frac{\Delta u_{y1}}{u_{yo}}\sin(\Delta\tau_2 + \Delta\tau_3 + \Delta\tau_4 - \theta_f) \\ +\frac{u_{xo}}{u_{yo}}\cos(t_f - \theta_f) + 2\sin(t_f - \theta_f) \end{bmatrix} \tag{E.55}$$

The solution to the critical times requires simultaneous solution to two nonlinear Equations (E.53) and (E.55). As stated earlier, the solution cannot be reached algebraically, i.e., it cannot be obtained analytically. For the four viable subcases (out of five)[2], the two simultaneous equations to be solved are:

Subcase I. (Y-X-Y)

[2]Earlier analysis showed that subcase V was not a viable control sequence.

The ρ-equation for this subcase is:

$$\frac{\rho_f^2-\rho_o^2}{2U_{max}^2}=\left[\begin{array}{l}23+\frac{\rho_o}{u_{yo}}\left(-2\cos\theta_o-\sin\theta_o\right)+4\frac{\rho_o}{u_{yo}}\cos\left(\Delta\tau_1+\theta_o\right)\\+2\frac{\rho_o}{u_{yo}}\sin\left(\Delta\tau_1+\Delta\tau_2+\theta_o\right)-4\frac{\rho_o}{u_{yo}}\cos\left(\Delta\tau_1+\Delta\tau_2+\Delta\tau_3+\theta_o\right)\\+\frac{\rho_o}{u_{yo}}\left[2\cos\left(t_f+\theta_o\right)-\sin\left(t_f+\theta_o\right)\right]\\-8\cos\Delta\tau_1+4\sin\Delta\tau_1+16\sin\Delta\tau_2+4\cos\Delta\tau_4+4\sin\Delta\tau_4\\+4\cos\left(\Delta\tau_1+\Delta\tau_2\right)-16\cos\left(\Delta\tau_2+\Delta\tau_3\right)-4\sin\left(\Delta\tau_2+\Delta\tau_3\right)\\-2\cos\left(\Delta\tau_3+\Delta\tau_4\right)+8\cos\left(\Delta\tau_1+\Delta\tau_2+\Delta\tau_3\right)\\+8\cos\left(\Delta\tau_2+\Delta\tau_3+\Delta\tau_4\right)-4\sin\left(\Delta\tau_2+\Delta\tau_3+\Delta\tau_4\right)\\+3\sin\left(\Delta\tau_1+\Delta\tau_2+\Delta\tau_3+\Delta\tau_4\right)\end{array}\right] \tag{E.56}$$

and the θ-equation is:

$$\frac{\rho_o}{u_{yo}}\sin\left(t_f+\theta_o-\theta_f\right)=\left[\begin{array}{l}\cos\theta_f+2\sin\theta_f+4\sin\left(\Delta\tau_4-\theta_f\right)\\-2\cos\left(\Delta\tau_3+\Delta\tau_4-\theta_f\right)\\-4\sin\left(\Delta\tau_2+\Delta\tau_3+\Delta\tau_4-\theta_f\right)\\+\cos\left(t_f-\theta_f\right)+2\sin\left(t_f-\theta_f\right)\end{array}\right] \tag{E.57}$$

Subcase II. (X-Y-X)

The ρ-equation for this subcase is:

$$\frac{\rho_f^2-\rho_o^2}{2U_{max}^2}=\left[\begin{array}{l}17+\frac{\rho_o}{u_{yo}}\left(-2\cos\theta_o+\sin\theta_o\right)-2\frac{\rho_o}{u_{yo}}\sin\left(\Delta\tau_1+\theta_o\right)\\+4\frac{\rho_o}{u_{yo}}\cos\left(\Delta\tau_1+\Delta\tau_2+\theta_o\right)+2\frac{\rho_o}{u_{yo}}\sin\left(\Delta\tau_1+\Delta\tau_2+\Delta\tau_3\theta_o\right)\\+\frac{\rho_o}{u_{yo}}\left[-2\cos\left(t_f+\theta_o\right)-\sin\left(t_f+\theta_o\right)\right]\\-2\cos\Delta\tau_1+4\sin\Delta\tau_1+8\sin\Delta\tau_2\\-6\cos\Delta\tau_4+4\sin\Delta\tau_4-8\cos\left(\Delta\tau_1+\Delta\tau_2\right)-4\sin\left(\Delta\tau_1+\Delta\tau_2\right)\\-4\cos\left(\Delta\tau_2+\Delta\tau_3\right)-8\cos\left(\Delta\tau_3+\Delta\tau_4\right)\\+2\cos\left(\Delta\tau_1+\Delta\tau_2+\Delta\tau_3\right)+2\cos\left(\Delta\tau_2+\Delta\tau_3+\Delta\tau_4\right)\\-4\sin\left(\Delta\tau_2+\Delta\tau_3+\Delta\tau_4\right)+3\sin\left(\Delta\tau_1+\Delta\tau_2+\Delta\tau_3+\Delta\tau_4\right)\end{array}\right] \tag{E.58}$$

and the θ-equation is:

$$\frac{\rho_o}{u_{yo}} \sin\left(t_f + \theta_o - \theta_f\right) = \begin{bmatrix} \cos\theta_f - 2\sin\theta_f - 2\cos\left(\Delta\tau_4 - \theta_f\right) \\ -4\sin\left(\Delta\tau_3 + \Delta\tau_4 - \theta_f\right) \\ +2\cos\left(\Delta\tau_2 + \Delta\tau_3 + \Delta\tau_4 - \theta_f\right) \\ -\cos\left(t_f - \theta_f\right) + 2\sin\left(t_f - \theta_f\right) \end{bmatrix} \tag{E.59}$$

Subcase III. (Y-X-X)

The ρ-equation for this subcase is:

$$\frac{\rho_f^2 - \rho_o^2}{2U_{max}^2} = \begin{bmatrix} 17 + \frac{\rho_o}{u_{yo}}\left(-2\cos\theta_o - \sin\theta_o\right) + 4\frac{\rho_o}{u_{yo}}\cos\left(\Delta\tau_1 + \theta_o\right) \\ +2\frac{\rho_o}{u_{yo}}\sin\left(\Delta\tau_1 + \Delta\tau_2 + \theta_o\right) - 2\frac{\rho_o}{u_{yo}}\sin\left(\Delta\tau_1 + \Delta\tau_2 + \Delta\tau_3\theta_o\right) \\ +\frac{\rho_o}{u_{yo}}\left[-2\cos\left(t_f + \theta_o\right) + \sin\left(t_f + \theta_o\right)\right] \\ -8\cos\Delta\tau_1 + 4\sin\Delta\tau_1 + 8\sin\Delta\tau_2 \\ -4\cos\Delta\tau_3 - 6\cos\Delta\tau_4 - 4\sin\Delta\tau_4 - 12\sin\left(\Delta\tau_2 + \Delta\tau_3\right) \\ +2\cos\left(\Delta\tau_3 + \Delta\tau_4\right) + 2\cos\left(\Delta\tau_1 + \Delta\tau_2 + \Delta\tau_3\right) \\ -8\cos\left(\Delta\tau_2 + \Delta\tau_3 + \Delta\tau_4\right) + 4\sin\left(\Delta\tau_2 + \Delta\tau_3 + \Delta\tau_4\right) \\ +3\sin\left(\Delta\tau_1 + \Delta\tau_2 + \Delta\tau_3 + \Delta\tau_4\right) \end{bmatrix} \tag{E.60}$$

and the θ-equation is:

$$\frac{\rho_o}{u_{yo}} \sin\left(t_f + \theta_o - \theta_f\right) = \begin{bmatrix} -\cos\theta_f - 2\sin\theta_f + 2\cos\left(\Delta\tau_4 - \theta_f\right) \\ -2\cos\left(\Delta\tau_3 + \Delta\tau_4 - \theta_f\right) \\ -4\sin\left(\Delta\tau_2 + \Delta\tau_3 + \Delta\tau_4 - \theta_f\right) \\ +\cos\left(t_f - \theta_f\right) + 2\sin\left(t_f - \theta_f\right) \end{bmatrix} \tag{E.61}$$

Subcase IV. (X-X-Y)

The ρ-equation for this subcase is:

$$\frac{\rho_f^2 - \rho_o^2}{2U_{max}^2} = \begin{bmatrix} 17 + \frac{\rho_o}{u_{yo}}\left(-2\cos\theta_o - \sin\theta_o\right) \\ +2\frac{\rho_o}{u_{yo}}\sin\left(\Delta\tau_1 + \theta_o\right) - 2\frac{\rho_o}{u_{yo}}\sin\left(\Delta\tau_1 + \Delta\tau_2 + \theta_o\right) \\ +4\frac{\rho_o}{u_{yo}}\cos\left(\Delta\tau_1 + \Delta\tau_2 + \Delta\tau_3 + \theta_o\right) \\ +\frac{\rho_o}{u_{yo}}\left[-2\cos\left(t_f + \theta_o\right) + \sin\left(t_f + \theta_o\right)\right] \\ -2\cos\Delta\tau_1 - 4\sin\Delta\tau_1 - 4\cos\Delta\tau_2 + 8\sin\Delta\tau_3 \\ -4\cos\Delta\tau_4 + 4\sin\Delta\tau_4 + 2\cos\left(\Delta\tau_1 + \Delta\tau_2\right) \\ +4\sin\left(\Delta\tau_2 + \Delta\tau_3\right) - 2\cos\left(\Delta\tau_3 + \Delta\tau_4\right) \\ -8\cos\left(\Delta\tau_1 + \Delta\tau_2 + \Delta\tau_3\right) + 2\cos\left(\Delta\tau_2 + \Delta\tau_3 + \Delta\tau_4\right) \\ +3\sin\left(\Delta\tau_1 + \Delta\tau_2 + \Delta\tau_3 + \Delta\tau_4\right) \end{bmatrix} \tag{E.62}$$

and the θ-equation is:

$$\frac{\rho_o}{u_{yo}}\sin\left(t_f + \theta_o - \theta_f\right) = \begin{bmatrix} -\cos\theta_f - 2\sin\theta_f - 4\sin\left(\Delta\tau_4 - \theta_f\right) \\ +2\cos\left(\Delta\tau_3 + \Delta\tau_4 - \theta_f\right) \\ -2\cos\left(\Delta\tau_2 + \Delta\tau_3 + \Delta\tau_4 - \theta_f\right) \\ +\cos\left(t_f - \theta_f\right) + 2\sin\left(t_f - \theta_f\right) \end{bmatrix} \tag{E.63}$$

E.3 CoState Boundary Conditions

The optimal theory provides the terminal costate in terms of the lagrange multiplier

$$\boldsymbol{\lambda}^T(t_f) = \boldsymbol{\nu}^T \frac{\partial \boldsymbol{\Psi}[\mathbf{x}(t_f), t_f]}{\partial \mathbf{x}(t_f)} \tag{E.64}$$

For $N = 3$, no additional relationship is gained from this condition (as it was for $N < 3$). However, there are additional observations for the four viable subcases of $N = 3$. For the control to be optimal, the velocity costate associated with the control switch must necessarily be zero at the corresponding switch times. The results are summarized in the Table E.1 below.

Table E.1 Velocity costate at switching times for four viable subcases of $N = 3$.

Subcases	Control Sequence	Velocity Costate
I.	Y-X-Y	$\lambda_{\dot{y}1} = \lambda_{\dot{x}2} = \lambda_{\dot{y}3} = 0$
II.	X-Y-X	$\lambda_{\dot{x}1} = \lambda_{\dot{y}2} = \lambda_{\dot{x}3} = 0$
III.	Y-X-X	$\lambda_{\dot{y}1} = \lambda_{\dot{x}2} = \lambda_{\dot{x}3} = 0$
IV.	X-X-Y	$\lambda_{\dot{x}1} = \lambda_{\dot{x}2} = \lambda_{\dot{y}3} = 0$

For convenience, the costate at t_3 is determined. The costate at t_1 and t_2 is transformed to via the costate transition matrix,

$$\boldsymbol{\lambda}_1^T = [\boldsymbol{\Phi}_\lambda^{-1}(t_3, t_1)\boldsymbol{\lambda}_3]^T = \boldsymbol{\lambda}_3^T \left[e^{-A^T(t_3 - t_1)}\right]^{-T} = \boldsymbol{\lambda}_3^T \boldsymbol{\Phi}_x(t_3, t_1) \tag{E.65a}$$

$$\boldsymbol{\lambda}_2^T = [\boldsymbol{\Phi}_\lambda^{-1}(t_3, t_2)\boldsymbol{\lambda}_3]^T = \boldsymbol{\lambda}_3^T \left[e^{-A^T(t_3 - t_2)}\right]^{-T} = \boldsymbol{\lambda}_3^T \boldsymbol{\Phi}_x(t_3, t_2) \tag{E.65b}$$

The appropriate velocity costate at t_1 and t_2 (appropriate to the subcases) are then used to generate two expressions relating the costate at t_3.

E.4 Transversality Condition and Hamiltonian

The Transversality condition must hold at t_f. However, the optimal theory for open final time states that the Hamiltonian will remain at zero. Then, the Transversality condition is reduced to the Equation (2.16), repeated here to facilitate the discussion.

$$\boldsymbol{\nu}^T \frac{\partial \boldsymbol{\Psi}\left(\mathbf{x}(t_f), t_f\right)}{\partial t_f} = \boldsymbol{\nu}^T \begin{bmatrix} 0 \\ 0 \\ 0 \end{bmatrix} = \mathbf{0} \tag{E.66}$$

since the terminal state constraint vector equation is not an explicit function of t_f.

Taking advantage of the Hamiltonian being zero at five different times, the choice of which of these to use is arbitrary.

$$\begin{aligned} H_o &= 1 + \boldsymbol{\lambda}_o^T(\mathbf{A}\mathbf{x}_o + \mathbf{B}\mathbf{u}_o) = 0 \\ H_1 &= 1 + \boldsymbol{\lambda}_1^T(\mathbf{A}\mathbf{x}_1 + \mathbf{B}\mathbf{u}_1) = 0 \\ H_2 &= 1 + \boldsymbol{\lambda}_2^T(\mathbf{A}\mathbf{x}_2 + \mathbf{B}\mathbf{u}_2) = 0 \\ H_3 &= 1 + \boldsymbol{\lambda}_3^T(\mathbf{A}\mathbf{x}_3 + \mathbf{B}\mathbf{u}_3) = 0 \\ H_f &= 1 + \boldsymbol{\lambda}_f^T(\mathbf{A}\mathbf{x}_f + \mathbf{B}\mathbf{u}_3) = 0 \end{aligned} \tag{E.67}$$

where $\mathbf{u}_f = \mathbf{u}_3$ for $N = 3$. However, since the aim is to find an equation that in linear withe respect to $\boldsymbol{\lambda}_3$, H_3 is chosen from above. H_3 can be written out explicitly:

$$\dot{x}_3\lambda_{x3} + \dot{y}_3\lambda_{y3} + (3x_3 + 2\dot{y}_3 + u_{x3})\,\lambda_{\dot{x}3} + (-2\dot{x}_3 + u_{y3})\,\lambda_{\dot{y}3} = -1 \tag{E.68}$$

which is linear in $\boldsymbol{\lambda}_3$ making it easy to calculate the it with linear algebra.

E.5 CoStates at the Third Control Switch

All the equations required to calculate the costate at t_3 have now been developed. The five perviously developed equations are Hamiltonian equation, the two equations for the two velocity costates at t_1, and the two equations for the two velocity costates at t_2. Combining these equations in a matrix form,

$$\boldsymbol{\Lambda}\boldsymbol{\lambda}_3 = \begin{bmatrix} -1 \\ \lambda_{\dot{x}1} \\ \lambda_{\dot{y}1} \\ \lambda_{\dot{x}2} \\ \lambda_{\dot{y}2} \end{bmatrix} \tag{E.69}$$

where $\mathbf{\Lambda}$ is given by,

$$\begin{bmatrix} \dot{x}_3 & \dot{y}_3 & 3x_3 + 2\dot{y}_3 + u_{x3} & -2\dot{x}_3 + u_{y3} \\ \sin(t_3 - t_1) & 2\left(\cos(t_3 - t_1) - 1\right) & \cos(t_3 - t_1) & -2\sin(t_3 - t_1) \\ 2\left(1 - \cos(t_3 - t_1)\right) & 4\sin(t_3 - t_1) - 3(t_3 - t_1) & 2\sin(t_3 - t_1) & 4\cos(t_3 - t_1) - 3 \\ \sin\Delta\tau_3 & 2\left(\cos\Delta\tau_3 - 1\right) & \cos\Delta\tau_3 & -2\sin\Delta\tau_3 \\ 2\left(1 - \cos\Delta\tau_3\right) & 4\sin\Delta\tau_3 - 3\Delta\tau_3 & 2\sin\Delta\tau_3 & 4\cos\Delta\tau_3 - 3 \end{bmatrix} \tag{E.70}$$

and $t_3 - t_1 = \Delta\tau_2 + \Delta\tau_3$. In all subcases only three of the five equations are used. The transversality equation, one of the velocity costate at t_1, and another velocity costate at t_2, result in a 3x3 matrix. The results for the four viable subcases are:

Subcase I. (Y-X-Y)

For this subcase, $\lambda_{\dot{y}3} = 0$, the transversality condition, $\lambda_{\dot{y}1} = 0$, and $\lambda_{\dot{x}2} = 0$ results in,

$$\mathbf{\Lambda}^I \begin{bmatrix} \lambda_{x3} \\ \lambda_{y3} \\ \lambda_{\dot{x}3} \end{bmatrix} = \begin{bmatrix} -1 \\ 0 \\ 0 \end{bmatrix} \tag{E.71}$$

where $\mathbf{\Lambda}^I$ is

$$\begin{bmatrix} \dot{x}_3 & \dot{y}_3 & 3x_3 + 2\dot{y}_3 + u_{x3} \\ 2\left(1 - \cos(t_3 - t_1)\right) & 4\sin(t_3 - t_1) - 3(t_3 - t_1) & 2\sin(t_3 - t_1) \\ \sin\Delta\tau_3 & 2\left(\cos\Delta\tau_3 - 1\right) & \cos\Delta\tau_3 \end{bmatrix} \tag{E.72}$$

Now, performing the matrix inverse algebraic operation,

$$\begin{bmatrix} \lambda_{x3} \\ \lambda_{y3} \\ \lambda_{\dot{x}3} \\ \lambda_{\dot{y}3} \end{bmatrix} = \frac{1}{D} \begin{bmatrix} -4\sin(\Delta\tau_2 + \Delta\tau_3) + 3(\Delta\tau_2 + \Delta\tau_3)\cos\Delta\tau_3 \\ 2\cos\Delta\tau_3 - 2\Delta\tau_2 \\ 4 + 4\cos\Delta\tau_2 - 4\alpha - 3(\Delta\tau_2 + \Delta\tau_3)\sin\Delta\tau_3 \\ 0 \end{bmatrix} \tag{E.73}$$

$$\begin{aligned} D &= (6x_3 + 8\dot{y}_3 - 4u_{xo})[\cos(\Delta\tau_2 + \Delta\tau_3) - 1] \\ &\quad + 4\dot{x}_3 \sin(\Delta\tau_2 + \Delta\tau_3) - \beta\cos\Delta\tau_2 \\ &\quad + [\beta - 3\dot{x}_3(\Delta\tau_2 + \Delta\tau_3)]\cos\Delta\tau_3 \\ &\quad + [(9x_3 + 6\dot{y}_3 - 3u_{xo})(\Delta\tau_2 + \Delta\tau_3)]\sin\Delta\tau_3 \end{aligned} \tag{E.74}$$

$$\alpha = \cos\Delta\tau_3 + \cos(\Delta\tau_2 + \Delta\tau_3) \tag{E.75}$$

$$\beta = 12x_3 + 6\dot{y}_3 - 4u_{xo} \tag{E.76}$$

Subcase II. (X-Y-X)

For this subcase, $\lambda_{\dot{x}3} = 0$, the transversality condition, $\lambda_{\dot{x}1} = 0$, and $\lambda_{\dot{y}2} = 0$ results in,

$$\mathbf{\Lambda}^{II} \begin{bmatrix} \lambda_{x3} \\ \lambda_{y3} \\ \lambda_{\dot{y}3} \end{bmatrix} = \begin{bmatrix} -1 \\ 0 \\ 0 \end{bmatrix} \tag{E.77}$$

where $\mathbf{\Lambda}^{II}$ is

$$\begin{bmatrix} \dot{x}_3 & \dot{y}_3 & -2\dot{x}_3 + u_{y3} \\ \sin(t_3 - t_1) & 2(\cos(t_3 - t_1) - 1) & -2\sin(t_3 - t_1) \\ 2(1 - \cos\Delta\tau_3) & 4\sin\Delta\tau_3 - 3\Delta\tau_3 & 4\cos\Delta\tau_3 - 3 \end{bmatrix} \tag{E.78}$$

Now, performing the linear algebra,

$$\begin{bmatrix} \lambda_{x3} \\ \lambda_{y3} \\ \lambda_{\dot{x}3} \\ \lambda_{\dot{y}3} \end{bmatrix} = \frac{1}{D} \begin{bmatrix} -6 - 8\alpha + 2\beta \\ \sin(\Delta\tau_2 + \Delta\tau_3) \\ 0 \\ -4 - 4\alpha + \beta + \cos(\Delta\tau_2 + \Delta\tau_3) \end{bmatrix} \tag{E.79}$$

$$\begin{aligned} D &= -2(\dot{x}_3 + 2u_{yo}) - 4u_{yo}\alpha \\ &\quad + 2(\dot{x}_3 + 2u_{yo})\cos(\Delta\tau_2 + \Delta\tau_3) \\ &\quad - (\dot{y}_3 - 3u_{yo}\Delta\tau_3)\sin(\Delta\tau_2 + \Delta\tau_3) \end{aligned} \tag{E.80}$$

$$\alpha = \cos\Delta\tau_2 - \cos\Delta\tau_3$$

$$\beta = 3\cos(\Delta\tau_2 + \Delta\tau_3) + 3\Delta\tau_3 \sin(\Delta\tau_2 + \Delta\tau_3) \tag{E.81}$$

Subcase III. (Y-X-X)

For this subcase, $\lambda_{\dot{x}3} = 0$, the transversality condition, $\lambda_{\dot{y}1} = 0$, and $\lambda_{\dot{x}2} = 0$ results in,

$$\mathbf{\Lambda}^{III} \begin{bmatrix} \lambda_{x3} \\ \lambda_{y3} \\ \lambda_{\dot{y}3} \end{bmatrix} = \begin{bmatrix} -1 \\ 0 \\ 0 \end{bmatrix} \tag{E.82}$$

where $\mathbf{\Lambda}^{III}$ is

$$\begin{bmatrix} \dot{x}_3 & \dot{y}_3 & -2\dot{x}_3 + u_{y3} \\ 2(1 - \cos(t_3 - t_1)) & 4\sin(t_3 - t_1) - 3(t_3 - t_1) & 4\cos(t_3 - t_1) - 3 \\ \sin\Delta\tau_3 & 2(\cos\Delta\tau_3 - 1) & -2\sin\Delta\tau_3 \end{bmatrix} \tag{E.83}$$

Now, performing the linear algebra,

$$\begin{bmatrix} \lambda_{x3} \\ \lambda_{y3} \\ \lambda_{\dot{x}3} \\ \lambda_{\dot{y}3} \end{bmatrix} = \frac{1}{D} \begin{bmatrix} 6 + 8\alpha - 6\beta \\ -\sin\Delta\tau_3 \\ 0 \\ 4 + 4\alpha - 3\beta - \cos\Delta\tau_3 \end{bmatrix} \tag{E.84}$$

$$\begin{aligned} D &= 2(\dot{x}_3 + 2u_{yo}) - (2\dot{x}_3 + u_{yo})\cos\Delta\tau_3 \\ &\quad +(\dot{y}_3)\sin\Delta\tau_3 + 4u_{yo}\alpha - 3u_{yo}\beta \end{aligned} \tag{E.85}$$

$$\alpha = \cos\Delta\tau_2 - \cos(\Delta\tau_2 + \Delta\tau_3)$$

$$\beta = \cos\Delta\tau_3 + (\Delta\tau_2 + \Delta\tau_3)\sin\Delta\tau_3 \tag{E.86}$$

Subcase IV. (X-X-Y)

For this subcase, $\lambda_{\dot{y}3} = 0$, the transversality condition, $\lambda_{\dot{x}1} = 0$, and $\lambda_{\dot{x}2} = 0$ results in,

$$\mathbf{\Lambda}^{IV} \begin{bmatrix} \lambda_{x3} \\ \lambda_{y3} \\ \lambda_{\dot{x}3} \end{bmatrix} = \begin{bmatrix} -1 \\ 0 \\ 0 \end{bmatrix} \tag{E.87}$$

where $\mathbf{\Lambda}^{IV}$ is

$$\begin{bmatrix} \dot{x}_3 & \dot{y}_3 & 3x_3 + 2\dot{y}_3 + u_{x3} \\ \sin(t_3 - t_1) & 2\left(\cos(t_3 - t_1) - 1\right) & \cos(t_3 - t_1) \\ \sin\Delta\tau_3 & 2\left(\cos\Delta\tau_3 - 1\right) & \cos\Delta\tau_3 \end{bmatrix} \tag{E.88}$$

Now, performing the linear algebra,

$$\begin{bmatrix} \lambda_{x3} \\ \lambda_{y3} \\ \lambda_{\dot{x}3} \\ \lambda_{\dot{y}3} \end{bmatrix} = \frac{1}{D} \begin{bmatrix} 2\alpha \\ \sin\Delta\tau_2 \\ -2\sin\Delta\tau_2 - 2\beta \\ 0 \end{bmatrix} \tag{E.89}$$

$$\begin{aligned} D &= (6x_3 + 3\dot{y}_3 + 2u_{xo})\sin\Delta\tau_2 \\ &\quad -2\dot{x}_3\alpha + 2(3x_3 + 2\dot{y}_3 + u_{xo})\beta \end{aligned} \tag{E.90}$$

$$\alpha = \cos\Delta\tau_3 - \cos(\Delta\tau_2 + \Delta\tau_3)$$

$$\beta = \sin\Delta\tau_3 - \sin(\Delta\tau_2 + \Delta\tau_3) \tag{E.91}$$

E.6 Initial CoState

Once, $\boldsymbol{\lambda}_3$ has been calculated, the calculation of initial costate relies once again on the use of costate transition matrix.

$$\boldsymbol{\lambda}_o = \boldsymbol{\Phi}_\lambda^{-1}(t_3, 0)\boldsymbol{\lambda}_3 \tag{E.92}$$

For the four viable subcases, the initial control pair can be either $+1$ or -1, but not both. This means the initial control options are reduced to two. Therefore, these calculations must be performed twice to ensure the signs correspond to

$$u_{xo} = -sgn\{\lambda_{\dot{x}o}\}U_{max} \tag{E.93a}$$

$$u_{yo} = -sgn\{\lambda_{\dot{y}o}\}U_{max} \tag{E.93b}$$

E.7 $N = 3$ for Stable Orbit to Stable Orbit Maneuver

In this section, a special case of the $N = 3$ case is presented for the problem of maneuvering from one stable and centered orbit to another; a reconfiguration maneuver. The results follow directly from the previous Section E with the conditions

$$a_o = a_f = 0 \qquad b_o = b_f = 0 \tag{E.94}$$

which means $\Delta a = \Delta b = 0$.

E.7.1 Critical Times Calculations. The critical times are now calculated based on the equations developed in the previous section with $\Delta a = \Delta b = 0$.

Equation (E.6) becomes

$$\Delta\tau_4 = -\frac{u_{y3}}{u_{yo}}\left[\Delta\tau_1 + \frac{u_{y1}}{u_{yo}}\Delta\tau_2 + \frac{u_{y2}}{u_{yo}}\Delta\tau_3\right] \tag{E.95}$$

The intermediate results for the four viable subcases of $N = 3$ are summarized in Table E.2 below.

Table E.2 Final Time for four viable subcases of $N = 3$ for stable to stable orbit maneuver.

Subcase	Control Sequence	$t_f = \Delta\tau_1 + \Delta\tau_2 + \Delta\tau_3 + \Delta\tau_4$
I.	Y-X-Y	$t_f = 2\left(\Delta\tau_2 + \Delta\tau_3\right)$
II.	X-Y-X	$t_f = 2\left(\Delta\tau_1 + \Delta\tau_2\right)$
III.	Y-X-X	$t_f = 2\Delta\tau_1$
IV.	X-X-Y	$t_f = 2\Delta\tau_4$

Equation (E.28) with $\Delta a = \Delta b = 0$ becomes

$$\frac{3}{2}\boldsymbol{\Delta T}^T \begin{bmatrix} \frac{u_{y3}}{u_{yo}} - 1 & \frac{u_{y1}}{u_{yo}}\frac{u_{y3}}{u_{yo}} - 1 & \frac{u_{y2}}{u_{yo}}\frac{u_{y3}}{u_{yo}} - 1 \\ \frac{u_{y1}}{u_{yo}}\frac{u_{y3}}{u_{yo}} - 1 & \frac{u_{y3}}{u_{yo}} - \frac{u_{y1}}{u_{yo}} & \frac{u_{y1}}{u_{yo}}\left(\frac{u_{y2}}{u_{yo}}\frac{u_{y3}}{u_{yo}} - 1\right) \\ \frac{u_{y2}}{u_{yo}}\frac{u_{y3}}{u_{yo}} - 1 & \frac{u_{y1}}{u_{yo}}\left(\frac{u_{y2}}{u_{yo}}\frac{u_{y3}}{u_{yo}} - 1\right) & \frac{u_{y3}}{u_{yo}} - \frac{u_{y2}}{u_{yo}} \end{bmatrix} \boldsymbol{\Delta T} + 2\boldsymbol{\Delta T}^T \begin{bmatrix} \left(\frac{u_{x3}}{u_{y3}} - \frac{u_{xo}}{u_{yo}}\right) & \left(\frac{u_{x3}}{u_{y3}}\frac{u_{y1}}{u_{yo}} - \frac{u_{xo}}{u_{yo}}\frac{u_{x1}}{u_{xo}}\right) & \left(\frac{u_{x3}}{u_{y3}}\frac{u_{y2}}{u_{yo}} - \frac{u_{xo}}{u_{yo}}\frac{u_{x2}}{u_{xo}}\right) \end{bmatrix} = 0$$

Details for the intermediate results using these equations for the four subcases of $N = 3$ are as follows:

Subcase I. (Y-X-Y)

$$\frac{3}{2}\boldsymbol{\Delta T}^T \begin{bmatrix} 0 & -2 & -2 \\ -2 & 2 & 2 \\ -2 & 2 & 2 \end{bmatrix} \boldsymbol{\Delta T} - 4\Delta\tau_1 + 4\Delta\tau_3 = 0 \tag{E.96}$$

$$\Delta\tau_1 = \frac{3\left(\Delta\tau_2 + \Delta\tau_3\right)^2 + 4\Delta\tau_3}{6\left(\Delta\tau_2 + \Delta\tau_3\right) + 4} \tag{E.97}$$

$$\Delta\tau_4 = \frac{3\left(\Delta\tau_2 + \Delta\tau_3\right)^2 + 4\Delta\tau_2}{6\left(\Delta\tau_2 + \Delta\tau_3\right) + 4} \tag{E.98}$$

Subcase II. (X-Y-X)

$$\frac{3}{2}\boldsymbol{\Delta T}^T \begin{bmatrix} -2 & -2 & 0 \\ -2 & -2 & 0 \\ 0 & 0 & 0 \end{bmatrix} \boldsymbol{\Delta T} + 4\Delta\tau_1 - 4\Delta\tau_3 = 0 \tag{E.99}$$

$$\Delta\tau_3 = \Delta\tau_1 - \frac{3}{4}\left(\Delta\tau_1 + \Delta\tau_2\right)^2 \tag{E.100}$$

$$\Delta\tau_4 = \Delta\tau_2 + \frac{3}{4}\left(\Delta\tau_1 + \Delta\tau_2\right)^2 \tag{E.101}$$

Subcase III. (Y-X-X)

$$-3\Delta\tau_1^2 - 4\Delta\tau_1 + 4\Delta\tau_3 = 0 \tag{E.102}$$

$$\Delta\tau_3 = \Delta\tau_1 + \frac{3}{4}\Delta\tau_1^2 \tag{E.103}$$

$$\Delta\tau_4 = -\Delta\tau_2 - \frac{3}{4}\Delta\tau_1^2 \tag{E.104}$$

Since all time intervals must be non-negative $\Delta\tau_1 = \Delta\tau_2 = 0$. Consequently, $\Delta\tau_3 = \Delta\tau_4 = 0$. This subcase becomes a non-viable option.

Subcase IV. (X-X-Y)

$$\frac{3}{2}\boldsymbol{\Delta T}^T \begin{bmatrix} -2 & -2 & -2 \\ -2 & -2 & -2 \\ -2 & -2 & -2 \end{bmatrix} \boldsymbol{\Delta T} - 4\left(\Delta\tau_1 + \Delta\tau_3\right) = 0 \tag{E.105}$$

$$\left(\Delta\tau_1 + \Delta\tau_3\right)^2 + \left(\frac{4}{3} + 2\Delta\tau_2\right)\left(\Delta\tau_1 + \Delta\tau_3\right) + \Delta\tau_2^2 = 0 \tag{E.106}$$

$$\Delta\tau_3 = -\Delta\tau_1 - \Delta\tau_2 - \frac{2}{3} + \frac{2}{3}\sqrt{1 + 3\Delta\tau_2} \tag{E.107}$$

$$\Delta\tau_4 = -\frac{2}{3} + \frac{2}{3}\sqrt{1 + 3\Delta\tau_2} \tag{E.108}$$

$$t_f = \Delta\tau_1 + \Delta\tau_2 + \Delta\tau_3 + \Delta\tau_4 = \frac{4}{3}\sqrt{1+3\Delta\tau_2} - \frac{4}{3} \tag{E.109}$$

$$\left(\frac{3}{4}t_f + 1\right)^2 = 1 + 3\Delta\tau_2 \tag{E.110}$$

$$\frac{3}{16}t_f^2 + \frac{1}{2}t_f = \Delta\tau_2 < t_f \tag{E.111}$$

$$t_f < \frac{8}{3} \tag{E.112}$$

Subcase III is also not a viable subcase for stable-to-stable orbit maneuvers reducing viable subcases to three. The results are summarized in Table E.3.

Table E.3 Time intervals for $N = 3$: stable-to-stable orbit maneuver

Subcase	Cntrl Seq.	$\Delta\tau_3$	$\Delta\tau_4$
I.	Y-X-Y	$\Delta\tau_1 - \Delta\tau_2 - \frac{2}{3} + \sqrt{\Delta\tau_1^2 + \frac{4}{3}\Delta\tau_2 + \frac{4}{9}}$	$-\frac{2}{3} + \sqrt{\Delta\tau_1^2 + \frac{4}{3}\Delta\tau_2 + \frac{4}{9}}$
II.[a]	X-Y-X	$\Delta\tau_1 - \frac{3}{4}\left(\Delta\tau_1 + \Delta\tau_2\right)^2$	$\Delta\tau_2 + \frac{3}{4}\left(\Delta\tau_1 + \Delta\tau_2\right)^2$
III.[b]	Y-X-X	$\Delta\tau_1 + \frac{3}{4}\Delta\tau_1^2$	$-\Delta\tau_2 - \frac{3}{4}\Delta\tau_1^2$
IV.[c]	X-X-Y	$-\Delta\tau_1 - \Delta\tau_2 - \frac{2}{3} + \frac{2}{3}\sqrt{1+3\Delta\tau_2}$	$-\frac{2}{3} + \frac{2}{3}\sqrt{1+3\Delta\tau_2}$

[a] $t_f \leq \frac{16}{3}$
[b] $\Delta\tau_1 = \Delta\tau_2 = \Delta\tau_3 = \Delta\tau_4 = t_f = 0$
[c] $t_f < \frac{8}{3}$

Finally, the relative orbit size parameter, $\rho(t)$, and the phase angle parameter, $\theta(t)$, are examined. Closer examination of these two equations show that they do not contain either Δa or Δb. Therefore, the two nonlinear Equations (E.53) and (E.55) remain valid and unchanged. The solution to the critical times will require a simultaneous solution to these two nonlinear equations because they cannot be obtained analytically.

E.7.2 Initial CoState. The calculation of initial costate is identical to the general $N = 3$ case as per Section E.6. However, only three subcases are viable, since as shown, subcases III and V are not viable for the stable-to-stable orbit maneuvers. The Hamiltonian condition remains the same as Equation (E.68). All the equation required

to calculate the costate at t_3 are exactly the same as in Equation (E.69) since Δa and Δb enter implicitly through the critical switching times. The remainder of the analysis is identical to the general $N = 3$ case as shown in Section E.5.

E.7.3 Reconfiguration Example. To illustrate the use of the method developed for in-plane satellite formation control, an example numerical problem is now presented. In this numerical example, the initial relative orbit is both stable and centered and the desired change is only in the relative size; θ_f is not specified. The relative orbit parameters for this example problem is

$$\begin{bmatrix} a_o = 0 \\ b_o = 0 \\ \rho_o = 1.0 \\ \theta_o = 0^o \end{bmatrix} \rightarrow \begin{bmatrix} a_f = 0 \\ b_f = 0 \\ \rho_f = 6.1 \\ \theta(t_f) \end{bmatrix} \tag{E.113}$$

with $U_{max} = 0.5$. The optimal control switch series is that of subcase I (Y-X-Y) with $u_{yo} = -U_{max} = u_{xo}$ and $\Delta\tau_i = \pi/2$. The total maneuver time is exactly one reference orbit long or 2π canonical units of time. Figure E.1 shows the state phase space trajectory of the satellite maneuvering from the circle symbol ($\bigcirc$) on the inner dashed-orbit where $\rho_o = 1$ and $\theta_o = 0^o$ to the diamond symbol ($\Diamond$) on the outer dashed-orbit where $\rho_f = 6.1$ and $\theta_f = 80.5^o$ in a counter-clockwise motion. The control switches occur at each of the delta symbols. In Figure E.2, the velocity costate (solid line) and the normalized optimal controls (dashed-line) are displayed. ($\triangle$). In Figure E.3, the optimality is confirmed by the Hamiltonian remaining zero for the full duration of the maneuver [3]. The initial costate for this problem is $\boldsymbol{\lambda}_o^T = \begin{bmatrix} 1.5 & 0 & 0 & 1 \end{bmatrix}$ which corresponds with the initial control of $u_{xo} = u_{yo} = -U_{max}$.

[3] The y-scale is 1×10^{-16}

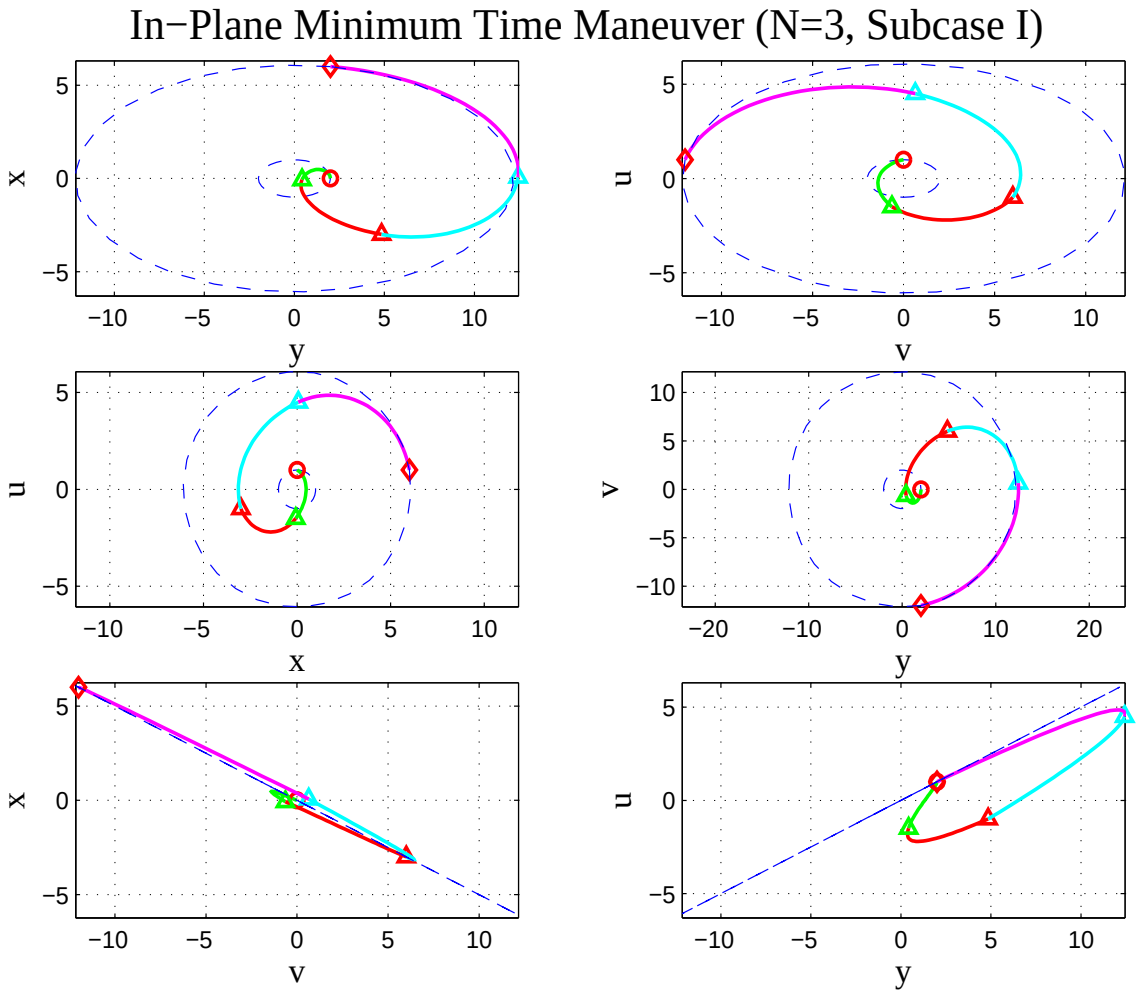

Figure E.1 State-phase space for in-plane minimum-time, Example 1 (N=3) u=$\dot{x}$, v=$\dot{y}$

E.7.4 Phasing Example Problem. In this example problem the initial relative orbit is again both stable and centered and only a phase shift is desired. In Figure E.4, the satellite is maneuvered from the circle symbol (◯) on the dashed-orbit where $\rho_o = 1$ and $\theta_o = 36.87^o$ to the diamond symbol (◊) on the same orbit where $\theta_f = 323.13^o$ in a counter-clockwise motion. The control switches occur at each of the delta symbols (△) with $N = 3$ and (Y-X-Y) series of control changes, i.e., subcase I with $U_{max} = 0.10$.

This was not an optimal maneuver; Hamiltonian was constant (2.0 for this example) during the maneuver, but is not zero. In Figure E.5, the time history of the costate (solid-line) and the normalized control (dashed-line) is shown.

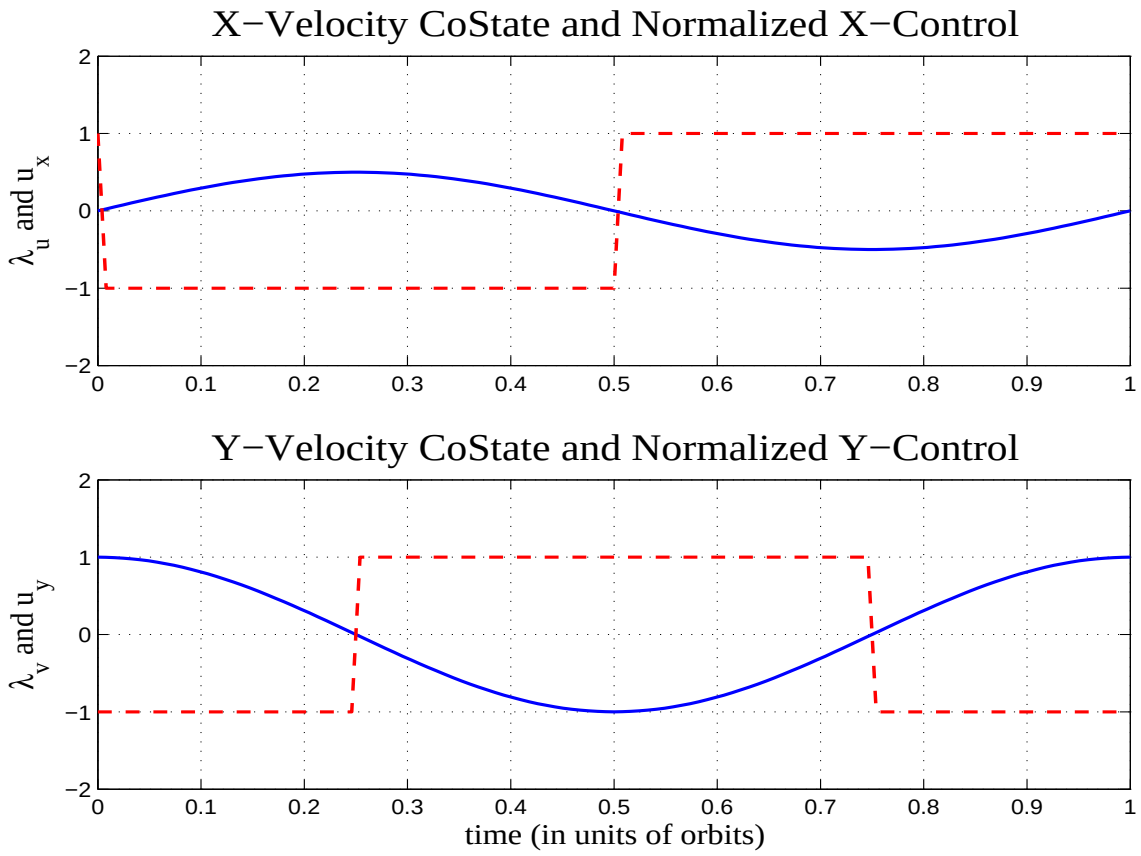

Figure E.2 Costate and normalized optimal control (N=3) $\lambda_u = \lambda_{\dot{x}}$, $\lambda_v = \lambda_{\dot{y}}$

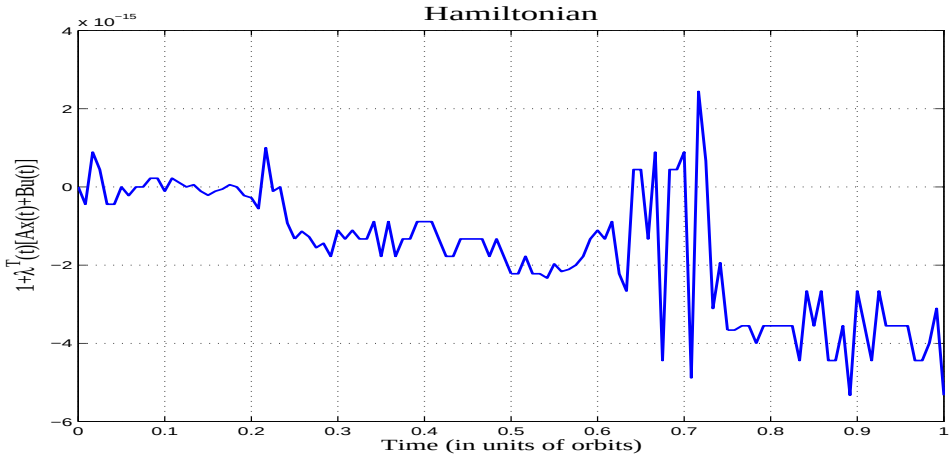

Figure E.3 Hamiltonian time history

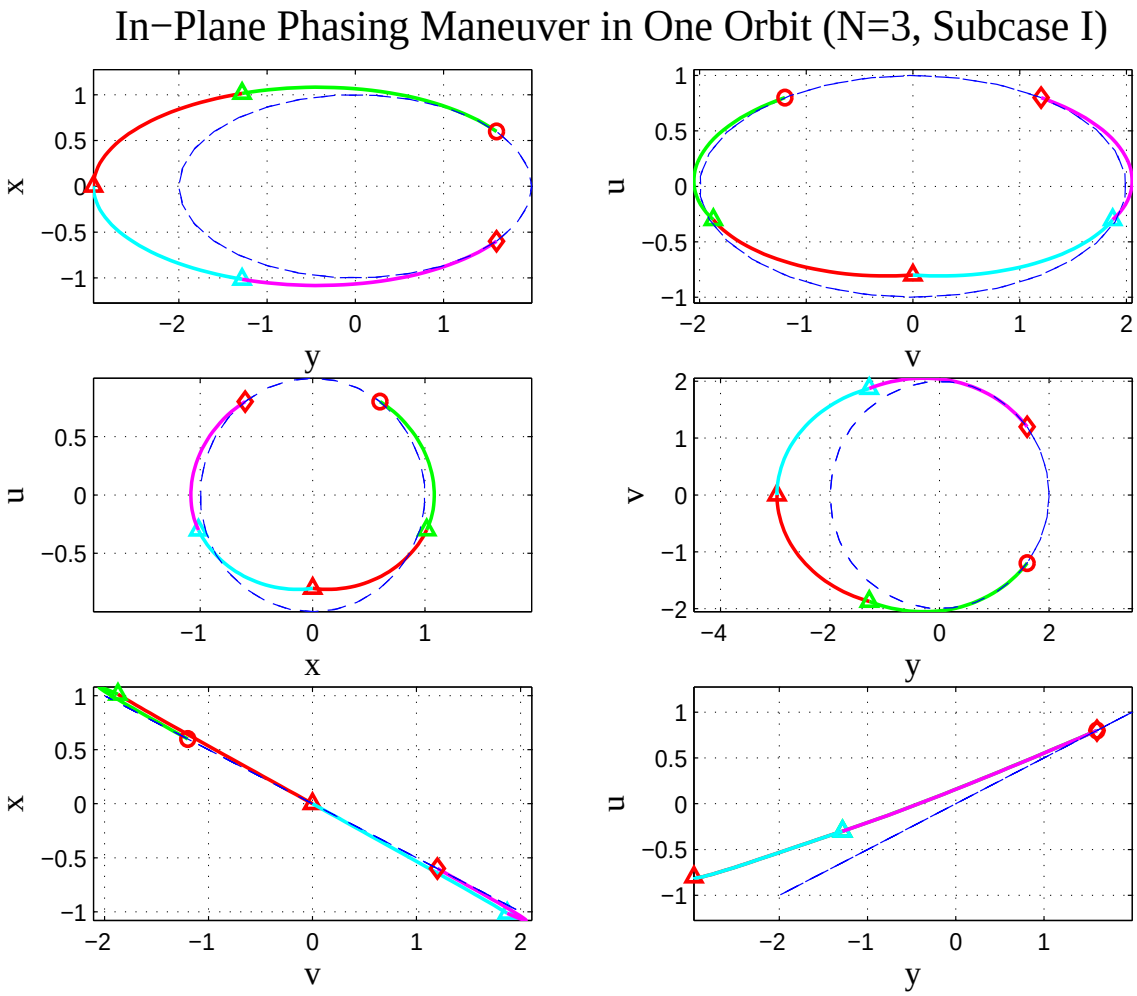

Figure E.4 State-phase space for in-plane minimum-time, Phasing Example (N=3) u=$\dot{x}$, v=$\dot{y}$

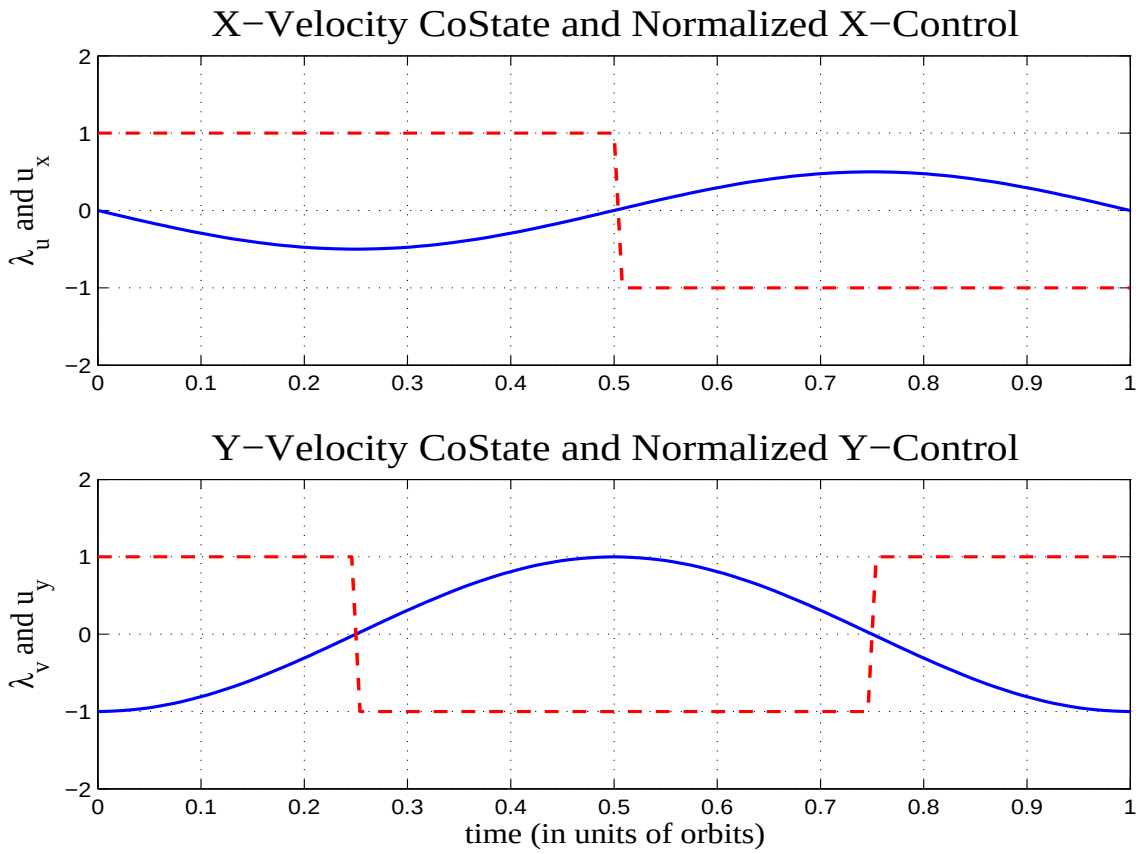

Figure E.5 Costate and normalized control for Phasing Example, (N=3) $\lambda_u = \lambda_{\dot{x}}$, $\lambda_v = \lambda_{\dot{y}}$

Appendix F. The First Order Variation for Minimum Time Problem with Initial Coasting

This appendix develops the first order necessary condition for minimum time problem with initial coasting. The derivation is a well known results from the optimal control theory using calculus of variation.

Performance Index:

$$J = t_f - t_o = \int_{t_o}^{t_f} dt \tag{F.1}$$

Dynamic Constraint:

$$\dot{\mathbf{x}}(t) = \mathbf{A}\mathbf{x}(t) + \mathbf{B}\mathbf{u}(t) \tag{F.2}$$

Corner State Constraint:

$$\boldsymbol{\Theta}(\mathbf{x}(t_c), t_c) = \mathbf{0} \tag{F.3}$$

Terminal State Constraint:

$$\boldsymbol{\Psi}(\mathbf{x}(t_f), t_f) = \mathbf{0} \tag{F.4}$$

Control Constraint:

$$|u_i(t)| \leq U_{max} \qquad i = x, y, z \tag{F.5}$$

Augmenting the Performance Index with constant lagrange multipliers for the corner and terminal state constraints and dynamic lagrange multipliers (also known as the Adjoint or Costate) for the dynamic constraint:

$$\widetilde{J} = \boldsymbol{\mu}^T \boldsymbol{\Theta}(\mathbf{x}(t_c), t_c) + \boldsymbol{\nu}^T \boldsymbol{\Psi}(\mathbf{x}(t_f), t_f) + \int_{t_o}^{t_f} \left(1 + \boldsymbol{\lambda}^T(t) \left[\mathbf{A}\mathbf{x}(t) + \mathbf{B}\mathbf{u}(t) - \dot{\mathbf{x}}(t)\right]\right) dt \tag{F.6}$$

Define the control or variational Hamiltonian: $H(\mathbf{x}(t), \mathbf{u}(t), \boldsymbol{\lambda}(t)) = 1 + \boldsymbol{\lambda}^T(t) \left[\mathbf{A}\mathbf{x}(t) + \mathbf{B}\mathbf{u}(t)\right]$

Then,

$$\widetilde{J} = \boldsymbol{\mu}^T \boldsymbol{\Theta}(\mathbf{x}(t_c), t_c) + \boldsymbol{\nu}^T \boldsymbol{\Psi}(\mathbf{x}(t_f), t_f) + \int_{t_o}^{t_f} \left(H(\mathbf{x}(t), \mathbf{u}(t), \boldsymbol{\lambda}(t))(t) - \boldsymbol{\lambda}^T(t)\dot{\mathbf{x}}(t)\right] dt \tag{F.7}$$

F.1 First Variation

Now, taking the first variation,

$$\begin{aligned}
\delta\widetilde{J} &= \boldsymbol{\mu}^T \frac{\partial \boldsymbol{\Theta}\left(\mathbf{x}(t_c), t_c\right)}{\partial t_c}\delta t_c + \boldsymbol{\mu}^T \frac{\partial \boldsymbol{\Theta}\left(\mathbf{x}(t_c), t_c\right)}{\partial \mathbf{x}(t_c)}\delta \mathbf{x}(t_c) \\
&+\boldsymbol{\nu}^T \frac{\partial \boldsymbol{\Psi}\left(\mathbf{x}(t_f), t_f\right)}{\partial t_f}\delta t_f + \boldsymbol{\nu}^T \frac{\partial \boldsymbol{\Psi}\left(\mathbf{x}(t_f), t_f\right)}{\partial \mathbf{x}(t_f)}\delta \mathbf{x}(t_f) \\
&+ \left[\left(H - \boldsymbol{\lambda}^T(t)\dot{\mathbf{x}}(t)\right)\delta t\right]\Big|_{t_o}^{t_{c-}} + \int_{t_o}^{t_{c-}} \left[\frac{\partial H}{\partial \mathbf{x}(t)}\widetilde{\delta}\mathbf{x}(t) + \frac{\partial H}{\partial \mathbf{u}(t)}\widetilde{\delta}\mathbf{u}(t) - \boldsymbol{\lambda}^T(t)\widetilde{\delta}\dot{\mathbf{x}}(t)\right] dt \\
&+ \left[\left(H - \boldsymbol{\lambda}^T(t)\dot{\mathbf{x}}(t)\right)\delta t\right]\Big|_{t_{c+}}^{t_f} + \int_{t_{c+}}^{t_f} \left[\frac{\partial H}{\partial \mathbf{x}(t)}\widetilde{\delta}\mathbf{x}(t) + \frac{\partial H}{\partial \mathbf{u}(t)}\widetilde{\delta}\mathbf{u}(t) - \boldsymbol{\lambda}^T(t)\widetilde{\delta}\dot{\mathbf{x}}(t)\right] dt
\end{aligned} \tag{F.8}$$

where $\delta(\cdot)$ is a total variation and $\widetilde{\delta}(\cdot)$is a partial variation. Since $\mathbf{x}(t)$ is continuous,

$$\widetilde{\delta}\dot{\mathbf{x}}(t) = \widetilde{\delta}\left(\frac{d\mathbf{x}(t)}{dt}\right) = \frac{d\left(\widetilde{\delta}\mathbf{x}(t)\right)}{dt} \tag{F.9}$$

Now, integrating the last term in the integrals by parts,

$$-\int_{t_o}^{t_{c-}} \boldsymbol{\lambda}^T(t)\widetilde{\delta}\dot{\mathbf{x}}(t)dt = -\int_{t_o}^{t_{c-}} \boldsymbol{\lambda}^T(t)d\left(\widetilde{\delta}\mathbf{x}(t)\right) = -\left[\boldsymbol{\lambda}^T(t)\widetilde{\delta}\mathbf{x}(t)\right]\Big|_{t_o}^{t_{c-}} + \int_{t_o}^{t_{c-}} \dot{\boldsymbol{\lambda}}^T(t)\widetilde{\delta}\mathbf{x}(t)dt \tag{F.10}$$

and we note that $\delta\mathbf{x}(t) = \widetilde{\delta}\mathbf{x}(t) + \dot{\mathbf{x}}(t)\delta t \;\rightarrow\; \widetilde{\delta}\mathbf{x}(t) = \delta\mathbf{x}(t) - \dot{\mathbf{x}}(t)\delta t$. So,

$$\begin{aligned}
-\int_{t_o}^{t_{c-}} \boldsymbol{\lambda}^T(t)\widetilde{\delta}\dot{\mathbf{x}}(t)dt &= -\left[\boldsymbol{\lambda}^T(t)\delta\mathbf{x}(t) - \boldsymbol{\lambda}^T(t)\dot{\mathbf{x}}(t)\delta t\right]\Big|_{t_o}^{t_{c-}} + \int_{t_o}^{t_{c-}} \dot{\boldsymbol{\lambda}}^T(t)\widetilde{\delta}\mathbf{x}(t)dt \\
&= -\left[\boldsymbol{\lambda}^T(t)\delta\mathbf{x}(t)\right]\Big|_{t_o}^{t_{c-}} + \left[\boldsymbol{\lambda}^T(t)\dot{\mathbf{x}}(t)\delta t\right]\Big|_{t_o}^{t_{c-}} + \int_{t_o}^{t_{c-}} \dot{\boldsymbol{\lambda}}^T(t)\widetilde{\delta}\mathbf{x}(t)dt \\
&= -\boldsymbol{\lambda}^T(t_{c-})\delta\mathbf{x}(t_c) + \boldsymbol{\lambda}^T(t_o)\delta t_o + \left[\boldsymbol{\lambda}^T(t)\dot{\mathbf{x}}(t)\right]|_{t_{c-}}\delta t_c - \left[\boldsymbol{\lambda}^T(t)\dot{\mathbf{x}}(t)\right]|_{t_o}\delta t_o \\
&\quad + \int_{t_o}^{t_{c-}} \dot{\boldsymbol{\lambda}}^T(t)\widetilde{\delta}\mathbf{x}(t)dt
\end{aligned} \tag{F.11}$$

where we used $\delta t_{c-} = \delta t_c$ for time is continuous and that $\delta \mathbf{x}(t_{c-}) = \delta \mathbf{x}(t_c)$ also because state is continuous. Similarly for the second integral,

$$\begin{aligned}
-\int_{t_{c+}}^{t_f} \boldsymbol{\lambda}^T(t)\widetilde{\delta}\dot{\mathbf{x}}(t)dt &= -\left[\boldsymbol{\lambda}^T(t)\delta\mathbf{x}(t) - \boldsymbol{\lambda}^T(t)\dot{\mathbf{x}}(t)\delta t\right]|_{t_{c+}}^{t_f} + \int_{t_{c+}}^{t_f} \dot{\boldsymbol{\lambda}}^T(t)\widetilde{\delta}\mathbf{x}(t)dt \\
&= -\left[\boldsymbol{\lambda}^T(t)\delta\mathbf{x}(t)\right]|_{t_{c+}}^{t_f} + \left[\boldsymbol{\lambda}^T(t)\dot{\mathbf{x}}(t)\delta t\right]|_{t_{c+}}^{t_f} + \int_{t_{c+}}^{t_f} \dot{\boldsymbol{\lambda}}^T(t)\widetilde{\delta}\mathbf{x}(t)dt \\
&= -\boldsymbol{\lambda}^T(t_f)\delta\mathbf{x}(t_f) + \boldsymbol{\lambda}^T(t_{c+})\delta t_c + \left[\boldsymbol{\lambda}^T(t)\dot{\mathbf{x}}(t)\right]|_{t_f}\delta t_f - \left[\boldsymbol{\lambda}^T(t)\dot{\mathbf{x}}(t)\right]|_{t_{c+}}\delta t_c \\
&\quad + \int_{t_{c+}}^{t_f} \dot{\boldsymbol{\lambda}}^T(t)\widetilde{\delta}\mathbf{x}(t)dt
\end{aligned} \tag{F.12}$$

where we used $\delta t_{c+} = \delta t_c$ and $\delta \mathbf{x}(t_{c+}) = \delta \mathbf{x}(t_c)$ for the same reasons stated above. The first variation now becomes,

$$\begin{aligned}
\delta\widetilde{J} &= \boldsymbol{\mu}^T\frac{\partial \boldsymbol{\Theta}\left(\mathbf{x}(t_c), t_c\right)}{\partial t_c}\delta t_c + \boldsymbol{\mu}^T\frac{\partial \boldsymbol{\Theta}\left(\mathbf{x}(t_c), t_c\right)}{\partial \mathbf{x}(t_c)}\delta\mathbf{x}(t_c) \\
&\quad + \boldsymbol{\nu}^T\frac{\partial \boldsymbol{\Psi}\left(\mathbf{x}(t_f), t_f\right)}{\partial t_f}\delta t_f + \boldsymbol{\nu}^T\frac{\partial \boldsymbol{\Psi}\left(\mathbf{x}(t_f), t_f\right)}{\partial \mathbf{x}(t_f)}\delta\mathbf{x}(t_f) \\
&\quad + H(t_{c-})\delta t_c - H(t_o)\delta t_o + \int_{t_o}^{t_{c-}} \left[\left(\frac{\partial H}{\partial \mathbf{x}(t)}\widetilde{\delta}\mathbf{x}(t) + \dot{\boldsymbol{\lambda}}^T(t)\right)\widetilde{\delta}\mathbf{x}(t) + \frac{\partial H}{\partial \mathbf{u}(t)}\widetilde{\delta}\mathbf{u}(t)\right]dt \\
&\quad - \boldsymbol{\lambda}^T(t_{c-})\delta\mathbf{x}(t_c) + \boldsymbol{\lambda}^T(t_o)\delta\mathbf{x}(t_o) \\
&\quad + H(t_f)\delta t_f - H(t_{c+})\delta t_c + \int_{t_{c+}}^{t_f} \left[\left(\frac{\partial H}{\partial \mathbf{x}(t)}\widetilde{\delta}\mathbf{x}(t) + \dot{\boldsymbol{\lambda}}^T(t)\right)\widetilde{\delta}\mathbf{x}(t) + \frac{\partial H}{\partial \mathbf{u}(t)}\widetilde{\delta}\mathbf{u}(t)\right]dt \\
&\quad - \boldsymbol{\lambda}^T(t_f)\delta\mathbf{x}(t_f) + \boldsymbol{\lambda}^T(t_{c+})\delta\mathbf{x}(t_c)
\end{aligned} \tag{F.13}$$

We again, have fixed initial time and initial state ($\delta t_o = \delta \mathbf{x}(t_o) = 0$), then

$$\begin{aligned}
\delta \widetilde{J} \;=\; & \left[\boldsymbol{\mu}^T \frac{\partial \boldsymbol{\Theta}\left(\mathbf{x}(t_c), t_c\right)}{\partial t_c} + H(t_{c-}) - H(t_{c+})\right] \delta t_c \\
& + \left[\boldsymbol{\mu}^T \frac{\partial \boldsymbol{\Theta}\left(\mathbf{x}(t_c), t_c\right)}{\partial \mathbf{x}(t_c)} + \boldsymbol{\lambda}^T(t_{c+}) - \boldsymbol{\lambda}^T(t_{c-})\right] \delta \mathbf{x}(t_c) \\
& + \left[\boldsymbol{\nu}^T \frac{\partial \boldsymbol{\Psi}\left(\mathbf{x}(t_f), t_f\right)}{\partial t_f} + H(t_f)\right] \delta t_f \\
& + \left[\boldsymbol{\nu}^T \frac{\partial \boldsymbol{\Psi}\left(\mathbf{x}(t_f), t_f\right)}{\partial \mathbf{x}(t_f)} - \boldsymbol{\lambda}^T(t_f)\right] \delta \mathbf{x}(t_f) \\
& + \int_{t_o}^{t_{c-}} \left[\left(\frac{\partial H}{\partial \mathbf{x}(t)} \widetilde{\delta}\mathbf{x}(t) + \dot{\boldsymbol{\lambda}}^T(t)\right) \widetilde{\delta}\mathbf{x}(t) + \frac{\partial H}{\partial \mathbf{u}(t)} \widetilde{\delta}\mathbf{u}(t)\right] dt \\
& + \int_{t_{c+}}^{t_f} \left[\left(\frac{\partial H}{\partial \mathbf{x}(t)} \widetilde{\delta}\mathbf{x}(t) + \dot{\boldsymbol{\lambda}}^T(t)\right) \widetilde{\delta}\mathbf{x}(t) + \frac{\partial H}{\partial \mathbf{u}(t)} \widetilde{\delta}\mathbf{u}(t)\right] dt
\end{aligned} \tag{F.14}$$

Now we choose the costate such that:

1. Costate/Adjoint Equation

$$\frac{\partial H}{\partial \mathbf{x}(t)} + \dot{\boldsymbol{\lambda}}^T(t) = 0 \qquad \rightarrow \qquad \dot{\boldsymbol{\lambda}}^T(t) = -\frac{\partial H}{\partial \mathbf{x}(t)} = -\boldsymbol{\lambda}^T(t)\mathbf{A} \tag{F.15}$$

   $\forall\ t \in [t_o, t_f]$. However, this does not imply that the costate is continuous at t_c. This equation along with $\dot{\mathbf{x}}(t) = \mathbf{A}\mathbf{x}(t) + \mathbf{B}\mathbf{u}(t)$.

2. Natural Boundary Condition

$$\boldsymbol{\nu}^T \frac{\partial \boldsymbol{\Psi}\left(\mathbf{x}(t_f), t_f\right)}{\partial \mathbf{x}(t_f)} - \boldsymbol{\lambda}^T(t_f) = 0 \qquad \rightarrow \qquad \boldsymbol{\lambda}^T(t_f) = \boldsymbol{\nu}^T \frac{\partial \boldsymbol{\Psi}\left(\mathbf{x}(t_f), t_f\right)}{\partial \mathbf{x}(t_f)} \tag{F.16}$$

3. Optimality Condition

$$\frac{\partial H}{\partial \mathbf{u}(t)} = 0 \qquad \rightarrow \qquad \boldsymbol{\lambda}^T(t)\mathbf{B} = 0 \tag{F.17}$$

$\forall\ t \in [t_o, t_f]$. $\boldsymbol{\lambda}^T(t)\mathbf{B}$ is the switching function for the Bang-Bang controller but is not necessarily continuous at t_c. $\boldsymbol{\lambda}^T(t_i)\mathbf{B} = 0$ where $t_c \leq t_i \leq t_f$ are the control switch times.

4. Transversality Condition

$$\begin{aligned} \boldsymbol{\nu}^T \frac{\partial \boldsymbol{\Psi}\left(\mathbf{x}(t_f), t_f\right)}{\partial t_f} &+ H(t_f) = 0 \\ \boldsymbol{\nu}^T \frac{\partial \boldsymbol{\Psi}\left(\mathbf{x}(t_f), t_f\right)}{\partial t_f} &+ \boldsymbol{\lambda}^T(t_f)\left[\mathbf{A}\mathbf{x}(t_f) + \mathbf{B}\mathbf{u}(t_f)\right] = -1 \end{aligned} \tag{F.18}$$

These are the same necessary conditions that we saw in the problem without the initial coasting. Then, the first variation is reduced to,

$$\begin{aligned} \delta\widetilde{J} \;=\; & \left[\boldsymbol{\mu}^T \frac{\partial \boldsymbol{\Theta}\left(\mathbf{x}(t_c), t_c\right)}{\partial t_c} + H(t_{c-}) - H(t_{c+})\right] \delta t_c \\ & + \left[\boldsymbol{\mu}^T \frac{\partial \boldsymbol{\Theta}\left(\mathbf{x}(t_c), t_c\right)}{\partial \mathbf{x}(t_c)} + \boldsymbol{\lambda}^T(t_{c+}) - \boldsymbol{\lambda}^T(t_{c-})\right] \delta\mathbf{x}(t_c) \end{aligned} \tag{F.19}$$

For an extremum, the first variation must necessarily be zero. The two remaining variations are independent and we must now require these additional necessary conditions:

5. Discontinuity of the Hamiltonian

$$\Delta H(t_c) = H(t_{c+}) - H(t_{c-}) = \boldsymbol{\mu}^T \frac{\partial \boldsymbol{\Theta}\left(\mathbf{x}(t_c), t_c\right)}{\partial t_c} \tag{F.20}$$

6. Discontinuity of Costate

$$\Delta\boldsymbol{\lambda}^T(t_c) = \boldsymbol{\lambda}^T(t_{c+}) - \boldsymbol{\lambda}^T(t_{c-}) = -\boldsymbol{\mu}^T \frac{\partial \boldsymbol{\Theta}\left(\mathbf{x}(t_c), t_c\right)}{\partial \mathbf{x}(t_c)} \tag{F.21}$$

Any control within the admissible set of controls (bounded by U_{max}) that satisfy these six enumerated first order conditions are extremum of this performance index.

Appendix G. The First Order Variation for Minimum Fuel Problem

This appendix describes the first order necessary condition for minimum time problem. The derivation is a well known results from the optimal control theory using calculus of variation.

Performance Index:

$$J = \int_{t_o}^{t_f} |\mathbf{u}(t)| dt \tag{G.1}$$

Dynamic Constraint:

$$\dot{\mathbf{x}}(t) = \mathbf{A}\mathbf{x}(t) + \mathbf{B}\mathbf{u}(t) \tag{G.2}$$

Terminal State Constraint:

$$\mathbf{\Psi}(\mathbf{x}(t_f), t_f) = 0 \tag{G.3}$$

Control Constraint:

$$|u_i(t)| \leq U_{max} \qquad i = x, y, z \tag{G.4}$$

Augmenting the Performance Index with constant lagrange multipliers for the terminal state constraint and dynamic lagrange multipliers (also known as the Adjoint or Costate) for the dynamic constraint:

$$\widetilde{J} = \boldsymbol{\nu}^T \mathbf{\Psi}(\mathbf{x}(t_f), t_f) + \int_{t_o}^{t_f} \left(|\mathbf{u}(t)| + \boldsymbol{\lambda}^T(t) \left[\mathbf{A}\mathbf{x}(t) + \mathbf{B}\mathbf{u}(t) - \dot{\mathbf{x}}(t) \right] \right) dt \tag{G.5}$$

Define the control or variational Hamiltonian: $H(\mathbf{x}(t), \mathbf{u}(t), \boldsymbol{\lambda}(t)) = |u(t)| + \boldsymbol{\lambda}^T(t) \left[\mathbf{A}\mathbf{x}(t) + \mathbf{B}\mathbf{u}(t) \right]$

Then,

$$\widetilde{J} = \boldsymbol{\nu}^T \mathbf{\Psi}(\mathbf{x}(t_f), t_f) + \int_{t_o}^{t_f} \left(H(\mathbf{x}(t), \mathbf{u}(t), \boldsymbol{\lambda}(t))(t) - \boldsymbol{\lambda}^T(t) \dot{\mathbf{x}}(t) \right] dt \tag{G.6}$$

G.1 First Variation

Now, taking the first variation,

$$\begin{aligned}\delta\widetilde{J} &= \boldsymbol{\nu}^T\frac{\partial\boldsymbol{\Psi}\left(\mathbf{x}(t_f),t_f\right)}{\partial t_f}\delta t_f+\boldsymbol{\nu}^T\frac{\partial\boldsymbol{\Psi}\left(\mathbf{x}(t_f),t_f\right)}{\partial\mathbf{x}(t_f)}\delta\mathbf{x}(t_f)+\left[\left(H-\boldsymbol{\lambda}^T(t)\dot{\mathbf{x}}(t)\right)\delta t\right]\Big|_{t_o}^{t_f}\\ &\quad+\int_{t_o}^{t_f}\left[\frac{\partial H}{\partial\mathbf{x}(t)}\widetilde{\delta}\mathbf{x}(t)+\frac{\partial H}{\partial\mathbf{u}(t)}\widetilde{\delta}\mathbf{u}(t)-\boldsymbol{\lambda}^T(t)\widetilde{\delta}\dot{\mathbf{x}}(t)\right]dt \qquad \text{(G.7)}\end{aligned}$$

where $\delta(\cdot)$ is a total variation and $\widetilde{\delta}(\cdot)$is a partial variation. Since $\mathbf{x}(t)$ is continuous,

$$\widetilde{\delta}\dot{\mathbf{x}}(t)=\widetilde{\delta}\left(\frac{d\mathbf{x}(t)}{dt}\right)=\frac{d\left(\widetilde{\delta}\mathbf{x}(t)\right)}{dt} \qquad \text{(G.8)}$$

Now, integrating the last term in the integral by parts,

$$-\int_{t_o}^{t_f}\boldsymbol{\lambda}^T(t)\widetilde{\delta}\dot{\mathbf{x}}(t)dt=-\int_{t_o}^{t_f}\boldsymbol{\lambda}^T(t)d\left(\widetilde{\delta}\mathbf{x}(t)\right)=-\left[\boldsymbol{\lambda}^T(t)\widetilde{\delta}\mathbf{x}(t)\right]\Big|_{t_o}^{t_f}+\int_{t_o}^{t_f}\dot{\boldsymbol{\lambda}}^T(t)\widetilde{\delta}\mathbf{x}(t)dt \qquad \text{(G.9)}$$

and we note that $\delta\mathbf{x}(t)=\widetilde{\delta}\mathbf{x}(t)+\dot{\mathbf{x}}(t)\delta t\ \rightarrow\ \widetilde{\delta}\mathbf{x}(t)=\delta\mathbf{x}(t)-\dot{\mathbf{x}}(t)\delta t$. So,

$$\begin{aligned}-\int_{t_o}^{t_f}\boldsymbol{\lambda}^T(t)\widetilde{\delta}\dot{\mathbf{x}}(t)dt &= -\left[\boldsymbol{\lambda}^T(t)\delta\mathbf{x}(t)-\boldsymbol{\lambda}^T(t)\dot{\mathbf{x}}(t)\delta t\right]\Big|_{t_o}^{t_f}+\int_{t_o}^{t_f}\dot{\boldsymbol{\lambda}}^T(t)\widetilde{\delta}\mathbf{x}(t)dt\\ &= -\left[\boldsymbol{\lambda}^T(t)\delta\mathbf{x}(t)\right]\Big|_{t_o}^{t_f}+\left[\boldsymbol{\lambda}^T(t)\dot{\mathbf{x}}(t)\delta t\right]\Big|_{t_o}^{t_f}+\int_{t_o}^{t_f}\dot{\boldsymbol{\lambda}}^T(t)\widetilde{\delta}\mathbf{x}(t)dt\\ &= -\boldsymbol{\lambda}^T(t_f)\delta\mathbf{x}(t_f)+\boldsymbol{\lambda}^T(t_o)\delta t_o+\left[\boldsymbol{\lambda}^T(t)\dot{\mathbf{x}}(t)\right]\Big|_{t_f}\delta t_f-\left[\boldsymbol{\lambda}^T(t)\dot{\mathbf{x}}(t)\right]\Big|_{t_o}\delta t_o\\ &\quad+\int_{t_o}^{t_f}\dot{\boldsymbol{\lambda}}^T(t)\widetilde{\delta}\mathbf{x}(t)dt \qquad \text{(G.10)}\end{aligned}$$

The first variation now becomes,

$$\begin{aligned}
\delta\widetilde{J} &= \nu\frac{\partial\boldsymbol{\Psi}\left(\mathbf{x}(t_f),t_f\right)}{\partial t_f}\delta t_f + \boldsymbol{\nu}^T\frac{\partial\boldsymbol{\Psi}\left(\mathbf{x}(t_f),t_f\right)}{\partial\mathbf{x}(t_f)}\delta\mathbf{x}(t_f) + \left(H-\boldsymbol{\lambda}^T(t)\dot{\mathbf{x}}(t)\right)|_{t_f}\delta t_f \\
&\quad - \left(H-\boldsymbol{\lambda}^T(t)\dot{\mathbf{x}}(t)\right)|_{t_o}\delta t_o + \int_{t_o}^{t_f}\left[\frac{\partial H}{\partial\mathbf{x}(t)}\widetilde{\delta}\mathbf{x}(t) + \frac{\partial H}{\partial\mathbf{u}(t)}\widetilde{\delta}\mathbf{u}(t)\right]dt \\
&\quad -\boldsymbol{\lambda}^T(t_f)\delta\mathbf{x}(t_f) + \boldsymbol{\lambda}^T(t_o)\delta t_o + \left[\boldsymbol{\lambda}^T(t)\dot{\mathbf{x}}(t)\right]|_{t_f}\delta t_f - \left[\boldsymbol{\lambda}^T(t)\dot{\mathbf{x}}(t)\right]|_{t_o}\delta t_o \\
&\quad + \int_{t_o}^{t_f}\dot{\boldsymbol{\lambda}}^T(t)\widetilde{\delta}\mathbf{x}(t)dt \\
&= \nu\frac{\partial\boldsymbol{\Psi}\left(\mathbf{x}(t_f),t_f\right)}{\partial t_f}\delta t_f + \boldsymbol{\nu}^T\frac{\partial\boldsymbol{\Psi}\left(\mathbf{x}(t_f),t_f\right)}{\partial\mathbf{x}(t_f)}\delta\mathbf{x}(t_f) + (H)|_{t_f}\delta t_f - (H)|_{t_o}\delta t_o \\
&\quad + \int_{t_o}^{t_f}\left[\left(\frac{\partial H}{\partial\mathbf{x}(t)} + \dot{\boldsymbol{\lambda}}^T(t)\right)\widetilde{\delta}\mathbf{x}(t) + \frac{\partial H}{\partial\mathbf{u}(t)}\widetilde{\delta}\mathbf{u}(t)\right]dt \\
&\quad -\boldsymbol{\lambda}^T(t_f)\delta\mathbf{x}(t_f) + \boldsymbol{\lambda}^T(t_o)\delta\mathbf{x}(t_o)
\end{aligned} \tag{G.11}$$

We also have fixed initial time, initial state and the final time ($\delta t_o = \delta\mathbf{x}(t_o) = \delta t_f = 0$), then

$$\begin{aligned}
\delta\widetilde{J} &= +\left[\boldsymbol{\nu}^T\frac{\partial\boldsymbol{\Psi}\left(\mathbf{x}(t_f),t_f\right)}{\partial\mathbf{x}(t_f)} - \boldsymbol{\lambda}^T(t_f)\right]\delta\mathbf{x}(t_f) \\
&\quad + \int_{t_o}^{t_f}\left[\left(\frac{\partial H}{\partial\mathbf{x}(t)} + \dot{\boldsymbol{\lambda}}^T(t)\right)\widetilde{\delta}\mathbf{x}(t) + \frac{\partial H}{\partial\mathbf{u}(t)}\widetilde{\delta}\mathbf{u}(t)\right]dt
\end{aligned} \tag{G.12}$$

Now we choose the costate such that:

1. Costate/Adjoint Equation

$$\frac{\partial H}{\partial\mathbf{x}(t)} + \dot{\boldsymbol{\lambda}}^T(t) = 0 \qquad \rightarrow \qquad \dot{\boldsymbol{\lambda}}^T(t) = -\frac{\partial H}{\partial\mathbf{x}(t)} = -\boldsymbol{\lambda}^T(t)\mathbf{A} \tag{G.13}$$

   This equation along with $\dot{\mathbf{x}}(t) = \mathbf{A}\mathbf{x}(t) + \mathbf{B}\mathbf{u}(t)$ are known as the Euler-Lagrange equations.

2. Natural Boundary Condition

$$\boldsymbol{\nu}^T\frac{\partial\boldsymbol{\Psi}\left(\mathbf{x}(t_f),t_f\right)}{\partial\mathbf{x}(t_f)} - \boldsymbol{\lambda}^T(t_f) = 0 \qquad \rightarrow \qquad \boldsymbol{\lambda}^T(t_f) = \boldsymbol{\nu}^T\frac{\partial\boldsymbol{\Psi}\left(\mathbf{x}(t_f),t_f\right)}{\partial\mathbf{x}(t_f)} \tag{G.14}$$

Then, the first variation is reduced to,

$$\delta\widetilde{J} = \int_{t_o}^{t_f} \frac{\partial H}{\partial \mathbf{u}(t)} \widetilde{\delta}\mathbf{u}(t)dt \tag{G.15}$$

For an extremum, the first variation must necessarily be zero. The final remaining necessary condition is:

3. Optimality Condition

$$\frac{\partial H}{\partial \mathbf{u}(t)} = 0 \qquad \rightarrow \qquad \frac{\partial |\mathbf{u}(t)|}{\partial \mathbf{u}(t)} + \boldsymbol{\lambda}^T(t)\mathbf{B} = 0 \tag{G.16}$$

   Notice this equation does not provide the optimal control directly. We must rely on Pontryagin's Minimum Principle which examined the second variation. The resulting optimal control minimizes the Hamiltonian and leads to a Bang-Off-Bang controller. We shall see that $\boldsymbol{\lambda}^T(t)\mathbf{B}$ is the switching function for the Bang-Bang controller and that $|\boldsymbol{\lambda}^T(t_i)\mathbf{B}| = 1$ where t_i are the control switch times.

Any control within the admissible set of controls (bounded by U_{max}) that satisfy these four enumerated first order conditions are extremum of this performance index.

G.2 Pontryagin's Minimum Principle Summary

A second order strong variation condition is known as the Weirstrauss condition. In Pontryagin's minimum principle, this condition was used, namely that the optimal control will be Hamilton-minimizer:

$$H(\mathbf{x}(t), \mathbf{u}^*(t), \boldsymbol{\lambda}(t)) \leq H(\mathbf{x}(t), \mathbf{u}(t), \boldsymbol{\lambda}(t)) \tag{G.17}$$

where $\mathbf{u}^*(t)$ is the optimal control and $\forall\ \mathbf{u}(t)$ in the admissible set of controls.

$$\begin{aligned} |\mathbf{u}^*(t)| + \boldsymbol{\lambda}^T(t)\left[\mathbf{A}\mathbf{x}(t) + \mathbf{B}\mathbf{u}^*(t)\right] &\leq |\mathbf{u}(t)| + \boldsymbol{\lambda}^T(t)\left[\mathbf{A}\mathbf{x}(t) + \mathbf{B}\mathbf{u}(t)\right] \\ |\mathbf{u}^*(t)| + \boldsymbol{\lambda}^T(t)\mathbf{B}\mathbf{u}^*(t) &\leq |\mathbf{u}(t)| + \boldsymbol{\lambda}^T(t)\mathbf{B}\mathbf{u}(t) \end{aligned} \tag{G.18}$$

The only controls within the admissible control that will make this inequality hold is

$$u_x^*(t) = \begin{cases} -sign\{\lambda_{\dot{x}}(t)\}U_{max} & , \quad |\lambda_{\dot{x}}(t)| > 1 \\ 0 & , \quad |\lambda_{\dot{x}}(t)| < 1 \end{cases} \tag{G.19}$$

with the other two controls being similarly defined.

Appendix H. Optimal Fuel Control of Satellite Formation

The focus of this research was on the minimum time (time-optimal) solution, but the minimum fuel solution is provided in this Appendix. The fuel concern for long term formation is crucial for the mission, but it requires the understanding of the minimum time solution.

For minimum fuel problem with final time unspecified, the minimum fuel control exists, but is not unique. Each different final time will provide a minimum fuel solution. For optimal time minimum fuel problem, the solution is unique. [44] The optimal solution will again be Hamiltonian-minimizing and will result in an on-off-on (or bang-off-bang) controller. In this minimum fuel formulation, the resulting on-off controller introduces coasting-arcs, for a normal problem.[1]

H.1 Minimum-Fuel Optimal Controller

The optimal fuel controller is Hamiltonian-minimizing and is given by,

$$\begin{aligned} u_x^*(t) &= 0 && if\ |\lambda_{\dot{x}}(t)| < 1 \\ u_x^*(t) &= -sgn\{\lambda_{\dot{x}}(t)\}U_{max} && if\ |\lambda_{\dot{x}}(t)| > 1 \\ 0 \le u_x^*(t) &\le U_{max} && if\ \lambda_{\dot{x}}(t) = -1 \\ -U_{max} \le u_x^*(t) &\le 0 && if\ \lambda_{\dot{x}}(t) = +1 \end{aligned} \tag{H.1}$$

with the corresponding control for $u_y^*(t)$ and $u_z^*(t)$. The control Hamiltonian must again satisfy the same canonical Euler-Lagrange equation (the adjoint equation) (2.12). See Appendix G for the details.

As in the minimum time problem, the optimal control minimum fuel is also determined by the last three costates: $\lambda_{\dot{x}}(t)$, $\lambda_{\dot{y}}(t)$, and $\lambda_{\dot{z}}(t)$. The costate dynamics do not

[1] A normal problem is a non-singular problem where the optimal control cannot be determined. The problem under study in this research was normal.

change and Equation (3.12) remains valid for minimum fuel problem. Recall that $\lambda_{\dot{z}}(t)$ is purely sinusoidal and that $\lambda_{\dot{x}}(t)$ has a constant offset and finally $\lambda_{\dot{y}}(t)$ has both an offset and a secular term linear in time. The remainder of this chapter presents the analytical solution for the out-of-plane minimum fuel problem.

H.2 Minimum Fuel Out-of-Plane Motion

For the out-of-plane minimum fuel problem, the costates does not stay at $+1$ or -1 for any open interval of time due to the sinusoidal nature of their solution, i.e., no singular control is optimal. The resulting optimal control will be the normal on-off controller. The coasting arcs ($u_x = u_y = u_z = 0$) will occur in an open interval of time (t_1, t_2), where $|\lambda_{\dot{x}}(t)| < 1, |\lambda_{\dot{y}}(t)| < 1, |\lambda_{\dot{z}}(t)| < 1 \ \forall \ t \in (t_1, t_2)$. For these coasting arcs, the state solution is the classical C-W solution, as shown in Sections 3.1.1 and 3.1.2.

The general dynamic equations for minimum-fuel problem has not changed. All the equations developed during the presentation of the minimum time problem remains valid. The reachable state from any given initial state is a function of both the desired final state and the magnitude of U_{max}. When the final state is specified (i.e. fixed terminal state) along with the fixed terminal time, the solution may not exist. This area needs further investigation and is recommended for future research.

The performance index to be minimized is $J = \int_0^{t_f} |u(t)| dt$, where t_f is now fixed. The initial state is specified by, $\mathbf{x}(t_o) = [z_o \ \dot{z}_o]^T = \mathbf{x}_o$.[2] The terminal state constraints discussion for minimum time in Section 4.1 also remains the same.

Unlike the minimum time problem with open final time, when the final time is specified, there is no transversality condition. However, optimal theory states that the Hamiltonian will be a non-zero constant.

[2]For convenience, the subscript $(\cdot)_z$ is not used in this Appendix.

$$
\begin{aligned}
H(t) = H(t_f) &= C \\
|u_z^*(t)| + \boldsymbol{\lambda}^T(t)\left[\mathbf{A}\mathbf{x}(t) + \mathbf{B}u_z^*(t)\right] &= |u_{zo}^*| + \boldsymbol{\lambda}_o^T\left[\mathbf{A}\mathbf{x}_o + \mathbf{B}u_{zo}^*\right] = C
\end{aligned}
\tag{H.2}
$$

The costate equation and the solution has not changed from those presented for the minimum time problem in Section 3.2. Again, this solution is viewed in the "costate phase-space", where the costate trajectory is a circle centered about the origin as seen in Figure H.1.

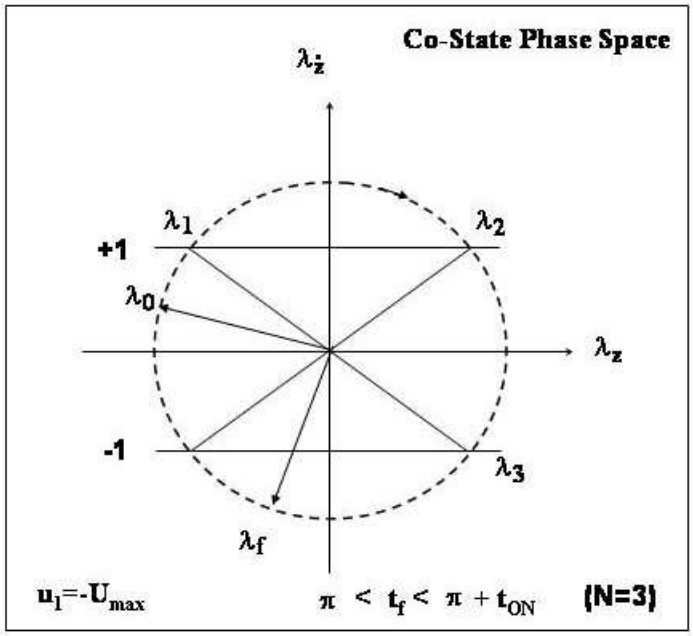

Figure H.1 Out-of-plane costate-phase space diagram .

From the previously developed necessary condition for the minimum fuel problem, the optimal control is zero whenever $|\lambda_{\dot{z}}(t)| < 1$, $+U_{max}$ when $\lambda_{\dot{z}}(t) < 1$ and $-U_{max}$

when $\lambda_{\dot{z}}(t) > 1$ with the switching occurring at $\lambda_{\dot{z}}(t) = \pm 1$. Notice the symmetry of the trajectory and also that the times of "off" (coasting arcs) and times of "on" (burning arcs) add up to π (canonical) units of time. As it was in the minimum time case, the Canonical units were used and the angles on the phase-space is directly proportional to the time; physical time is equal to $t/\omega = \alpha/\omega$, where α is the angle in the phase-space. Also note that $R_\lambda > 1$ for non-trivial solution; i.e., if $R_\lambda \leq 1$, then $u^*(t) = 0 \; \forall t \geq 0$.

It is easier to see here what it means to not specify the final time. A minimum fuel solution may require an infinitesimal burning arc and nearly half-of-an-orbit of coasting with only a small change in the trajectory radius per orbit. In this case the radius of the costate trajectory (R_λ) would approach unity; $R_\lambda = 1 + \epsilon$. On the other hand, if $R_\lambda \to \infty$ then the coasting arcs will approach zero and the solution would approach the solution for the minimum time problem.

Some simple cases were examined to gain understanding of this problem. In the following examples, the final state is assumed reachable with the specified control switches. Also assumed is that final arc is a burning arc; i.e., $u_{zN} \neq 0$. The final assumption for these examples is that the final time is specified a priori.

H.3 Single Arc (No Switching: $N = 0$)

With the final arc assumed a non-coasting arc, $u_{zo} \neq 0$. The radius of the final state, R_{zf}, must be bounded by R_{min} below and R_{max} above. With no coasting arc, the minimum and maximum radii are computed using $t_{on} = \pi$.

$$R_{min}, R_{max} = \sqrt{(-z_o \pm 2U_{max})^2 + \dot{z}_o^2} \tag{H.3}$$

where the sign $\pm U_{max}$ is a function of initial state, $\mathbf{x}_o$. A unique solution is achieved by forcing the final time to equal the burning arc. Then, from the geometry, $\lambda_{\dot{z}_f} = \lambda_{\dot{z}_o} = \pm 1$

$$\cos\left[\frac{1}{2}(t_f)\right] = \frac{1}{R_\lambda} \tag{H.4}$$

and $\lambda_{z_f} = -\lambda_{zo}$.

$$(\lambda_{zo}, \lambda_{\dot{z}_o}) = \begin{cases} (+\sqrt{R_\lambda^2 - 1}, -1) & , u_{zo} = +U_{max} \\ (-\sqrt{R_\lambda^2 - 1}, +1) & , u_{zo} = -U_{max} \end{cases} \tag{H.5}$$

See Figure H.2. By forcing $t_f = t_{on}$ a solution was found, but this also means the initial

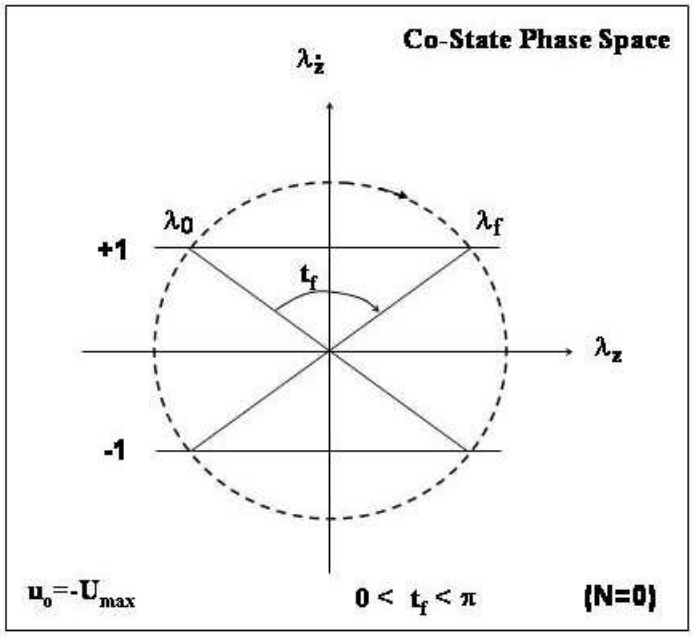

Figure H.2 Out-of-plane costate-phase space diagram for N=0.

costate is not unique. Any initial costate which provides the burning time larger than the specified final time will work.

H.4 Two Arcs, Single Controlled Arc (One Switch: $N = 1$)

In this case the optimal control sequence is $u_z^* = \{0, \pm U_{max}\}$. The maximum (and minimum) radius change occur if an initial coast is followed by a control initiated when

the velocity first reach zero; $\dot{z}(t_m) = 0$, where

$$\tan(t_m) = \frac{\dot{z}_o}{z_o} \tag{H.6}$$

and

$$R_{min}, R_{max} = \sqrt{(R_{zo} - u_{z1})^2 + 2u_{z1}(u_{z1} - R_{zo})\frac{z_o}{R_{zo}} + u_{z1}^2} \tag{H.7}$$

where $u_{z1} = \pm U_{max}$. See Figure H.3.

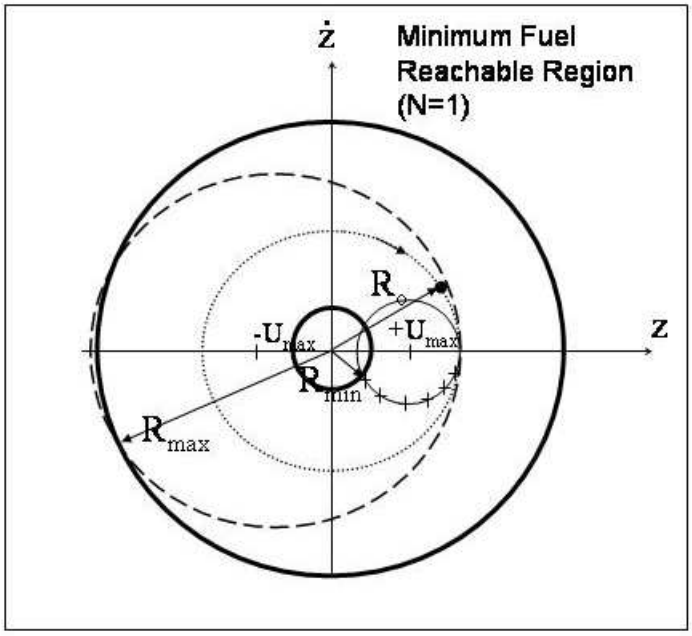

Figure H.3 Out-of-plane reachable region for N=1.

This time there are two options: 1) force $(t_f - t_1) = t_{on}$, or 2) force $t_1 = t_{off}$. See Figure H.4. Again, the initial costate is not unique for this case. In either case, the

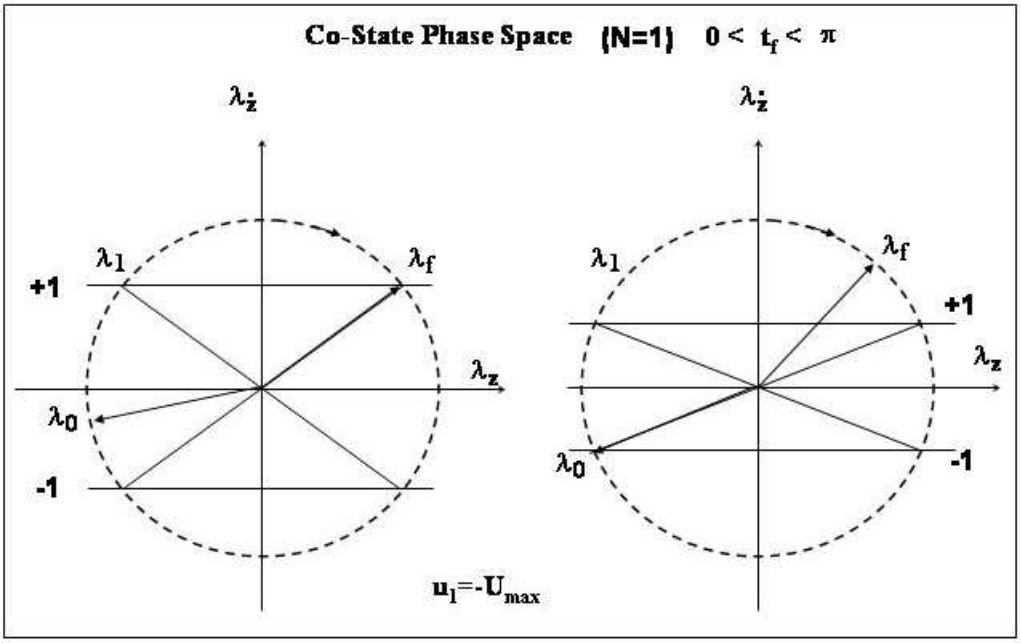

Figure H.4 Out-of-plane costate-phase space diagram for N=1.

switch time t_1 is calculated first. t_1 is solved using the state equation.[3]

$$\begin{aligned}
\mathbf{x}(t_f) &= \mathbf{\Phi}(t_f, t_1)\mathbf{x}_1 + \int_{t_1}^{t_f} \mathbf{\Phi}(t_f, \tau)\mathbf{B}u_1 d\tau \\
&= \mathbf{\Phi}(t_f, t_1)\left[\mathbf{\Phi}(t_1, 0)\mathbf{x}_o\right] + \int_{t_1}^{t_f} \mathbf{\Phi}(t_f, \tau)\mathbf{B}u_1 d\tau \\
&= \mathbf{\Phi}(t_f, 0)\mathbf{x}_o + \int_{t_1}^{t_f} \mathbf{\Phi}(t_f, \tau)\mathbf{B}u_1 d\tau
\end{aligned} \tag{H.8}$$

[3]For the remainder of this Appendix, the subscript $(\cdot)_z$ will be dropped for convenience. All state vector and control will be that of the out-of-plane motion.

performing the integration and some algebra,

$$\mathbf{x}_f - \mathbf{\Phi}(t_f, 0)\mathbf{x}_o = \begin{bmatrix} 1 - \cos(t_f - t_1) \\ \sin(t_f - t_1) \end{bmatrix} u_1 \tag{H.9}$$

writing out the left side more explicitly,

$$\begin{bmatrix} z_f \\ \dot{z}_f \end{bmatrix} - \begin{bmatrix} \cos(t_f) & \sin(t_f) \\ -\sin(t_f) & \cos(t_f) \end{bmatrix} \begin{bmatrix} z_o \\ \dot{z}_o \end{bmatrix} - \begin{bmatrix} u_1 \\ 0 \end{bmatrix} = \begin{bmatrix} -\cos(t_f - t_1) \\ \sin(t_f - t_1) \end{bmatrix} u_1 \tag{H.10}$$

Now $t_f - t_1$ can be solved,

$$\cos(t_f - t_1) = \frac{1}{u_1}(z_o \cos(t_f) + \dot{z}_o \sin(t_f) + u_1 - z_f) \tag{H.11}$$

and since t_f is given,

$$t_1 = t_f - (t_f - t_1) \tag{H.12}$$

By setting $(t_f - t_1) = t_{on}$,

$$\cos\left[\frac{1}{2}(t_f - t_1)\right] = \frac{1}{R_\lambda} \tag{H.13}$$

By setting $t_1 = t_{off}$,

$$\sin\left[\frac{1}{2}(t_1)\right] = \frac{1}{R_\lambda} \tag{H.14}$$

Now, t_1 and R_λ are known.

$$(\lambda_{z1}, \lambda_{\dot{z}_1}) = \begin{cases} (+\sqrt{R_\lambda^2 - 1}, -1) & , u_1 = +U_{max} \\ (-\sqrt{R_\lambda^2 - 1}, +1) & , u_1 = -U_{max} \end{cases} \tag{H.15}$$

Then, the initial costate is solved by:

$$\boldsymbol{\lambda}_o = \mathbf{\Phi}^{-1}(t_1, 0)\boldsymbol{\lambda}_1 \tag{H.16}$$

where $\boldsymbol{\lambda}_1 = [\lambda_{z1}\ \lambda_{\dot{z}1}]^T$.

H.5 Three Arcs, Single Coasting Arc (Two Switch: $N = 2$)

Now the optimal control sequence is $u^* = \{\pm U_{max}, 0, \mp U_{max}\}$. In this case, there is no longer an option of choosing when the first switch or the final switch occurs. The solution requires that $(t_2 - t_1) = t_{off}$. See Figure H.5. Now, both switching times, t_1

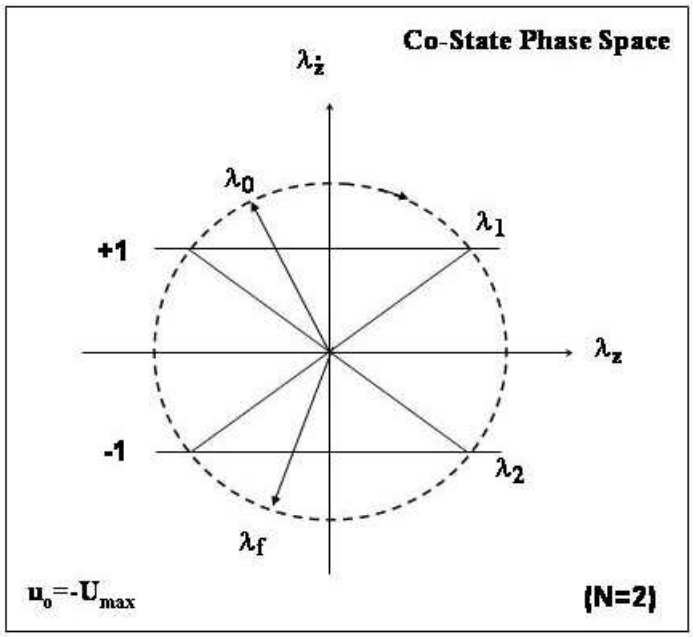

Figure H.5 Out-of-plane costate-phase space diagram for N=2.

and t_2, need to be calculated. Using the state solution again,

$$\begin{aligned} \mathbf{x}_f &= \mathbf{\Phi}(t_f, t_2)\mathbf{x}_2 + \int_{t_2}^{t_f} \mathbf{\Phi}(t_f, \tau)\mathbf{B}u_2 d\tau \\ \mathbf{x}_2 &= \mathbf{\Phi}(t_2, t_1)\mathbf{x}_1 \\ \mathbf{x}_1 &= \mathbf{\Phi}(t_1, 0)\mathbf{x}_o + \int_0^{t_1} \mathbf{\Phi}(t_1, \tau)\mathbf{B}u_o d\tau \end{aligned} \tag{H.17}$$

$$
\begin{aligned}
\mathbf{x}_f &= \mathbf{\Phi}(t_f,0)\mathbf{x}_o + \int_0^{t_1} \mathbf{\Phi}(t_f,\tau)\mathbf{B}u_o d\tau - \int_{t_2}^{t_f} \mathbf{\Phi}(t_f,\tau)\mathbf{B}u_o d\tau \\
&= \mathbf{\Phi}(t_f,0)\mathbf{x}_o + u_o \left\{ \begin{bmatrix} \cos(t_f - t_1) - \cos(t_f) \\ -\sin(t_f - t_1) + \sin(t_f) \end{bmatrix} - \begin{bmatrix} 1 - \cos(t_f - t_2) \\ \sin(t_f - t_2) \end{bmatrix} \right\} \\
&= \mathbf{\Phi}(t_f,0)\mathbf{x}_o - u_o \begin{bmatrix} 1 + \cos(t_f) \\ -\sin(t_f) \end{bmatrix} + u_o \begin{bmatrix} \cos(t_f - t_1) + \cos(t_f - t_2) \\ -\sin(t_f - t_1) - \sin(t_f - t_2) \end{bmatrix} \qquad \text{(H.18)}
\end{aligned}
$$

Using trigonometric identities and performing algebraic manipulations,

$$
\mathbf{x}_f - \mathbf{\Phi}(t_f,0)\mathbf{x}_o + u_o \begin{bmatrix} 1 + \cos(t_f) \\ -\sin(t_f) \end{bmatrix} = u_o \begin{bmatrix} \cos(t_f) & \sin(t_f) \\ -\sin(t_f) & \cos(t_f) \end{bmatrix} \begin{bmatrix} \cos(t_1) + \cos(t_2) \\ \sin(t_1) + \sin(t_2) \end{bmatrix}
$$

Notice the leading matrix on the right-side is $\Phi(t_f, 0)$. Multiplying by the inverse,

$$
\frac{\mathbf{\Phi}^{-1}(t_f,0)}{u_o} \left[\mathbf{x}_f - \mathbf{\Phi}(t_f,0)\mathbf{x}_o + u_o \begin{bmatrix} 1 + \cos(t_f) \\ -\sin(t_f) \end{bmatrix} \right] = \begin{bmatrix} \cos(t_1) + \cos(t_2) \\ \sin(t_1) + \sin(t_2) \end{bmatrix} \qquad \text{(H.19)}
$$

where everything on the left-side are known. Let the left side be called a constant vector with elements a_2 and b_2; $[a_2\ b_2]^T$. The solutions for this set of two equations and two unknowns are given in terms of the two constants,

$$
\cos(t_1) = \frac{1}{2}\left(a_2 \mp b_2 \sqrt{\frac{4}{a_2^2 + b_2^2} - 1} \right) \qquad \text{(H.20)}
$$

$$
\cos(t_2) = \frac{1}{2}\left(a_2 \pm b_2 \sqrt{\frac{4}{a_2^2 + b_2^2} - 1} \right) \qquad \text{(H.21)}
$$

The signs are chosen such that $t_2 > t_1 > 0$.

With the knowledge of these two switching times, $t_{off} = t_2 - t_1$, R_λ can be found.

$$
\sin\left[\frac{1}{2}(t_2 - t_1) \right] = \frac{1}{R_\lambda} \qquad \text{(H.22)}
$$

Now that R_λ is known, the costate at t_2 is easily found,

$$\boldsymbol{\lambda}_2 = \begin{cases} (+\sqrt{R_\lambda^2 - 1}, -1) & , u_2 = +U_{max} \\ (-\sqrt{R_\lambda^2 - 1}, +1) & , u_2 = -U_{max} \end{cases} \tag{H.23}$$

Finally, the initial costate is provided by

$$\boldsymbol{\lambda}_o = \boldsymbol{\Phi}^{-1}(t_2, 0)\boldsymbol{\lambda}_2 \tag{H.24}$$

H.6 Four Arcs, Two Coasting Arcs(Three Switch: $N = 3$)

Now the optimal control sequence is $u^* = \{0, \pm U_{max}, 0, \mp U_{max}\}$. Since the coasting and burning arcs must add up to π; i.e., $t_{on} + t_{off} = \pi$. Furthermore,

$$\begin{aligned} (t_2 - t_1) &= t_{on} \\ (t_3 - t_2) &= t_{off} \\ (t_3 - t_1) &= \pi \end{aligned} \tag{H.25}$$

Using the state solution again,

$$\begin{aligned} \mathbf{x}_1 &= \boldsymbol{\Phi}(t_1, 0)\mathbf{x}_o + \int_0^{t_1} \boldsymbol{\Phi}(t_1, \tau)\mathbf{B}u_o d\tau = \boldsymbol{\Phi}(t_1, 0)\mathbf{x}_o \\ \mathbf{x}_2 &= \boldsymbol{\Phi}(t_2, t_1)\mathbf{x}_1 + \int_{t_1}^{t_2} \boldsymbol{\Phi}(t_2, \tau)\mathbf{B}u_1 d\tau \\ &= \boldsymbol{\Phi}(t_2, 0)\mathbf{x}_o + \int_{t_1}^{t_2} \boldsymbol{\Phi}(t_2, \tau)\mathbf{B}u_1 d\tau \\ \mathbf{x}_3 &= \boldsymbol{\Phi}(t_3, t_2)\mathbf{x}_2 = \boldsymbol{\Phi}(t_3, 0)\mathbf{x}_o + \int_{t_1}^{t_2} \boldsymbol{\Phi}(t_3, \tau)\mathbf{B}u_1 d\tau \\ \mathbf{x}_f &= \boldsymbol{\Phi}(t_f, t_3)\mathbf{x}_3 + \int_{t_3}^{t_f} \boldsymbol{\Phi}(t_f, \tau)\mathbf{B}u_3 d\tau \\ &= \boldsymbol{\Phi}(t_f, 0)\mathbf{x}_o + \int_{t_1}^{t_2} \boldsymbol{\Phi}(t_f, \tau)\mathbf{B}u_1 d\tau + \int_{t_3}^{t_f} \boldsymbol{\Phi}(t_f, \tau)\mathbf{B}u_3 d\tau \end{aligned} \tag{H.26}$$

substituting $u_3 = -u_1$ and carrying out the integration,

$$\mathbf{x}_f = \mathbf{\Phi}(t_f, 0)\mathbf{x}_o + u_1 \left\{ \begin{bmatrix} \cos(t_f - t_2) - \cos(t_f - t_1) \\ -\sin(t_f - t_2) + \sin(t_f - t_1) \end{bmatrix} - \begin{bmatrix} 1 - \cos(t_f - t_3) \\ \sin(t_f - t_3) \end{bmatrix} \right\} \quad \text{(H.27)}$$

becomes after substituting $t_3 = t_1 + \pi$ and expanding using trigonometric identities,

$$\begin{aligned} \mathbf{x}_f - \mathbf{\Phi}(t_f, 0)\mathbf{x}0 + u_1 \begin{bmatrix} 1 + \cos(t_f) \\ -\sin(t_f) \end{bmatrix} & \\ = \quad u_1 \begin{bmatrix} \cos(t_f) & \sin(t_f) \\ -\sin(t_f) & \cos(t_f) \end{bmatrix} \begin{bmatrix} \cos(t_2) - 2\cos(t_1) \\ \sin(t_2) - 2\sin(t_1) \end{bmatrix} & \quad \text{(H.28)} \end{aligned}$$

As it was in the $N = 2$ case, the first matrix on the right hand side is $\Phi(t_f, 0)$. Multiplying by the inverse,

$$\frac{\mathbf{\Phi}^{-1}(t_f, 0)}{u_1} \left(\mathbf{x}_f - \mathbf{\Phi}(t_f, 0)\mathbf{x}0 + u_1 \begin{bmatrix} 1 + \cos(t_f) \\ -\sin(t_f) \end{bmatrix} \right) = \begin{bmatrix} \cos(t_2) - 2\cos(t_1) \\ \sin(t_2) - 2\sin(t_1) \end{bmatrix} \quad \text{(H.29)}$$

Once again everything on the left hand side are known. Labelling the left constant vector as $[a_3 \; b_3]^T$, the two switching times can be found from

$$\begin{bmatrix} a_3 \\ b_3 \end{bmatrix} = \begin{bmatrix} \cos(t_2) - 2\cos(t_1) \\ \sin(t_2) - 2\sin(t_1) \end{bmatrix} \quad \text{(H.30)}$$

More explicitly,

$$\begin{aligned} \cos(t_1) &= \frac{1}{4}\left[a_3 \left(\frac{-3}{a_3^2 + b_3^2} - 1 \right) \mp \frac{b_3}{2} \sqrt{\frac{-9}{(a_3^2 + b_3^2)^2} + \frac{10}{a_3^2 + b_3^2} - 1} \right] \\ \cos(t_2) &= \frac{1}{4}\left[a_3 \left(\frac{-3}{a_3^2 + b_3^2} + 1 \right) \pm \frac{b_3}{2} \sqrt{\frac{-9}{(a_3^2 + b_3^2)^2} + \frac{10}{a_3^2 + b_3^2} - 1} \right] \end{aligned}$$

The signs are chosen such that $t_2 > t_1 > 0$. With the first two switching times known, the final switching time is easily calculated by Equation (H.25). The costate radius, R_λ is using either of the two equivalent ways,

$$\cos\left[\frac{1}{2}(t_2 - t_1)\right] = \frac{1}{R_\lambda} \tag{H.31}$$

$$\sin\left[\frac{1}{2}(t_3 - t_2)\right] = \frac{1}{R_\lambda} \tag{H.32}$$

$$\tag{H.33}$$

Now that R_λ is known, the costate at t_3 is easily found,

$$\boldsymbol{\lambda}_3 = \begin{cases} (+\sqrt{R_\lambda^2 - 1}, -1) & , u_3 = +U_{max} \\ (-\sqrt{R_\lambda^2 - 1}, +1) & , u_3 = -U_{max} \end{cases} \tag{H.34}$$

See Figure H.6. Finally, the initial costate is provided by

$$\boldsymbol{\lambda}_o = \boldsymbol{\Phi}^{-1}(t_3, 0)\boldsymbol{\lambda}_3 \tag{H.35}$$

H.7 Five Arcs, Two Coasting Arcs (Four Switch: $N = 4$)

Now the optimal control sequence is $u^* = \{\pm U_{max}, 0, \mp U_{max}, 0, \pm U_{max}\}$. Again, the coasting and burning arcs must add up to π; i.e., $t_{on} + t_{off} = \pi$. Furthermore,

$$\begin{aligned} (t_2 - t_1) &= (t_4 - t_3) = t_{off} \\ (t_3 - t_2) &= t_{on} \\ (t_3 - t_1) &= (t_4 - t_2) = \pi \end{aligned} \tag{H.36}$$

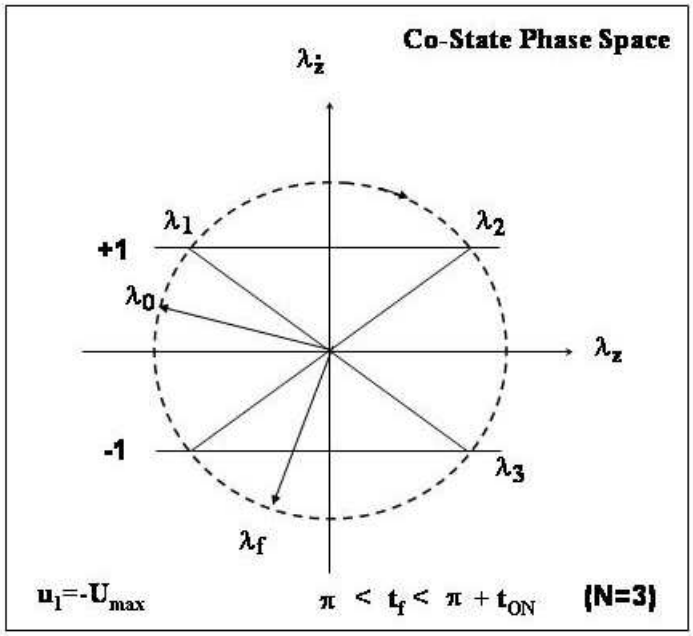

Figure H.6 Out-of-plane costate-phase space diagram for N=3 .

Using the state solution again,

$$\begin{aligned}
\mathbf{x}_1 &= \mathbf{\Phi}(t_1,0)\mathbf{x}_o + \int_0^{t_1} \mathbf{\Phi}(t_1,\tau)\mathbf{B}u_o d\tau \\
\mathbf{x}_2 &= \mathbf{\Phi}(t_2,t_1)\mathbf{x}_1 + \int_{t_1}^{t_2} \mathbf{\Phi}(t_2,\tau)\mathbf{B}u_1 d\tau = \mathbf{\Phi}(t_2,t_1)\mathbf{x}_1 \\
\mathbf{x}_3 &= \mathbf{\Phi}(t_3,t_2)\mathbf{x}_2 + \int_{t_2}^{t_3} \mathbf{\Phi}(t_3,\tau)\mathbf{B}u_2 d\tau \\
\mathbf{x}_4 &= \mathbf{\Phi}(t_4,t_3)\mathbf{x}_3 + \int_{t_3}^{t_4} \mathbf{\Phi}(t_4,\tau)\mathbf{B}u_3 d\tau = \mathbf{\Phi}(t_4,t_3)\mathbf{x}_3 \\
\mathbf{x}_f &= \mathbf{\Phi}(t_f,t_4)\mathbf{x}_4 + \int_{t_4}^{t_f} \mathbf{\Phi}(t_f,\tau)\mathbf{B}u_4 d\tau
\end{aligned} \tag{H.37}$$

substituting $u_1 = u_3 = 0$, $u_2 = -u_o$, $u_4 = u_o$ and carrying out the integration,

$$\begin{aligned}
\mathbf{x}_f &= \mathbf{\Phi}(t_f, 0)\mathbf{x}_o \\
&+ u_o \begin{bmatrix} \cos(t_f - t_1) - \cos(t_f) \\ -\sin(t_f - t_1) + \sin(t_f) \end{bmatrix} \\
&- u_o \begin{bmatrix} \cos(t_f - t_3) - \cos(t_f - t_2)) \\ -\sin(t_f - t_3) + \sin(t_f - t_2) \end{bmatrix} \\
&+ u_o \begin{bmatrix} 1 - \cos(t_f - t_4) \\ \sin(t_f - t_4) \end{bmatrix}
\end{aligned} \tag{H.38}$$

becomes after substituting $t_3 = t_1 + \pi$, $t_4 = t_2 + \pi$ and expanding using trigonometric identities,

$$\begin{aligned}
&\mathbf{x}_f - \mathbf{\Phi}(t_f, 0)\mathbf{x}_o - u_o \begin{bmatrix} 1 - \cos(t_f) \\ +\sin(t_f) \end{bmatrix} \\
= \; & u_o \begin{bmatrix} \cos(t_f) & \sin(t_f) \\ -\sin(t_f) & \cos(t_f) \end{bmatrix} \begin{bmatrix} 2\cos(t_2) + 2\cos(t_1) \\ 2\sin(t_2) + 2\sin(t_1) \end{bmatrix}
\end{aligned} \tag{H.39}$$

As it was in the $N = 2$ and $N = 3$ cases, the first matrix on the right hand side is $\Phi(t_f, 0)$. Multiplying by the inverse,

$$\frac{\mathbf{\Phi}^{-1}(t_f, 0)}{2u_o} \left(\mathbf{x}_f - \mathbf{\Phi}(t_f, 0)\mathbf{x}0 - u_o \begin{bmatrix} 1 - \cos(t_f) \\ \sin(t_f) \end{bmatrix} \right) = \begin{bmatrix} \cos(t_1) + \cos(t_2) \\ \sin(t_1) + \sin(t_2) \end{bmatrix} \tag{H.40}$$

Once again everything on the left hand side are known. Labelling the left constant vector as $[a_4 \; b_4]^T$, the two switching times can be found from

$$\begin{bmatrix} a_4 \\ b_4 \end{bmatrix} = \begin{bmatrix} \cos(t_1) + \cos(t_2) \\ \sin(t_1) + \sin(t_2) \end{bmatrix} \tag{H.41}$$

More explicitly,

$$\cos(t_1) = \frac{1}{2}\left[a_4 \mp b_4\sqrt{\frac{4}{a_4^2+b_4^2}-1}\right] \tag{H.42}$$

$$\cos(t_2) = \frac{1}{2}\left[a_4 \pm b_4\sqrt{\frac{4}{a_4^2+b_4^2}-1}\right] \tag{H.43}$$

The signs are chosen such that $t_2 > t_1 > 0$. With the first two switching times known, the third and fourth switching times are easily calculated by Equation (H.36). The costate radius, R_λ is using either of the three equivalent ways,

$$\sin\left[\frac{1}{2}(t_2-t_1)\right] = \frac{1}{R_\lambda} = \sin\left[\frac{1}{2}(t_4-t_3)\right] \tag{H.44}$$

$$\cos\left[\frac{1}{2}(t_3-t_2)\right] = \frac{1}{R_\lambda} \tag{H.45}$$

$$\tag{H.46}$$

See Figure H.7. Now that R_λ is known, the costate at t_4 is easily found,

$$\boldsymbol{\lambda}_4 = \begin{cases} (+\sqrt{R_\lambda^2-1}, -1) & , u_4 = +U_{max} \\ (-\sqrt{R_\lambda^2-1}, +1) & , u_4 = -U_{max} \end{cases} \tag{H.47}$$

Finally, the initial costate is provided by

$$\boldsymbol{\lambda}_o = \boldsymbol{\Phi}^{-1}(t_4, 0)\boldsymbol{\lambda}_4 \tag{H.48}$$

H.8 General Case (N Switches)

In general, the first two switching times (in addition to the specified final time) will be required for cases with $N \geq 2$. These two switching times are derived from the solution to the state (dynamic) equation. This can be accomplished since all switching times after the second switch are a function of the first two switching times; i.e., $t_3 = t_1 + \pi$, and

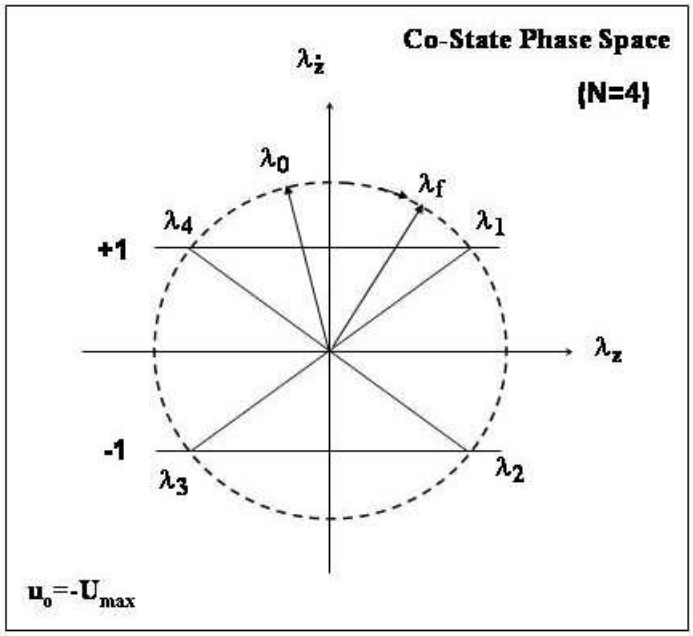

Figure H.7 Out-of-plane costate-phase space diagram for N=4.

$t_4 = t_2 + \pi$, etc. The analytic state solution is

$$\begin{aligned}
\mathbf{x}_f &= \mathbf{\Phi}(t_f,0)\mathbf{x}_o + \int_0^{t_f} \mathbf{\Phi}(t_f,\tau)\mathbf{B}u(\tau)d\tau \\
&= \mathbf{\Phi}(t_f,0)\mathbf{x}_o + \int_0^{t_1} \mathbf{\Phi}(t_f,\tau)\mathbf{B}d\tau u_o + \int_{t_N}^{t_f} \mathbf{\Phi}(t_f,\tau)\mathbf{B}d\tau u_N \\
&+ \sum_{i=1}^{N-1} \int_{t_i}^{t_i+1} \mathbf{\Phi}(t_f,\tau)\mathbf{B}d\tau u_i \\
&= \mathbf{\Phi}(t_f,0)\mathbf{x}_o + \begin{bmatrix} \cos(t_f - t_1) - \cos(t_f) \\ -\sin(t_f - t_1) + \sin(t_f) \end{bmatrix} u_o + \begin{bmatrix} 1 - \cos(t_f - t_N) \\ \sin(t_f - t_N) \end{bmatrix} u_N \\
&+ \sum_{i=1}^{N-1} \begin{bmatrix} \cos(t_f - t_{i+1}) - \cos(t_f - t_i) \\ -\sin(t_f - t_{i+1}) + \sin(t_f - t_i) \end{bmatrix} u_i
\end{aligned} \tag{H.49}$$

The integration can be carried out when u_i is expressed in terms of u_N. The solutions can be broken into two separate cases; one for when N is even and the other when N is odd.

(N is EVEN, N $\geq$ 2)

$$\begin{aligned} & \frac{\mathbf{x}_f - \mathbf{\Phi}(t_f, 0)\mathbf{x}_o}{u_N} - \begin{bmatrix} 1 \\ 0 \end{bmatrix} + \begin{bmatrix} (-1)^{\frac{N}{2}-1} & 0 \\ 0 & (-1)^{\frac{N}{2}} \end{bmatrix} \begin{bmatrix} \cos(t_f) \\ \sin(t_f) \end{bmatrix} \\ = & \frac{N}{2} \begin{bmatrix} (-1)^{\frac{N}{2}} & 0 \\ 0 & (-1)^{\frac{N}{2}-1} \end{bmatrix} \begin{bmatrix} \cos(t_f - t_1) + \cos(t_f - t_2) \\ \sin(t_f - t_1) + \sin(t_f - t_2) \end{bmatrix} \end{aligned} \tag{H.50}$$

where the first matrix on the right side of the equation has an inverse equal to itself.

$$\begin{bmatrix} (-1)^{\frac{N}{2}} & 0 \\ 0 & (-1)^{\frac{N}{2}-1} \end{bmatrix}^{-1} = \begin{bmatrix} (-1)^{\frac{N}{2}} & 0 \\ 0 & (-1)^{\frac{N}{2}-1} \end{bmatrix} \tag{H.51}$$

Now, multiplying both sides by this inverse, we can isolate all the known values to the left side. If we call the left side $[a_N^{'}\ b_N^{'}]^T$,

$$\begin{bmatrix} a_N^{'} \\ b_N^{'} \end{bmatrix} = \frac{2}{N} \begin{bmatrix} (-1)^{\frac{N}{2}} & 0 \\ 0 & (-1)^{\frac{N}{2}-1} \end{bmatrix} \left\{ \frac{\mathbf{x}_f - \mathbf{\Phi}(t_f, 0)\mathbf{x}_o}{u_N} - \begin{bmatrix} 1 + (-1)^{\frac{N}{2}-1} \cos(t_f) \\ (-1)^{\frac{N}{2}} \sin(t_f) \end{bmatrix} \right\} \tag{H.52}$$

The resulting equation is:

$$\begin{bmatrix} a_N^{'} \\ b_N^{'} \end{bmatrix} = \begin{bmatrix} \cos(t_f - t_1) + \cos(t_f - t_2) \\ \sin(t_f - t_1) + \sin(t_f - t_2) \end{bmatrix} \tag{H.53}$$

Now, the right hand side needs to be expanded using the trigonometric identities

$$\begin{bmatrix} \cos(t_f - t_1) + \cos(t_f - t_2) \\ \sin(t_f - t_1) + \sin(t_f - t_2) \end{bmatrix} = \begin{bmatrix} \cos(t_f) & \sin(t_f) \\ \sin(t_f) & -\cos(t_f) \end{bmatrix} \begin{bmatrix} \cos(t_1) + \cos(t_2) \\ \sin(t_1) + \sin(t_2) \end{bmatrix} \tag{H.54}$$

Multiplying the left hand side by the inverse of the first right matrix,

$$\begin{bmatrix} a_N \\ b_N \end{bmatrix} = \begin{bmatrix} \cos(t_f) & \sin(t_f) \\ \sin(t_f) & -\cos(t_f) \end{bmatrix}^{-1} \begin{bmatrix} a_N^{'} \\ b_N^{'} \end{bmatrix} = \begin{bmatrix} \cos(t_1) + \cos(t_2) \\ \sin(t_1) + \sin(t_2) \end{bmatrix} \tag{H.55}$$

which can be solved for the first two switching times:

$$\cos(t_1) = \frac{1}{2}\left(a_N \mp b_N \sqrt{\frac{4}{a_N^2 + b_N^2} - 1} \right) \tag{H.56}$$

$$\cos(t_2) = \frac{1}{2}\left(a_N \pm b_N \sqrt{\frac{4}{a_N^2 + b_N^2} - 1} \right) \tag{H.57}$$

where the sign is used to ensure that $t_2 > t_1 > 0$. The coasting arc is defined by these two switching times

$$t_{off} = t_2 - t_1 \tag{H.58}$$

$$t_{on} = \pi - t_{off} \tag{H.59}$$

(N is ODD, N $\geq$ 3) For these cases, the left hand side is simpler

$$\begin{bmatrix} a_N^{'} \\ b_N^{'} \end{bmatrix} = \frac{\mathbf{x}_f - \mathbf{\Phi}(t_f, 0)\mathbf{x}_o}{u_N} - \begin{bmatrix} 1 \\ 0 \end{bmatrix} \tag{H.60}$$

but, the right hand side is a bit messier,

$$\begin{bmatrix} a_N^{'} \\ b_N^{'} \end{bmatrix} = \begin{bmatrix} c_N \cos(t_f - t_1) - d_N \cos(t_f - t_2) \\ -c_N \sin(t_f - t_1) + d_N \sin(t_f - t_2) \end{bmatrix} \tag{H.61}$$

where

$$c_N = \left(\frac{N+1}{2}\right)(-1)^{\frac{N+1}{2}} \tag{H.62}$$

$$d_N = \left(\frac{N-1}{2}\right)(-1)^{\frac{N+1}{2}} \tag{H.63}$$

$$= sgn\{c_N\}(|c_N|-1) \tag{H.64}$$

The right side can be expanded using the trigonometric identities as it was done for the even cases.

$$\begin{aligned}
&\begin{bmatrix} c_N\cos(t_f-t_1)-d_N\cos(t_f-t_2) \\ -c_N\sin(t_f-t_1)+d_N\sin(t_f-t_2)\end{bmatrix} \\
= &\begin{bmatrix}\cos(t_f) & \sin(t_f)\\ -\sin(t_f) & \cos(t_f)\end{bmatrix}\begin{bmatrix} c_N\cos(t_1)-d_N\cos(t_2) \\ c_N\sin(t_1)-d_N\sin(t_2)\end{bmatrix} \\
= &\ \mathbf{\Phi}(t_f,0)\begin{bmatrix} c_N\cos(t_1)-d_N\cos(t_2) \\ c_N\sin(t_1)-d_N\sin(t_2)\end{bmatrix} \\
= &\ c_N\mathbf{\Phi}(t_f,0)\begin{bmatrix} \cos(t_1)-D_N\cos(t_2) \\ \sin(t_1)-D_N\sin(t_2)\end{bmatrix}
\end{aligned} \tag{H.65}$$

where $D_N = d_N/c_N = (N-1)/(N+1)$. Multiplying the left hand side by $\Phi^{-1}(t_f,0)$ and dividing by c_N,

$$\begin{bmatrix} a_N \\ b_N\end{bmatrix} = \frac{\mathbf{\Phi}^{-1}(t_f,0)}{c_N}\begin{bmatrix} a_N' \\ b_N'\end{bmatrix} = \begin{bmatrix} \cos(t_1)-D_N\cos(t_2) \\ \sin(t_1)-D_N\sin(t_2)\end{bmatrix} \tag{H.66}$$

The equation can still be solved for the first two switching times:

$$\cos(t_1) = \frac{1}{2}\left[a_N\left(\frac{1-D_N^2}{a_N^2+b_N^2}+1\right)\pm b\sqrt{L-1}\right] \tag{H.67}$$

$$\cos(t_2) = \frac{1}{2D_N}\left[a_N\left(\frac{1-D_N^2}{a_N^2+b_N^2}-1\right)\pm b\sqrt{L-1}\right] \tag{H.68}$$

where

$$L = \frac{2(1+D_N^2)}{a_N^2+b_N^2} + \frac{D_N^2(2-D_N^2)-1}{(a_N^2+b_N^2)^2} - 1 \tag{H.69}$$

and the sign is used to ensure that $t_2 > t_1 > 0$. The thrusting arc is defined by these two switching times.

$$t_{on} = t_2 - t_1 \tag{H.70}$$

$$t_{off} = \pi - t_{on} \tag{H.71}$$

(N is ODD or EVEN, N $\geq$ 2) Once the first two switching times are calculated, the radius of the costate trajectory can be calculated

$$\frac{1}{R_\lambda} = \begin{cases} \cos\left[\frac{1}{2}t_{on}\right] & , \ N \ is \ odd \\ \sin\left[\frac{1}{2}t_{off}\right] & , \ N \ is \ even \end{cases} \tag{H.72}$$

Next, the costate at the last switch is calculated,

$$\boldsymbol{\lambda}_N = \begin{cases} (+\sqrt{R_\lambda^2-1}, -1) & , \ u_N = +U_{max} \\ (-\sqrt{R_\lambda^2-1}, +1) & , \ u_N = -U_{max} \end{cases} \tag{H.73}$$

Finally, the initial costate can be calculated by

$$\boldsymbol{\lambda}_o = \boldsymbol{\Phi}^{-1}(t_N, 0)\boldsymbol{\lambda}_N \tag{H.74}$$

where the last switching time, t_N, can be calculated using t_1 and t_2.

$$t_N = \begin{cases} t_1 + \left(\frac{N-1}{2}\right)\pi & , \ N \ is \ odd \\ t_2 + \left(\frac{N-2}{2}\right)\pi & , \ N \ is \ even \end{cases} \tag{H.75}$$

H.9 Minimum Fuel versus Minimum Time

There are some key differences between the optimal time solution and optimal fuel solution.

1. One of the main difference between these two problems is that the final time is specified for the minimum fuel problem and the optimal solution must result in a constant Hamiltonian. For the minimum time problem, the final time is calculated and we have the Transversality Condition which remains zero for all time.
2. The minimum time problem required the calculations of the first and last intersection points where the switches occur, but the remaining intersection points were easily calculated due to the intermediate time intervals being exactly π canonical units of time.
3. The minimum fuel problem required the calculation of the first two switching times whereas the minimum time problem required only the first switching time.
4. The test for sufficient condition is not required; i.e., the difficult Hamilton-Jacobi equation need not be solved. Both the minimum time and minimum fuel problem minimizes a convex function with linear constraints. Therefore, it is a global minimum.
5. The number of control switching for the minimum fuel problem is a function of the fixed final time. This fixed final time must be larger than the minimum time. As the specified final time for the minimum fuel problem increases, the number of control switching increases. The lower bound is the N^* from the minimum time solution. More research is required for understanding the number of control switching required for the minimum fuel problem.

H.10 Out-of-Plane Example Problem

This section provides the result of a sample problem with $U_{max} = 0.25$ and $\omega = 1$ for both the minimum time and minimum fuel problem. The problem was to find an

optimal controls that will take the given initial state to the given final state in minimum time and secondly using minimum fuel given the final time.

1. Initial and final states:

$$\begin{aligned} \mathbf{x}_o &= [z_o \ \dot{z}_o]^T = [1 \ \ 1]^T \\ \mathbf{x}_f &= [z_f \ \dot{z}_f]^T = [-1.1339 \ \ -1.2374]^T \end{aligned} \tag{H.76}$$

with $R_{zo} = \sqrt{\mathbf{x}_o^T \mathbf{x}_o} = 1.4142$ and $R_{zf} = \sqrt{\mathbf{x}_f^T \mathbf{x}_f} = 1.6784$.
See Figure H.8 below.

2. State-Space Diagram:

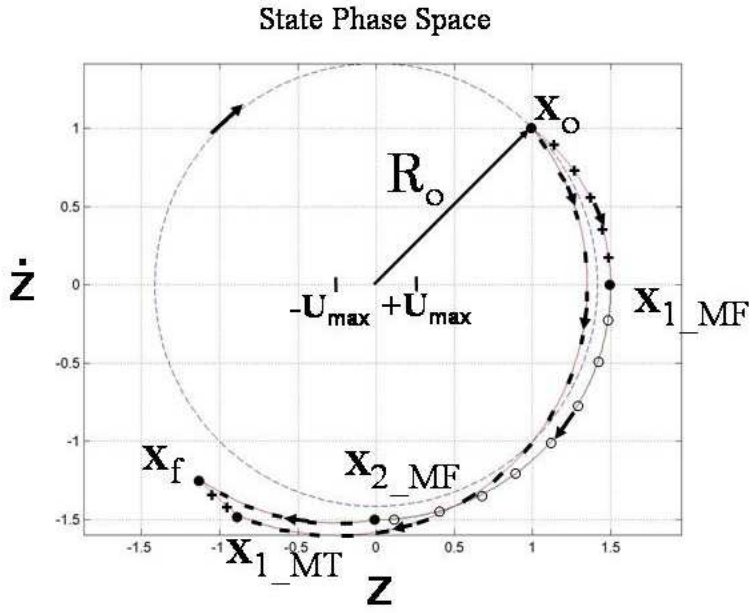

Figure H.8 Out-of-plane state-phase space diagram for both minimum time and minimum fuel example problem.

The minimum time solution required one control switch with $u_o = -U_{max}$ and $u_1 = U_{max}$. The switch occurs at $\mathbf{x}_{1\_MT}$. The minimum fuel solution required two

control switches with $u_o = U_{max}$ and $u_1 = 0$ and $u_2 = -U_{max}$. The switches occur at $\mathbf{x}_{1\_MF}$ and $\mathbf{x}_{2\_MF}$. See Figure(H.8).

3. Results Table:

   See Appendix I for details of the calculations.

Table H.1 Summary of out-of-plane numerical results

	Minimum Time	Minimum Fuel
N	1	2
$\mathbf{x}_N$	$\mathbf{x}_1 = [-0.8838, -1.47]^T$	$\mathbf{x}_1 = [1.5, 0]^T$ $\mathbf{x}_2 = [0, -1.5]^T$
t_N	$t_1 = 2.6526$	$t_1 = 0.9273$ $t_2 = 2.4981$
t_f	$t^*_{MT} = 2.8368$	$t_f = 3.2835$
R_λ	0.6803	1.4142
$\boldsymbol{\lambda}_N$	$\boldsymbol{\lambda}_1 = [0.6803, 0]^T$	$\boldsymbol{\lambda}_1 = [-1, -1]^T$ $\boldsymbol{\lambda}_2 = [-1, 1]^T$
$\boldsymbol{\lambda}_o$	$\boldsymbol{\lambda}_o = [-0.6006, 0.3195]^T$	$\boldsymbol{\lambda}_o = [0.2, -1.4]^T$
$u^*_z(t)$	$-sgn\{\lambda_{\dot{z}}(t)\}U_{max}$	$\begin{cases} 0 & \lvert\lambda_{\dot{z}}(t)\rvert < 1 \\ -sgn\{\lambda_{\dot{z}}(t)\}U_{max} & \lvert\lambda_{\dot{z}}(t)\rvert > 1 \end{cases}$
$\lambda_{\dot{z}}(t)$	$-\lambda_{zo}\sin(t) + \lambda_{\dot{z}_o}\cos(t)$	$-\lambda_{zo}\sin(t) + \lambda_{\dot{z}_o}\cos(t)$
ΔV	0.7092	0.4282

4. Costate Phase Diagrams:

   Figure(H.9) illustrates the difference in the costate for the minimum time and minimum fuel solutions. Notice that the radius for the minimum time is less than unity, which cannot happen in the minimum fuel case.

H.11 Summary

In this chapter, the minimum fuel solution for the out-of-plane motion was presented analytically. The minimum fuel solution was more complex than the minimum time solution. Also, the optimal N^* for the minimum fuel requires further research.

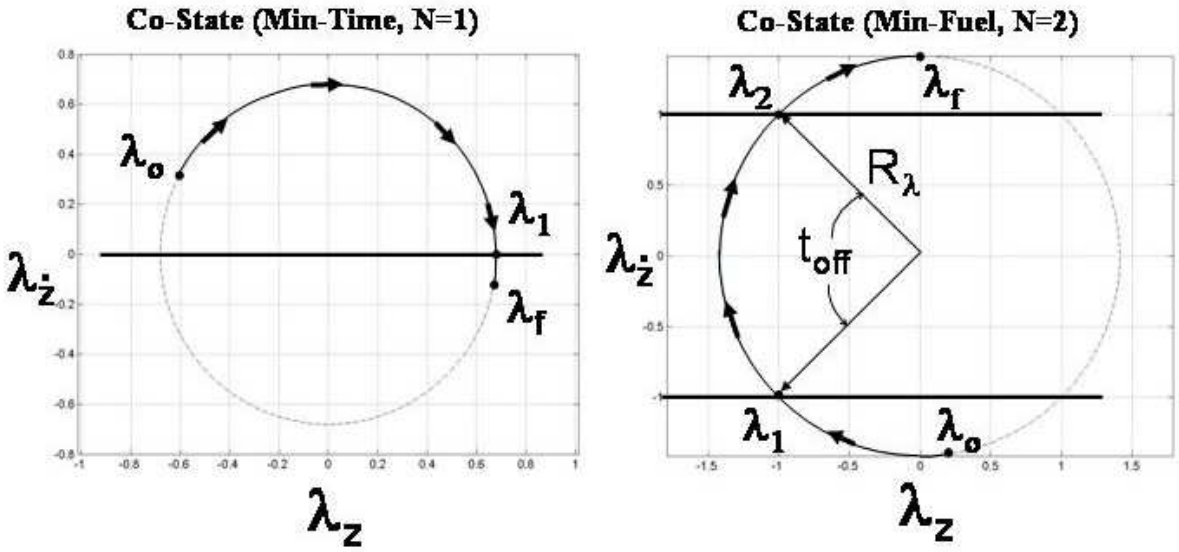

Figure H.9 Comparison costate-phase space diagrams.

Appendix I. Out-of-Plane Minimum-Time and Minimum-Fuel Example Problem Calculations

This appendix provides the detailed calculation for the out-of-plane example problem discussed in Section H.10.

I.1 Minimum-Time Calculations

A. Number of Control Switches

$N = \left\lfloor \frac{|R_f - R_o|}{2U_{max}} \right\rfloor = \left\lfloor \frac{|1.6784 - 1.4142|}{0.5} \right\rfloor = \lfloor 0.5284 \rfloor = 0$ did not produce a minimum time solution. Therefore, N was incremented by one; $N^*_{MT} = 1$.

B. State at the first control switch

With $u_o = -U_{max}$,

$$\begin{aligned} z_1 &= \frac{R_f^2 - R_o^2}{4Nu_o} + \frac{z_o - (-1)^N z_f}{2N} - (N-1)u_o \\ &= \frac{2.8169 - 2.0}{-1.0} + \frac{1 - 1.1339}{2} = -0.8838 \end{aligned} \tag{I.1}$$

and

$$\begin{aligned} \dot{z}_1^2 &= (z_o - u_o)^2 + \dot{z}_o^2 - (z_1 - u_o)^2 \\ &= (1 + 0.25)^2 + 1^2 - (-0.8838 + 0.25)^2 = 2.1608 \\ \dot{z}_1 &= -1.4700 \end{aligned} \tag{I.2}$$

C. Time of first control switch

$$\begin{aligned} \tan(t_1) &= \frac{\dot{z}_o(z_1 - u_o) - \dot{z}_1(z_o - u_o)}{\dot{z}_o\dot{z}_1 + (z_o - u_o)(z_1 - u_o)} \\ &= \frac{1 \cdot (-0.88381 + 0.25) - (-1.4700)(1 + 0.25)}{1 \cdot (-1.4700) + (1 + 0.25)(-0.8838 + 0.25)} \\ t_1 &= 2.6526 = 151.99^o \end{aligned} \tag{I.3}$$

D. Initial Co-state

$$\begin{aligned}\lambda_{zo} &= \frac{1}{(z_o - u_o)\tan(t_1) - \dot{z}_o} \\ &= \frac{1}{(1+0.25)\tan(151.99^o) - 1} = -0.6006 \end{aligned} \tag{I.4}$$

$$\begin{aligned}\lambda_{\dot{z}_o} &= \frac{\tan(t_1)}{(z_o - u_o)\tan(t_1) - \dot{z}_o} \\ &= \frac{\tan(151.99^o)}{(1+0.25)\tan(151.99^o) - 1} = 0.3195 \end{aligned} \tag{I.5}$$

The initial co-state $\boldsymbol{\lambda}_o = [-0.6006\ 0.3195]^T$.

E. Optimal Control

The optimal control is given by

$$u_z^*(t) = -sgn\{\lambda_{\dot{z}}(t)\}U_{max} \tag{I.6}$$

where

$$\begin{aligned}\lambda_{\dot{z}}(t) &= \mathbf{B}^T\boldsymbol{\lambda}(t) = \mathbf{B}^T\boldsymbol{\Phi}_\lambda(t,0)\boldsymbol{\lambda}_o \\ &= -\lambda_{zo}\sin(t) + \lambda_{\dot{z}_o}\cos(t) \end{aligned} \tag{I.7}$$

F. Minimum Time

Minimum time, $t_f - t_1$,

$$\begin{aligned}\tan(t_f - t_1) &= \frac{\dot{z}_1[z_f - (-1)^1 u_0] - \dot{z}_f[z_1 + (2\cdot 1 - 1)u_o]}{\dot{z}_1\dot{z}_f + [z_1 + (2\cdot 1 - 1)u_o][z_f - (-1)^1 u_o]} \\ &= \frac{-1.4700[-1.1339 - 0.25] - (-1.2374)[-0.8838 - 0.25]}{(-1.4700)(-1.2374) + [-0.8838 - 0.25][-1.1339 - 0.25)]} \\ (t_f - t_1) &= 0.1842 = 10.55^o \end{aligned} \tag{I.8}$$

Then the total time is

$$t_f^* = t_1 + (t_f - t_1) = 2.6526 + 0.1842 = 2.8368 = 162.54^o \tag{I.9}$$

G. Fuel Usage

The total fuel usage is simply $\Delta V = t_f^* U_{max} = 0.7092$.

I.2 Minimum-Fuel Calculations

a. Final Time

$t_f = 3.2835$ rad $= 188.1301^o$

b. Number of Control Switches

$N = 2$ with the optimal control sequence of $u_z^* = \{-u_2, 0, u_2\}$ and $u_2 = -U_{max}$.

c. Times of first two Control switches

First two control switch times are calculated, but we first need the intermediate values, a_N and b_N,

$$\begin{aligned}
\begin{bmatrix} a_2' \\ b_2' \end{bmatrix} &= \frac{2}{2} \begin{bmatrix} (-1)^{\frac{2}{2}} & 0 \\ 0 & (-1)^{\frac{2}{2}-1} \end{bmatrix} \left\{ \frac{\mathbf{x}_f - \mathbf{\Phi}_x(t_f, 0)\mathbf{x}_o}{u_2} - \begin{bmatrix} 1 + (-1)^{\frac{2}{2}-1}\cos(t_f) \\ (-1)^{\frac{2}{2}}\sin(t_f) \end{bmatrix} \right\} \\
&= \begin{bmatrix} -1 & 0 \\ 0 & 1 \end{bmatrix} \left\{ \frac{\begin{bmatrix} -1.1339 \\ -1.2374 \end{bmatrix} - \mathbf{\Phi}_x(t_f, 0) \begin{bmatrix} 1 \\ 1 \end{bmatrix}}{-0.25} - \begin{bmatrix} 1 + \cos(t_f) \\ -\sin(t_f) \end{bmatrix} \right\} \\
&= \begin{bmatrix} 0.0 \\ 1.4142 \end{bmatrix}
\end{aligned} \tag{I.10}$$

$$\begin{bmatrix} a_2 \\ b_2 \end{bmatrix} = \begin{bmatrix} \cos(t_f) & \sin(t_f) \\ \sin(t_f) & -\cos(t_f) \end{bmatrix}^{-1} \begin{bmatrix} 0.0 \\ 1.4142 \end{bmatrix} = \begin{bmatrix} -0.2000 \\ 1.4000 \end{bmatrix} \tag{I.11}$$

$$
\begin{aligned}
\cos(t_1) &= \frac{1}{2}\left(a_2 + b_2\sqrt{\frac{4}{a_2^2+b_2^2}-1}\right) \\
&= \frac{1}{2}\left(-0.2000 + 1.400\sqrt{\frac{4}{(-0.2000)^2+(1.4000)^2}-1}\right) \\
t_1 &= \cos^{-1}(0.600) = 0.9273 = 53.13^o \\
\cos(t_2) &= \frac{1}{2}\left(a_2 - b_2\sqrt{\frac{4}{a_2^2+b_2^2}-1}\right) \\
&= \frac{1}{2}\left(-0.2000 - 1.400\sqrt{\frac{4}{(-0.2000)^2+(1.4000)^2}-1}\right) \\
t_2 &= \cos^{-1}(-0.800) = 2.4981 = 143.13^o
\end{aligned}
$$

The coasting arc lasts from t_1 to t_2; $t_{off} = t_2 - t_1 = \pi/2$.

d. Initial co-state

First we need to calculate the Radius of the Co-state trajectory. Since $N = 2$,

$$R_\lambda = \frac{1}{\sin(\frac{1}{2}t_{off})} = \csc\left(\frac{\pi}{4}\right) = 1.4142 = \sqrt{2} \tag{I.12}$$

Now, the co-state the second control switch is determine by,

$$\boldsymbol{\lambda}_2 = (-\sqrt{R_\lambda^2 - 1}, +1) = \begin{bmatrix} -1 \\ 1 \end{bmatrix} \tag{I.13}$$

Finally, the initial co-state is calculated using,

$$
\begin{aligned}
\boldsymbol{\lambda}_o &= \boldsymbol{\Phi}_\lambda^{-1}(t_2, 0)\boldsymbol{\lambda}_2 \\
&= \begin{bmatrix} \cos(t_2) & \sin(t_2) \\ -\sin(t_2) & \cos(t_2) \end{bmatrix}^{-1} \begin{bmatrix} -1 \\ 1 \end{bmatrix} = \begin{bmatrix} 0.2000 \\ -1.4000 \end{bmatrix}
\end{aligned} \tag{I.14}
$$

e. Optimal Control

The optimal-fuel control is given by

$$u_z^*(t) = \begin{cases} 0 & , |\lambda_{\dot{z}}(t)| < 1 \\ -sgn\{\lambda_{\dot{z}}(t)\} U_{max} & , |\lambda_{\dot{z}}(t)| > 1 \end{cases} \tag{I.15}$$

where as it was in the minimum-time case

$$\begin{aligned} \lambda_{\dot{z}}(t) &= \mathbf{B}^T \boldsymbol{\lambda}(t) = \mathbf{B}^T \boldsymbol{\Phi}_\lambda(t,0) \boldsymbol{\lambda}_o \\ &= -\lambda_{zo} \sin(t) + \lambda_{\dot{z}_o} \cos(t) \end{aligned} \tag{I.16}$$

f. Fuel Usage

The total fuel usage is simply $\Delta V = (t_f - t_{off}) U_{max} = 0.4282$.

Appendix J. Optimal Control for Minimum-Time and Minimum-Fuel

J.1 Minimum Time

Table J.1 depicts all the possible control for the bang-bang minimum-time optimal control as well as the signs of the costates that correspond to each control. The missing case is the off condition once the final state is achieved.

Table J.1 Bang-Bang Minimum-Time Control and Costate Table

Subcase	$\frac{u_x}{U_{max}}$	$\frac{u_y}{U_{max}}$	$\frac{u_z}{U_{max}}$	$\lambda_{\dot{x}}$	$\lambda_{\dot{y}}$	$\lambda_{\dot{z}}$
MT 1	+1	+1	+1	< 0	< 0	< 0
MT 2	+1	+1	-1	< 0	< 0	> 0
MT 3	+1	-1	+1	< 0	> 0	< 0
MT 4	+1	-1	-1	< 0	> 0	> 0
MT 5	-1	+1	+1	> 0	< 0	< 0
MT 6	-1	+1	-1	> 0	< 0	> 0
MT 7	-1	-1	+1	> 0	> 0	< 0
MT 8	-1	-1	-1	> 0	> 0	> 0

J.2 Minimum Fuel

Similar tables can be constructed for the minimum-fuel problem. Table J.2 below depicts all the possible control for the on-off minimum-fuel optimal control. From these tables it is easy to see that the minimum-time and minimum-fuel optimal control will be the same if in the minimum-fuel problem there are no coasting arcs; u_x, u_y, and u_z cannot be zero. Another way of saying this is Table J.1 is a subset of Table J.2; i.e. cases MF 1, MF 3, MF 7, MF 9, MF 19, MF 21, MF 25, and MF 27 of Table J.2 are exactly the cases to MT 1 through MT 8 in Table J.1. This can only happen if the costates for the min-fuel problem do not cross +1 or -1. However, in Equation (**??**), the costate corresponding to the cross-track motion ($\lambda_{\dot{z}}$), is sinusoidal about zero, which imply u_z will be zero for some part of the maneuver. Thus minimum-fuel problem will never be

equal to minimum-time unless the problem is strictly in the plane of the reference orbit; i.e. no out-of-plane motion.

Table J.2 ON-OFF Minimum-Fuel Control Table

Subcase	$\frac{u_x}{U_{max}}$	$\frac{u_y}{U_{max}}$	$\frac{u_z}{U_{max}}$
MF 1	+1	+1	+1
MF 2	+1	+1	0
MF 3	+1	+1	-1
MF 4	+1	0	+1
MF 5	+1	0	0
MF 6	+1	0	-1
MF 7	+1	-1	+1
MF 8	+1	-1	0
MF 9	+1	-1	-1
MF 10	0	+1	+1
MF 11	0	+1	0
MF 12	0	+1	-1
MF 13	0	0	+1
MF 14	0	0	0
MF 15	0	0	-1
MF 16	0	-1	+1
MF 17	0	-1	0
MF 18	0	-1	-1
MF 19	-1	+1	+1
MF 20	-1	+1	0
MF 21	-1	+1	-1
MF 22	-1	0	+1
MF 23	-1	0	0
MF 24	-1	0	-1
MF 25	-1	-1	+1
MF 26	-1	-1	0
MF 27	-1	-1	-1

Subcase	$\lvert\lambda_{\dot{x}}\rvert$	$\lvert\lambda_{\dot{y}}\rvert$	$\lvert\lambda_{\dot{z}}\rvert$
MF 1	> 1	> 1	> 1
MF 2	> 1	> 1	< 1
MF 3	> 1	> 1	> 1
MF 4	> 1	< 1	> 1
MF 5	> 1	< 1	< 1
MF 6	> 1	< 1	> 1
MF 7	> 1	> 1	> 1
MF 8	> 1	> 1	< 1
MF 9	> 1	> 1	> 1
MF 10	< 1	> 1	> 1
MF 11	< 1	> 1	< 1
MF 12	< 1	> 1	> 1
MF 13	< 1	< 1	> 1
MF 14	< 1	< 1	< 1
MF 15	< 1	< 1	> 1
MF 16	< 1	> 1	> 1
MF 17	< 1	> 1	< 1
MF 18	< 1	> 1	> 1
MF 19	> 1	> 1	> 1
MF 20	> 1	> 1	< 1
MF 21	> 1	> 1	> 1
MF 22	> 1	< 1	> 1
MF 23	> 1	< 1	< 1
MF 24	> 1	< 1	> 1
MF 25	> 1	> 1	> 1
MF 26	> 1	> 1	< 1
MF 27	> 1	> 1	> 1

Bibliography

1. Clohessy, W. and R.S. Wiltshire. "Terminal Guidance System for Satellite Rendezvous," *Journal of the Aerospace Sciences*, *27*:653–658 (1960).
2. Visher, P. "Satellite Clusters," *Satellite Communications*, *1*(1):22–4,27 (1979).
3. Parker, T.W. "Permutational Metric Optimization of an Earth Orbiting Satellite." Ph.D. Prospectus, 2001.
4. Space Vehicles Directorate, AFRL. *TechSat 21 - Space Missions Using Satellite Clusters*. Technical Report, http://www.vs.afrl.af.mil/TechProgs/TechSat21/NGSC.html, 2001.
5. Burns, R. and C. McLaughlin and J. Keitner and M. Martin. "TechSat21: Formation Design, Control, and Simulation." edited by anonymous. 2001.
6. Hartman, K., et al. "Relative Navigation for Spacecraft Formation Flying," *Advances in the Astronautical Sciences*, *100*(Part II):685–699 (1998).
7. Conkey, D. and J. Bristow. "EO-1 Formation Flying Using AutoCon," *IEEE*, 55–61 (2000).
8. Guzman, J.J. and E. Ariel. "Flying a Four-Spacecraft Formation by the Moon ... Twice." *13th AAS/AIAA Space Flight Mechanics Meeting*. AAS Publications Office, 2003.
9. Sabol, C. and R. Burns and C.A. McLaughlin. "Satellite Formation Flying Design and Evolution," *Advances in astronautical sciences*, *102*(1):265–284 (1999).
10. Sedwick, R.J. and D.W. Miller and E.M.C. Kong. "Mitigation of Differential Perturbations in Clusters of Formation Flying Satellites," *Advances in Astronautical Sciences*, *102*(1):323–342 (1999).
11. Inalhan, G. and M. Tillerson and How J. "Relative Dynamics and Control of Spacecraft Formations in Eccentric Orbits," *Journal of Guidance, Control, and Dynamics*, *25*(1):48–59 (Jan/Feb 2002).
12. Wiesel, W. "Optimal Impulsive Control of Relative Satellite Motion," *Journal of Guidance, Control, and Dynamics* (2002).
13. Schweighart, S.A. and R.J. Sedwick. "High-fidelity Linearized J_2 Model for Satellite Formation Flight," *Journal of Guidance, Control, and Dynamics*, *25*(6):1073–1080 (2002).
14. Schaub, J. and K.T. Alfriend. "J_2 Invariant Relative Orbits For Spacecraft Formations." *1999 Flight Mechanics Symposium*, edited by J.P. Lynch. 125–139. NASA Goddard Space Flight Center, 1999.

15. Alfriend, K.V. and S.R. Vadali and H. Schaub. "Formation flying satellites: control by an astrodynamicist," *Celestial Mechanics and Dynamical Astronomy*, *81*(No. 1-2):57–62 (2001).

16. Vallado, D.A. *Fundamentals of Astrodynamics and Applications*. Space Technology Series, The McGraw-Hill Companies, Inc., 1997.

17. Melton, R.G. "Relative Motion of Satellites in Elliptical Orbits," *Advances in the Astronautical Sciences*, *97*(Part II):2075–2094 (1997).

18. Kechichian, J.A. "The Analysis of the Relative Motion in General Elliptic Orbit with Respect to a Dragging and Precessing Coordinate Frame," *Advances in the Astronautical Sciences*, *97*(P 2):2053–2074 (1997).

19. Yan, Q. and G. Yang and V. Kapila and M.S. Queiroz. "Nonlinear Dynamics and Output Feedback Control of Multiple Spacecraft in Elliptical Orbits." *American Control Conference*. 839–843. IEEE, 2000.

20. Yamanaka, K. and F. Ankersen. "New State Transition Matrix for Relative Motion on an Arbitrary Elliptical Orbit," *Journal of Guidance, Control, and Dynamics*, *23*(1):60–66 (2000).

21. Schaub, H. and K. Alfriend. "Hybrid Cartesian and Orbit Element Feedback Law for Formation Flying Spacecraft," *Journal of Guidance, Control, and Dynamics*, *25*(2):387–393 (Mar/Apr 2002).

22. Ross, I.M. and J.T. King and F. Fahroo. "Designing Optimal Spacecraft Formations." *AIAA/AAS Astrodynamics Specialist Conference and Exhibit*. AIAA, 2002.

23. Hujsak, R.S. "Nonlinear dynamical model of relative motion for the orbiting debris problem," *Journal of Guidance, Control, and Dynamics*, *14*(2):460–465 (1990).

24. Vaddi, S.S. and S.R. Vadali. "Linear and Nonlinear Control Laws for Formation Flying." *13th AAS/AIAA Space Flight Mechanics Meeting*. AAS Publications Office, 2003.

25. Wiesel, W.E. "The Dynamics of Relative Satellite Motion." *AAS/AIAA Space Flight Mechanics Meeting*. AAS Publications Office, 2001.

26. Coverstone-Carrol, V. and J.E. Prussing. "Optimal Cooperative Power-Limited Rendezvous Between Neighboring Circular Orbits," *Journal of Guidance, Control, and Dynamics*, *16*(6):1045–1054 (1993).

27. Wiesel, W. "Relative Satellite Motion About an Oblate Planet," *Journal of Guidance, Control, and Dynamics*, *25*(4):776–785 (2002).

28. Carter, T.E. and S.A. Alvarez. "Quadratic-based computation of four-impulse optimal rendezvous near circular orbit," *Journal of Guidance, Control, and Dynamics*, *23*(1):109–117 (1999).

29. Ulybyshev, Y. "Long-Term Formation Keeping of Satellite Constellation Using Linear-Quadratic Controller," *Journal of Guidance, Control, and Dynamics*, *21*(1):109–115 (1998).

30. Kechichian, J.A. "Minimum-Fuel Time-Fixed Rendezvous Using Constant Low Thrust," *Advances in the Astronautical Sciences*, *82*(P 1):479–500 (1993).

31. Kechichian, J.A. "Optimal Power-Limited Rendezvous for Linearized Equations of Motion," *Journal of Guidance, Control, and Dynamics*, *17*(5):1082–1086 (1994).

32. Kechichian, J.A. "Optimal Low-Thrust Transfer Using Variable Bounded Thrust," *Acta Astronautica*, *36*(7):357–365 (1995).

33. Kechichian, J.A. "Optimal Low-Thrust Rendezvous Using Equinotial Orbit Elements," *Acta Astronautica*, *38*(1):1–14 (1996).

34. Kechichian, J.A. "Minimum-Time Low-Thrust Rendezvous and Transfer Using Epoch Mean Longtiude Formulation," *Journal of Guidance, Control, and Dynamics*, *22*(3):421–432 (1999).

35. Kechichian, J.A. "Minimum-Time Constant Acceleration Orbit Transfer with First-Order Oblateness Effect," *Journal of Guidance, Control, and Dynamics*, *23*(4):595–603 (2000).

36. DeCou, A.B. "Orbital Station-Keeping for Multiple Spacecraft Interferometry," *The Journal of the Astronautical Sciences*, *39*(3):283–297 (1991).

37. Guelman, M. and M. Aleshin. "Optimal Bounded Low Thrust Rendezvous with Fixed Terminal Approach Direction." *AAS/AIAA Astrodynamics Conference*, edited by F. Hoots and B. Kaufman and P. Cefola and D. Spencer. 739–758. AAS, 1997.

38. Pardis, C.J. and Carter T. "Optimal Power-Limited Rendezvous with Thrust Saturation," *Journal of Guidance, Control, and Dynamics*, *18*(5):1145–1150 (1995).

39. Yan, Q. and V. Kapila and A.G. Sparks. "Pulse-Based Periodic Control for Spacecraft Formation Flying." *IEEE American Control Conference*. 374–378. IEEE, 2000.

40. Vadali, S. and H. Schaub and K. Alfriend. "Initial Conditions and Fuel-optimal Control for Formation Flying Satellites," *AIAA Guidance, Navigation, and Control Conference and Exhibit* (1999).

41. Irvin, D.J. *A Study of Linear vs. Nonlinear Control Techniques for the Reconfiguration of Satellite formations*. Masters Thesis, Air Force Institute of Technology (AFIT), 2001.

42. Irvin, D.J. "Linear vs. Nonlinear Control Techniques For The Reconfiguration Of Satellite Formations." *AIAA Guidance, Navigation, and Control Conference and Exhibit*. AIAA, 2001.

43. Queiroz, M. and V. Kapila and Q. Yan. "Adaptive Nonlinear Control of Multiple Spacecraft Formation Flying," *Journal of Guidance, Control, and Dynamics*, *25*(4):385–390 (2000).

44. Athans, M. and P.L. Falb. *Optimal Control - An Introduction to the Theory and Its Applications*. McGraw-Hill Book Company, 1966.

45. Milam, M.B. and N. Petit and R.M. Murray. "Constrained Trajectory Generation For Micro-Satellite Formation Flying." *AIAA Guidance, Navigation, and Control Conference and Exhibit*. AIAA, 2001.

46. Maybeck, P.S. *Stochastic Models, Estimation, and Control, Volume 1*, *1*. Mathematics in Science and Engineering. Academic Press, Inc., 1994.

47. Chang, S.S.L. "Sufficient Condition for Optimal Cotnrol of Linear Systems with Nonlinar Cost Functions." *1964 Joint Automatic Control Conference*, edited by Zadeh L. A. Placone R. C. Franklin, G. 295–296. 1964.

48. Wiesel, W.E. *Spaceflight Dynamics*. The McGraw-Hill, Inc., 1989.

49. Yeh, H.-H. and A. Sparks. "Geometry and Control of Satellite Formations." *American Control Conference*. 384–388. IEEE, 2000.

50. Seo, John S. and William E. Weisel. "Low Thrust Control Optimization for Satellite Formation." *14th AAS/AIAA Space Flight Mechanics Conference*. AAS Publications Office, 2004.

51. Maybeck, P.S. *Stochastic Models, Estimation, and Control, Volume 3*, *3*. Mathematics in Science and Engineering. Academic Press, Inc., 1994.

52. Parker, T.W. *Mean Performance Optimization of an Orbiting Distributed Aperture by Warped Aperture Image Plane Comparisons*. Ph.D. Dissertation, Air Force Institute of Technology, 2002.

Vita

Major John S. Seo was born in Seoul, Korea. At age ten, his family immigrated to Michigan where he attended West Bloomfield High School. After graduating as a valedictorian of his high school class, he attended the University of Michigan in 1986. In 1990, he earned his Bachelors of Science degree in Aerospace Engineering with academic distinction and at the same time received his commission in the Air Force through Detachment 390 as a distinguished ROTC graduate. His first assignment was to the Computational Fluid Dynamics (CFD) branch in the Air Vehicle's Directorate of Air Force Research Laboratory at Wright-Patterson AFB. He was then selected to serve as the Engineer/Scientist Exchange Program (ESEP) officer to the Republic of Korea's Agency for Defense Development (ROK ADD) from 1994-1996 and worked on CFD software in support of ROK's indigenous trainer aircrafts, KTX-1 and KTX-2. He returned to the United States to attend the US Air Force Test Pilot School as a student of the Flight Test Engineering Course. After graduation, he was assigned to the 418 Flight Test Squadron, Edwards AFB from 1997-1999 where he participated in the C-141C GPS Enhanced Navigation System (GPSENS) testing. He was then interviewed and selected for the position of academic instructor in the Department of Astronautical Engineering at the United States Air Force Academy (USAFA/DFAS) from 1999-2001. He arrived at the Air Force Institute of Technology (AFIT) for his PhD program under the direction of Dr. William E. Wiesel. Upon graduation, he will be assigned to AFIT's Systems Engineering Directorate with the follow-on assignment returning him to the USAFA in 2006 as an Assistant Professor of Astronautical Engineering. Major Seo and his lovely wife have a son and a daughter.

REPORT DOCUMENTATION PAGE

Form Approved
OMB No. 0704–0188

1. REPORT DATE *(DD–MM–YYYY)*	2. REPORT TYPE	3. DATES COVERED *(From — To)*
30–09–2004	Doctoral Dissertation	Oct 2001 — Sep 2004

4. TITLE AND SUBTITLE

Analytical Solution for Low-Thrust Minimum Time Control of a Satellite Formation

5a. CONTRACT NUMBER

5b. GRANT NUMBER

5c. PROGRAM ELEMENT NUMBER

6. AUTHOR(S)

Seo, John S., Major, USAF

5d. PROJECT NUMBER

5e. TASK NUMBER

5f. WORK UNIT NUMBER

7. PERFORMING ORGANIZATION NAME(S) AND ADDRESS(ES)

Air Force Institute of Technology
Graduate School of Engineering and Management (AFIT/EN)
2950 Hobson Way
WPAFB OH 45433-7765

8. PERFORMING ORGANIZATION REPORT NUMBER

AFIT/DS/ENY/04-04

9. SPONSORING / MONITORING AGENCY NAME(S) AND ADDRESS(ES)

AFRL/VSES
Attn: Dr. Richard K. de Jonckheere and Dr. Thomas A. Lovell
3550 Aberdeen Ave, SE
Kirtland AFB, NM 87117 DSN:246-5054

10. SPONSOR/MONITOR'S ACRONYM(S)

11. SPONSOR/MONITOR'S REPORT NUMBER(S)

12. DISTRIBUTION / AVAILABILITY STATEMENT

Approval for public release; distribution is unlimited.

13. SUPPLEMENTARY NOTES

14. ABSTRACT

Satellite formations or distributed satellite systems provide advantages not feasible with single satellites. Efficient operation of this platform requires the use of optimal control of the entire satellite formation. While the optimal control theory is well established, only a very simple dynamical system affords an analytical solution. Any practical optimal control problem solves the resulting two-point boundary value (TPBV) problem numerically. The relative satellite dynamics using Hill's coordinate system and approximations made by Clohessy and Wiltshire, combined with body-fixed thruster control, result in a linearized dynamic system. This dissertation provides the analysis for the minimum time satellite formation control by decoupling the in-plane motion from the out-of-plane motion. While the out-of-plane motion is fully analytic, the in-plane motion is only semi-analytic. The TPBV problem is transformed to solving simultaneous nonlinear equations for the critical control switching times, resulting in an open-loop, bang-bang controller.

15. SUBJECT TERMS

satellite formation; optimal control; minimum time control; Clohessy-Wiltshire; continuous low-thrust; distributed satellite system; bang-bang control; satellite rendezvous; proximity operations; Hill's equation

16. SECURITY CLASSIFICATION OF:			17. LIMITATION OF ABSTRACT	18. NUMBER OF PAGES	19a. NAME OF RESPONSIBLE PERSON
a. REPORT	b. ABSTRACT	c. THIS PAGE			William E. Wiesel, PhD (ENY)
U	U	U	UU	268	19b. TELEPHONE NUMBER *(include area code)* (937) 255-6565, ext 4312